



'Sangola Taluka Shetkari Shikshan Prasarak Mandal Sangola's

# VIDNYAN MAHAVIDYALAYA SANGOLA

(Arts & Science, E.C.S. & B.C.A.)

Off. (02187) 220508

Tal. Sangola Dist. Solapur Pin. 413 307 (Maharashtra)

Mob. No. 9421045987

(Affiliated to P. A. H. Solapur University)

Email : vidnyanms@yahoo.co.in

Website : www.vmssangola.org

**Acting Principal : Dr. R. A. Fule**  
M.A., Ph.D.

**Third Cycle Accredited by NAAC**  
with 'B' Grade (CGPA of 2.24)

Ref. No.

Date :

/

120



## Number of workshops/seminars conducted on Research Methodology, Intellectual Property Rights (IPR) and entrepreneurship during the year-2021-22

This year nine international/national conferences were organized by the different departments and one IPR workshop is also organised.

Year	Name of the workshop/ seminar	Number of Participants	Date From - To
2021-22	International e-Conference on Proteomics Application To Biomedical Research-2022 (PABR-2022)	147	10/04/2022 To 11/04/2022
2021-22	International e-Conference on Recent Trend in Nano-Materials and Its Applications-2023 (RTNA-2022)	167	22/04/2022 To 23/04/2023
2021-22	International conference on Nurture the Nature To Strengthen the Future	87	
2021-22	Food processing and fruit preservation	49	17/02/2022
2021-22	Workshop on stress management and stress removal	136	22/02/2022
2021-22	Workshop on STSSP teaching and learning application	72	20/01/2022
2021-22	Workshop on IPR	156	30/05/2022

**Dr. S.S. Dhasade**  
Coordinator, IQAC  
Vidnyan Mahavidyalaya, Sangola

**Acting Principal**  
Vidnyan Mahavidyalaya, Sangola  
Tal. Sangola Dist. Solapur



**3.2.2 - Number of workshops/seminars conducted  
on Research Methodology, Intellectual  
Property Rights (IPR) and entrepreneurship  
during the year-2021-22**

**Documents**

**3.2.2 PABR-2022 chemistry**

## " विज्ञान महाविद्यालयामध्ये रसायनशास्त्र विभागाचे आंतरराष्ट्रीय चर्चासत्र संपन्न "

विज्ञान महाविद्यालय सांगोला येथे रसायनशास्त्र विभाग व I.Q.A.C यांच्या संयुक्त विद्यमाने " Proteomics Application to BioMedical Research 2022 " ( PABR -2022 ) या विषयावरील दोन दिवसीय आंतरराष्ट्रीय चर्चासत्र संपन्न झाले.

सदर चर्चासत्राच्या उदघाटन सोहळ्यास प्रमुख पाहुणे म्हणून Dr.G.B.Zore ( Raman Fellow ) School of Life Science S.R.T.M.U. Nanded हे उपस्थित होते. तर चर्चासत्राच्या पहिल्या दिवशी प्रमुख वक्ते म्हणून डॉ. बालाजी रोकडे, वरिष्ठ वैज्ञानिक EliLilli, Kinsale, Ireland तसेच डॉ. डी. के. सोनवणे, विभागप्रमुख, रसायनशास्त्र विभाग, शिवाजी विद्यापीठ, कोल्हापूर हे लाभले होते.

कार्यक्रमाच्या उदघाटन प्रसंगीच्या प्रमुख भाषणामध्ये प्रा. जी. बी. झोरे यांनी Proteomics या विज्ञानाच्या शाखेचे मानवी जीवनामध्ये असलेले महत्त्व स्पष्ट केले. तसेच या क्षेत्रामध्ये संशोधनासाठी उपलब्ध असणा-या विविध संधीची माहिती चर्चासत्रामध्ये सहभागी झालेल्या संशोधकांना व विद्यार्थ्यांना दिली.

कार्यक्रमातील पुढील सत्रामध्ये डॉ. डी. के. सोनवणे, विभागप्रमुख, रसायनशास्त्र विभाग, शिवाजी विद्यापीठ, कोल्हापूर हे प्रमुख वक्ते म्हणून लाभले होते तर या सत्राचे अध्यक्ष म्हणून प्रा. एस. बी. पटवारी, विभागप्रमुख, रसायनशास्त्र विभाग, एल.बी.एस. कॉलेज, धर्माबाद, जि. नांदेड हे लाभले होते. डॉ. डी. के. सोनवणे यांनी Proteomics या विषयावरील त्यांनी केलेले संशोधन कार्य विशद केले. सदरील दिवसाच्या तिस-या सत्रामध्ये डॉ. बालाजी रोकडे, वरिष्ठ शास्त्रज्ञ Eli Lilli, Ireland ) हे प्रमुख वक्ते म्हणून लाभले होते व या सत्राचे अध्यक्ष म्हणून प्रा. एस. एच. गायकवाड ( B.O.S. Chairman) पुण्यश्लोक अहिल्यादेवी होळकर सोलापूर विद्यापीठ, सोलापूर हे उपस्थित होते.

डॉ. बालाजी रोकडे यांनी " Asymmetric Synthesis " या विषयावरील त्यांचे संशोधन कार्य विस्तारीतपणे उपस्थितांना सांगितले. संशोधन कार्य करित असताना त्या विषयातील सखोल अभ्यासाची संशोधनास जोड देणे कसे आवश्यक आहे हे उदाहरणे देऊन उपस्थितांना सांगितले. सत्राची सांगता संशोधकांशी चर्चा करून तसेच संशोधकांनी केलेल्या पोस्टर प्रेझेंटेशनच्या सादरीकरणाने झाली.

दुस-या दिवसाच्या पहिल्या सत्रासाठी प्रमुख वक्ते म्हणून डॉ. अतुल देशमुख, ज्येष्ठ शास्त्रज्ञ, कोपनहेगन विद्यापीठ, डेन्मार्क हे उपस्थित होते. त्यांनी कोपनहेगन विद्यापीठामध्ये चालू असलेल्या अद्यावत संशोधन कार्याची माहिती उपस्थित संशोधकांनी दिली. संशोधकांनी संशोधन क्षेत्रातील कार्य करित असताना येणा-या अडचणींवरती प्रश्न विचारले. तसेच डॉ. अतुल देशमुख यांनी सकारात्मक उत्तरे देऊन संशोधकांचे समाधान केले.

कार्यक्रमातील दुस-या सत्रामध्ये Dr. Diana Samodova, Scientist, University Of Copenhagan, Denmark हया उपलब्ध होत्या. त्यांनी Proteomics संशोधित केलेल्या त्यांच्या संशोधनावबदल सखोल माहिती दिली. तसेच या संशोधनामुळे मानवी जीवनामध्ये वैद्यकीय क्षेत्रात होऊ शकत असणा-या सुविधांचे महत्त्व विशद केले.

कार्यक्रमाची सांगता डॉ. शंकर धसाडे, को-ऑर्डिनेटर, I.Q.A.C यांनी आभार प्रदर्शनांनी केली.



Sangola Taluka Shetkari Shikshan Prasarak Mandal Sangola's

**Vidnyan Mahavidyalaya, Sangola.**

Tal-Sangola, Dist-Solapur, MH-413307, India.



(Affiliated to Punyashlok Ahilyadevi Holkar Solapur University, Solapur.)

**Department of Chemistry in Collaboration with Internal Quality Assurance Cell (IQAC)**

organizes

**International e-Conference on Proteomics Application to Biomedical Research-2022(PABR-2022)**

(dated April 10-11, 2022)

**Resource Persons**



**Dr. Atul Deshmukh**  
University of Copenhagen,  
Denmark

**Dr. Diana Samodova**  
University of Copenhagen,  
Denmark

**Dr. Balaji Rokade**  
Senior Scientist  
Eli Lilly Kinsale Ireland

**Dr. K. D. Sonwane**  
Shivaji University,  
Kolhapur

**Chief Patron**

**Mr. Ramchandra Khatkale**  
President, STSSPM

**Mr. Chandrakant Deshmukh**  
Director, STSSPM

**Dr. Aniket Deshmukh**  
Director, STSSPM

**Mr. Vitthalrao Shinde**  
Secretary, STSSPM

**Organizing Committee**

**Dr. R. A. Fule**  
Acting Principal

**Mr. R. S. Gaikwad**  
Convener

**Dr. S. S. Dhasade**  
Coordinator IQAC

**Dr. S. N. Kadam**  
Organizing Secretary

**Mr. N. P. Adlinge**  
Treasurer

**Dr. S. R. Shinde**  
Member

**Dr. R. B. Bhosale**  
Member  
(PAH University Solpur )

**Dr. J. V. Thombare**  
Member

**Mr. A. R. Ingawale**  
Member

**Dr. B. S. Dawane**  
Member  
(S.R.T. M. University Nanded)

**Dr. S. B. Patwari**  
Member  
(S.R.T. M. University Nanded)

**Dr. V. P. Ubale**  
Member

**About Registration & Conference proceeding**

E-Certificate to be provided to those who will register, attend and fill the feedback form.

**Last date of registration:** 09 April, 2022.

**Registration Link:**

<https://forms.gle/aUghRAaZMgnfrY7i6>

Email: pabr2022@gmail.com

Conference Date: April 10-11, 2022

Paper Publication

Research papers will be published in

•UGC Approved Journal Number 64011

•International Peer reviewed Thomson

Reuters, Open access Scientific Journal

•Online ISSN: 2395-602X

•Print ISSN: 2395-6011

•DOI: 10.32628, Index Copernicus :49.58

•Individual certificate to soft copy to all authors

Soft copy of CD cover and proceeding of the conference if needed.

Contact No.: **9028548942**, 9766234273, 9970448413

Registration Fees submission details: The registration fees along with paper publication charges may be paid online/ Paytm/ Phone pay / Internet Banking to

Account Name: Vidnyan Mahavidyalaya, Sangola

Bank Name: Bank of Maharashtra

Branch: Sangola, Account Number: 60101820852

IFSC: MAHB0001467; MICR Code: 413014079

Fees details:

Category	Registration fee	Paper Publication charges
Students	Rs. 100/-	Rs. 700/-
Academics	Rs. 200/-	Rs. 700/-
Industry	Rs. 1000/-	Rs. 700/-
Foreign Delegates	USD 20	USD 50

Submission of Papers: Interested authors are requested to submit full-length manuscript of research paper in MS-Word 2007 or MS-Word 2010 including Paper Title, Names of all the authors and e-mail address of corresponding authors. The font should be Times New Roman, Size-12. The maximum length of manuscripts is limited to four pages. Paper sent by e-mail to conference E-mail address: pabr2022@gmail.com.





Sangola Taluka Shetkari Shikshan Prasarak Mandal Sangola's

## Vidnyan Mahavidyalaya, Sangola

Tal-Sangola, Dist-Solapur, MH- 413307, India.  
(Affiliated to Punyashlok Ahilyadevi Holkar Solapur  
University, Solapur)



Department of Chemistry in collaboration with Internal Quality Assurance Cell (IQAC) organizes an  
**International e-Conference on Proteomics Application to  
Biomedical Research-2022 (PABR-2022)** Dated on April 10-11, 2022  
Conference E-mail: pabr2022@gmail.com

-:Program Schedule:-

**Day 1<sup>st</sup>: Sunday**

**Date: April 10, 2022**

**Session-I: Inauguration of Conference;**

**Ses. Coordinator: Dr. J. V. Thombare**

Sr. No.	Time in IST*	Description/Name of Program	Name
01	12:50 pm to 12:55 pm	Introduction and Welcome	Mr. R S Gaikwad <b>Convener</b>
02	12:55 pm to 01.00 pm	Introduction to chief Guest	Dr. S. S. Dhasade <b>Coordinator IQAC</b>
03	01:00 pm to 01:40 pm	Keynote Address	<b>Resource Person:</b> Prof. G. B. Zore School of chemical science, Swami Ramanand Teerth Marathwada University, Nanded
04	01:40 pm to 01:45 pm	Presidential Address	Dr. R. A. Fule Acting Principal, V. M. Sangola
05	01:45 pm to 01:50 pm	Vote of thanks	Mr. A. R. Ingawale,
<b>Session-II: Invited Talk; Session Coordinator: Dr. S. N. Kadam</b>			
06	02:00 pm to 02:50 pm	<b>Resource Person:</b> Prof. D K Sonwane Head, Dept. Of Chemistry Shivaji University, Kolhapur	<b>Chairperson:</b> Prof. S. B. Patwari Head, Dept. Of Chemistry LBS college, Dhramabad
07	02:50 pm to 02:55 pm	Discussion and vote of Thanks	
08	02:55 am to 03:00 pm	Short break	

\*IST-Indian Standard Time (Time is mentioned in IST)

**Session-III: Invited Talk; Session Coordinator: Mr. R. S. Gaikwad**

09	03:00 pm to 3.45pm	<b>Resource Person:</b> <b>Dr. Balaji Rokade</b> Researcher Eli Lillya Kinsale, Ireland	<b>Chairperson:</b> <b>Prof. S. H. Gaikwad</b> BOS, Chairman Punyashlok Ahilyadevi Holkar University, Solapur
10	3.45pm to 3.50pm	Discussion	
	3.50 pm to 4.00 pm	Short break	
<b>Session-IV: Oral Presentations; Session Coordinator: Mr. A. R. Ingawale</b>			
11	4.00 pm to 4.10 pm	OP-01	<b>Chairperson:</b> <b>Dr. Lalasaheb Kashid</b> Vidyaprathisthan Arts, Science and commerce college, Baramati
	4.10 pm to 4.20pm	OP-02	

**Day 2<sup>nd</sup>: Monday**

**Date: April 11, 2022**

**Session-V: Invited Talk;**

**session coordinator: Dr. J. V. Thombare**

12	01:30 pm to 02:15 pm	<b>Resource Person:</b> <b>Dr. Atul Deshmukh</b> Scientist, University of Copenhagen, Denmark	<b>Chairperson:</b> <b>Dr. Deokar S. S.</b> Head, Department of chemistry Shankarrao Mohite Mahavidyalay Akluj
	02:15 pm to 02:30 pm	Discussion and vote of thanks	

**Session-VI: Invited Talk; Session Coordinator: Dr. Shital R. shinde**

13	2.30pm to 3.00pm	<b>Resource Person:</b> <b>Dr. Diana Samodova</b> Scientist, University of Copenhagen, Denmark	<b>Chairperson:</b> <b>Dr. Bachute Madhusudan</b> Principal Sangola College Sangola
----	------------------	--	--

\*IST-Indian Standard Time (Time is mentioned in IST)

14	3.00pm to 3.15 pm	Discussion and vote of thanks	
<b>Session-VII: Valedictory Function Session Coordinator: Mr. N P Adlinge</b>			
15	03:20 pm to 03:25 pm	Conference Overview	<b>Mr. R S Gaikwad</b> Convener
16	03:25 pm to 03:35 pm	Feedback from Participants	--
17	03:35 pm to 03:55 pm	Valedictory address	<b>Dr. Bachute Madhusudan</b> Principal Sangola College Sangola
18	03:55 pm to 4:00 pm	Presidential remark	<b>Prof. V. P. Ubale</b> Principal DBF Dayanand college, Solapur
19	04:00 pm to 04:05 noon	Vote of Thanks	<b>Dr Shankar S Dhasade</b> Coordinator IQAC

\*IST-Indian Standard Time (Time is mentioned in IST)



Sangola Taluka Shetkari Shikshan Prasarak Mandal Sangola's  
**Vidnyan Mahavidyalaya, Sangola.**

Tal-Sangola. Dist-Solapur. MH-413307, India.  
Affiliated to Purnyashlok Abhilyadevi Holkar Solapur  
University, Solapur.



## Certificate

This is to certify that Prof./Dr./Mr./Ms.: **KARANDE SHIVAJI SAMRATA** (Paper presenter)  
of **Vidnyan mahavidyalaya sangola**

has participated at **International e-Conference on Proteomics Application to  
Biomedical Research-2022 (PABR-2022)**, organized by Department of Chemistry in  
collaboration with Internal Quality Assurance Cell (IQAC), Vidnyan Mahavidyalaya, Sangola.

Date: April 10-11, 2022.

**Mr. R. S. Gaikwad**  
Convener,  
PABR-2022

**Dr. S. S. Dhasade**  
Coordinator,  
IQAC

Online ISSN : 2395-602X

Print ISSN : 2395-6011

www.ijsrst.com



## **International e-conference on Proteomics Application to Biomedical Research (PABR-2022)**

Organized By  
Department of Chemistry,  
Sangola Taluka Shetkari Shikshan Prasarak  
Mandal Sangola's, Vidnyan Mahavidyalaya, Sangola  
Tal-Sangola, Dist-Solapur, MH-413307, India  
Collaboration with  
Internal Quality Assurance Cell (IQAC)

**VOLUME 9, ISSUE 12, MARCH-APRIL-2022**

# **INTERNATIONAL JOURNAL OF SCIENTIFIC RESEARCH IN SCIENCE AND TECHNOLOGY**

Email : [editor@ijsrst.com](mailto:editor@ijsrst.com) Website : <http://ijsrst.com>



## **International e-conference on Proteomics Application to Biomedical Research (PABR-2022)**

**10th and 11th April, 2022**

Organised by

Department of Chemistry in Collaboration with Internal Quality  
Assurance Cell (IQAC)

Sangola Taluka Shetkari Shikshan Prasarak Mandal Sangola's  
Vidnyan Mahavidyalaya, Sangola

Tal-Sangola, Dist-Solapur, MH-413307, India

Affiliated to Punyashlok Ahilyadevi Holkar Solapur University,  
Solapur, Maharashtra, India

In Association with

International Journal of Scientific Research in Science and Technology

Print ISSN: 2395-6011 Online ISSN : 2395-602X

Volume 9, Issue 12, March-April-2022

International Peer Reviewed, Open Access Journal

Published By

Technoscience Academy



(The International Open Access Publisher)

website: [www.technoscienceacademy.com](http://www.technoscienceacademy.com)

## Resource Persons



**Dr. Atul Deshmukh**  
University of Copenhagen,  
Denmark



**Dr. Diana Samodova**  
University of Copenhagen,  
Denmark



**Dr. Balaji Rokade**  
Researcher Eli Lillya Kinsale  
Ltd. Ireland



**Dr. D K Sonwane**  
Shivaji University,  
Kolhapur

## Chief Patron

**Mr. Ramchandra  
Khatkale**  
President, STSSPM

**Mr. Chandrakant  
Deshmukh**  
Director, STSSPM

**Dr. Aniket  
Deshmukh**  
Director, STSSPM

**Mr. Vitthalrao  
Shinde**  
Secretary, STSSPM

## Organizing Committee

**Mr. Ramchandra  
Khatkale**  
President, STSSPM

**Mr. Chandrakant  
Deshmukh**  
Director, STSSPM

**Dr. Aniket  
Deshmukh**  
Director, STSSPM

**Mr. Vitthalrao  
Shinde**  
Secretary, STSSPM

### Organizing Committee

**Dr. R. A. Fule**  
Acting Principal

**Mr. R. S Gaikwad**  
Convener

**Dr. S. S. Dhasade**  
Coordinator IQAC

**Dr. S. N. Kadam**  
Organizing Secretary

**Mr. N. P. Adlinge**  
Treasurer

**Dr. S. R. Shinde**  
Member

**Mr. S. S. Karande**  
Member

**Dr. J. V. Thombare**  
Member

**Mr. A. R. Ingawale**  
Member

**Dr. B. S. Dawane**  
Member

**Dr. S. B. Patwari**  
Member

**Dr. V. P. Ubale**  
Member

## About US

The Institution, Sangola Taluka Shetkari Shikshan Prasarak Mandal Sangola, was established in 23-Sep-1991, with the aim of giving availability and facility of education to socially backward society, to Bahun society including Harijan, Girijan, farmers, labours and socially deprived from progress in the region of sangola taluka since its establishment, the sansthas has started highschool department, professional courses of +2 section and vidnyan mahavidyalay, etc. vidnyan mahavidyalay was established 23rd september 1991. There is the facility of B.C.S, B.C.A (degree courses), Bsc(comp) & Msc education in the college. The college has started M.A (english) course from the year 2004 & Msc (comp science) from 2009 from 2012 since its establishment the college has been progressing ahead and has now become an important academic center in the region of sangola taluka the college is accredited by NAAC with Grade "B" in the year 2004 Along with an intellectual & all round development of students, to develop their academic carrier, there are various departments under Arts & Science College faculties During the last year the no. of students in this college were 1600. The big building of the college, with its large play ground, is near by S.T stand.

## CONTENTS

Sr. No	Article/Paper	Page No
2	<b>Synthesis, Characterization of Cr<sup>+3</sup>, Mn<sup>+2</sup> Metal Ion Chelates with Newly Synthesized Benzothiazolyl Hydrazone Derivatives</b> Bhagat S. M	11-18
3	<b>An Efficient One Pot Synthesis of Polyhydroquinolines Using TS1 Catalyst Under Solvent Free Conditions</b> S.K. Ghumbre, A. S. Renge	19-21
4	<b>One Pot Three Component Eco-Friendly Synthesis of Quinoline-3-Carbonitrile Derivatives</b> Kadam S. N, Ambhore Ajay, Shringare S. N., Shinde S. R., Gaikwad R. S., Adlinge N. P., Ingawale A. R.	22-27
5	<b>Highly Proficient Extractive Studies on The Behaviour of Neodymium (III) Assisted By 2-Octylaminopyridine from Weak Succinate Media</b> Gurupad D. Kore, Sunil B. Zanje, Mansing A. Anuse, Sanjay S. Kolekar	28-37
6	<b>Ammonium Chloride in PEG As an Efficient Catalyst for Synthesis Dihydropyrano [3,2-C] Chromene-3-Carbonitrile Derivatives</b> Manojkumar R. Tapare, Rahul Kamble	38-45
7	<b>Synthesis of Spiro-fused Heterocycles under Aerobic Conditions by using Polymer Gel Entrapped Catalyst</b> Shinde S. R, Gaikwad R. S, Adlinge N. P, Ingawale A. R, Kadam S. N, Rajashri Salunkhe	46-51
8	<b>DBU Catalyzed One Pot Four-Component Synthesis of Pyrano Pyrazole Derivatives with their Antioxidant Activity</b> Ashok R. Karad, Navanand B. Wadwale, Gopinath S. Khansole, Sunil.S.Choudhare, Swapnil V. Navate Vijay N. Bhosale	52-60



## Synthesis, Characterization of Cr<sup>+3</sup>, Mn<sup>+2</sup> Metal Ion Chelates with Newly Synthesized Benzothiazolyl Hydrazone Derivatives

Bhagat S.M<sup>1</sup>

<sup>1</sup>Department of Chemistry, I.C.S. College of Art's, Comm. And Science, Khed, Dist.- Ratnagiri, Maharashtra, India

### ABSTRACT

The transition Metal ion chelates of Cr<sup>+3</sup>, Mn<sup>+2</sup> is synthesized by using 2-(4'-dimethylamion phenyl)-4-bromo-6-ethoxy benzothiazolyl hydrazones and characterized by different analytical procedure and spectral study. These metal ion chelates are insoluble in common organic solvents. Infrared spectrum showed the bonding through azomethizine N and ring N.

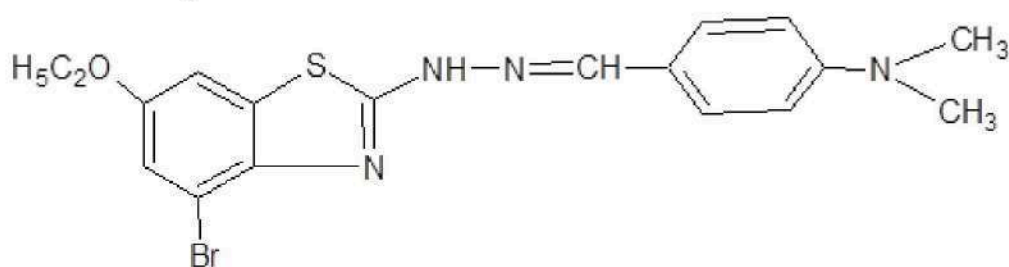
**Keywords:** - benzothiazolyl hydrazones, Metal ion chelates.

### I. INTRODUCTION

Chemistry of ligand:- The coordination chemistry of hydrazones is an intensive area of study and numerous metal complexes of these ligand have been investigated<sup>1</sup>. The development of the field of bioinorganic chemistry has increased the interest in Schiff base complexes, since it has been recognized that many of these complexes may serve as models for biologically important species<sup>2-4</sup>. The hydrazones metal complexes have found application in various process like sensor, medicine, nonlinear optics etc. they are well known for their metal binding ability and exhibit interesting coordinating behavior with transition metal ion<sup>5,6</sup>. Coordination compound derived from aryl hydrazones have been reported because of their anti-tuberculosis, antimicrobial and corrosion inhibitor<sup>7-9</sup>. Hydrazones have been drawing much attention from coordination chemistry to transition metal<sup>10</sup>. In the context of the above application we have tried to the synthesis and characterization of transition metal complexes of 2-(4'-dimethyl amino phenyl)-4-bromo-6-ethoxy benzothiazolyl hydrazones. Prepared complexes were dried and the physical and chemical properties were recorded. analysis of the complexes and different spectral studies like I.R. , Electronic spectra of the complex were used for find out the donor site of the ligand.

## II. SYNTHESIS OF LIGAND

Preparation of 2-(4'-dimethylamion phenyl)-4-bromo-6-ethoxy benzothiazolyl hydrazones from 4-bromo-6-ethoxy benzothiazolyl hydrazones. To the ethanolic solution of 4-bromo-6-ethoxy benzothiazol was added in ethanolic solution of 4-dimethylaminobenzaldehyde. The mixture was refluxed on water bath for two hours. Obtained solid is cooled filtered, washed with ethanol and recrystallized from hot benzene  
Structure of ligand.



2-(4'-dimethylamion phenyl)-4-bromo-6-ethoxy benzothiazolyl hydrazones

Physical parameter-

## III. SYNTHESIS OF COMPLEXES.

i) Synthesis of Bis 2-(4'-dimethylamion phenyl)-4-bromo-6-ethoxy benzothiazolyl hydrazones Cr <sup>III</sup> chloride complex

100 ml 0.1 M CrCl<sub>3</sub>.6H<sub>2</sub>O were prepared in alcohol and 2-(4'-dimethylamion phenyl)-4-bromo-6-ethoxy benzothiazolyl hydrazones, 0.2 M solution were prepared in ethyl alcohol. These two solutions were mixed and transfer into 500 ml round bottom flask attached water condenser, 6.5 pH is of the reaction mixture were adjusted by adding basic buffer solution pH-10. Reaction mixture were fefluxed for one hour in water bath. The precipitate was obtained . it is digested, after cooling it is filtered through buckner funnel , the precipitate of complex were furified by washing with ethyl alcohol, the complex were dried by keeping it in oven. The product was packed into sample bottle.

ii) Synthesis of Bis 2-(4'-dimethylamion phenyl)-4-bromo-6-ethoxy benzothiazolyl hydrazones Mn II chloride complex

100 ml 0.1M alcoholic solution of MnCl<sub>2</sub>.4H<sub>2</sub>O were treated with 100 ml of alcoholic ,0.2 M 2-(4'-dimethylamion phenyl)-4-bromo-6-ethoxy benzothiazolyl hydrazones in 500 ml flask. The Ph of reaction mixture were kept 6-8 by adding alcoholic solution of basic buffer solution drop by drop. The precipitate was further digested and cooled and the precipitate was filtered through Buckner funnel, the precipitate was washed with alcohol and dried it by keeping in oven.

#### IV. PHYSICAL PARAMETER AND ELEMENTAL ANALYSIS

Decomposition point was determined with the help of melting point apparatus by open capillary method. M:L ratio was determined by heating known weight of complex in platinum crucible. Metal ion percentage in a complex is determined by E.D.T.A. titration method. Chloride is estimated by Mohr's method.

Physical parameter and analytical data of the Cr(III), Mn(II), complexes and ligand 2-(4'-dimethylamion phenyl)-4-bromo-6-ethoxy benzothiazolyl hydrazones (MAPBEBTH). Are given in table no. 5.1. metal ligand ratio and empirical formula were assigned on the basis of T.G.A. measurement and elemental analysis is given in table no.5.2.

#### V. CHARACTERIZATION OF COMPLEXES

U.V. and visible spectra of complexes and ligand recorded on U.V. SHIMADZU UV3600 spectrophotometer at range 200-800 nm by using D.M.S.O. solvent at P.G. department of chemistry Shivaji University Kolhapur. I.R. spectra of ligand were recorded at Yeshwant Mahavidyala Nanded and I.R. spectra of complexes are recorded at PERKIN ELMER spectrum-100/79720 by KBr platelet method at Shivaji University Kolhapur. Thermo gravimetric analysis (T.G./D.T.A.) measurement are recorded on thermo gravimetric analyzer on TA model S.T.D-2960 at Shivaji University Kolhapur in Nitrogen atmosphere. XRD pattern of the complexes recorded on PW-3719/1710 Philips -Holland spectrometer at Shivaji University Kolhapur and E.S.R. is recorded at IIT, pawai, Mumbai.

#### VI. RESULT AND DISCUSSION

The complexes of Cr(III), Mn(II). are prepared with the ligand 2-(4'-dimethylamion phenyl)-4-bromo-6-ethoxy benzothiazolyl hydrazones (MAPBEBTH). This complexes are coloured. These complexes are soluble in D.M.S.O. but insoluble in water, alcohol, chloroform, and D.M.F. Decomposition point of complexes are in the range of 240-300°C. It suggest that they have good thermal stability at room temperature

Table.5.1: physical property of (MAPBEBTH) metal complexes.

Complex	color	D.P.	Yield%	%Cl
[Cr (MAPBEBTH) <sub>2</sub> Cl <sub>2</sub> ] <sub>2</sub> H <sub>2</sub> O Cl	Light blue	272-276	70	10.492
[Mn (MAPBEBTH) <sub>2</sub> (H <sub>2</sub> O) <sub>2</sub> ] Cl <sub>2</sub> .	Creamy	270-278	63	7.097

Table.2.2: Percent C,H,N and metal ion in HMPBMBTH metal *complex*

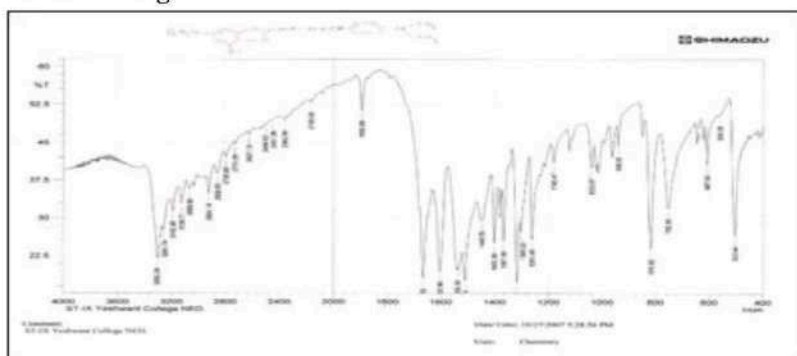
compond	M.wt	Empirical formula	%C	%H	%N	%M
MAPBEBTH	419.20	C <sub>18</sub> H <sub>19</sub> N <sub>4</sub> BrSO	51.576	4.532	13.365	-
[Cr (MAPBEBTH) <sub>2</sub> Cl <sub>2</sub> ] <sub>2</sub> H <sub>2</sub> O Cl	1015	C <sub>36</sub> H <sub>40</sub> Cl <sub>3</sub> CrN <sub>8</sub> S <sub>2</sub> Br <sub>2</sub> O <sub>3</sub>	42.602	3.940	11.034	5.124
[Mn (MAPBEBTH) <sub>2</sub> (H <sub>2</sub> O) <sub>2</sub> ] Cl <sub>2</sub>	1000.3	C <sub>36</sub> H <sub>42</sub> Cl <sub>2</sub> MnN <sub>8</sub> S <sub>2</sub> Br <sub>2</sub> O <sub>4</sub>	43.228	4.198	11.196	5.488

## U.V.

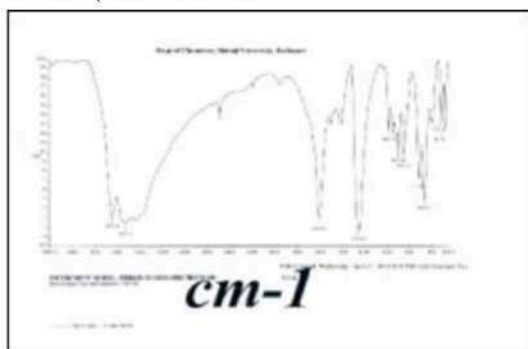
U.V. and visible spectra of complexes and ligand recorded on U.V. SHIMADZU UV3600 spectrophotometer at range 200-800 nm by using D.M.S.O. solvent at P.G. department of chemistry Shivaji University Kolhapur. The ligand 2-(4'-dimethylamion phenyl)-4-bromo-6-ethoxy benzothiazolyl hydrazones has exhibited one characteristic maxima in U.V. region at 246 nm where in  $[\text{Cr}(\text{MAPBEBTH})_2\text{Cl}_2]\text{H}_2\text{O}$  Cl complex it is shifted at 258 nm and in complex  $[\text{Mn}(\text{MAPBEBTH})_2(\text{H}_2\text{O})_2]\text{Cl}_2$ . Band is observed at 266 nm this shifting of band is due the complex formation.

## I.R. spectra-

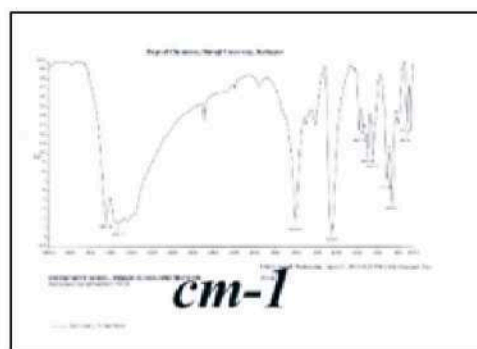
A sharp strong band is observed in I.R. spectra of ligand at 1665 in ligand it is due to the C=N of thiazole ring nitrogen. This band is shifted in  $\text{Cr}^{+3}$  complex as well as in  $\text{Mn}^{+2}$  complex. In  $\text{Cr}^{+3}$  complex it is observed at 1645 and in  $\text{Mn}^{+2}$  complex it is observed at 1606 this shifting of band in both complexes it indicate that the Nitrogen of thiazole ring is involve in the complex formation. Another band is observed at 1602 in ligand. This band is support to the presence of C=N (azomethazine) group in ligand. This band is shifted in  $\text{Cr}^{+3}$  and  $\text{Mn}^{+2}$  complexes. The band is observed in  $\text{Cr}^{+3}$  complex at 1590 where in  $\text{Mn}^{+2}$  complex it is observed at 1510. This shifting of band indicate that the azomethazine nitrogen involve in the complex formation. One band is observed at 3302 in ligand it may be due to the presence of N-H group. This band is not observed in  $\text{Cr}^{+3}$  and  $\text{Mn}^{+2}$  complexes it is evidence that the N-H group is involve in the complex formation. One more band is observed at 481 where as in  $\text{Mn}^{+2}$  complex it is observed at 468 but not in ligand it indicate that there is a formation of M-L bond. Thus the ligand act as a bidentate. It coordinate through azomethazine, Nitrogen of thiazole ring.



I.R. of (MAPBEBTH)



I.R. of  $[\text{Cr}(\text{MAPBEBTH})_2\text{Cl}_2]\text{H}_2\text{O}$  Cl



I.R. of  $[\text{Mn}(\text{MAPBEBTH})_2(\text{H}_2\text{O})_2]\text{Cl}_2$ .

### Thermal analysis:-

Results of TG analysis were used to determine the nature of water molecules present and decomposition pattern of the complexes. Lattice water molecules were lost in the 70-110 °C temperature range while coordinate water molecules were eliminated at relatively high temperature range of 150-240 °C. complete decomposition of ligand occur at about 800 °C and observed residue corresponds to respective metaloxide. Present losses of material as obtained from TGA curve are good agreement with calculated percent loss in mass. Thermo gravimetric results coincide well with DTA peaks. TGA/DTA scans are depicted in fig.

#### TGA/DTA of [Cr (MAPBEBTH)<sub>2</sub>Cl<sub>2</sub>] H<sub>2</sub>O Cl

TGA/DTA plot of [Cr (MAPBEBTH)<sub>2</sub>Cl<sub>2</sub>] H<sub>2</sub>O Cl shows five peak of decomposition. The first peak is observed at the temperature range 50-130°C and 9.023% loss of mass is observed . This loss of mass is due to the elimination of lattice chloride and water molecule from the compound. In second peak 18.047% loss is observed in the temperature range 130-280°C. The loss of mass is due to the elimination of two molecule of N(CH<sub>3</sub>) and ethoxy group form the complex. Third peak is observed in the temperature range 280-430°C and 15.411% mass is lost . This loss in mass is due to the elimination of two benzene ring from the molecule. In the fourth peak 31.228% mass is lost in the temperature range 430-570°C. The loss of mass is due to the elimination of two bromobenzene rings from the complex. Last peak is observed in the temperature range 570-760°C . In this peak 20.277% mass is lost. This loss in weight is due to the elimination of thiazole ring part and its substituent chain NH-N=CH. From the temperature 760°C curve of graph show constant value. It indicate that remaining mass is of metal oxide. Calculated value are coincide with observed value.

#### TGA/DTA [Mn (MAPBEBTH)<sub>2</sub> (H<sub>2</sub>O)<sub>2</sub>] Cl<sub>2</sub> complex

TGA/DTA plot of [Mn (MAPBEBTH)<sub>2</sub> (H<sub>2</sub>O)<sub>2</sub>] Cl<sub>2</sub> Complex Shows five peaks of decomposition. First peak is observed at temperature range 50-110°C and 6.208% mass is lost. This loss in mass is due to the elimination of lattice chloride from the complex. In second peak 9.356% mass is lost in the temperature range 110-260°C. This loss in weight is due to the burning of coordinate chloride and water molecule. Observed values are in good agreement with calculated values. Third peak is observed at the temperature range 260-490°C . In this temperature range 15.564% weight is lost form the complex compound . this loss of mass is due to the elimination of N(CH<sub>3</sub>)<sub>2</sub> and OC<sub>2</sub>H<sub>5</sub> group from complex. Fourth peak is observed at temperature range 490-620°C and 40.622% weight is lost. This loss in weight is due to the elimination of bromobenzen ring. In last fifth peak 17.488% mass is lost in the temperature range 620-770°C this loss in mass is due to the elimination of thiazole ring part and its substituent chain NH-N=CH. Form the temperature range 770°C curve of the graph show constant value of weight of complex it indicate that remaining mass is of metal oxide. Observed figures and calculated figures are approximately equal.

Temp. range °C	% loss	Nature of decomposition
50-130	9.023(9.087)	Lattice chloride & water molecule
130-280	18.047(18.022)	N(CH <sub>3</sub> ) <sub>2</sub> & OC <sub>2</sub> H <sub>5</sub>

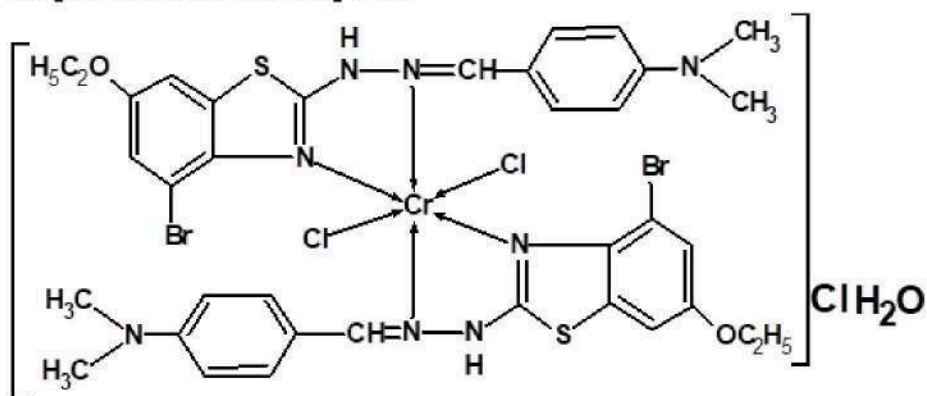
280-430	15.411(15.241)	Two benzene ring
430-570	31.228(31.385)	Two bromo Benzene ring
5570-760	20.277 (20.262)	Thiazole ring part and substituted chain.

Thermal decomposition value of  $[\text{Cr}(\text{MAPBEBTH})_2\text{Cl}_2]\text{H}_2\text{O Cl}$  complex

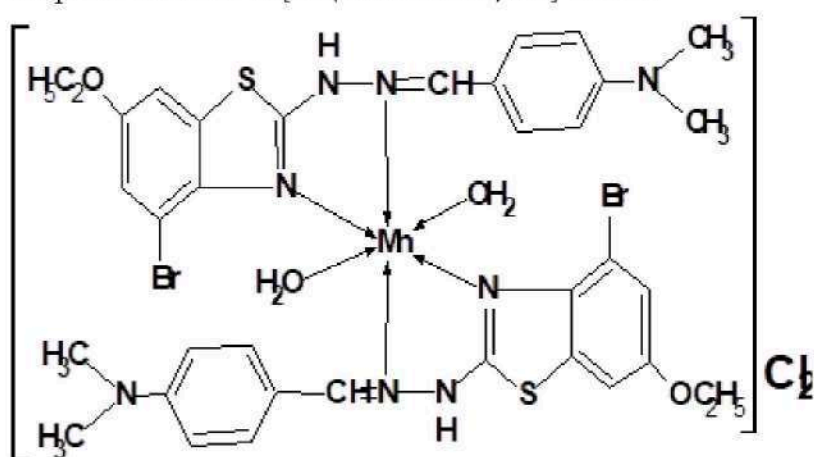
Temp. range °C	% loss	Nature of decomposition
50-130	9.023(9.087)	Lattice chloride & water molecule
130-280	18.047(18.022)	$\text{N}(\text{CH}_3)_2$ & $\text{OC}_2\text{H}_5$
280-430	15.411(15.241)	Two benzene ring
430-570	31.228(31.385)	Two bromo Benzene ring
5570-760	20.277 (20.262)	Thiazole ring part and substituted chain.

Thermal decomposition value of  $[\text{Mn}(\text{MAPBEBTH})_2(\text{H}_2\text{O})_2]\text{Cl}_2$  metal

Proposed structure of complexes

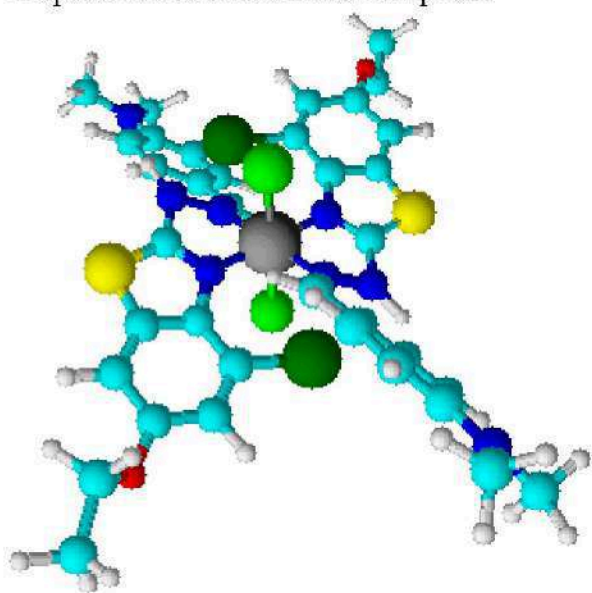
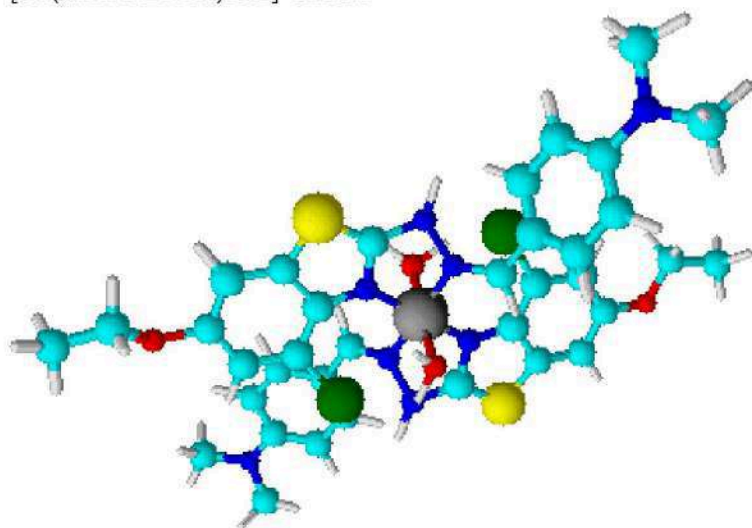


Proposed structure of  $[\text{Cr}(\text{MAPBEBTH})_2\text{Cl}_2]\text{Cl H}_2\text{O}$



Proposed structure of  $[\text{Mn}(\text{MAPBEBTH})_2(\text{H}_2\text{O})_2]\text{Cl}_2\text{H}_2\text{O}$

## Proposed 3D structure metal complexes

 $[Cr(MAPBEBTH)_2Cl_2] Cl H_2O$  $[Mn(MAPBEBTH)_2(H_2O)_2] Cl_2H_2O$ 

## VII. REFERENCES

- [1]. Sondhi S.M., M.Dinodia. and A. Kumar., Bioorg.Med.Chem.,2006, 14,4657.
- [2]. C. Jayabalkrishnan and K. Natarajan., Rect.Inorg. Met- Org.Chem.,2001.,31,980.
- [3]. Dharmaraj N.P.,Viswanathmurthi and K. Natarajan., 2001.,Trans.met.Chem., 26, 105.
- [4]. Jeeworth T., H.L.K. Waall, M.G.Bhowon,D. Ghoorhoo and K. Babooram., Rect.Inorg.Met-org.Chem.,2000, 30,1063.
- [5]. Gudasi K.B., R.V.Shenoy, R.S. Vadavi, A.S. Patil and M.Nethaji., J. Mol.struct.,2006,788(1-3),22-29.
- [6]. Kuriakose M., M.R. Prathapachandra Kurup and E. Suresh., Polyhedron,2007,26(2),2713-2718.

- [7]. A.S. Fouda, G.E. Badr and M.N. El-Haddad., J. Korean Chem. Soc.,2008,2,124.
- [8]. M.A. Ali., M.H. Kabir, M.Nazimuddin, S.M.H. Majumder, M.T.H. Tarafder and M.A.Khair., Indian J. Chem., 1988., 27A., 1064.
- [9]. Feerari M.B.,S. Capacchi, G. Pelosi, G. Refto, P. Tarasconi, R. Alberlini, S. Pinelli and P. Lunghi., Inorg.Chim.Acta.,1999,286,134.
- [10].Mishra D., S. Naskar, A.J. Blake and S. Chattopadhyay. Inorg. Chimica Acta.,2007,360(7),2291-2297.
- [11].Aswar A.S., V.V. Dhande and V.B. Badwaik., Russ. J. Inorg. Chem., 2007,52,1206.
- [12].Aswar A.S., A.R.Yaul, V.V. Dhande and N.J. Suryawanshi., Polish J. Chem., 2009.,29,556.
- [13].Mautya M.R. , A. Syamal. Indian J. Chem., 1985, 24A,836.
- [14].Kumar D., P.K. Gupta and A. Syamal., J. Indian Chem. Soc., 2003., 80,3.
- [15].Sarika R. Yaul, Amit R. Yaul, Gaurav B. Pethe. And Anand S. Aswar. , Am-Euras. J. Sci., 2009, 4(4),229-234.
- [16].Aswar. A. S., A. D. Bansod, S.R. Aswale and P. R. Mandlik., Indian J. Chem., 2004., 43A, 1892.
- [17].Singh P.K. and D.N. Kumar., Spectrochimica Acta., 2006, part A, 64(4), 853-858.
- [18].Sanjeev R. Dudhal, Shrikant Kulkarni IJETSR volume 5, Issue 3 (2018)



## An Efficient One Pot Synthesis of Polyhydroquinolines Using TS1 Catalyst Under Solvent Free Conditions

S.K. Ghumbre<sup>1\*</sup>, A.S. Renge<sup>2</sup>

<sup>1\*</sup>Department of Chemistry, I.C.S. College of Arts, Commerce and Science, Khed, Dist. Ratnagiri-415709, Maharashtra, India

<sup>2</sup>Department of Chemistry, K.G.K. of Arts, Commerce and Science, Karjat, Dist. Raigad-402107, Maharashtra, India

### ABSTRACT

The synthesis of polyhydroquinoline derivatives via Hantzsch condensation is excellent route by using four component coupling reaction of aldehydes, dimedone, ethyl acetoacetate and ammonium acetate in the presence of heterogeneous catalyst TS1 under solvent free condition.

**Keywords:** Aldehyde; Dimedone; TS1 catalyst; Hantzsch reaction.

### I. INTRODUCTION

4 Substituted 1,4 dihydropyridine (1,4-DHP) nucleus is a fertile source of biologically important molecules possessing various important pharmacological properties such as vasodilator, antihypertensive, bronchodilator antithrombotic, hepto-protective, antitumor, antimutagenic, geroprotective and antidiabetic agents<sup>1-4</sup>. From recent studies 1-4 DHP shows several medicinal applications which include neuroprotectant and platelet anti-aggregatory activity, in addition cerebral antiischemic activity in the treatment in the of Alzheimer's disease<sup>5-7</sup>. An efficient Hantzsch condensation polyhydroquinoline derivatives via a four component coupling reaction of aldehydes, dimedone, ethyl acetoacetate and ammonium acetate in the presence of HClO<sub>4</sub>-SiO<sub>2</sub> under solvent free conditions at 90°C temperature<sup>8</sup>. Yb(OTf)<sub>3</sub> promoted one pot synthesis of polyhydroquinoline derivatives via Hantzsch reaction of aldehydes, dimedone, ethyl acetoacetate and ammonium acetate at ambient temperature in excellent yield<sup>9</sup>. Photocatalytic oxidation of 1,4 dihydropyridine to pyridine has been extensively investigated<sup>10</sup>. Here in the present work, developed new efficient method for synthesis of polyhydroquinoline using TS1 catalyst under solvent free conditions.

## II. MATERIAL AND METHODS:

A mixture of aldehyde (1mmol), dimedone (1mmol), ethyl acetoacetate (1mmol), ammonium acetate (1.5mmol), TS1 (50mg) were refluxed under solvent free conditions. The reaction was confirmed by thin layer chromatography, the resulting solid product was treated with EtOAc followed by water and a brine solution and dried with anhydrous  $\text{Na}_2\text{SO}_4$ . The solution was concentrated in vacuum to afford the crude product. The pure product was obtained by further recrystallization using absolute alcohol.

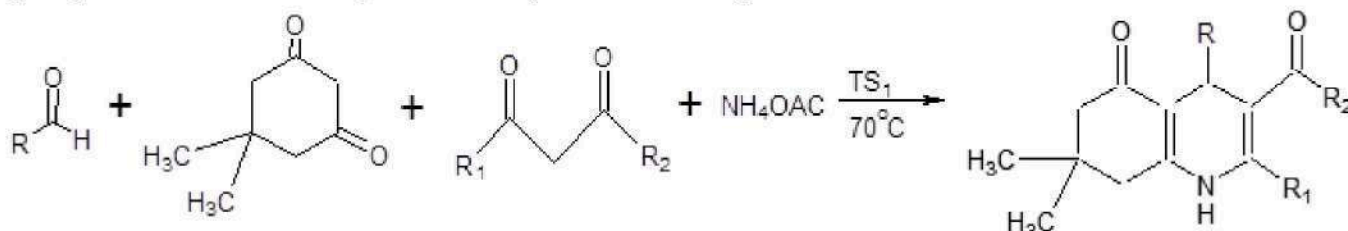


**Table:** TS1 catalyzed Hantzsch condensation for synthesis of polyhydroquinolines derivatives under solvent free conditions.

Entry	R	R1	R2	Time (min.)	Product	Yield	Melting point (°C) Observed	Melting point (°C) Reported
1	C <sub>6</sub> H <sub>5</sub>	CH <sub>3</sub>	OEt	20	2a	85	203-204	202-204 <sup>9</sup>
2	4-F-C <sub>6</sub> H <sub>4</sub>	CH <sub>3</sub>	OEt	22	2b	82	185-186	184-186 <sup>9</sup>
3	4-OCH <sub>3</sub> -C <sub>6</sub> H <sub>4</sub>	CH <sub>3</sub>	OEt	24	2c	84	256-257	257-259 <sup>9</sup>
4	4-CH <sub>3</sub> -C <sub>6</sub> H <sub>4</sub>	CH <sub>3</sub>	OEt	21	2d	80	261-262	260-261 <sup>9</sup>
5	3-NO <sub>2</sub> -C <sub>6</sub> H <sub>4</sub>	CH <sub>3</sub>	OEt	22	2e	82	178-179	177-178 <sup>10</sup>

The structure of the product were determined from their spectroscopic (UV, IR, NMR, Mass) data.

## III. SPECTROSCOPIC DATA

### Ethyl-1,4,7,8-tetrahydro-2,7,7-trimethyl-4-(4-fluorophenyl)-5(6*H*)-oxoquinolin-3-carboxylate

(2b). Yellow solid, mp 185-186 °C. IR (KBr): 3292, 2959, 1696, 1649, 1608, 1487, 1380, 1219, 1025, 764 cm<sup>-1</sup>. <sup>1</sup>H NMR (400 MHz, CDCl<sub>3</sub>):  $\delta$  = 0.92 (s, 3H, CH<sub>3</sub>), 1.07 (s, 3H, CH<sub>3</sub>), 1.18 (t,  $J$  = 7.3 Hz, 3H, CH<sub>3</sub>), 2.13-2.25 (m, 4H, 2  $\times$ CH<sub>2</sub>), 2.38 (s, 3H, CH<sub>3</sub>), 4.05 (q,  $J$  = 7.33 Hz, 2H, CH<sub>2</sub>), 5.02 (s, 1H, CH), 5.8 (s, 1H, NH), 6.85-6.89 (m, 2H, ArH), 7.23-7.27 (m, 2H, ArH). <sup>13</sup>C NMR (75 MHz, CDCl<sub>3</sub>)  $\delta$  14.1, 18.2, 26.4, 29.0, 32.1, 35.2, 50.1, 50.3, 59.0, 103.4, 110.0, 114.2, 114.3, 114.4, 129.0, 129.1, 144.1, 145.1, 149.4, 169.8, 194.2. LCMS:  $m/z$  = 356 (M-H)<sup>-</sup>. Anal. Calcd for C<sub>21</sub>H<sub>24</sub>NO<sub>3</sub>F: C, 70.58; H, 6.72; N, 3.92; F, 5.32. Found: C, 70.52; H, 6.79; N, 3.87; F, 5.28.

### Ethyl-1,4,7,8-tetrahydro-2,7,7-trimethyl-4-(4-methoxyphenyl)-5(6*H*)-oxoquinolin-3-carboxylate

(2c). Yellow solid, mp 256-257 °C. IR (KBr): 3276, 2956, 1703, 1648, 1606, 1496, 1381, 1215, 1031, 765 cm<sup>-1</sup>. <sup>1</sup>H NMR (200 MHz, CDCl<sub>3</sub> + DMSO-d<sub>6</sub>):  $\delta$  = 0.95 (s, 3H, CH<sub>3</sub>), 1.09 (s, 3H, CH<sub>3</sub>), 1.21 (t,  $J$  = 7.2 Hz, 3H, CH<sub>3</sub>), 2.01-2.10 (m, 4H, 2  $\times$ CH<sub>2</sub>), 2.30 (s, 3H, CH<sub>3</sub>), 3.70 (s, 3H OCH<sub>3</sub>), 4.00 (q,  $J$  = 7.2 Hz, 2H, CH<sub>2</sub>), 4.80 (s, 1H, CH), 6.65 (d,  $J$  = 7.3 Hz, 2H, ArH), 7.10 (d,  $J$  = 7.3 Hz, 2H, ArH), 8.65 (s, 1H, NH). <sup>13</sup>C NMR (75 MHz, DMSO-d<sub>6</sub>)

$\delta$  14.1, 18.2, 26.4, 29.1, 32.1, 34.7, 50.2, 50.5, 54.8, 58.9, 103.2, 110.1, 113.0, 113.1, 128.2, 128.3, 139.8, 144.6, 149.1, 157.2, 166.9, 194.2. LCMS:  $m/z = 368$  (M-H)<sup>-</sup>. Anal. Calcd for C<sub>22</sub>H<sub>27</sub>NO<sub>4</sub>: C, 71.54; H, 7.31; N, 3.79; Found: C, 71.59; H, 7.35; N, 3.84.

#### IV. RESULT AND DISCUSSION

The classical method for the preparation of polyhydroquinoline derivatives involves the reaction of aldehyde with ethyl acetoacetate and ammonia, in acetic acid or in refluxing in alcohol. However, this method suffers from several drawbacks such as long reaction time, excess of organic solvent and lower product yield<sup>11</sup>. All the starting materials in the ratio of 1:1:1:1 mixture of aldehyde, dimedone, ethyl acetoacetate and ammonium acetate catalyzed by TS1 catalyst is a green reaction in solvent free condition.

#### V. CONCLUSION

In conclusion, we reported TS1 recyclable and reused green catalyst for Hantzsch reaction. Some of the efficient feature for this method such as simplicity of the experiment, mild reaction condition, high yield, short reaction time and easy work up. Hence such simple and lucidness makes this method attractive for the synthesis of polyhydroquinoline derivatives.

#### VI. REFERENCES

- [1]. Godfraid, T.; Miller, R.; Wibo, M. *Pharmacol. Rev.* 1986, 38, 321.
- [2]. Sausins, A.; Duburs, G. *Heterocycles* 1988, 27, 269.
- [3]. Mager, P. P.; Coburn, R. A.; Solo, A. J.; Triggle D. J.; Rothe, H. *Drug Design Discovery* 1992, 8, 273.
- [4]. Mannhold, R.; Jablonka, B.; Voigdt, W.; Schoenafinger, K.; SchraVan, K. *Eur. J. Med. Chem.* 1992, 27, 229.
- [5]. Klusa, V. *Drugs Fut.* 1995, 20, 135.
- [6]. Bretzel, R. G.; Bollen, C. C.; Maeser, E.; Federlin, K. F. *Am. J. Kidney. Dis.* 1993, 21, 53.
- [7]. Bretzel, R. G.; Bollen, C. C.; Maeser, E.; Federlin, K. F. *Drugs Fut.* 1992, 17, 465.
- [8]. M. Maheswara, V. Siddaiah, *ARKIVOC* 2006 (II) 201-206.
- [9]. L.M. Wang, j. Sheng, *Tetrahedron*, 2005,61,1539-1543.
- [10]. Sainani, J. B.; Shah, A. C.; Arya, V. P. *Indian J. Chem, Sect B* 1994, 33, 526.
- [11]. Mohammad Ziarani.; Ghodsi. *Iran. J. Chem. Chem. Eng.* 2010, 29, 2



## One Pot Three Component Eco-Friendly Synthesis of Quinoline-3-Carbonitrile Derivatives

Kadam S. N.<sup>1</sup>, Ambhore Ajay<sup>2</sup>, Shringare S. N.<sup>3</sup>, Shinde S. R.<sup>1</sup>, Gaikwad R. S.<sup>1</sup>, Adlinge N. P.<sup>1</sup>, Ingawale A. R.<sup>1</sup>

<sup>1</sup>Department of Chemistry, Vidnyan Mahavidyalaya Sangola, Solapur, 413307, Maharashtra, India

<sup>2</sup>Department of Chemistry, Padmabhushan Dr. Vasantraodada Patil Mahavidyalaya, Tasgaon, Sangli 416312, Maharashtra, India

<sup>3</sup>School Of Chemical Sciences P.A.H. Solapur University, Solapur – 413 255, Maharashtra, India

### ABSTRACT

New derivatives of quinoline-3-carbonitrile have synthesized with a direct one pot three component eco-friendly protocol. The present protocol displays a mild and easy access for the Knoevenagel condensation utilizing heterocyclic aldehyde, 2-cyanoacetohydrazide, and substituted anilines. The method includes use of recyclable catalyst Bleaching earth clay (PH12.5) incorporated with the PEG-400 as a green solvent. All the synthesized compounds were characterized for their spectral analysis.

**Keyword:** Bleaching earth clay (BEC), PEG-400, Heterocyclic aldehyde, recyclability.

### I. INTRODUCTION

The predominant occurrence of the quinoline-3-carbonitrile derivative in various natural products and established medicinal compounds<sup>1-3</sup> had proven to be a versatile scaffold in organic and medicinal chemistry. quinoline-3-carbonitrile have recognized to acquire varied biological activities such as antibacterial<sup>4</sup>, antiviral<sup>5</sup>, anticancer<sup>6</sup>, antifungal<sup>7</sup>, antimalarial<sup>8</sup>, anti H.I.V<sup>9</sup>, anti-inflammatory<sup>10</sup>. Quinoline-3-carbonitrile derivative are acknowledged medicinal compounds known to be present in the bioactive natural products<sup>11</sup>. Heterocyclic aldehydes are proven to contain varied biological activities<sup>12</sup>. By interpreting these points we combine the heterocyclic aldehydes with anilines and 2-cyanoacetohydrazide assuming that the present combination may lead to formation of improved biological hybrid.

There is always been quest for advancement of the synthetic rout for the conversion of readily available reagent in to widely used organic compounds. For accomplishing this multicomponent reaction (MCR) are recognized as an important tool from economic as well as environmental point of view<sup>13</sup>. Along with the MCR method, use of green solvent is also considered to be an environmental benign access. Amongst the green solvents used for MCR strategy PEG-400 is considered to be well known green solvent<sup>14</sup>.

In the previous literature there are abundant synthetic strategies for the synthesis of quinoline-3-carbonitrile derivatives<sup>15</sup>. Development of an heterogenous catalyst for the synthesis of numerous important organic

motifs was always been a center of interest for organic chemistry students<sup>16-17</sup>. Ease of handling, reusability, easy extraction are some peculiar advantages of heterogenous catalysts. Amongst those heterogeneous catalysts Bleaching earth clay (BEC) is considered as a remarkable heterogenous catalyst for various organic transformations<sup>18</sup>. Taking in account these facts we represent an MCR protocol for synthesis of by Consolidation of heterocyclic aldehydes with anilines and 2-cyanoacetohydrazide Manipulating Bleaching earth clay as catalyst and PEG-400 as green solvent.

## II. RESULT AND DISCUSSION

A facile one pot three component protocol for the synthesis of new quinoline-3-carbonitrile derivative **4a-j** is reported by utilizing equimolar heterocyclic aldehydes **2a-j**, anilines **3a-c** and 2-cyanoacetohydrazide **1** **Scheme 1**. The synthetic protocol commences with sequential addition of 2-cyanoacetohydrazide and heterocyclic aldehydes in round bottom flask previously filled with catalytic amount of BEC and PEG-400 as green solvent, after completion of reaction as indicated by TLC the anilines was added in the same pot and the reaction mixture was further stirred at 80°C for the formation of product. the first attempt was made using the Triethylamine as a catalyst which results in formation of the product with 50% yield and time required for completion of reaction was 65 minutes Entry1 Table1. Observing these results, we moved for other catalysts piperidine and morpholine Entry 2and 3 Table 1 respectively which the outcomes of 40 and 30% yield with the time of 70 and 60 minutes. When we moved for using BEC as a catalyst 1 Wt% resulting in production of improved 60% yield Entry 4 table1. Enthused with these results we further investigate different wt% compositions of BEC (pH 12.5). We came to investigation that satisfactory yield was obtained when we utilized 15wt% of BEC. The yield was found to hampered when 10 wt% and 20wt% BEC were used Entry 5 and 7 Table 1. However, there was no formation of product when reaction was carried out in absence of catalyst when stirred at RT Entry 8. Even though when reaction mixture was stirred at 80°C without catalyst the formation of product was not observed Entry 9 Table 1. The optimized reaction conditions were found when 15wt% of BEC was used.

Table1: Optimized reaction conditions

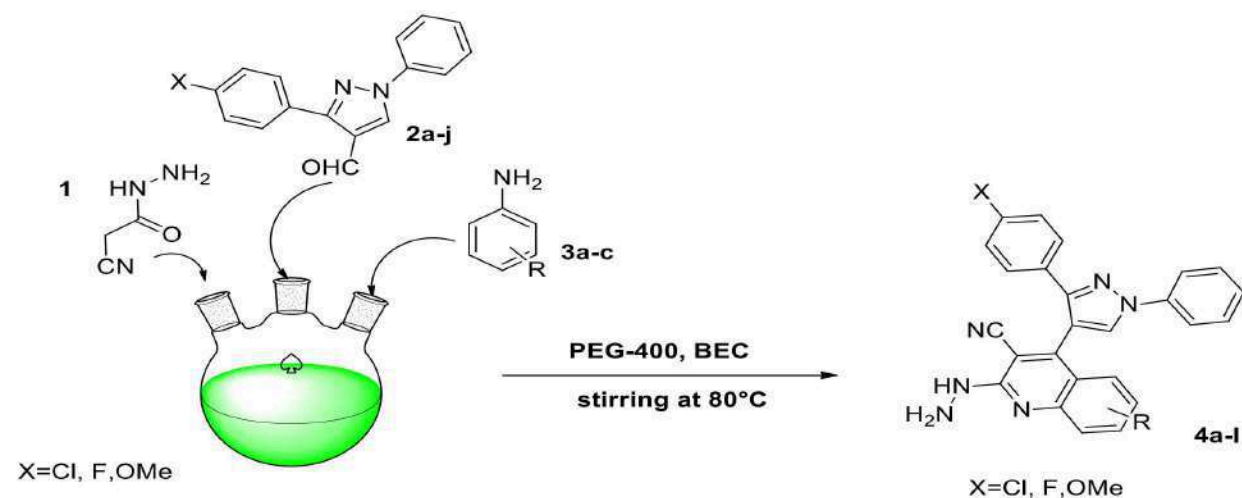
Entry	Catalyst (Mol/wt%)	Temp (°C)	Time (Min)	Yield of 4a (%)
1	Triethylamine (Mol%)	70	65	50
2	Piperidine (Mol%)	80	70	40
3	Morpholine (Mol%)	80	60	30
4	Bleaching earth Clay 1 wt%	80	50	60
5	Bleaching earth Clay 10 wt%	80	40	70
6	Bleaching earth Clay 15 wt%	80	35	90
7	Bleaching earth Clay 20 wt%	80	20	70
8	No catalyst	RT	70	0
9	No catalyst	80	80	0

<sup>a</sup> Reaction progress was monitored by thin layer chromatography (TLC)

<sup>b</sup> Yield refers to isolated yield

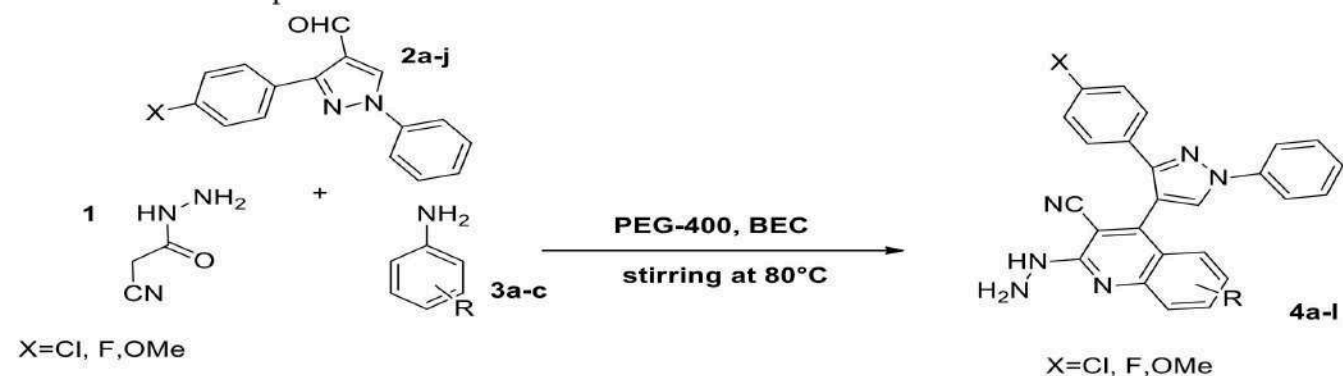
With these optimized conditions we initiated to find the substrate scope the reaction condition was found to operate for varied substrate scope Table 2.

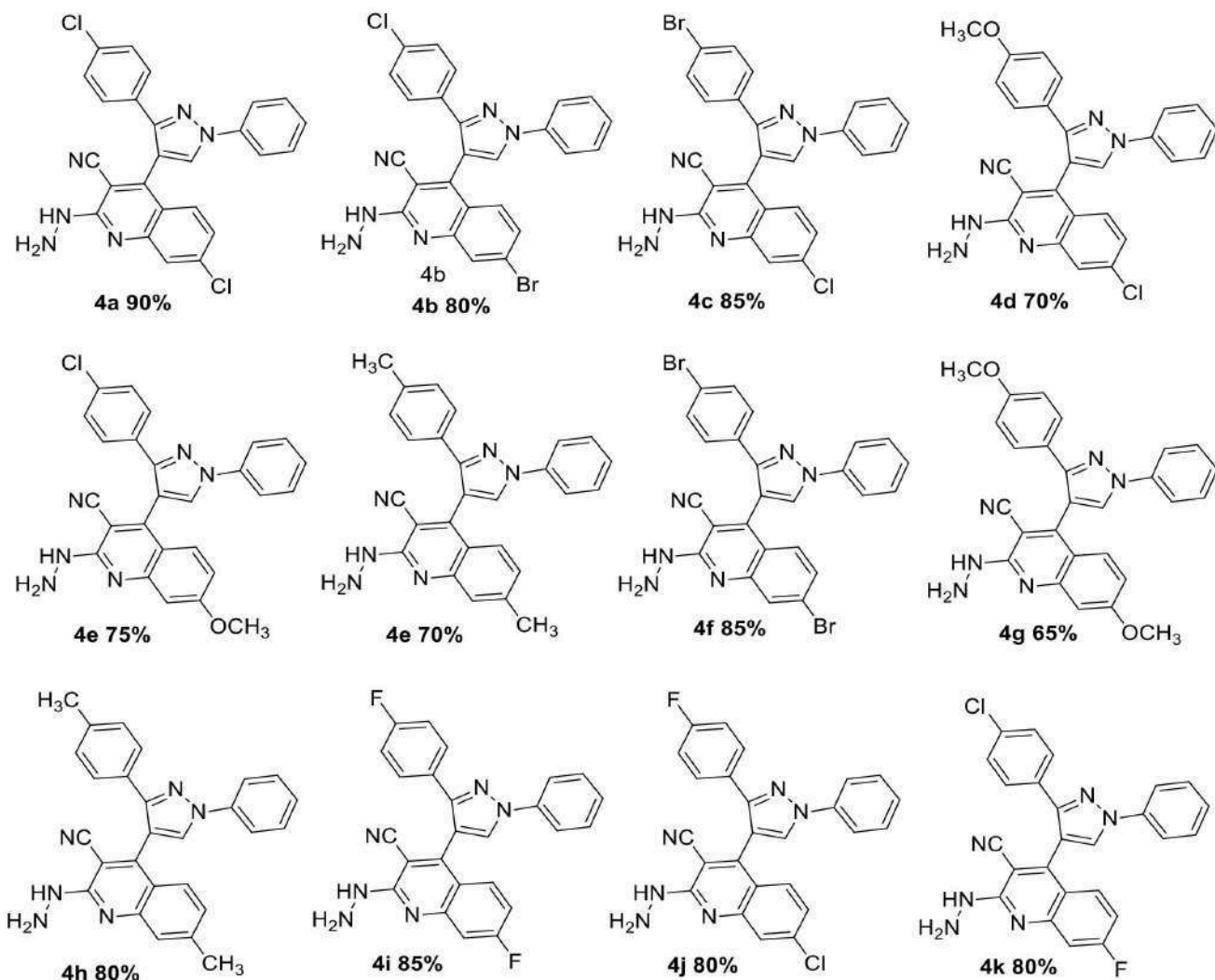
### Scheme 1



The finding of the substrate scope indicates that the MCR strategy allows variety of substrate to undergo smoothly with formation of product with satisfactory yield. Interpretation of the yield of the substrate scope indicate that the reactant with electron donating group either on aldehyde 2a-j or on the anilines 3a-c renders the product yield. The substrates with electron withdrawing groups on the aldehydes or on the anilines are providing the products with good yield.

Table 2 Substrate Scope

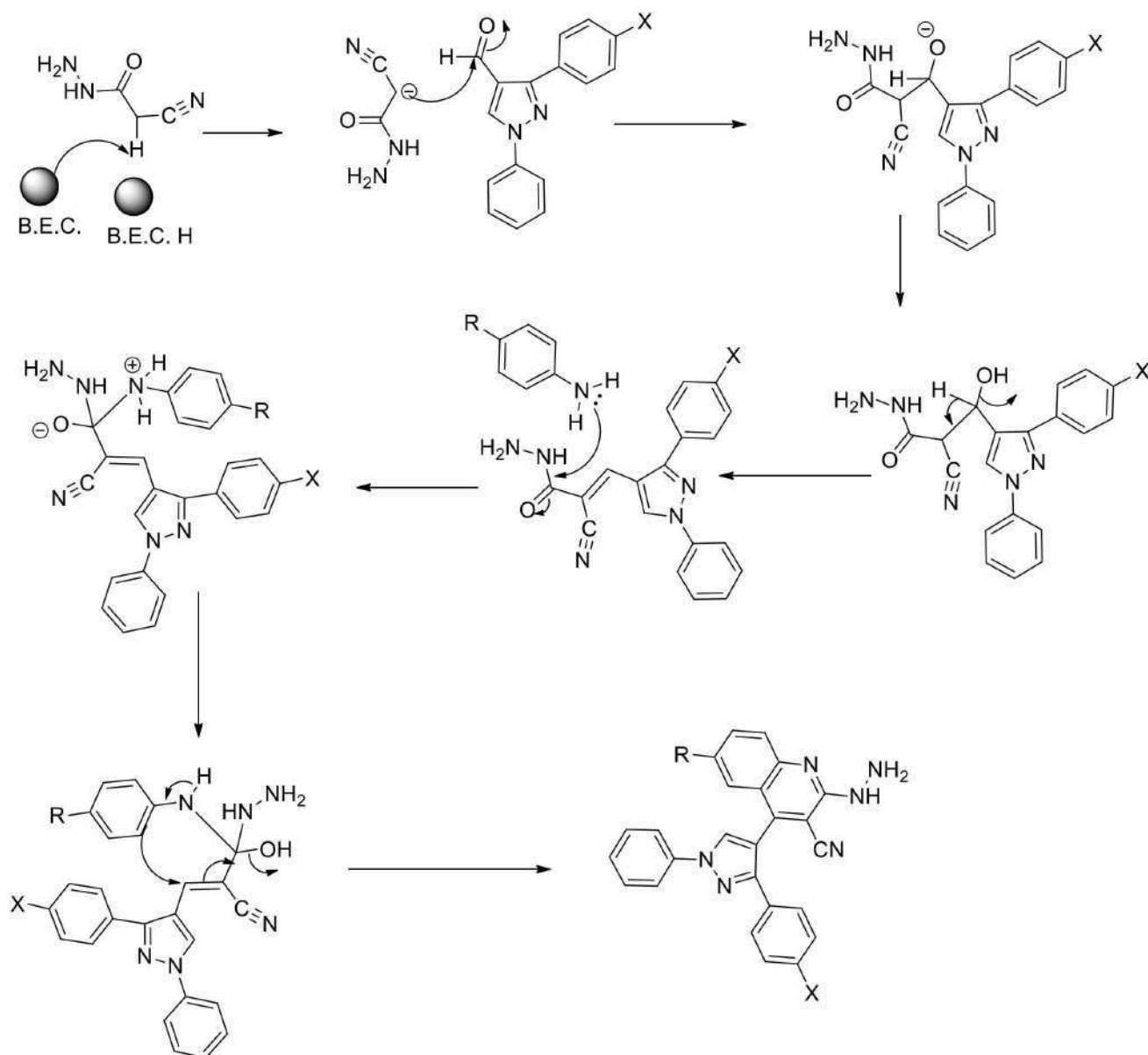




<sup>a</sup>Yield refers to the isolated product after column chromatography

The plausible mechanistic path was proposed in Scheme 2. The mechanism indicate reaction was proceed through abstraction of proton from 2-cyanoacetohydrazide by BEC then the anion attack on the carbonyl of heterocyclic aldehyde. Furthermore addition of substituted anilines leads to formation of final product.

Scheme 2 Plausible mechanism



### III. CONCLUSION

The proposed protocol provides an easy access for the synthesis of quinoline-3-carbonitrile derivatives. The MCR strategy for the synthesis is woven with the environmental benign approach through the use of BEC as a catalyst and PEG-400 as a solvent. The protocol delivers an efficient access for the formation of new hybrid product with coupling of easily available reactants which may lead to improved biological activities.

## IV. REFERENCES

- [1]. Nainwal, L. M., Tasneem, S., Akhtar, W., Verma, G., Khan, M. F., Parvez, S., Shaquiquzzaman, M., Akhter, M., Alam M. Eur. J. Med. Chem. 2019, 164, 121-170.
- [2]. Mukherjee, S., Pal, M. Drug Discov. Today, 2013, 18, 389-398.
- [3]. Chung, P. Y., Bian, Z. X., Pun, H. Y., Chan, D., Chan, A.S.C., Chui, C. H., Tang, J.C.O., Lam, K. H. Future Med. Chem. 2015, 7, 947-967.
- [4]. Khan, S. A., Asiri, A. M., Basisi, H. M., Asad, M., Zayed, M. E., Sharma, K., Wani, M. Y., Bioorg. Chem. 2019, 88, 102968.
- [5]. Ibrahim, M. A., Badran, A. S. Syn. Commun. 2020, 50, 1871-1882.
- [6]. Liu, B., You, Q. D., Li, Z. Y. Chin. Chem. Lett. 2010, 21, 554-557.
- [7]. Gholap, A. R., Toti, K. S., Shirazi, F., Kumari, R., Bhat, M. K., Deshpande, M. V., Srinivasan, K. V. Biorg. Med. Chem. 2007, 15, 6705-6715.
- [8]. Shah, N. M., Patel, M. P., Patel, R. G. Eur. J. Med. Chem. 2012, 54, 239-247.
- [9]. Jentsch, N. G., Hart, A. P., Hume, J. D., Sun, J., McNeely, K. A., Lama, C., Julia, A., Pigza, M. G., Donahue G., Kessler, J. J., ACS Med. Chem. Lett. 2018, 9, 1007-1012.
- [10]. Tu, S. J., Jiang, B., Jia, R. H., Zhang, J. Y., Zhang, Y., Yao, C. S., Shi, F. Org. Biomol. Chem. 2006, 4, 3664-3668.
- [11]. Kawanishi, N., Sugimoto, T., Shibata, J., Nakamura, K., Masutani, K., Ikuta, M., Hirai, H. Biorg. Med. Chem. 2006, 16, 5122-5126.
- [12]. Vo, C. V. T., Luescherf, M. U., Bode, J. W., Nature Chemistry, 2014, 6, 310-314.
- [13]. Eydokimov, N. M., Kireev, A. S., Yakovenko, A. A., Antipin, M. Y., Magedov, I. V., Kornienko, A., J. Org. Chem. 2007, 72, 3443-3453.
- [14]. Shitole, N. V., Shelke, K. F., Sadaphal, S. A., Shingate, B. B., Shingare, M. S., Green chem. Lett. Rev. 2010, 3, 83-87.
- [15]. Aly, R. M., Serya, R. A., El-Motwally, A. M., Esmat, A., Abbas, S., Abou El Ella, D. A., Bioorg. Chem. 2017, 75, 368-392.
- [16]. Argyle, M. D., Bartholomew, C. H., Catalysts, 2015, 5, 145-269.
- [17]. Boey, P. L., Maniam, G. P., Abd Hamid, S., Chem. Eng. J., 2011, 168, 15-22.
- [18]. Gaikwad, M. V., Kamble, R. D., Hese, S. V., Acharya, A. P., Mogle, P. P., Kadam, S. N., Dawane B. S., Res. Chem, Intermed. 2015, 41, 4673-4678.



## Highly Proficient Extractive Studies on The Behaviour of Neodymium (III) Assisted By 2-Octylaminopyridine from Weak Succinate Media

Gurupad D. Kore<sup>1,2\*</sup>, Sunil B. Zanje<sup>3</sup>, Mansing A. Anuse<sup>1</sup>, Sanjay S. Kolekar<sup>1</sup>

<sup>1</sup>Analytical Chemistry Laboratory, Shivaji University, Kolhapur-416004, Maharashtra, India

<sup>2</sup>Department of Chemistry, Padmabhushan Vasantdada Patil Mahavidyalaya, Kavathemahankal-416405,  
Maharashtra, India

<sup>3</sup>Department of Chemistry, J. M. Patel Arts, Commerce and Science College, Bhandara-441904, Maharashtra,  
India

### ABSTRACT

The extraction behaviour studies of neodymium(III) from sodium succinate medium at pH 7.5 with 2-octylaminopyridine in xylene. The extracted neodymium(III) was stripped with 0.1 M HCl from the organic phase and determined by arsenazo. Physicochemical parameters like diluents study, phase ratio, and loading capacity to name a few were optimized for the quantitative extraction of neodymium(III). Neodymium(III) was selectively extracted and separated from binary and ternary mixtures.

**Keywords:** - Extraction, Neodymium (III), 2-octylaminopyridine, Succinate media.

### I. INTRODUCTION

Neodymium is one most abundant element in earth crust but never occur in nature as a native element, its main source is ores of Monazite, Xenotime and Bastnaesite [1]. Neodymium is used as a permanent magnet, neodymium, boron, and iron tetragonal alloy (Nd<sub>2</sub>Fe<sub>14</sub>B) have been used in a wide range of applications requiring high coercive force and high energy product (e.g. Hybrid electric vehicles and miniature high capacity hard disk drives) [2,3]. Neodymium is rare and valuable therefore their recycling and extraction are mandatory for technical, environmental, economic, and resource conservation reasons.

Separation of neodymium from natural resources by environmentally friendly approaches is most significant. Therefore, man strategies for the isolation of neodymium have been developed. Among which solvent extraction is the most often used technique. Different extractants have been used for the extraction of neodymium such as 8-hydroxyquinoline [4], Cyanex 921 [5], trioctylphosphine oxide (TOPO) and trialkylphosphine oxide [6], 2-ethylhexylphosphoric acid [7]. Tributylphosphate in supercritical carbon dioxide solvent has been successfully used for the quantitative recovery of neodymium [8]. Mono-2-ethylhexyl ester [9]. The extractantdialkylphosphate in the ionic liquid has been studied for the extraction of neodymium [10].

Long-chain crown ethers such as poly[dibenzo-18-crown-6] [11], dicycloheano-18-crown-6 [12], and TODGA [13] were used.

As per as the robustness of the work is concerned. In earlier work, Nd(III) was extracted with different extractants. However those required either mineral acid media, the high time of extraction, high concentration of extractant, etc. Whereas in the present method, the extraction was carried out in 0.005 M sodium succinate at pH – 7.5, and extractant concentration was 0.05 M indicating the method is relatively eco-friendly and a step ahead towards green Chemistry.

The proposed study aimed to develop a more greener and precise method for the extraction of Nd(III). Efforts have been made to optimize the extraction system. The novelty of the system lies in the minimum use of concentration of extractant and use of greener weak acid media. The method has a good recovery of solvent and does not require too much of instrumentation.

## II. EXPERIMENTAL

### Apparatus

Digital spectrophotometer optimized  $\alpha$  was used for the absorption measurement using 1 cm quartz cells. An Elico digital pH meter model LI-127 was used to measure the pH. METLER TOLEDO was used for weighing operations model ML-204/-01 having accuracy  $1 \times 10^{-4}$ g.

### Reagents

#### Standard Neodymium(III) 500 $\mu\text{g}/\text{ml}$ stock solution

The stock solution of neodymium (III) was prepared to dissolve 1.165 g. of neodymium oxide in 40 ml of perchloric acid and the final volume was brought to 1000 ml with double distilled water.

#### 2-Octylaminopyridine (2-OAP)

2-OAP was synthesized by Borsch and Petrukhin [14] and the working extractant solution having molarity (0.05M) was prepared in xylene.

#### Arsenazo-I

Arsenazo-I (0.05% w/v) was prepared by dissolving 0.05 g. of arsenazo-I (s. d. Fine-chem limited) in water.

#### Triethanolamine buffer

Added 200 ml 15% triethanolamine in 160 ml of 1M  $\text{HNO}_3$  and 40 ml of water. Adjust the pH of the solution to 7.2 with dilute  $\text{NH}_3$  or  $\text{HNO}_3$ .

All reagents and metal salts used are of analytical grade and their solutions were prepared in water and mineral acid.

### Recommended Procedure

A solution containing 75 µg neodymium(III), was made to 0.005 M w/v with sodium succinate, and pH was brought to 7.5 with dilute mineral acid and base by maintaining total dilution volume to 25 ml and then transferred to 125 ml separatory funnel to this added 10 ml 0.05 M 2-OAP in xylene as an extractant and shaken for 5 min, two phases were allowed to disengage. The neodymium(III) extracted in the organic phase was stripped with 0.1 M HCl ( $3 \times 10$ ) ml as a strippant solution.

The stripped solution containing neodymium(III) was evaporated to moist dryness. To this added 5% sulphosalicylic acid. After two minutes added 5 ml of the Arsenazo-I [15] (0.05% w/v) solution, 10 ml of triethanolamine buffer, water to 40 ml, and ammonia till the pH was 7.2. Transfer the solution to a 50 ml volumetric flask, diluted up to the mark with water, and measured the absorbance at 580 nm using reagent solution as a reference.

## III. RESULTS AND DISCUSSION

### Effect of pH

The formation of a complex of metal with a particular extractant and the subsequent extraction was greatly influenced by the pH of the solution. The influence of the pH on the extraction of neodymium(III), was studied in the range from 1-10 (Fig. 1). The required  $H^+$  ion concentration at various pH was reached by adding dil. HCl or NaOH. The extraction of ion-pair complex of neodymium(III) was increased with pH and became quantitative in the pH range 7.0 - 8.2, above this optimum pH range neodymium(III) extraction decreases. Therefore 7.5pH was selected throughout the experiment.

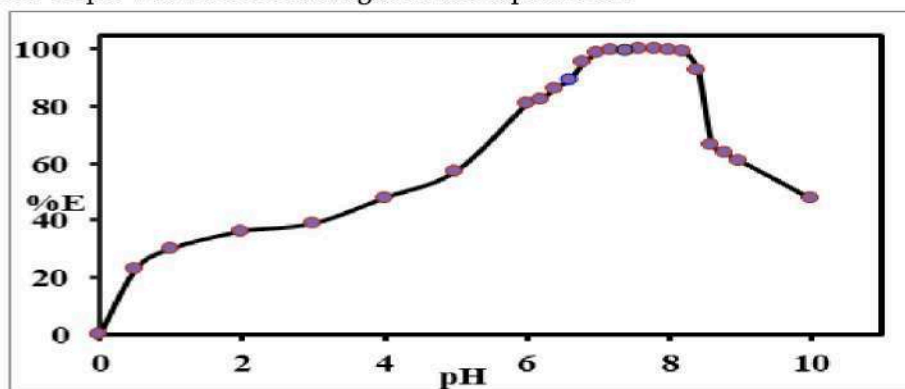


Fig. 1 Effect of pH on extraction of Nd(III) - 2-OAP complex.

### Influence of 2-OAP concentration on extraction of neodymium(III)

The concentration of extractant is one of the most important factors for the extraction of any metal. Hence extraction performance of neodymium(III) greatly depended on the concentration of 2-OAP. To elucidate the effect of 2-OAP concentration on the neodymium(III) extraction, the experiment was carried out at a various concentration of 2-OAP from 0.001- 0.10 M (Fig. 2), and other parameters such as pH 7.5, 0.005 M sodium succinate, phase ratio 2.5:1 were kept constant and extraction was carried out. The results illustrate that the extraction commences at 0.001 M 2-OAP concentration and becomes quantitative in the range of 0.04-0.06 M,

further increase in concentration beyond 0.06 M there was a decrease in the extraction of neodymium(III). For the further study, 10 ml of 0.05 M 2-OAP was adopted as an optimum concentration of extractant for the quantitative extraction of neodymium(III). The recycling capacity of the reagent for quantitative extraction of neodymium(III) was observed to be three times.

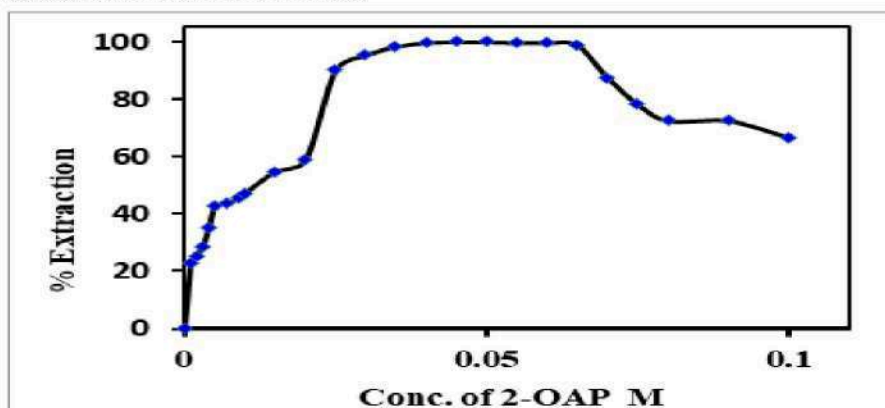


Fig. 2 Impact of conc. of 2- OAP on extraction of Nd(III)

#### Impact of weak organic acid concentration

The extraction of neodymium(III) was investigated at pH 7.5 with 10 ml of 0.05 M 2-OAP in xylene in the presence of a varying concentration of different weak organic anions like acetate, succinate, malonate and citrate. Quantitative extraction of neodymium(III) was found from succinate media. The weak acid curve of sodium succinate indicates that quantitative extraction was taking place in the concentration range of 0.003 to 0.010 M. In general procedure 0.005 M sodium succinate was recommended throughout the experiment (Fig. 3). The salicylate, malonate, citrate, and ascorbate do not give quantitative extraction of neodymium(III) as there was no formation of stable ion-pair complexes.

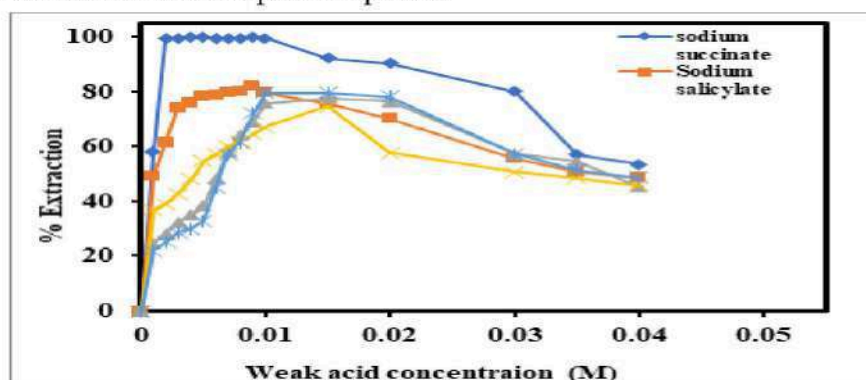


Fig. 3 Impact of weak organic acid concentration

#### Metal Loading Capacity

The extraction behaviour of neodymium(III) was studied concerning the metal loading capacity was demonstrated at a varying concentration of neodymium(III) in the range 25  $\mu\text{g}$  to 900  $\mu\text{g}$ . The analysis elucidates that the nearly hundred percent extractions take place in the range of 25 to 700  $\mu\text{g}$ . It means up to 700  $\mu\text{g}$  of neodymium(III) 10 ml of 0.05 M 2-OAP is sufficient and after 700  $\mu\text{g}$  neodymium(III) decrease in

extraction demonstrates that there might be a deficiency of 2-OAP. Thus this study indicates that 700 µg of neodymium(III) is a maximum capacity for 10 ml 0.05 M 2-OAP.

### Impact of stripping reagents on the extraction of neodymium(III)

Stripping is a back extraction and is reverse to that of extraction. If the extraction took place in a basic medium, usually the acidic strippants become more efficient and vice versa. The loaded organic phase of 2-OAP, was back-extracted with various stripping reagents as shown in Fig. 4. The results demonstrate that, the extraction efficiency of the different stripping reagents like ammonia buffer, water, ammonia, HCl, H<sub>2</sub>SO<sub>4</sub> and HNO<sub>3</sub>. The study illustrates that neodymium(III) was extracted with 2-OAP in xylene and stripped out completely with HCl, while other reagents showed incomplete stripping of neodymium(III) from the loaded organic phase. Therefore, the stripping of neodymium(III) from the loaded organic phase was carried out with 0.1 M HCl (3 × 10 ml) solution. The stripping mechanism-

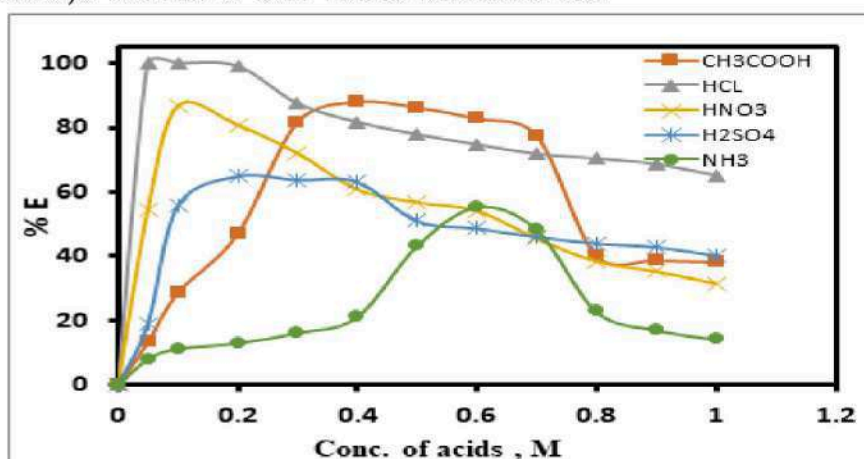


Fig. 4 Impact of strippants on extraction of Nd(III)

### Solvent Study

The use of suitable solvents is very important in solvent extraction. The different solvents were studied such as amyl alcohol, 1,2-dichloroethane, xylene, n-butanol, kerosene, methyl isobutylketone, chloroform, toluene, benzene, carbon tetrachloride (Fig. 5). The extraction of neodymium(III) was found to be quantitative in xylene and toluene with 0.05 M 2-OAP. It was found that there was no significant relationship between dielectric constant and percentage extraction. Hence xylene was selected as a solvent for extraction of neodymium(III) which has low cost and showed clear phase separation.

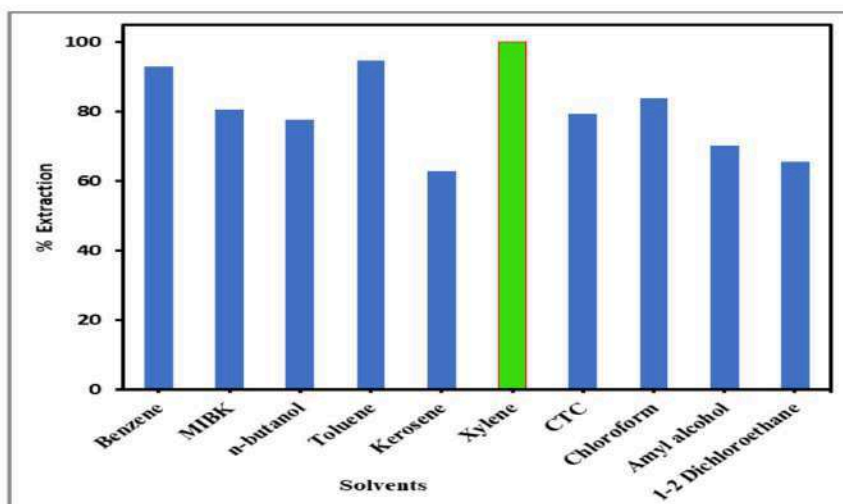


Fig. 5 Effect of solvents

### Effect of organic to aqueous volume ratio

The different volume of aqueous phase to non-aqueous phase was examined by keeping organic phase volume fixed. The analysis was carried out in the range of 1:1 to 1:30. The study reveals that 1:1 to 1:6 ratios give quantitative extraction of neodymium(III). Beyond 1:6 ratio the distribution ratio decreases because of lack of 2-OAP extractant due to an increase in volume (Fig. 6). Therefore 1:2.5 ratio of organic to aqueous was recommended for the proposed method for practical suitability and to avoid the losses of chemicals.

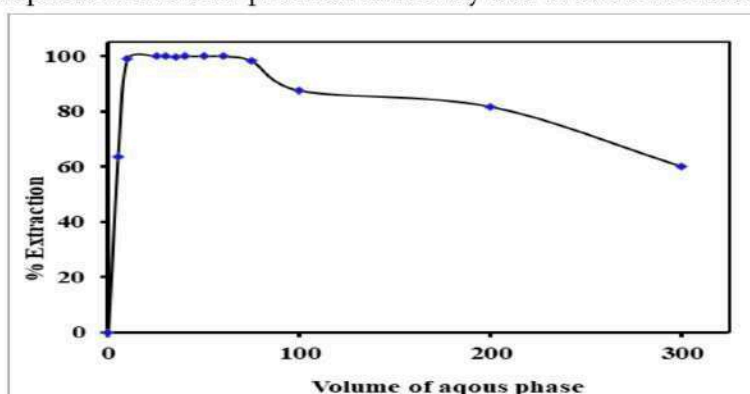
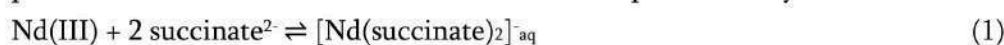


Fig. 6 Effect of organic to aqueous volume ratio

### Stoichiometry of extracted species

The mechanism of extraction of neodymium(III) was proposed by evaluating the experimental information and based on slope ratio study. The plot of  $\log D_{[\text{Nd(III)}}]$  Vs  $\log C_{[\text{succinate}]}$  at fixed pH 5.5 and 9.5 was linear with slopes 2.02 and 2.03 respectively. This illustrates that two succinate ions react with one Nd(III) species (Fig. 7). The plot of  $\log D_{[\text{Nd(III)}}]$  Vs  $\log C_{[2\text{-OAP}]}$  at fixed pH 5.5 and 9.5 showed a slope of 1.18 and 1.09 respectively. This illustrates that one mole of 2-OAP takes part in reaction with one mole of neodymium(III) (Fig. 8). Therefore the slope ratio method proposes the possible combination of species as 1:2:1 (Metal: succinate: 2-OAP). The probable mechanism of extraction based on the slope ratio analysis method was as follows



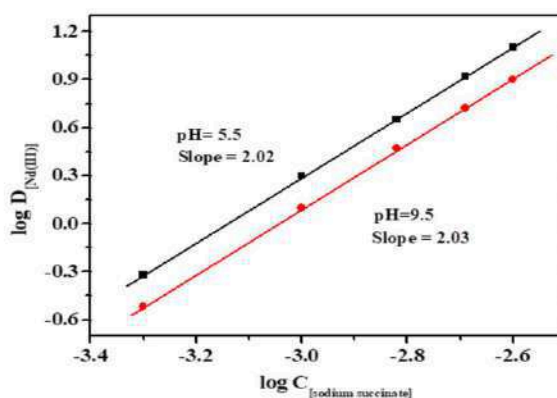
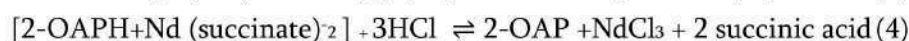
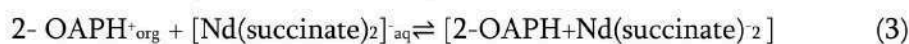


Fig.7 Plot  $\log D_{[\text{Nd(III)}]}$  Vs  $\log C_{[\text{sodium succinate}]}$

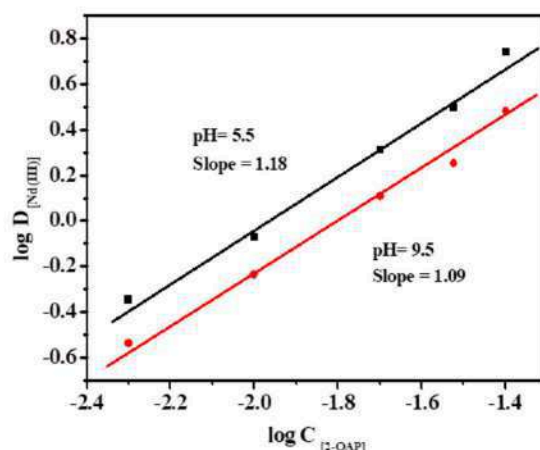


Fig. 8 Plot of  $\log D_{[\text{Nd(III)}]}$  Vs  $\log C_{[2\text{-OAP}]}$

#### IV. APPLICATIONS

##### Separation of neodymium(III) from associated metal ions

The influence of commonly associating ions in the ore samples on the extraction recovery of neodymium(III) was studied. Various salts and metal ions were added individually to a solution containing 75  $\mu\text{g}$  of neodymium(III) in 25 ml aqueous volume and an extraction procedure was employed. The tolerance limit of the associating ions, defined as the largest amount making the recovery of neodymium(III) less than 95 %. Most of the metal ions and anions do not interfere in the extraction of the neodymium(III) even at the milligram level. The versatility of the proposed method was checked by carrying out extraction of neodymium(III) with various associated metal ions such as Zr(IV), Ce(IV), Y(III), Th(IV), La(III), Gd(III), Sm(III), Cd(II), Pb(II), Ba(II), Ru(III), Se(IV), Mg(II), Sr(II), Mo(VI), U(VI), V(V), Zn(II), Ca(II), Cr(VI),

W(VI), Ti(IV), Nb(V), Co(II), Mn(II), Fe(II), Ta(V), Ni(II), Eu(III), Pd(II), As(III), Cu(II), Bi(III), Te(IV) and Sb(III) with 10 ml of 0.05 M 2-OAP in xylene from 0.005 M succinate medium (Table 1). Added metal ion was estimated by a classical method using a selective reagent spectrophotometrically whereas neodymium (III) was determined spectrophotometrically by the Aresnazo-I method.

**Table 1 The influence of foreign ions on extraction of neodymium(III)**

Tolerance limit in mg	Foreign ions added
0.5	Gd(III) <sup>f</sup>
1	U(VI) <sup>a</sup> , V(V) <sup>a</sup> , Fe(II), Ta(v) <sup>a</sup> , Ce (IV) <sup>a</sup> , Pb(II) <sup>b</sup> , Al(III) <sup>d</sup> , Ni(II) <sup>c</sup>
2	La(III), Y(III), Mo(II), Zr(IV) <sup>a</sup> , Zn (II), Ba(II), Mn(II), Sb(II), Ru(III), Th(IV) <sup>a</sup>
3	Se(IV), Bi(III), Te(IV), Co(II), Eu(III)
4	Mg(II)
5	Cd(II), Ti(IV), Nb(V), Cu(II)
7	Pd(II)
10	Sr(II), Cr(VI), Sm(III) <sup>e</sup> , W(VI), Fluoride, Nitrite, phosphate, EDTA
15	Ascorbate, Tartarate, Iodide, Thiourea, Chloride, Salicylate, Thiocyanate
25	Acetate, Nitrate, Thiosulphate, Citrate, Ca(II), Sulphate, Succinate
50	Bromide , Oxalate ,

a = Fluoride, b = thiosulphate, c = thiocyanate, d = oxalate, e = ascorbate ,

f = thiourea

#### Separation of neodymium(III) from ternary mixture

A ternary mixture of neodymium (III) with Th(IV) Zr(IV):La(III) Ce(IV): Cd(II), Fe(II): Th(IV), Fe(II): Th(IV), Y(III) :Y(III), La(III) : Sm(III), U (VI): Zr(IV), Mo(VI): Eu(III), U(VI):Bi(III), La(III):U(VI), Ce(IV) and U(VI) Th(IV) were prepared and analyzed by general procedure (Table 2).

**Table 2 Separation of neodymium(III) from synthetic mixtures.**

Metal ions	Amount taken in $\mu\text{g}$	% Recovery of Nd(III)*	RSD, %
Nd(III)	75	99.75	0.07
Th(IV)	40		
Zr(IV)	400		
Nd(III)	75	99.72	0.15
La(II)	250		
Ce(IV)	300		
Nd(III)	75	99.68	0.07
Bi(III)	300		

La(III)	250		
Nd(III)	75		
Th(IV)	40	99.75	0.17
Ce(IV)	300		
Nd(III)	75		
Y(III)	75	99.78	0.10
La(III)	250		
Nd(III)	75		
Eu(III)	150	99.62	0.19
U(VI)	200		
Nd(III)	75		
Sm(III)	200	99.78	0.16
U(VI)	200		
Nd(III)	75		
Zr(IV)	400	99.48	0.13
Mo(VI)	150		
Nd(III)	75		
Fe(III)	400	99.58	0.09
Cd(II)	40		
Nd(III)	75		
Y(III)	75	99.62	0.11
Th(IV)	40		
Nd(III)	75		
U(VI)	200	99.72	0.15
Ce(IV)	300		
Nd(III)	75		
U(VI)	200	99.70	0.17
Th(IV)	40		

\* Average five determinations

Added metal ions remained in a non-organic phase whereas from loaded non-aqueous phase containing neodymium(III) was back-extracted with 0.1 M HCl ( $3 \times 10$ ) ml and determined spectrophotometrically by arsenazo-I. To check and confirm the accuracy of the method average three determinations were carried out.

## V. CONCLUSION

- I]. The ion-pair complex of neodymium(III) succinate with the 2-OAP in xylene was good enough for separating the various binary, ternary mixtures which are commonly associated with it.

- II]. During extraction of neodymium(III) there was no need for the addition of any surfactant or modifier for quantitative extraction in a single step from weak acid media at 7.5 pH and at room temperature.
- III]. The neodymium(III) from the loaded organic phase of 2-OAP was back-extracted by stripping the non-aqueous phase with 0.1 M HCl ( $3 \times 10$  ml) solution.
- IV]. The extractant 2-OAP was extended for separating the neodymium(III) from binary and ternary mixtures.
- V]. The strippants used for the separation are simple.
- VI]. The probable composition of the proposed method was 1:2:1 (metal: succinate: 2-OAP extractant).

## VI. REFERENCES

- [1]. R. Banda, H. Jeon, and M. Lee, *J. Korean Inst. Resour. Recycl.* 20, 46 (2011).
- [2]. M. Tanaka, T. Oki, K. Koyama, H. Narita, and T. Oishi, *Handbook on the physics and chemistry of rare earths*. Amsterdam: Elsevier B.V., (2013).
- [3]. D. Brown, B. Ma, and Z. Chen, *J. Magn. Magn. Mater.* 248, 432 (2002).
- [4]. T. Miaomiao, J. Qiong, and L. Wuping, *J. Rare Earths.* 31, 604 (2013).
- [5]. N. Panda, N. Devi, and S. Mishra, *J. Rare Earths.* 30, 794 (2012).
- [6]. Y. El-Nadi, *Hydrometallurgy* 119, 23 (2012).
- [7]. D. Wu, Q. Zhang, and B. Bao, *Hydrometallurgy.* 88, 210 (2007).
- [8]. R. Fox, R. Ball, P. Harrington, H. Rollins, J. Jolley, and C. Wai, *J. Supercrit Fluid.* 31, 273 (2004).
- [9]. Z. Yongqi, L. Jianning, H. Xiaowei, W. Chunmei, Z. Zhaowu, and Z. Guocheng, *J. Rare Earth.* 26, 688 (2008).
- [10]. A. Rout, J. Kotlarska, W. Dehaen and K. Binnemans, *PCCP* 15, 16533 (2013).
- [11]. S. Lad, and B. Mohite, *J. Radioanal. Nucl. Chem.* 302, 1481 (2014).
- [12]. T. Fujii, T. Yamamoto, J. Inagawaa, K. Gunji, K. Watanabe and K. Nishizawa, *Solvent Extract. Ion Exchange.* 18, 1155 (2000).
- [13]. P. Vernekar, Y. Jagdale, A. Sharma, A. Patwardhan, A. Patwardhan, S. Ansari, and P. Mohapatra, *Sep. Sci. Technol.* 49, 1509 (2014).
- [14]. N. Borsch, and O. Petrukhin, *Zh Anal Khim.* 33, 1805 (1978).
- [15]. Z. Marckzenko *Spectrophotometric determination of trace elements*, 1st edn. Wiley, (1976) Chichester.



## Ammonium Chloride in PEG As an Efficient Catalyst for Synthesis Dihydropyrano [3,2-C] Chromene-3-Carbonitrile Derivatives

Manojkumar R. Tapare<sup>1</sup>, Rahul Kamble\*<sup>1</sup>

<sup>1</sup>Department of Chemistry, Amruteshwar Arts, Commerce and Science College, Vinzar, Pune- 412213,  
Maharashtra, India

### ABSTRACT

The present paper reports a green, efficient, and rapid method for the synthesis of 2-amino-5-oxo-4-phenyl-4,5-dihydropyrano[3,2-c]chromene-3-carbonitrile derivatives by one-pot condensation of 4-hydroxy-2H-chromen-2-one, aldehyde, and malononitrile in the presence of ammonium chloride in PEG-400. The method has the advantages of operational simplicity, mild reaction conditions, short reaction time, and no environmental impact.

**Keywords:** Ammonium chloride, Green chemistry, PEG-400.

### I. INTRODUCTION

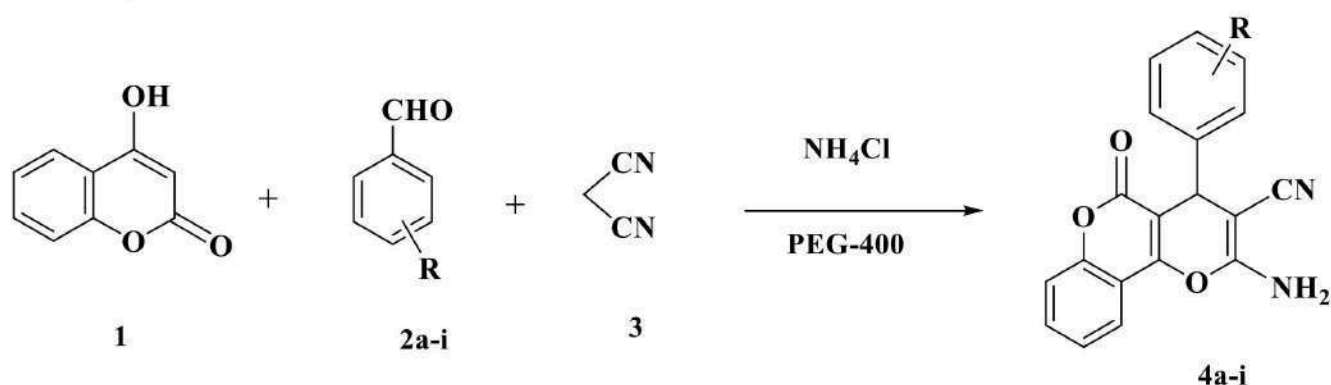
Advances in organic synthesis enable chemists to prepare most natural product targets. Even with state of the art methods, however, syntheses often require many synthetic manipulations and purifications, resulting in low overall yields and generation of large amounts of chemical waste. To address these issues, increasing synthetic efficiency and reducing E-factors (defined as the ratio of the mass of waste produced to the mass of product) are becoming more important in designing synthetic routes [1]. One approach to streamline organic synthesis is through tandem and sequential reactions that accomplish multiple steps in a single flask and minimize isolations, purifications, and solvent use. Recently, we have reported several MCRs on the synthesis of Pyrano-[2,3- c ]-pyrazoles [2-4]. It is well known that pyrans are important core units in a number of natural products [4] and photochromic materials [5]. Compounds with pyran ring system have many pharmacological properties and play important roles in biochemical process [5]. Moreover, 4H-pyrans are useful intermediates for the synthesis of various compounds, such as pyranopyridine derivatives [6], polyazanaphthalenes [7], pyrano[2]pyrimidines [8], and pyridin-2-ones [9]. Therefore, preparation of this heterocyclic nucleus has gained great importance in organic synthesis. There are many sound reports expressing that pyrano[3,2- c]chromene is a class of vital heterocycles with a wide range of biological effects [10] such as spasmolytic, diuretic, anticoagulant, anti-cancer and anti-anaphylactic activity [11]. Moreover fused chromene derivatives have a relatively broad spectrum with high activity profile against various bacteria and fungi [12]<sup>26</sup> along with antiproliferative [13], sexpheromonal [14], mutagenic [15],

antitumor [16], anti-viral [17,18] and central nervous system activities [19]. Recently, several methods have been reported for the synthesis of pyran derivatives via a three-component condensation of  $\beta$ -dicarbonyl compounds with aldehydes and malononitrile [20].

As there is increasing environmental consciousness in chemical research and industry, the challenge for a sustainable environment calls for clean procedures that can avoid using volatile organic solvents and heavy metal ions as catalysts. Together with the volatile character and very poor environmental and toxicological profiles of the most commonly used compounds, there is a need for alternative solvents that may replace the present ones [1, 21, 22]. Several approaches within the green chemistry framework have been proposed in the last few years; supercritical fluids and ionic liquids being the most promising and extended ones among academia. In spite of the promising characteristics of these alternative fluids, their extension to large scale industrial applications is very scarce nowadays, especially for ionic liquids. Among these alternative organic solvents with adequate properties, polyethylene glycol-400 (PEG-400) [22] is one of the most promising ones.

## II. RESULT AND DISCUSSION

As part of a continuing effort in our laboratory toward the development of new multi-component condensation reactions, we became interested in the possibility of developing environmental friendly methodologies for the preparation of 2-amino-5-oxo-4-phenyl-4, 5-dihydropyrano[3,2-c]chromene-3-carbonitrile derivatives through a three-component condensation reaction of 4-hydroxyquinolin-2(1H)-one, aldehydes, and malononitrile. By a preliminary experiment, we found that this three-component condensation reaction in PEG-400 using ammonium chloride as a promoter worked very well. Therefore, we herein report a green, efficient, and rapid procedure for the one-pot synthesis of 2-amino-5-oxo-4-phenyl-4, 5-dihydropyrano[3,2-c]chromene-3-carbonitrile derivatives by using ammonium chloride as the catalyst in excellent yields (Scheme 1).



**Scheme 1.** Synthetic route of 2-amino-5-oxo-4-phenyl-4, 5-dihydropyrano[3,2-c]chromene-3-carbonitrile derivatives

Initially, we investigated the three-component condensation reaction of 4-hydroxy-2H-chromen-2-one 1, benzaldehyde 2a, and malononitrile 3 in PEG-400 as green solvent in the presence of different catalysts and the results are summarized in Table 1.

**Table 1.** Comparison of Catalytic Activity of Various Catalysts for synthesis of pyrano[3,2-c]chromene-3-carbonitrile derivatives

Entry	Catalyst (mol/wt %)	Time (min)	Yield of 4a <sup>a</sup> (%)
1	PTSA (20)	>60	70
2	NH <sub>2</sub> SO <sub>3</sub> H (20)	>60	58
3	SiO <sub>2</sub> -NaHSO <sub>3</sub> H (10)	>60	60
4	ZnCl <sub>2</sub> (20)	>60	52
5	MgCl <sub>2</sub> (20)	>60	62
6	TEA (20)	30	70
7	Piperidine (20)	20	78
8	MgO (20)	20	60
9	Ammonium chloride (1)	25	75
10	Ammonium chloride (5)	22	89
11	Ammonium chloride (10)	20	94
12	Ammonium chloride (20)	25	91
13	KF-Al <sub>2</sub> O <sub>3</sub> (0.3 g)	120	78

<sup>a</sup>Isolated yields.

In this three-component reaction, we found that catalysts had significant effects on the reaction time and yields (Table 1). The results indicated that in the presence of proton acids and classical Lewis acids as catalysts the yields at lower side in EtOH under reflux conditions for 60 min, such as TsOH, NH<sub>2</sub>SO<sub>3</sub>H, SiO<sub>2</sub>-NaHSO<sub>3</sub>, ZnCl<sub>2</sub>, and MgCl<sub>2</sub> (Table 1, entries 1–5). The model reaction was carried out using ammonium chloride in PEG, to our delight, the desired condensation product 4a was obtained in moderate to excellent yields (50–94%), which meant that this three-component condensation reaction of 4-hydroxy-2H-chromen-2-one 1, benzaldehyde 2a, and malononitrile 3 could proceed smoothly catalyzed by mild acidic condition. As shown in Table 1, ammonium chloride was found to be the most effective catalyst in terms of reaction time and yields (Table 1, entries 9–12). Further-more, we found that the yields of 4a were improved as the amount of ammonium chloride increased from 5% to 10%, and the yields plateaued when the amount of ammonium chloride was further in-creased from 20% to 50% (Table 1, entries 11–14). However, only 78% yield of the desired product was obtained in the presence of KF-Al<sub>2</sub>O<sub>3</sub> as catalyst for 5 h (Table 1, entry 13). Therefore, 10 wt % of ammonium chloride was considered to be the most suitable.

As shown in Table 2, only a trace amount of the target product 4a was observed when the mixture was heated for 60 min in the presence of 10 wt % of ammonium chloride in ethanol, methanol, DMF as well as under a solvent-free condition (Table 2, entries 1-4). The increasing interest of organic chemists in the use of PEG (Table 2, entries 5-8) as a solvent of choice and its unique properties [2-4] attracted our attention to its use as a green solvent in the present study. The reaction using PEG-400 (94%) as the solvents gave the corresponding product 4a in high yields and in short reaction time (Table 2, entries 7 and 12). From the economic and environmental point of view, PEG-400 was chosen as the reaction medium for all further

reactions. Therefore, the best reaction conditions were obtained by using 10 wt % of ammonium chloride as the catalyst in PEG-400.

**Table 2.** Study of effect of solvent on synthesis of pyrano[3,2-c]chromene-3-carbonitrile derivatives.

Entry	Solvent	Temp °C	Time (Min)	Yield <sup>a</sup> (%)
1	None	100	120	Traces
2	Ethanol	60	60	50
3	Methanol	60	60	46
4	DMF	100	30	80
5	PEG-200	60	30	82
6	PEG-400	Rt	25	89
7	PEG-400	60	20	94
8	PEG-600	60	30	88

<sup>a</sup> Isolated Yields.

Having established the optimized reaction conditions, we then successfully synthesized a variety of 2-amino-5-oxo-4-phenyl-4, 5-dihydropyrano[3,2-c]chromene-3-carbonitrile derivatives **4** and the results were summarized in Table 3.

**Table 3.** Physical data of ammonium chloride catalyzed synthesis of pyrano[3,2-c]chromene-3-carbonitrile derivatives.

Product	Ar	Yield <sup>a</sup> (%)	MP°C Found(Reported)
2a	C <sub>6</sub> H <sub>5</sub> <b>2a</b>	94	255-257 (256-258)[23]
2b	4-CH <sub>3</sub> C <sub>6</sub> H <sub>4</sub> <b>2b</b>	92	252-254 (250-252)[23]
2c	4-CH <sub>3</sub> O-C <sub>6</sub> H <sub>4</sub> <b>2c</b>	90	241-244 (240-242)[23]
2d	4-F-C <sub>6</sub> H <sub>4</sub> <b>2d</b>	89	210-212
2e	4-Cl-C <sub>6</sub> H <sub>4</sub> <b>2e</b>	92	264-267 (263-265)[23]
2f	4-Br-C <sub>6</sub> H <sub>4</sub> <b>2f</b>	91	247-250 (249-251)[23]
2g	3-CH <sub>3</sub> O-4-HOC <sub>6</sub> H <sub>3</sub> <b>2g</b>	94	228-230
2h	4-OH-C <sub>6</sub> H <sub>4</sub> <b>2h</b>	87	258-260
2i	3-OH-C <sub>6</sub> H <sub>4</sub> <b>2i</b>	89	263-265
2j	4-NO <sub>2</sub> -C <sub>6</sub> H <sub>4</sub> <b>2j</b>	90	259-261 (258-260)[23]
2k	3-NO <sub>2</sub> -C <sub>6</sub> H <sub>4</sub> <b>2k</b>	87	261-263 (262-264) [23]
2l	2-Cl-C <sub>6</sub> H <sub>4</sub> <b>2l</b>	93	275-277
2m	2,4-Cl <sub>2</sub> C <sub>6</sub> H <sub>3</sub> <b>2m</b>	90	256-258 (257-259)[23]
2n	2-OH-C <sub>6</sub> H <sub>4</sub> <b>2i</b>	88	280-282

<sup>a</sup>Isolated yields.

A series of aromatic, heterocyclic, and aliphatic aldehydes were selected to undergo the condensation in the presence of ammonium chloride. As shown in Table 3, aromatic aldehydes **2** carrying either electron-donating or electron-withdrawing substituent reacted efficiently giving excellent yields (Table 3, entries 1–14). Hence, the effect of the nature of the substituent on the aromatic ring showed no obvious effect on this

conversion. The experimental procedure is an efficient, green, convenient, rapid and has the ability to tolerate a variety of other functional groups, such as methoxyl, nitro, hydroxyl, and halides under these reaction conditions.

### III. CONCLUSIONS

In summary, the present method discloses a new and simple modification of the condensation of 4-hydroxyquinolin-2(1H)-one **1**, aldehyde **2**, malononitrile **3** to the synthesis of 2-amino-5-oxo-4-phenyl-4, 5-dihydropyrano[3,2-c]chromene-3-carbonitrile derivatives **4** by using ammonium chloride as a catalyst in PEG-400. The present method has the advantages of operational simplicity, mild reaction conditions, short reaction time, improved yields of the products and characteristic recyclable ability of catalyst, thus making it a useful and important addition to the existing methods. Undoubtedly, this reaction should be useful to design a simple work up procedure for the synthesis of 2-amino-5-oxo-4-phenyl-4, 5-dihydropyrano[3,2-c]chromene-3-carbonitrile derivatives **4**.

### IV. EXPERIMENTAL

All the melting points were uncorrected and determined in an open capillary tube. The chemicals and solvents used were of laboratory grade and were purified. Completion of the reaction was monitored by thin layer chromatography on precoated sheets of silica gel-G (Merck, Germany) using iodine vapour for detection. IR spectra were recorded in KBr pellets on a FTIR Shimadzu spectrophotometer. <sup>1</sup>H NMR (300MHz) and <sup>13</sup>C NMR (75 MHz) spectra were recorded in DMSO-*d*<sub>6</sub> with an Avance spectrometer (Bruker, Germany) at a 300-MHz frequency using TMS as an internal standard. Mass spectra were recorded on an EI-Shimadzu QP 2010 PLUS GC-MS system (Shimadzu, Japan). Elemental analyses were performed on a Carlo Erba 106 Perkin-Elmer model 240 analyzer (Perkin-Elmer, USA).

**4.1. General procedure for the synthesis of 2-amino-5-oxo-4-phenyl-4, 5-dihydropyrano[3,2-c]chromene-3-carbonitrile derivatives 4:** A mixture of 4-hydroxy-2H-chromen-2-one **1** (1 mol), aldehyde (2a-2l) (1.1 mol), malononitrile **3** (1.1 mmol), and ammonium chloride (10 wt %) in PEG-400 (10 mL) was heated to 60°C under stirring for the given time (Table 3). After completion (by TLC), the reaction mixture was filtered to separate catalyst then cooled to room temperature, then ice cold water (50 mL) was added to the mixture and stirred magnetically for 5-10 min. The solid was filtered and recrystallized from EtOH to afford the pure products **4 a-i**.

**4.1.1. Product 4a:** Pale yellow powder; Yield: 294 mg, 93 %; m.p. 255-257 °C (recrystallized from EtOH); IR (KBr) cm<sup>-1</sup>: 3323, 3204, 2195, 1720, 1668, 1601, 1519, 1381, 1264, 1143, 1048, 761, 481; <sup>1</sup>H NMR (300 MHz, DMSO-*d*<sub>6</sub> TMS) δ ppm; 4.41 (1H, s, CH), 7.21-7.30 (5H, m, arom.), 7.36 (2H, s, NH<sub>2</sub>), 7.40-7.48 (2H, m, arom.), 7.69 (1H, t, J = 7.2 Hz, arom.), 7.86 (1H, d, J = 7.2 Hz, arom.); <sup>13</sup>C NMR(75 MHz, DMSO-*d*<sub>6</sub>, TMS) δ ppm; 37.1, 58.1, 104.1, 113.0, 116.6, 119.3, 122.6, 124.7, 127.2, 127.7, 128.6, 133.0, 143.4, 152.2, 153.5, 158.1, 159.6; Anal. Calcd for C<sub>19</sub>H<sub>12</sub>N<sub>2</sub>O<sub>3</sub>: C, 72.15; H, 3.82; N, 8.86 %. Found: C, 72.11; H, 3.81; N, 8.84 %.

4.1.2. Product 4b: Grayish solid; Yield: 304 mg, 92 %; m.p. 252-254 °C (recrystallized from EtOH); IR (KBr)  $\text{cm}^{-1}$ : 3319, 3310, 3195, 2196, 1718, 1676, 1608, 1377, 1057, 954, 757, 506;  $^1\text{H}$  NMR (300 MHz, DMSO- $d_6$  TMS)  $\delta$  ppm; 2.21 (3H, s,  $\text{CH}_3$ ), 4.36 (1H, s, CH), 7.05-7.11 (4H, m, arom.), 7.34 (2H, s,  $\text{NH}_2$ ), 7.39-7.47 (2H, m, arom.), 7.66 (1H, t,  $J = 9.0$  Hz, arom.), 7.86 (1H, d,  $J = 9.0$  Hz, arom.);  $^{13}\text{C}$  NMR(75 MHz, DMSO- $d_6$ , TMS)  $\delta$  ppm; 20.7, 36.7, 58.2, 104.2, 113.1, 116.6, 117.8, 119.3, 122.5, 124.7, 127.6, 129.1, 132.9, 136.3, 140.5, 152.2, 153.3, 158.0, 159.6. Anal. Calcd for  $\text{C}_{20}\text{H}_{14}\text{N}_2\text{O}_3$ : C, 72.72; H, 4.27; N, 8.48 %. Found: C, 72.74; H, 4.27; N, 8.47 %.

4.1.3. Product 4c: White solid; Yield: 304 mg, 88 %; m.p. 221-223 °C (recrystallized from EtOH); IR (KBr)  $\text{cm}^{-1}$ : 3370, 3290, 3182, 2191, 1709, 1671, 1605, 1571, 1507, 1459, 1379, 1319, 1251, 1178, 1111, 1052, 1026, 951, 834, 756, 564, 529;  $^1\text{H}$  NMR (300 MHz, DMSO- $d_6$  TMS)  $\delta$  ppm; 3.68 (3H, s,  $\text{OCH}_3$ ), 4.35 (1H, s, CH), 6.82 (2H, d,  $J = 8.4$  Hz, arom.), 7.13 (2H, d,  $J = 8.4$  Hz, arom.), 7.33 (2H, s,  $\text{NH}_2$ ), 7.38-7.47 (1H, m, arom.), 7.63-7.69 (1H, m, arom.), 7.84 (1H, dd,  $J = 7.5$  Hz,  $J = 1.2$  Hz, arom.), 7.93 (1H, d,  $J = 9.0$  Hz, arom.);  $^{13}\text{C}$  NMR(75 MHz, DMSO- $d_6$ , TMS)  $\delta$  ppm; 36.2, 55.1, 58.4, 104.3, 114.0, 115.3, 116.6, 119.4, 122.5, 124.8, 128.8, 132.9, 133.5, 135.5, 152.2, 153.1, 158.0, 159.6, 160.5; Anal. Calcd for  $\text{C}_{20}\text{H}_{14}\text{N}_2\text{O}_4$ : C, 69.36; H, 4.07; N, 8.09 %. Found: C, 69.38; H, 4.06; N, 8.10 %.

4.1.4. Product 4e: Light yellow colored solid; Yield: 315 mg, 90 %; m.p. 265-267 °C (recrystallized from EtOH); IR (KBr)  $\text{cm}^{-1}$ : 3402, 3323, 3204, 2197, 1714, 1670, 1604, 1509, 1379, 1264, 1143, 1047, 761, 481;  $^1\text{H}$  NMR (300 MHz, DMSO- $d_6$  TMS)  $\delta$  ppm; 4.46 (1H, s, CH), 7.23 (2H, d,  $J = 8.4$  Hz, arom.), 7.43-7.50 (6H, m,  $\text{NH}_2$ +arom.), 7.68-7.72 (1H, m, arom.), 7.88 (1H, d,  $J = 7.2$  Hz, arom.);  $^{13}\text{C}$  NMR(75 MHz, DMSO- $d_6$ , TMS)  $\delta$  ppm; 36.4, 57.7, 103.6, 113.1, 116.6, 119.1, 122.6, 124.8, 128.6, 129.6, 131.7, 133.1, 142.4, 152.3, 153.6, 158.1, 159.7; Anal. Calcd for  $\text{C}_{19}\text{H}_{11}\text{ClN}_2\text{O}_3$ : C, 65.06; H, 3.16; N, 7.99 %. Found: C, 65.11; H, 3.19; N, 8.02 %.

4.1.5. Product 4f: Yellow colored solid; Yield: 367 mg, 93 %; m.p. 220-222 °C (recrystallized from EtOH); IR (KBr)  $\text{cm}^{-1}$ : 3385, 3305, 3188, 2191, 1712, 1674, 1606, 1375, 1060, 759, 510;  $^1\text{H}$  NMR (300 MHz, DMSO- $d_6$  TMS)  $\delta$  ppm; 5.12 (1H, s, CH), 7.17-7.23 (3H, m,  $\text{NH}_2$ +arom.), 7.34 (3H, t,  $J = 8.7$  Hz, arom.), 7.46 (4H, t,  $J = 10.1$  Hz, arom.);  $^{13}\text{C}$  NMR(75 MHz, DMSO- $d_6$ , TMS)  $\delta$  ppm; 37.0, 56.6, 116.5, 116.9, 119.5, 120.7, 124.8, 125.1, 125.8, 129.8, 130.4, 131.9, 134.5, 142.5, 150.3, 154.1, 159.0; Anal. Calcd for  $\text{C}_{19}\text{H}_{11}\text{BrN}_2\text{O}_3$ : C, 57.74; H, 2.81; N, 7.09 %. Found: C, 57.77; H, 2.82; N, 7.08 %.

4.1.6. Product 4j: Yellow colored solid; Yield: 336 mg, 93 %; m.p. 251-253 °C (recrystallized from EtOH); IR (KBr)  $\text{cm}^{-1}$ : 3390, 3212, 3179, 2197, 1662, 1575, 1465, 1409, 1260, 1227, 746, 548;  $^1\text{H}$  NMR (300 MHz, DMSO- $d_6$  TMS)  $\delta$  ppm; 4.64 (1H, s, CH), 7.44 (2H, t,  $J = 7.5$  Hz, arom.), 7.49-7.54 (2H, m, arom.), 7.57 (2H, s,  $\text{NH}_2$ ), 7.69 (1H, t,  $J = 7.5$  Hz, arom.), 7.87 (1H, d,  $J = 7.5$  Hz, arom.), 8.14 (2H, d,  $J = 8.4$  Hz, arom.);  $^{13}\text{C}$  NMR(75 MHz, DMSO- $d_6$ , TMS)  $\delta$  ppm; 22.3, 36.9, 43.9, 56.9, 102.9, 113.0, 116.7, 118.9, 122.7, 123.8, 124.8, 129.2, 133.2, 146.7, 150.8, 152.4, 154.0, 158.1, 159.6. Anal. Calcd for  $\text{C}_{19}\text{H}_{11}\text{N}_3\text{O}_5$ : C, 63.16; H, 3.07; N, 11.63 %. Found: C, 63.17; H, 3.08; N, 11.65 %.

4.1.7. Product 4k: Yellow colored solid; Yield: 332 mg, 92 %; m.p. 257-258 °C (recrystallized from EtOH); IR (KBr)  $\text{cm}^{-1}$ : 3382, 3235, 3179, 2193, 1728, 1663, 1600, 1416, 1298, 1173, 1119, 1010, 753, 472;  $^1\text{H}$  NMR (300 MHz, DMSO- $d_6$  TMS)  $\delta$  ppm; 4.69 (1H, s, CH), 7.42 (1H, d,  $J = 8.7$  Hz, arom.), 7.48 (1H, d,  $J = 7.8$  Hz, arom.), 7.52 (2H, s,  $\text{NH}_2$ ), 7.59 (1H, t,  $J = 7.8$  Hz, arom.), 7.68 (1H, dt,  $J = 8.0$  Hz,  $J = 8.0$  Hz,  $J = 1.4$  Hz, arom.), 7.76

(1H, t, J = 7.8 Hz, arom.), 7.87 (1H, d, J = 7.2 Hz, arom.), 8.08 (2H, d, J = 7.8 Hz, arom.); <sup>13</sup>C NMR(75 MHz, DMSO-d<sub>6</sub>, TMS) δ ppm; 22.3, 36.8, 43.9, 57.1, 103.0, 113.0, 116.7, 119.0, 122.5, 124.8, 130.2, 133.2, 134.8, 145.6, 148.0, 152.4, 154.0, 158.3, 159.7. Anal. Calcd for C<sub>19</sub>H<sub>11</sub>N<sub>3</sub>O<sub>5</sub>: C, 63.16; H, 3.07; N, 11.63 %. Found: C, 63.19; H, 3.06; N, 11.66 %.

## V. ACKNOWLEDGENTS

The author MVG gratefully acknowledge to Savitribai Phule Pune University, Pune for Financial Assistance in the form of Minor Research Project.

## VI. REFERENCES

- [1]. Sheldon, R. A. Green Chem. 2007, 9, 1273–1283; b) Sheldon, R. A. Green Chem., 2005, 7, 267-278.
- [2]. Kamble, R. D.; Dawane, B. S.; Yemul, O. S.; Kale A. B.; Patil, S. D. Res Chem Intermed., 2013, 39, 3859–3866.
- [3]. Chobe, S. S.; Kamble R. D.; Patil, S. D.; Acharya, A. P.; Hese, S. V.; Yemul, O. S.; Dawane, B. S. Med Chem Res., 2013, 22, 5197–5203.
- [4]. Dawane, B. S.; Yemul, O. S.; Chobe, S. S.; Mandawad, G. G.; Kamble, R. D.; Shinde, A. V.; Kale, V. S.; Hurne, A. O.; Pawde, M. A.; Kale, M. P.; Desai, N. P.; Salgare, R. R.; Patil, M. B.; Mundhe S. N.; and Chavan, S. R. Der Pharma Chemica, 2011, 3(3), 300-305.
- [5]. Kumar, S.; Hernandez, D.; Hoa, B.; Lee, Y.; Yang, J. S.; McCurdy, A. Org. Lett. 2008, 10, 3761–3764.
- [6]. O'Callaghan, C. N.; McMurry, T. B. H. J. Chem. Res., Synop. 1995, 214-217.
- [7]. Adbel-Fattah, A. H.; Hesien, A. M.; Metwally, S. A.; Elnagdi, M. H. Liebigs Ann. Chem. 1989, 585–588.
- [8]. Quintela, J. M.; Peinador, C.; Moreira, M. J. Tetrahedron, 1995, 51, 5901–5912.
- [9]. Srivastava, S.; Batra, S.; Bhaduri, A. P. Indian J. Chem., Sect. B 1996, 35B, 602–604
- [10]. Green, G.R.; Evans, J.M.; Vong, A.K.; Katritzky, A.R. ; Rees, C.W. E.F. Scriven(Eds.), Comprehensive Heterocyclic Chemistry II, 5, Pergamon Press, Oxford, 1995, p. 469.
- [11]. Foye, W.O. Principi Di Chemico Farmaceutic. Piccin, Padova, Italy, 1991, 416-420.
- [12]. Khafagy, M.M.; El-Wahab, A.H.F.A.; Eid, F.A.; El-Agrody, A.M.; Farmaco 2002, 57, 715-722.
- [13]. Dell, C.P.; Smith, C.W. Eur. Patent Appl. EP537949 Chem. Abstr. 1993, 119, 139102d.
- [14]. Bianchi, G.; Tava, A. Agric. Biol. Chem. 1987, 51, 200-2002.
- [15]. Hiramoto, K.; Nasuhara, A.; Michiloshi, K.; Kato, T.; Kikugawa, K. Mutat. Res. 1997, 395, 47-56.
- [16]. Mohr, S. J.; Chirigos, M. A.; Fuhrman, F. S.; Pryor, J. W. Cancer Res. 1975, 35, 3750-37-54.
- [17]. Smith, W. P.; Sollis, L. S.; Howes, D. P.; Cherry, C. P.; Starkey, D. I.; Cogley, N. K. J. Med.Chem. 1998, 41, 787-797.
- [18]. Martinez, A.G.; Marco, L.J. Bioorg. Med. Chem. Lett. 1997, 7, 3165-3170.
- [19]. Eiden, F.; Denk, F. Arch. Pharm. Weinheim Ger. Arch. Pharm. 1991, 324, 353.
- [20]. Peng, Y.; Song, G. Catal. Commum. 2007, 8, 111–114.

- [21].DeSimone, J. M. *Science*, 2002, 297, 799-803.
- [22].Capello, C.; Fischer, U. and Hungerbuhler, K. *Green Chem.*, 2007, 9, 927-943.
- [23].Mohammadi, A. S. and Balalaie, S. *Tetrahedron Letters*, 2007, 48, 3299–3303.



## Synthesis of Spiro-fused Heterocycles under Aerobic Conditions by using Polymer Gel Entrapped Catalyst

Shinde S. R<sup>1</sup>, Gaikwad R. S<sup>1</sup>, Adlinge N. P<sup>1</sup>, Ingawale A. R<sup>1</sup>, Kadam S. N<sup>1</sup>, Rajashri Salunkhe<sup>2\*</sup>

<sup>1</sup>Department of Chemistry, Vidnyan Mahavidyalaya Sangola, 413307, Maharashtra, India

<sup>2</sup>Department of Chemistry, Shivaji University, Kolhapur, 416004, Maharashtra, India

### ABSTRACT

Spiro-fused heterocycles were synthesized in good to excellent yields by a pseudo three-component reaction of an aldehyde, urea and Meldrum's acid or barbituric acid at ambient temperature.

**Keyword:** Aldehydes, Gel Entrapped-ZnCl<sub>2</sub>, modified Biginelli reaction, recyclability.

### I. INTRODUCTION

Multi-component reactions (MCRs) have recently emerged as valuable tools in the preparation of structurally diverse chemical libraries of drug-like heterocyclic compounds [1]. The Biginelli reaction is a well-known multi-component reaction involving a one-pot cyclocondensation of an aldehyde, active methylene compounds like Meldrum's acid or barbituric acid and urea [2-4]. Multi-component reactions (MCRs) have recently gained tremendous importance in organic and medicinal chemistry. The main contributing factors are the high atom economy, wide application in combinatorial chemistry and diversity-oriented synthesis [5-11]. Typical examples of the various homogeneous catalysts employed are polyphosphate ester [12], LaCl<sub>3</sub>·7H<sub>2</sub>O [13] and LiClO<sub>4</sub> [14]. Recently Lewis acid catalyzed Biginelli reactions have been extensively reported in the literature.

The use of Lewis acids in organic synthesis, especially in catalysis is one of most rapidly developing fields in synthetic organic chemistry [15]. While various kinds of Lewis acids catalyzed reactions have been developed and many of them applied in industries, these reactions must be carried out strictly under moisture-free conditions [16, 17]. After the completion of reaction, the only viable alternative for separating them is by a destructive water quench. This fact makes the use of Lewis acids as a prime source of the huge quantities of inorganic waste produced within chemical industries. An intriguing line of development in this regard is to replace stoichiometries technologies involving hazardous reagents like Lewis acids with cleaner alternatives. In this regard, we envisioned that the entrapment of Lewis acids in matrix of agar-agar, the concept acronymed as gel entrapped Lewis acids (GELAs), can prove to be highly attractive strategy to alleviate the problems associated with Lewis acids. The agar-agar is natural hydrosoluble carbohydrate polymer composed

of linear chains of repeating agarobiose units alternating between 3-linked- $\beta$ -D-galactopyransoyl (G) and 4-linked 3,6-anhydro- $\alpha$ -L-galactopyransoyl(LA) units (**Fig. 1**). The bioavailability and potent biocompatibility of agar-agar explains the interest taken by us for entrapment. We hypothesized that concept of GELA can combine the properties of Lewis acids with that of solid support thus facilitating significant advances in selectivity and activity. Additionally, we envisioned the intact network structure of GELAs will allow for a robust recycling with excellent activity.

Meldrum's acid (2,2-dimethyl-1,3-dioxane-4,6-dione isopropylidene malonate) is an active methylene compound having rigid cyclic structure with high acidity ( $pK_a=4.97$ ) which undergoes hydrolysis very easily. Barbituric acid or malonylurea or 6-hydroxyuracil is an organic compound based on a pyrimidine heterocyclic skeleton. It is an odorless powder soluble in water. Barbituric acid is the parent compound of barbiturate drugs, although barbituric acid itself is not pharmacologically active. Knowing the chemical and pharmacological importance the spiro-fused heterocycles and as a part of our continuing efforts towards the development of sustainable routes for preparation of biologically active compounds, we report herein an efficient multi-component synthesis of spiro-fused heterocycles by using GELAs.

## II. RESULTS AND DISCUSSION

Initially, we focused our attention towards the preparation of GELAs. The  $ZnCl_2$  and  $AlCl_3$  were used as the prototype Lewis acid in these studies. A series of experiments were under taken in which different concentrations of selected Lewis acids (5-25 %) were dissolved in a varying amount of agar-agar in water. After a substantial experimentation, we found that 20 % w/w of agar-agar aqua gel containing 10 % Lewis acids resulted in the formation of soft gel that served as GELAs in the present work. The GELAs are white jelly like substance that could be cut into pieces. The changes in physical nature of GELAs were studied in different solvents like ethanol, dichloromethane, toluene, acetone, dichloromethane and isopropanol. We found that gel remained intact in these organic solvents. On the contrary, the GELAs swelled in water and became soft.

Thermal behaviour of GELAs was investigated by thermogravimetric analysis (TGA) and differential thermal analysis (DTA) (**Fig. 2**). The thermograms displayed an initial weigh loss upto 225 °C accompanied by an endotherm corresponding to loss of water molecules accumulated in the GELAs. A second weight loss which occurs between 225 °C to 520 °C can be attributed to thermal decomposition polymeric matrix of agar-agar. This is followed by small weight loss (~ 4%) which can be attributed to the decomposition of metal halide resulting in the formation metallic species. These results revealed that the entrapment of Lewis acids into matrix of agar-agar does not affect the thermal stability of polymer.

Our next task was to demonstrate the catalytic activity of GELA in the synthesis of Spiro-fused heterocycles. A model reaction between the Meldrum's acid/ barbituric acid (5 mmol), urea (5 mmol) and benzaldehyde (5x3 mmol) was carried out. Typically, the reactions were carried out at ambient temperature in open air using 1 gm of GELAs with 5 mmol of substrates in ethanol. The reaction proceeded efficiently yielding the Spiro-fused heterocycles in excellent yield within very short time. In order to delineate the role of GELAs, a control experiment was carried out in which the model reaction was performed without gel catalyst. No reaction was

observed even after prolonged reaction time. We further examined the effect of different atmospheres on the model reaction. We observed that the reaction carried out under aerobic conditions.

As better results were obtained for ZnCl<sub>2</sub>-GELA as compared to AlCl<sub>3</sub>, we employed this particular catalyst for further studies. The generality of the protocol was validated by reacting commercially available Meldrum's acid (pK<sub>a</sub>=4.97) / barbituric acid (pK<sub>a</sub>=4.01) (5 mmol), urea (5 mmol) and benzaldehyde (5x3 mmol) (Scheme 1) under aerobic conditions. In general the corresponding Spiro-fused heterocycles were obtained in good to excellent yields. No significant effects were observed for the substituents on benzaldehydes. The striking feature of all the reactions was the isolation of products. During the course of the reaction the product precipitates out and can be isolated simply by filtration. The product obtained after sufficient washing with ethanol was found to be practically pure. The identity of all the compounds was ascertained on the basis of IR, <sup>1</sup>H NMR, <sup>13</sup>C NMR and mass spectroscopy data. The physical and spectroscopic data are in consistent with the proposed structures.

It has been well established that in case of the gel entrapped catalysts, the reagent trapped in the gel may leach into the solvent. Atomic absorption spectroscopy was used for assessing the stability of ZnCl<sub>2</sub>-GELA towards leaching. The analysis revealed that only 65.5 mg/L is leached from 1 gm of catalyst. These results confirm that ZnCl<sub>2</sub>-GELA is stable under the operating conditions used in experiment. Using the amount of ZnCl<sub>2</sub> same as that leached out, the reaction between Meldrum's acid/ barbituric acid (5 mmol), urea (5 mmol) and benzaldehyde (5x3 mmol) did not give quantitative yield of the corresponding product. This clearly demonstrated that catalysis was solely due to intact gel rather than leached ZnCl<sub>2</sub>. Moreover, hot filtration experiments proved that these catalysts are truly heterogeneous.

Applications of green chemistry and for industrial point of view, the recovery and reusability of catalyst is an important factor. To investigate the possibility of catalyst recycling, the model reaction using ZnCl<sub>2</sub>-GELA in ethanol was carried out. After completion of the reaction, the ZnCl<sub>2</sub>-GELA was recovered by simple filtration, washed with ethanol and subsequently reused in another catalytic cycle with identical substrates. We were delighted to find that the catalyst could be reused for seven runs with excellent yield of product (Fig. 3). In addition, the catalyst can be stored and handled in air without deterioration. It was interesting to note that the rates and yields of the reactions were almost same when the catalyst was used after one month of storage on the bench top in air at room temperature.

### III. EXPERIMENTAL SECTION

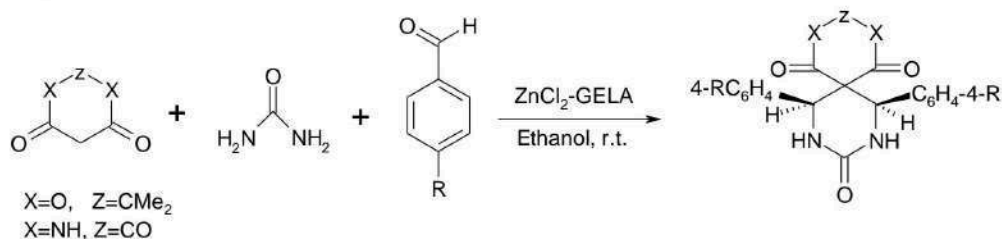
Melting points were determined in an open capillary and are uncorrected. Infrared spectra were recorded on a PerkinElmer FT-IR spectrometer. The samples were examined as KBr discs ~5 % w/w. <sup>1</sup>H NMR and <sup>13</sup>C NMR spectra were recorded on a Bruker Avon 300 spectrometer using DMSO-d<sub>6</sub> as solvent and TMS as internal reference. The mass spectrum was recorded on Thermo, LCQ Tune spectrometer. TGA-DTA analysis was recorded on SDS Q600 N20.9 in nitrogen. All the chemicals were obtained from s. d. FiNE CHEM, SPECTROCHEM and used without further purification.

### Preparation of Gel Entrapped ZnCl<sub>2</sub> (GELA)

A mixture of agar-agar (20 g) in water (140 mL) was prepared first and then added the solution of ZnCl<sub>2</sub> (10 g) in water (10 mL). The resultant solution was boiled with stirring for few minutes and cooled in ice bath to yield the desired GELAs. The GELA is a milky jelly like substance that can be cut into small cubes.

### Synthesis of Spirofused Heterocyclic Compound

A mixture of Meldrum's acid/ barbituric acid (5 mmol), urea (5 mmol) and benzaldehyde (5x3 mmol) was stirred in the presence of GELA (1 g) in 5 mL of ethanol at ambient temperature till the completion of the reaction as monitored by TLC. The resulting crude product was filtered and recrystallized from ethanol to yield the desired product.



**Scheme 1:** GELA catalyzed multi-component synthesis of spirofused heterocyclic compound

## IV. CONCLUSION

In conclusion, the present method is an operationally simple and environmental friendly procedure for the synthesis of spirofused heterocyclic compounds using ZnCl<sub>2</sub>-GELA at ambient temperature. In addition recyclability, cost effective, short reaction time, easy handling, clean reaction profile, excellent yields of products without any use of more purification and no energy consumption make this methodology a valid contribution to existing processes in the field of spirofused heterocyclic compounds synthesis. To the best of our knowledge, this procedure provides the first example of ZnCl<sub>2</sub>-GELA catalyzed efficient synthetic method for spirofused heterocyclic derivatives.

## V. ACKNOWLEDGEMENTS

We gratefully acknowledge the financial support from the Department of Science Technology and University Grants Commission for FIST and SAP respectively. One of the author Miss Shital Shinde thanks UGC, New Delhi for the research fellowship.

## VI. REFERENCES

- [1]. Ugi, I.; Dömling, A.; Hörl, W. Endeavour 1994, 18,115. (b) Tietze, L. F.; Modi, A. Med.Res. Rev. 2000, 20, 304. (c) Ugi, I.; Dömling, A.; Werner, B. J. Heterocyclic Chem. 2000, 37, 647. (d) Orru R. V. A.; de Greef, M. Synthesis 2003, 1471.
- [2]. Biginelli, P. Gazz. Chim. Ital. 1893, 23, 360-413.

- [3]. Kappe, C. O. *Acc. Chem. Res.* 2000, 33, 879–888. doi:10.1021/ar000048h
- [4]. Lusch, M. J.; Tallarico, J. A. *Org. Lett.* 2004, 6, 3237–3240. doi:10.1021/ol048946r
- [5]. Ramón, D. J.; Yus, M. *Angew. Chem., Int. Ed.* 2005, 44, 1602–1634. doi:10.1002/anie.200460548
- [6]. Ramachary, D. B.; Barbas, C. F., III. *Chem.–Eur. J.* 2004, 10, 5323–5331. doi:10.1002/chem.200400597
- [7]. Denmark, S. E.; Fan, Y. J. *Am. Chem. Soc.* 2003, 125, 7825–7827. doi:10.1021/ja035410c
- [8]. Andreana, P. R.; Liu, C. C.; Schreiber, S. L. *Org. Lett.* 2004, 6, 4231–4233. doi:10.1021/ol0482893
- [9]. Cozzi, P. G.; Rivalta, E. *Angew. Chem., Int. Ed.* 2005, 44, 3600–3603. doi:10.1002/anie.200462757
- [10]. Armstrong, R. W.; Combs, A. P.; Tempest, P. A.; Brown, S. D. Keating, T. A. *Acc. Chem. Res.* 1996, 29, 123–131. doi:10.1021/ar9502083
- [11]. Burke, M. D.; Schreiber, S. L. *Angew. Chem., Int. Ed.* 2004, 43, 46–58. doi:10.1002/anie.200300626
- [12]. Kappe, C. O.; Falsone, S. F. *Synlett* 1998, 718–720. doi:10.1055/s-1998-1764
- [13]. Lu, J.; Bai, Y.; Wang, Z.; Yang, B.; Ma, H. *Tetrahedron Lett.* 2000, 41, 9075–9078. doi:10.1016/S0040-4039(00)01645-2
- [14]. Yadav, J. S.; Reddy, B. V. S.; Srinivas, R.; Venugopal, C.; Ramalingam, T. *Synthesis* 2001, 1341–1345 doi:10.1055/s-2001-15229.
- [15]. (a) K. Ishihara, in *Lewis Acids in Organic Synthesis*, ed. H. Yamamoto, Wiley-VCH: Weinheim, Germany, 2000, vol. 1, pp. 89-133; (b) S. Kobayashi, K. Manabe, *Acc. Chem. Res.*, 2002, 35, pp. 209-217; (c) K. Manabe, Y. Mori, T. Wakabayashi, S. Nagayama, S. Kobayashi, *J. Am. Chem. Soc.*, 2002, 122, pp. 7202-7207; (d) S. Kobayashi, *Pure Appl. Chem.*, 1998, 70, pp. 1019–1026; (e) S. Hu, Z. Zhang, J. Song, Y. Zhou, B. Han, *Green. Chem.*, 2009, 11, pp. 1746-1749; (f) H. E. Lanman, R. -V. Nguyen, X. Yao, T. -H. Chan, C. -J. Li, *J. Mol. Catal. A: Chem.*, 2008, 279, pp. 218-222.
- [16]. A. G. Posternak, R. Y. Garlyauskayte, L. M. Yagupolskii, *Tetrahedron Lett.*, 2009, 50, pp. 446–447.
- [17]. S. Kobayashi, K. Manabe, *Pure Appl. Chem.*, 2000, 72, pp. 1373–1380.
- [18]. A. Shaabani, A. Bazgir, *Tetrahedron. Lett.*, 2004, 45, 2575.

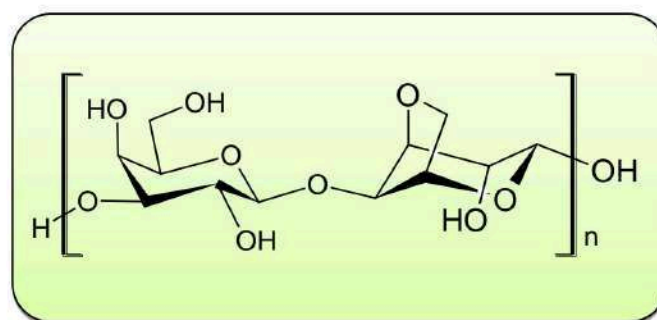


Fig.1 Structure of agarose

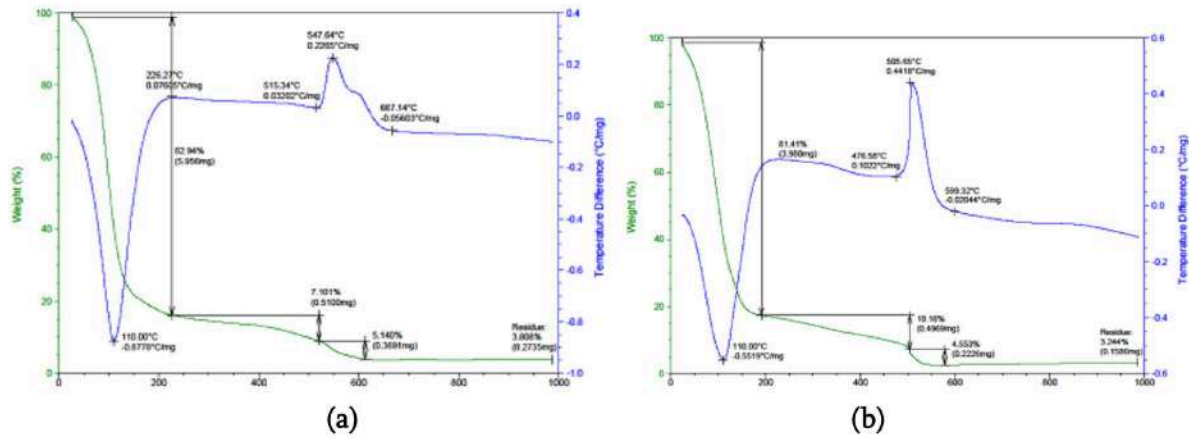


Fig.2 DSC-TGA graph of (a) ZnCl<sub>2</sub>-GELA and (b) AlCl<sub>3</sub>-GELA

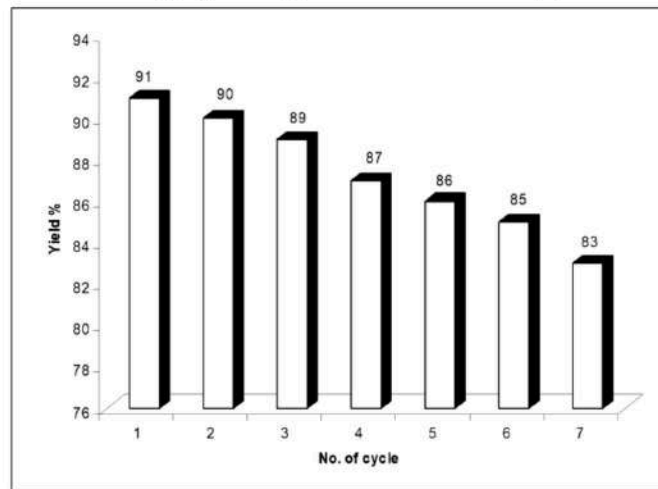


Fig. 3 Recyclic use of GELA in spirofused heterocyclic compound



## DBU Catalyzed One Pot Four-Component Synthesis of Pyrano Pyrazole Derivatives with their Antioxidant Activity

Ashok R. Karad<sup>a</sup>, Navanand B. Wadwale<sup>b</sup>, Gopinath S. Khansole<sup>c</sup>, Sunil.S.Choudhare<sup>d</sup>, Swapnil V. Navate<sup>e</sup>  
Vijay N. Bhosale<sup>e\*</sup>

- a. Department of Chemistry, Mahatma Gandhi Mahavidyalaya, Ahmedpur Dist.Latur (M.S.) India.  
b. P.G. Research Centre, Department of Chemistry, M.S.G. College Malegaon,(M.S) 423105 India.  
c. Department of Chemistry, D. A. B. N. College, Chikhali, Sangli District, Maharashtra, 415408 India  
d. Department of Chemistry, S. D. College, Soegaon, Aurangabad District, Maharashtra, 431120 India.  
e. P.G. Research Centre, Department of Chemistry, Yeshwant Mahavidyalaya, Nanded (M.S.) India.  
email-: vijaynbhosale77@gmail.com

### ABSTRACT

A green, efficient and simple procedure has been developed for the synthesis of Pyrano [2,3-*c*] Pyrazoles from a one pot four component condensation of Ethylacetoacetate, Malononitrile, Hydrazine hydrate and different substituted aromatic Aldehydes using 1,8-diazabicyclo [5.4.0] undec-7-ene (DBU) as catalyst in ethanol-water. The synthesized Pyrano [2,3-*c*] Pyrazoles were screened for their Antioxidant activity. These newly synthesized compounds were evaluated by their using various spectroscopic techniques and also elemental analysis.

Keywords : Pyrano pyrazoles, MCRs, DBU

### I. INTRODUCTION

Multicomponent Reactions (MCRs) are very proficient in the synthesis of organic molecule<sup>1-3</sup>. In this protocol single step reaction gives magnificent yield without any isolation of intermediate and intimately associated with the principals of green chemistry.<sup>4</sup>

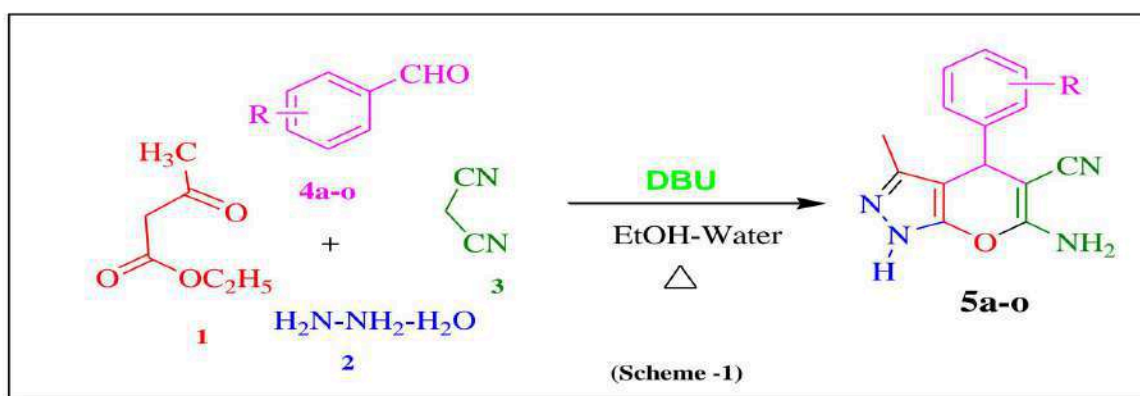
Pyrano pyrazole derivatives has vital role in the class of organic compounds because of their broad spectrum of biological as well as pharmacological importance. The Pyrano pyrazole moieties of the drug with wide medicinal application such as antimicrobial<sup>5-6</sup>, antitumor<sup>7</sup>, antipyretic<sup>8</sup>, anti-inflammatory<sup>9</sup>, antidepressant<sup>10</sup>, antihypertensive<sup>11</sup>, and peptide deformylase inhibitor<sup>12</sup>. Moreover, Dihydro pyrano [2,3-*c*] pyrazole showed hypotensive and hypoglycemic agents<sup>13</sup>, molluscicidal activity<sup>14</sup> and as well as a screening hit for Chkl kinase inhibitor<sup>15</sup>.

Chemists have reported various methods for the synthesis of Pyrano pyrazole derivatives. Various method of four component synthesis by using Thiamine hydrochloride (VB<sub>1</sub>)<sup>16</sup>, CsF<sup>17</sup>, ZnO nanoparticle<sup>18</sup>, CAPB<sup>19</sup>, NaHSO<sub>3</sub> using ultrasound mediated,<sup>20</sup> TBAHS,<sup>21</sup> and molecular iodine non recoverable<sup>22</sup> also have

been reported. Overall, all these reported methods are effective but requires long time, expensive catalyst. So in order to overcome these problems, keeping green approach in mind, in this present investigation we have reported synthesis of the Pyrano pyrazole derivatives by simple, efficient and eco-friendly method. We have synthesized Pyrano pyrazoles derivatives by using as a catalyst.

We decide to investigate DBU as an homogeneous catalyst for the synthesis of dihydropyrano [3,2-*c*]chromene derivatives in aqueous ethanol. Catalyst used (DBU) 1,8-diazabicyclo[5.4.0]undec-7-ene acts as homogeneous catalyst and it execute much organic transformation under placid condition. As a part of our constant efforts toward the development of well-organized, cost-effective and novel methods using green catalysts and solvents, we investigated the activity of the readily available and environmentally benign DBU as catalyst for the synthesis of pyrano pyrazole derivatives.

## RESULT AND DISCUSSION:



As a Initial steps, we have focused on model reaction (**Scheme 1**) by refluxing equimolar amount of Ethylacetoacetate (**1**) (3.0 mmol), Hydrazine hydrate (80%) (**2**) (3.0 mmol), Malononitrile (**3**) (3.0 mmol), and different substituted aromatic aldehydes (**4**) (3.0 mmol) in ethanol-water (1:1) buy using DBU (1,8-diazabicyclo[5.4.0]undec-7-ene) (10 mol%) for three hour at 60°C which results in the formation of compound **5b** with 80% yield (Table 1, entry 7). The investigating the effectiveness of different polar and non polar solvent using catalytic amount of DBU (10 mol%). Solvent optimization clearly suggested that ethanol-water is the best solvent for the desired transformation due to fast reaction rate and high yield (Table1, entry 7). The other polar protic solvents gives moderate yield (Table1, entry 6).while other a protic solvent like DCM, THF, Acetonitrile, and Toluene displayed slow reaction rates leading lower yield (Table1, entry 1-4). Also,carried out the model reaction using different stoichiometric amount of DBU catalyst. The catalyst screening result are summarized in Table 2. It was observed that the excellent yield was achieved by using 10 mol% of DBU (1,8-diazabicyclo[5.4.0]undec-7-ene) (Table 2, entry 6).

After optimization the reaction condition, the scope of the method was investigated with a series of substituted aromatic aldehydes and the result are summarized in Table 3.

These synthesized products (**5a-o**) were completely characterized from IR, 1H-NMR, Mass and 13C-NMR spectroscopic technique and also elemental analysis. We proposed tentative plausible mechanism for

the formation of Pyrano [2,3-c] pyrazoles (5a-o) in the presence of DBU as a catalyst. The overall, mechanism takes place according to Knoevenagels-Michael reaction (Scheme-II).

**Table 1.** Optimization of the reaction conditions using different solvents.<sup>[a]</sup>

Entry	Solvent	Reaction Time (h)	Yield (%) <sup>[b]</sup>
1	DCM	7.0	30
2	THF	6.5	35
3	Acetonitrile	6.0	40
4	Toluene	5.5	45
5	Ethanol	3.0	65
6	Water	3.0	70
7	Ethanol-Water	3.0	80

<sup>[a]</sup> **Reaction conditions:** Ethylacetoacetate (**1**) (3.0 mmol), hydrazine hydrate (80%) (**2**) (3.0 mmol), malononitrile (**3**) (3.0 mmol), and different substituted aromatic aldehydes (**4**) (3.0 mmol) in Ethanol-Water and DBU (1,8-diazabicyclo[5.4.0]undec-7-ene) were refluxed at 60°.

<sup>[b]</sup> Isolated yields.

**Table 2:** Optimization Study for the amount of DBU (1,8-diazabicyclo[5.4.0]undec-7-ene) (<sup>[a]</sup>

Entry	Catalyst (mole %)	Temperature (°C)	Reaction Time (h)	Yield % <sup>[b]</sup>
1	01	60	3.0	30
2	02	60	3.0	50
3	05	60	3.0	60
4	06	60	3.0	60
5	08	60	3.0	70
6	10	60	3.0	80
7	15	60	3.0	80

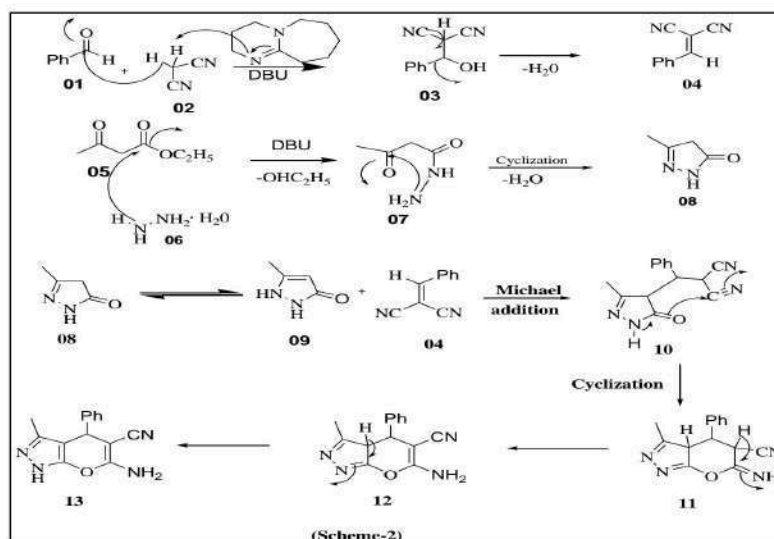
<sup>[a]</sup> **Reaction conditions:** Ethylacetoacetate (**1**) (3.0 mmol), Hydrazine hydrate (80%) (**2**) (3.0 mmol), Malononitrile (**3**) (3.0 mmol), and different substituted Aromatic aldehydes (**4**) (3.0 mmol) in Ethanol-Water and DBU (1,8-diazabicyclo[5.4.0]undec-7-ene) as a catalyst were refluxed for three hours at 60°C. <sup>[b]</sup> Isolated yields.

**Table 3.** Synthesis of pyrano [2,3-*c*] pyrazoles derivatives .<sup>[a]</sup>

Entry	Ar	Time (Hrs)	Yield% <sup>[a]</sup>	M.P. (°C)	
				Found	Lit. Ref
5a	C <sub>6</sub> H <sub>5</sub>	3.5	68	245-246	244-245 <sup>22</sup>
5b	4'-OCH <sub>3</sub> -C <sub>6</sub> H <sub>4</sub>	3.0	80	209-210	209-211 <sup>22</sup>
5c	4'-CH <sub>3</sub> -C <sub>6</sub> H <sub>4</sub>	3.0	78	205-207	205-207 <sup>23</sup>
5d	4'-Br -C <sub>6</sub> H <sub>4</sub>	3.0	70	179-181	177-179 <sup>24</sup>
5e	4'-Cl -C <sub>6</sub> H <sub>4</sub>	3.5	70	233-235	234-235 <sup>23</sup>
5f	4'-NO <sub>2</sub> -C <sub>6</sub> H <sub>4</sub>	4.0	60	248-250	251-252 <sup>23</sup>
5g	4'-OH -C <sub>6</sub> H <sub>4</sub>	3.0	75	221-223	223-225 <sup>25</sup>
5h	4'-F -C <sub>6</sub> H <sub>4</sub>	3.5	65	172-174	170-171 <sup>23</sup>
5i	4'-OCH <sub>3</sub> , 3'-OCH <sub>3</sub> -C <sub>6</sub> H <sub>3</sub>	3.0	80	310-312	311-313 <sup>23</sup>
5j	4'- OCH <sub>3</sub> ,3'-OH-C <sub>6</sub> H <sub>3</sub>	3.0	80	242-244	244-246 <sup>22</sup>
5k	3'- Br -C <sub>6</sub> H <sub>4</sub>	3.5	66	223-224	223-225 <sup>23</sup>
5l	3'- NO <sub>2</sub> -C <sub>6</sub> H <sub>4</sub>	3.5	56	193-195	190-192 <sup>26</sup>
5m	3'- OH -C <sub>6</sub> H <sub>4</sub>	3.0	72	223-225	221-223 <sup>27</sup>
5n	2'- OH -C <sub>6</sub> H <sub>4</sub>	3.0	65	207-208	207-209 <sup>28</sup>
5o	2'- Cl -C <sub>6</sub> H <sub>4</sub>	3.5	68	143-144	143-145 <sup>28</sup>

<sup>[a]</sup> **Reaction conditions:** Ethylacetoacetate (**1**) (**3.0 mmol**), Hydrazine hydrate(80%) (**2**) (**3.0 mmol**), Malononitrile (**3**) (**3.0 mmol**), and different substituted Aromatic aldehydes (**4**) (**3.0 mmol**) in Ethanol-Water and DBU (1,8-diazabicyclo[5.4.0]undec-7-ene) as a catalyst were refluxed for three hours at 60°C.<sup>[b]</sup> Isolated yields.

### Probable Mechanism:



**Experimental:**

Melting points were determined on electro-thermal melting point apparatus and are uncorrected. IR (KBr) spectra were recorded using Perkin-Elmer FTIR spectrophotometer. Mass spectral data were recorded on liquid chromatography mass spectrometer (Shimadzu 2010Ev) using ESI probe. The  $^1\text{H}$  and  $^{13}\text{C}$  NMR spectra were recorded on spectrometer at 300MHz using TMS as an internal standard. All the reactions were monitored by thin layer chromatography, carried out on 0.25 mm thick silica gel-G plate using iodine vapour for detection.

**General procedure for the synthesis of 4-substituted derivatives of 4- phenyl Pyrano [2,3-c] pyrazoles (5a-5o):**

A mixture of Ethylacetoacetate (1) (3.0 mmol), Hydrazine hydrate (80%) (2) (3.0 mmol), Malononitrile (3) (3.0 mmol), was refluxed independently with different substituted Aromatic aldehydes (4) (3.0 mmol) in presence of DBU (1,8-diazabicyclo[5.4.0]undec-7-ene) (10 mol%) as catalyst in ethanol-water as solvent for three hours at 60°C. The progress of reaction were monitored by TLC, the product obtained was filtered, and recrystallized from ethanol (5ml) to give the pure products of 5(a-o), (Table 3).

**Spectral Characterization of Representative Compounds.****6-amino-1,4-dihydro-3-methyl-4-phenylpyrano[2,3-c]pyrazole-5-carbonitrile (5a):**

Yellow solid, IR (KBr /  $\text{cm}^{-1}$ ) 3410,3340 ( $-\text{NH}_2$ ), 3120( $-\text{NH}$ ), 2220 ( $-\text{C}\equiv\text{N}$ ), 1665 ( $\text{C}=\text{N}$ ), 1270( $-\text{C}-\text{O}-\text{C}-$ );  $^1\text{H}$  NMR (300MHz,  $\text{DMSO}-d_6$  / ppm)  $\delta$  1.72(s,3H); 4.5 (s,1H,-CH); 6.70(s, 2H); 7.10-7.40 (m,5H, Ar-H); 12.06(s,1H,-NH); EI-MS (m/z: RA %): 253 ( $\text{M}^+ +1$ , 100%). Elemental analysis calculated data for  $\text{C}_{14}\text{H}_{12}\text{N}_4\text{O}$ ; C, 66.65; N, 22.11. Found: C, 66.63; N, 22.09.

**6-amino-1,4-dihydro-4-(4-methoxyphenyl)-3-methylpyrano[2,3-c]pyrazole-5-carbonitrile (5b):**

Yellow solid, IR (KBr/  $\text{cm}^{-1}$ ) 3400, 3250 ( $-\text{NH}_2$ ), 3110 ( $-\text{NH}$ ), 2192 ( $-\text{C}\equiv\text{N}$ ), 1655 ( $\text{C}=\text{N}$ ), 1250 ( $-\text{C}-\text{O}-\text{C}-$ );  $^1\text{H}$  NMR (300MHz,  $\text{DMSO}-d_6$  / ppm)  $\delta$  1.70 (s,3H); 3.7 (s,3H, Ar-OCH<sub>3</sub>); 4.5(s,1H,-CH); 7.0 (s,2H); 7.2 -6.7 (m,4H, Ar-H); 12.0(s,1H,-NH); EI-MS (m/z: RA %): 283 ( $\text{M}^+ +1$ , 100%).  $^{13}\text{C}$  NMR (300 MHz,  $\text{DMSO}-d_6$  / ppm)  $\delta$ : 36.8, 55.5, 99.2, 114.0, 120.1,127.2, 129.6, 144.2, 159.0. Elemental analysis calculated data for  $\text{C}_{15}\text{H}_{14}\text{N}_4\text{O}_2$ ; C, 63.82; N, 19.82. Found: C, 63.79; N, 19.80.

**6-amino-1,4-dihydro-3-methyl-4-p-tolylpyrano[2,3-c]pyrazole-5-carbonitrile(5c):**

Yellow solid, IR (KBr/  $\text{cm}^{-1}$ ) 3317, 3409 ( $-\text{NH}_2$ ), 3190 ( $-\text{NH}$ ), 2190 ( $-\text{C}\equiv\text{N}$ ), 1647 ( $\text{C}=\text{N}$ ), 1157 ( $-\text{C}-\text{O}-\text{C}-$ );  $^1\text{H}$  NMR (300MHz,  $\text{DMSO}-d_6$  / ppm)  $\delta$  1.77 (s,3H); 2.26 (s,3H, Ar-OCH<sub>3</sub>); 4.54(s,1H,-CH); 6.8 (s,2H); 7.02 -7.12 (m,4H, Ar-H); 12.07 (s,1H,-NH); EI-MS (m/z: RA %): 267 ( $\text{M}^+ +1$ , 100%). Elemental analysis calculated data for  $\text{C}_{15}\text{H}_{14}\text{N}_4\text{O}$ ; C, 67.65; N, 21.40. Found: C, 67.63; N, 21.38.

**6-amino-4-(4-bromophenyl)-1,4-dihydro-3-methylpyrano[2,3-c]pyrazole-5-carbonitrile(5d):**

White solid, IR (KBr/  $\text{cm}^{-1}$ ) 3474, 3325 ( $-\text{NH}_2$ ), 3190 ( $-\text{NH}$ ), 2192 ( $-\text{C}\equiv\text{N}$ ), 1658 ( $\text{C}=\text{N}$ ), 1157 ( $-\text{C}-\text{O}-\text{C}-$ );  $^1\text{H}$  NMR (300MHz,  $\text{DMSO}-d_6$  / ppm)  $\delta$  1.7 (s,3H); 4.6 (s,1H,-CH); 6.93 (s,2H); 7.12 -7.52 (m,4H, Ar-H); 12.14 (s,1H,-NH); EI-MS (m/z: RA %): 330( $\text{M}^+$ ) 332 ( $\text{M}^+ +1$ , 100%).  $^{13}\text{C}$  NMR (300 MHz,  $\text{DMSO}-d_6$  / ppm)  $\delta$ : 35.0, 56.0, 97.2, 119.0, 120.1, 131.0, 143.0, 154.0, 160.0. Elemental analysis calculated data for  $\text{C}_{15}\text{H}_{14}\text{Br N}_4\text{O}$ ; C, 50.77; N, 16.92. Found: C, 50.75; N, 16.90.

**6-amino-4-(4-chlorophenyl)-1,4-dihydro-3-methylpyrano[2,3-c]pyrazole-5-carbonitrile(5e):**

White solid, IR (KBr /  $\text{cm}^{-1}$ ) 3425 , 3325 (-NH<sub>2</sub>), 3174 (-NH) , 2200 (-C≡N) 1647 (C=N), 1184 (-C-O-C-) ; <sup>1</sup>H NMR (300MHz, DMSO-d<sub>6</sub>/ ppm)  $\delta$  1.79 (s,3H); 4.63 (s,1H,-CH); 6.93 (s,2H); 7.18 -7.20 (m,4H, Ar-H); 12.00 (s,1H,-NH); EI-MS (m/z: RA %): 287(M<sup>+</sup>) 288 (M<sup>+</sup> +1, 100%). Elemental analysis calculated data for C<sub>15</sub>H<sub>14</sub>Cl N<sub>4</sub>O; C, 58.65 ; N, 19.54. Found: C, 58.63; N, 19.54.

**Biological Evaluation:****Antioxidant Activity:****a) DPPH (1,1-diphenyl-2-picrylhydrazyl) radical scavenging assay :**

DPPH (1, 1-diphenyl-2-picrylhydrazyl) radical scavenging assay was proceed by reported method. Take 1 ml (1 mM) of the test sample is added to equimolar quantity of 0.1 mM solution of DPPH in ethanol. After incubation at room temperature for 25 min, then the DPPH reduction was takes places and measured by Reading the absorbance at 517 nm. Ascorbic acid (1mM) used as reference compound.

The compound **5(d, f, k, l & o)**, (Table 4) showed remarkable antioxidant activity against DDPH radical scavenging activity with reference of ascorbic acid.

**b) OH radical scavenging assay:**

Hydroxy radicals scavenging activity was measured with Fenton's reaction (Rollet –Labelle et al., 1998). The reaction mixture contained 60  $\mu\text{l}$  of FeCl<sub>2</sub> (1mM), 90  $\mu\text{l}$  of 1,10-phenanthroline(1mM), 2.4 ml of phosphate buffer (pH 7.8),150  $\mu\text{l}$  of 0.17M H<sub>2</sub>O<sub>2</sub> and 1.5 ml of individual newly synthesized organic compounds (1mM). The reaction mixture was kept at room temperature for 5 minutes incubation and the absorbance was recorded at 560 nm using UV-Visible spectrophotometer. Ascorbic acid (1mM) was used as the reference compound. The OH radical scavenging activity, the OH radical in which oxygen species are most reactive. The effective OH radical stabilizing potential observed strong absorption maximum at 560 nm using standard Ascorbic acid (89.5  $\pm$  0.021) drug.

The compound **5(d, f, k & l)**, (Table 4) showed remarkable antioxidant activity against OH radical scavenging activity with reference of ascorbic acid.

**Table 4 : Antioxidant activity of tested compounds (5a-5o.)**

Entry	Compound Code	% Radical scavenging activity	
		DPPH radical scavenging	OH radical scavenging
01	5a	55.7 $\pm$ 1.03	53.2 $\pm$ 1.39
02	5b	68.5 $\pm$ 0.79	60.3 $\pm$ 2.20
03	5c	60.2 $\pm$ 0.54	65.2 $\pm$ 1.30
04	5d	81.1 $\pm$ 1.50	80.2 $\pm$ 1.28
05	5e	79.1 $\pm$ 0.72	73.6 $\pm$ 0.69
06	5f	88.5 $\pm$ 1.68	84.2 $\pm$ 1.40

07	5g	50.2 ± 0.32	55.2 ± 1.66
08	5h	60.4 ± 0.66	65.2 ± 2.00
09	5i	58.2 ± 1.44	49.2 ± 0.80
10	5j	61.2 ± 0.08	45.2 ± 2.10
11	5k	<b>89.5 ± 2.68</b>	<b>86.2 ± 0.28</b>
12	5l	<b>82.8 ± 1.04</b>	<b>86.2 ± 0.10</b>
13	5m	44.0 ± 0.30	55.8 ± 2.11
14	5n	58.1 ± 1.60	59.2 ± 1.80
15	5o	82.7 ± 1.70	78.2 ± 2.60
16	Ascorbic Acid (Standard)	<b>91.4 ± 0.021</b>	<b>89.5 ± 0.021</b>

### Conclusion:

The method we used for the synthesis of 4-substituted derivatives of Pyrano [2,3-c] pyrazoles derivatives by using DBU (1,8-diazabicyclo[5.4.0]undec-7-ene ) is efficient catalyst. The product can be easily isolated by simple workup technique, requires ambient reaction condition, short time, less expensive and give excellent yield. Among these synthesized compounds few compounds shows potent antioxidant activity.

### Acknowledgments:

Authors are grateful to thanks Principal, Yeshwant Mahavidyalaya, Nanded for providing laboratory facilities, Director, Indian Institute of Chemical Technology, Hyderabad and Vishnu chemical limited for providing spectra.

### References:

1. Nair V, Rajesh C, Vinod AU, Bindu S ,Sreekenath AR, Balagopal LS. Strategies for Heterocyclic Construction via Novel Multicomponent Reactions Based on Isocyanides and Nucleophilic Carbenes. *Acc chem Res*, **2003**; 36(12); 899-907.
2. Orru RVA, de Greef M. Recent Advances in Solution-Phase Multicomponent Methodology for the Synthesis of Heterocyclic Compounds. *Synthesis*, **2003**; 10; 1471-1499.
3. Bienaymé H, Hulme C , Odon G , Schmitt P. Maximizing Synthetic Efficiency: Multi-Component Transformations Lead the Way. *Chem.A. Eur. J*, **2000**, 6(18); 3321-3329.
4. Ganem B. Strategies for Innovation in Multicomponent Reaction Design. *Acc. Chem. Res.*, **2009**; 42 (3); 463-472.

5. Eid F A, Abd El-Wahab AHF, El-Hag Ali GA M, Khafagy M M. **Synthesis and antimicrobial evaluation of naphtho[2,1-b]pyrano[2,3-d]pyrimidine and pyrano[3,2-e] [1,2,4]triazolo[1,5-c]pyrimidine derivatives**, Acta Pharmaceutica. **2004**: 54; 13-26.
6. El-Agrody A M, Abd-Latif M S, Fakery A H, Bedair A H. Heteroaromatization with 4-Hydroxycoumarin Part II: Synthesis of Some New Pyrano[2,3-d] pyrimidines, [1,2,4]triazolo[1,5-c]pyrimidines and Pyrimido[1,6-b]-[1,2,4] triazine Derivatives. *Molecule*, **2001**: 6(6): 519-527.
7. Park H J, Lee K, Park S J, Ahn B, Lee J C, Cho H Y, Lee K I. Identification of antitumor activity of pyrazole oxime ethers. *Bioorg. Med. Chem. Lett.*, **2005**: 15 (13); 3307-3312
8. Shafiee A, Bagheri M, Abdollahi M. Shekarchi M., The antinociceptive activities of 1-(4-aryl-2-thiazolyl)-3,5-disubstituted-2 pyrazolines in mouse writhing test. *J. Pharm. Sci.*, **2003**: 6(3); 360-362.
9. Ren X L, Li H B, Wu C, Yang H Z., Synthesis of a small library containing substituted pyrazoles, *Arkivoc*, **2005**: 15 ; 59-67.
10. Prasad Y R, Rao A L, Prasoon L, Murali K P, Kumar R., Synthesis and Antidepressant Activity of Some 1,3,5-Triphenyl-2-Pyrazolines and 3-(2-Hydroxy Naphthalen-1-yl)-1,5-Diphenyl-2-Pyrazolines *Bioorg. Med. Chem. Lett.* **2005**: 15 (22); 5030-5034.
11. Almansa C, de Arriba AF, Cavalcanti FL, Gómez LA, Miralles A, Merlos M, García-Rafanell J, Forn J. Synthesis and SAR of a new series of COX-2-selective inhibitors: pyrazolo[1,5-a] pyrimidines. *J. Med. Chem.* **2001**: 44(3); 350-61.
12. Calí P, Naerum L, Mukhija S, Hjelmencrantz A., Isoxazole-3-hydroxamic acid derivatives as peptide deformylase inhibitors and potential antibacterial agents. *Bioorg. Med. Chem. Lett.*, **2004**: 14(24); 5997-6000.
13. Kuo SC, Huang LJ, Nakamura H., Studies on heterocyclic compounds. 6. Synthesis and analgesic and antiinflammatory activities of 3,4-dimethylpyrano[2,3-c]pyrazol-6-one derivatives. *J Med Chem.* **1984**: 4; 539-44.
14. Abdelrazek FM, Metz P, Kataeva O, Jäger A, El-Mahrouky SF. Synthesis and molluscicidal activity of new chromene and pyrano[2,3-c]pyrazole derivatives. *Arch. Pharm. Chem. Life Sci.* **2007**, 340, 543–548.
15. Foloppe N, Fisher LM, Howes R, Potter A, Robertson AG, Surgenor AE. Identification of chemically diverse Chk1 inhibitors by receptor-based virtual screening. *Bioorg Med Chem.* **2006**: 14(14); 4792-4802.
16. Nikam M D, Mahajan P S, Chate AV, Dabhade S K, Gill C H., An Efficient And Green Protocol For The Synthesis Of Dihydropyrano [2,3-C] Pyrazoles In Aqueous Medium Using Thiamine Hydrochloride As A Catalyst. *J. Chil. Chem. Soc.*, **2015**: 60;2847-2850.
17. Bhosale VN, Khansole GS, Angulwar JA, Choudhare SS, Cesium Fluoride Catalysed tandem Knoevenagel- Michael reaction for the synthesis of 6-amino-1,4-dihydro-3-methyl-1,4-phenyl pyrano [2,3-c]pyrazoles., *Der Pharma Chemica*, **2015**: 7(6);126-130.
18. Tekale SU, Kauthale SS, Jadhav K M, Pawar R P. Nano-ZnO Catalyzed Green and Efficient One-Pot four-component synthesis of Pyranopyrazoles. *Journal of Chemistry*, **2013**;10; 1155-1162.

19. Tamaddon F, Alizadeh M., A four component synthesis of dihydropyrano [2,3-c] pyrazoles in a new water based worm-like micellar medium. *Tetrahedron Letters*, **2014**: 55; 3588-3591.
20. Darandale S N, Sangshetti J N ,Shinde D B. Ultrasound mediated, Sodium Bisulfite catalyzed, solvent free synthesis of 6-amino-3-methyl-4-substituted-2,4-dihydro pyrano [2,3-c] pyrazole-5-carbonitrile., *Journal of the Korean Chemical Society*, **2012** :56(3); 328-333.
21. Bhosale VN,Khansole GS ,AngulwarJA, , Choudhare SS,Karad AR, One Pot, Four-Component for the Synthesis of Pyrano Pyrazole Derivatives using TBAHS as Green Catalyst and Their Biological Evaluation. *Asian J. Research Chem.* **2017**: 10(6).
22. Madhusudana Reddy M B, Pasha M A. One-pot, multicomponent synthesis of 4H-pyrano [2,3-c] pyrazoles in water at 25°C. *Indian Journal of Chemistry*. **2012**: 51B; 537-541.
23. Yadav D K,Quaraishi M A. Eletrochemical investigation of substituted pyranopyrazoles absorption on mild steel in acid solution. *Ind.Eng.Chem.Res.***2012**: 51; 8194-8210.
24. Bora P P, Bihani M., Bez G. Beyond enzymatic promiscuity: asymmetric induction by L-proline on lipase catalyzed synthesis of polyfunctionalized 4H-pyrans, *J. of Molecular Catalysis B: Enzymatic*, **2013**: 92; 24.
25. Babaie M , Sheibani H. Nanosized magnesium oxide as a highly effective heterogeneous base catalyst for the rapid synthesis of pyranopyrazoles via a tandem four-component reaction *Arabian Journal of Chemistry*, **2011**: 4; 159–162.
26. Makawana JA, Mungra DC, Patel MP, Patel RG. Microwave assisted synthesis and antimicrobial evaluation of new fused pyran derivatives bearing 2-morpholinoquinoline nucleus. *Bioorg Med Chem Lett.* 2011: 21(20); 6166-6169.
27. Bihani M, Bora P P, Bez G, Askari H . Amberlyst A21 Catalyzed Chromatography-Free Method for Multicomponent Synthesis of Dihydropyrano[2,3-c]pyrazoles in Ethanol *ACS Sustainable Chem. Eng.*, 2013: 1 (4); 440–447.
28. Heravi M M, Ghods A, Derikvand F, Bakhtiari K, Bamoharram F F., H14[NaP5W30O110] catalyzed one-pot three-component synthesis of dihydropyrano[2,3-c] pyrazole and pyrano[2,3-d]pyrimidine derivatives, *Journal of the Iranian Chemical Society*, 2010: 7 ( 3); 615–620.
29. Kanagraj K, Pitchumani K., Solvent –free multicomponent synthesis of pyranopyrazoles: per-6-amino- $\beta$ -cyclodextrin as a remarkable catalyst and host. *Tetrahedron Lett.* 2010: 51: 3312-3316.



'Sangola Taluka Shetkari Shikshan Prasarak Mandal Sangola's

# VIDNYAN MAHAVIDYALAYA SANGOLA

(Arts & Science, E.C.S. & B.C.A.)

Off. (02187) 220508

Tal. Sangola Dist. Solapur Pin. 413 307 (Maharashtra)  
(Affiliated to P. A. H. Solapur University)

Mob. No. 9421045987  
Email : vidnyanms@yahoo.co.in  
Website : www.vmssangola.org

Acting Principal : Dr. R. A. Fule  
M.A., Ph.D.

Third Cycle Accredited by NAAC  
with 'B' Grade (CGPA of 2.24)

Ref. No. 39/2021-22

Date : 13/4/2022

## Thanking Letter

To,

**Dr. Diana Samodova**  
Senior Scientist,  
University of Copenhagen, Denmark

**Subject :** - Thanking you for your presence as a resource person in the International e-Conference on Proteomics application to Biomedical Research-(PABR-2022).

Respected sir,

We are heartily thankful to you for your valuable presence as a resource person in the International e-Conference on Proteomics application to Biomedical Research-(PABR-2022) arranged by department of chemistry in our college. We are also thankful to you for your stimulating speech on Proteomics and your current research in concerned field. Your comments were especially helpful for the participants accomplishing research work in their concerned area. Your enthusiasm is contagious and we hope to use your suggestion in our future campaigns.

Thank you

Principal

**Acting Principal**

Vidnyan Mahavidyalaya, Sangola  
Tal. Sangola Dist. Solapur



'Sangola Taluka Shetkari Shikshan Prasarak Mandal Sangola's

# VIDNYAN MAHAVIDYALAYA SANGOLA

(Arts & Science, E.C.S. & B.C.A.)

Off. (02187) 220508

Tal. Sangola Dist. Solapur Pin. 413 307 (Maharashtra)

Mob. No. 9421045987

(Affiliated to P. A. H. Solapur University)

Email : vidnyanms@yahoo.co.in

Website : www.vmsangola.org

Acting Principal : Dr. R. A. Fule  
M.A., Ph.D.

Third Cycle Accredited by NAAC  
with 'B' Grade (CGPA of 2.24)

Ref. No. 40/2021-22

Date : 13/4/2022

## Thanking Letter

To,

**Dr. Atul Deshmukh**  
Senior Scientist,  
University of Copenhagen, Denmark

**Subject :** - Thanking you for your presence as a resource person in the International e-Conference on Proteomics application to Biomedical Research-(PABR-2022).

Respected sir,

We are heartily thankful to you for your valuable presence as a resource person in the International e-Conference on Proteomics application to Biomedical Research-(PABR-2022) arranged by department of chemistry in our college. We are also thankful to you for your stimulating speech on Proteomics and your current research in concerned field. Your comments were especially helpful for the participants accomplishing research work in their concerned area. Your enthusiasm is contagious and we hope to use your suggestion in our future campaigns.

Thank you

Principal

**Acting Principal**

Vidnyan Mahavidyalaya, Sangola  
Tal. Sangola Dist. Solapur



'Sangola Taluka Shetkari Shikshan Prasarak Mandal Sangola's

# VIDNYAN MAHAVIDYALAYA SANGOLA

(Arts & Science, E.C.S. & B.C.A.)

Off. (02187) 220508

Tal. Sangola Dist. Solapur Pin. 413 307 (Maharashtra)  
(Affiliated to P. A. H. Solapur University)

Mob. No. 9421045987  
Email : vidnyanms@yahoo.co.in  
Website : www.vmssangola.org

Acting Principal : Dr. R. A. Fule  
M.A., Ph.D.

Third Cycle Accredited by NAAC  
with 'B' Grade (CGPA of 2.24)

Ref. No. 41/2021-22

Date : 13/4/2022

## Thanking Letter

To,

**Dr. Balaji Rokade**  
Senior Scientist,  
Eli Lilly Kinsale, Ireland

**Subject :** - Thanking you for your presence as a resource person in the International e-Conference on Proteomics application to Biomedical Research-(PABR-2022).

Respected sir,

We are heartily thankful to you for your valuable presence as a resource person in the International e-Conference on Proteomics application to Biomedical Research-(PABR-2022) arranged by department of chemistry in our college. We are also thankful to you for your stimulating speech on Proteomics and your current research in concerned field. Your comments were especially helpful for the participants accomplishing research work in their concerned area. Your enthusiasm is contagious and we hope to use your suggestion in our future campaigns.

Thank you

Principal

**Acting Principal**

Vidnyan Mahavidyalaya, Sangola  
Tal. Sangola Dist. Solapur



'Sangola Taluka Shetkari Shikshan Prasarak Mandal Sangola's

# VIDNYAN MAHAVIDYALAYA SANGOLA

(Arts & Science, E.C.S. & B.C.A.)

Off. (02187) 220508

Tal. Sangola Dist. Solapur Pin. 413 307 (Maharashtra)

Mob. No. 9421045987

(Affiliated to P. A. H. Solapur University)

Email : vidnyanms@yahoo.co.in

Website : www.vmsangola.org

Acting Principal : Dr. R. A. Fule

M.A., Ph.D.

Third Cycle Accredited by NAAC  
with 'B' Grade (CGPA of 2.24)

Ref. No. 38/2021-22

Date : 13/4/2022

## Thanking Letter

To,

**Prof. G. B. Zore**

School of Chemical science,

S. R. T. M. University, Nanded

**Subject :** - Thanking you for your presence as a chief guest for the Inaugural function of International e-Conference on Proteomics application to Biomedical Research-(PABR-2022).

Respected sir,

We are heartily thankful to you for your valuable presence as a chief guest of inaugural function of International e-Conference on Proteomics application to Biomedical Research-(PABR-2022) arranged by department of chemistry in our college. We are also thankful to you for your stimulating key note address on Proteomics and your current research in concerned field. Your comments were especially helpful for the participants accomplishing research work in their concerned area. Your enthusiasm is contagious and we hope to use your suggestion in our future campaigns.

*o/c*

Thank you

Principal

**Acting Principal**

Vidnyan Mahavidyalaya, Sangola  
Tal. Sangola Dist. Solapur



'Sangola Taluka Shetkari Shikshan Prasarak Mandal Sangola's

# VIDNYAN MAHAVIDYALAYA SANGOLA

(Arts & Science, E.C.S. & B.C.A.)

Off. (02187) 220508

Tal. Sangola Dist. Solapur Pin. 413 307 (Maharashtra)  
(Affiliated to P. A. H. Solapur University)

Mob. No. 9421045987  
Email : vidnyanms@yahoo.co.in  
Website : www.vmssangola.org

Acting Principal : Dr. R. A. Fule  
M.A., Ph.D.

Third Cycle Accredited by NAAC  
with 'B' Grade (CGPA of 2.24)

Ref. No. 37/2021-22

Date : 13/14/2022

## Thanking Letter

To,

**Prof. K. D. Sonawane**  
Head  
Department of Chemistry  
Shivaji University, Kolhapur

**Subject : -** Thanking you for your presence as a resource person in the International e-Conference on Proteomics application to Biomedical Research-(PABR-2022).

Respected sir,

We are heartily thankful to you for your valuable presence as a resource person in the International e-Conference on Proteomics application to Biomedical Research-(PABR-2022) arranged by department of chemistry in our college. We are also thankful to you for your stimulating speech on Proteomics and your current research in concerned field. Your comments were especially helpful for the participants accomplishing research work in their concerned area. Your enthusiasm is contagious and we hope to use your suggestion in our future campaigns.

o/c

Thank you

Principal

**Acting Principal**  
Vidnyan Mahavidyalaya, Sangola  
Tal. Sangola Dist. Solapur



'Sangola Taluka Shetkari Shikshan Prasarak Mandal Sangola's

# VIDNYAN MAHAVIDYALAYA SANGOLA

(Arts & Science, E.C.S. & B.C.A.)

Tal. Sangola Dist. Solapur Pin. 413 307 (Maharashtra)  
(Affiliated to P. A. H. Solapur University)

Off. (02187) 220508

Mob. No. 9421045987

Email : vidnyanms@yahoo.co.in

Website : www.vmssangola.org

Acting Principal : **Dr. R. A. Fule**  
M.A., Ph.D.

Third Cycle Accredited by NAAC  
with 'B' Grade (CGPA of 2.24)

Ref. No. 36/2021-22

Date : 13/4/2022

## Thanking Letter

To,

**Dr. S. B. Patwari**  
Head,  
L.B.S. College, Dharmabad

**Subject :** - Thanking you for your presence as a Chairperson in the International e-Conference on Proteomics application to Biomedical Research-(PABR-2022).

Respected sir,

We are heartily thankful to you for your valuable presence as a chairperson in the International e-Conference on Proteomics application to Biomedical Research-(PABR-2022) arranged by department of chemistry in our college. We are also thankful to you for your stimulating speech on Proteomics and your current research in concerned field. Your comments were especially helpful for the participants accomplishing research work in their concerned area. Your enthusiasm is contagious and we hope to use your suggestion in our future campaigns.

Thank you

o/c

  
Principal

**Acting Principal**  
Vidnyan Mahavidyalaya, Sangola  
Tal. Sangola Dist. Solapur



'Sangola Taluka Shetkari Shikshan Prasarak Mandal Sangola's

# VIDNYAN MAHAVIDYALAYA SANGOLA

(Arts & Science, E.C.S. & B.C.A.)

Off. (02187) 220508

Tal. Sangola Dist. Solapur Pin. 413 307 (Maharashtra)

Mob. No. 9421045987

(Affiliated to P. A. H. Solapur University)

Email : vidnyanms@yahoo.co.in

Website : www.vmsangola.org

Acting Principal : Dr. R. A. Fule

M.A., Ph.D.

Third Cycle Accredited by NAAC  
with 'B' Grade (CGPA of 2.24)

Ref. No. 35/2021-22

Date : 13/14/2022

## Thanking Letter

To,

**Dr. S. H. Gaikwad**

BOS Chairman,

PAH Solapur University, Solapur

**Subject :** - Thanking you for your presence as a Chairperson in the International e-Conference on Proteomics application to Biomedical Research-(PABR-2022).

Respected sir,

We are heartily thankful to you for your valuable presence as a chairperson in the International e-Conference on Proteomics application to Biomedical Research-(PABR-2022) arranged by department of chemistry in our college. We are also thankful to you for your stimulating speech on Proteomics and your current research in concerned field. Your comments were especially helpful for the participants accomplishing research work in their concerned area. Your enthusiasm is contagious and we hope to use your suggestion in our future campaigns.

Thank you

O/C

  
Principal

**Acting Principal**  
Vidnyan Mahavidyalaya, Sangola  
Tal. Sangola Dist. Solapur



'Sangola Taluka Shetkari Shikshan Prasarak Mandal Sangola's

# VIDNYAN MAHAVIDYALAYA SANGOLA

(Arts & Science, E.C.S. & B.C.A.)

Off. (02187) 220508

Tal. Sangola Dist. Solapur Pin. 413 307 (Maharashtra)

Mob. No. 9421045987

(Affiliated to P. A. H. Solapur University)

Email : vidnyanms@yahoo.co.in

Website : www.vmssangola.org

Acting Principal : Dr. R. A. Fule

M.A., Ph.D.

Third Cycle Accredited by NAAC  
with 'B' Grade (CGPA of 2.24)

Ref. No. By past

Date : 12/4/2022

## Thanking Letter

To,

**Dr. Lalasaheb Kashid**

Vidyaprathisthan Arts, Science, Commerce  
College, Baramati

**Subject :** - Thanking you for your presence as a Chairperson in the International e-Conference on Proteomics application to Biomedical Research-(PABR-2022).

Respected sir,

We are heartily thankful to you for your valuable presence as a chairperson in the International e-Conference on Proteomics application to Biomedical Research-(PABR-2022) arranged by department of chemistry in our college. We are also thankful to you for your stimulating speech on Proteomics and your current research in concerned field. Your comments were especially helpful for the participants accomplishing research work in their concerned area. Your enthusiasm is contagious and we hope to use your suggestion in our future campaigns.

Thank you

o/c

  
Principal

**Acting Principal**  
Vidnyan Mahavidyalaya, Sangola  
Tal. Sangola Dist. Solapur



'Sangola Taluka Shetkari Shikshan Prasarak Mandal Sangola's

# VIDNYAN MAHAVIDYALAYA SANGOLA

(Arts & Science, E.C.S. & B.C.A.)

Tal. Sangola Dist. Solapur Pin. 413 307 (Maharashtra)  
(Affiliated to P. A. H. Solapur University)

Off. (02187) 220508

Mob. No. 9421045987

Email : vidnyanms@yahoo.co.in

Website : www.vmssangola.org

Acting Principal : **Dr. R. A. Fule**  
M.A., Ph.D.

Third Cycle Accredited by NAAC  
with 'B' Grade (CGPA of 2.24)

Ref. No. 31/2021-22

Date : 12/14/2022

## Thanking Letter

To,

**Dr. V. P. Ubale**  
Principal,  
DBF Dayanand College, Solapur

**Subject :** - Thanking you for your presence as a Chairperson in the International e-Conference on Proteomics application to Biomedical Research-(PABR-2022).

Respected sir,

We are heartily thankful to you for your valuable presence as a chairperson in the International e-Conference on Proteomics application to Biomedical Research-(PABR-2022) arranged by department of chemistry in our college. We are also thankful to you for your stimulating speech on Proteomics and your current research in concerned field. Your comments were especially helpful for the participants accomplishing research work in their concerned area. Your enthusiasm is contagious and we hope to use your suggestion in our future campaigns.

Thank you

o/c

  
Principal

**Acting Principal**  
Vidnyan Mahavidyalaya, Sangola  
Tal. Sangola Dist. Solapur



'Sangola Taluka Shetkari Shikshan Prasarak Mandal Sangola's

# VIDNYAN MAHAVIDYALAYA SANGOLA

(Arts & Science, E.C.S. & B.C.A.)

Off. (02187) 220508

Tal. Sangola Dist. Solapur Pin. 413 307 (Maharashtra)

Mob. No. 9421045987

(Affiliated to P. A. H. Solapur University)

Email : vidnyanms@yahoo.co.in

Website : www.vmssangola.org

Acting Principal : Dr. R. A. Fule

M.A., Ph.D.

Third Cycle Accredited by NAAC  
with 'B' Grade (CGPA of 2.24)

Ref. No. 33 / 2021-22

Date : 13/4 / 2022

## Thanking Letter

To,

**Dr. Deokar S. S.**

Head,

Department of Chemistry,

Shankarro Mohite College, Akluj

**Subject :** - Thanking you for your presence as a Chairperson in the International e-Conference on Proteomics application to Biomedical Research-(PABR-2022).

Respected sir,

We are heartily thankful to you for your valuable presence as a chairperson in the International e-Conference on Proteomics application to Biomedical Research-(PABR-2022) arranged by department of chemistry in our college. We are also thankful to you for your stimulating speech on Proteomics and your current research in concerned field. Your comments were especially helpful for the participants accomplishing research work in their concerned area. Your enthusiasm is contagious and we hope to use your suggestion in our future campaigns.

Thank you

O/c

**Acting Principal**  
Vidnyan Mahavidyalaya, Sangola  
Tal. Sangola Dist. Solapur



'Sangola Taluka Shetkari Shikshan Prasarak Mandal Sangola's

# VIDNYAN MAHAVIDYALAYA SANGOLA

(Arts & Science, E.C.S. & B.C.A.)

Off. (02187) 220508

Tal. Sangola Dist. Solapur Pin. 413 307 (Maharashtra)  
(Affiliated to P.A. H. Solapur University)

Mob. No. 9421045987  
Email : vidnyanms@yahoo.co.in  
Website : www.vmssangola.org

Acting Principal : Dr. R. A. Fule  
M.A., Ph.D.

Third Cycle Accredited by NAAC  
with 'B' Grade (CGPA of 2.24)

Ref. No. 32/2021-22

Date : 13/4/2022

## Thanking Letter

To,

**Dr. Bachute Madhusudan**  
Principal,  
Sangola college Sangola

**Subject :** - Thanking you for your presence as a Chairperson in the International e-Conference on Proteomics application to Biomedical Research-(PABR-2022).

Respected sir,

We are heartily thankful to you for your valuable presence as a chairperson in the International e-Conference on Proteomics application to Biomedical Research-(PABR-2022) arranged by department of chemistry in our college. We are also thankful to you for your stimulating speech on Proteomics and your current research in concerned field. Your comments were especially helpful for the participants accomplishing research work in their concerned area. Your enthusiasm is contagious and we hope to use your suggestion in our future campaigns.

Thank you

o/c

  
Principal

**Acting Principal**  
Vidnyan Mahavidyalaya, Sangola  
Tal. Sangola Dist. Solapur



'Sangola Taluka Shetkari Shikshan Prasarak Mandal Sangola's

# VIDNYAN MAHAVIDYALAYA SANGOLA

(Arts & Science, E.C.S. & B.C.A.)

Off. (02187) 220508

Tal. Sangola Dist. Solapur Pin. 413 307 (Maharashtra)  
(Affiliated to P. A. H. Solapur University)

Mob. No. 9421045987  
Email : vidnyanms@yahoo.co.in  
Website : www.vmssangola.org

Acting Principal : **Dr. R. A. Fule**  
M.A., Ph.D.

Third Cycle Accredited by NAAC  
with 'B' Grade (CGPA of 2.24)

Ref. No. 48/2022-23

Date : 16/11/2022

To,

**Prof. Patwari S. B.**  
Department of Chemistry  
LBS Mahavidyalaya Dharmabad

**Subject :** - Thanking you for working as Organizing committee member for the International e-Conference on Proteomic application to Biomedical Research-(PABR-2022).

Respected sir,

We are heartily thankful to you for working as a committee member for International e-Conference on Proteomic application to Biomedical Research-(PABR-2022) arranged by department of chemistry in our college. We are also thankful to you for your support and sharing of your current research in concerned field. Your suggestions were especially helpful for the organizing committee to convey the conference with ease. Your enthusiasm is contagious, and we hope to use your suggestion in our future campaigns.

Thank you

o/c

  
**Acting Principal**  
Principal  
Vidnyan Mahavidyalaya, Sangola  
Tal. Sangola Dist. Solapur



'Sangola Taluka Shetkari Shikshan Prasarak Mandal Sangola's

# VIDNYAN MAHAVIDYALAYA SANGOLA

(Arts & Science, E.C.S. & B.C.A.)

Off. (02187) 220508

Tal. Sangola Dist. Solapur Pin. 413 307 (Maharashtra)  
(Affiliated to P. A. H. Solapur University)

Mob. No. 9421045987  
Email : vidnyanms@yahoo.co.in  
Website : www.vmssangola.org

Acting Principal : Dr. R. A. Fule  
M.A., Ph.D.

Third Cycle Accredited by NAAC  
with 'B' Grade (CGPA of 2.24)

Ref. No. 42/2021-22

Date : 13/4/2022

## Appreciation Letter

To,

**Dr. Sunil Gaikwad**

D. Y. Patil women's college pimpari-chinchwad, Pune

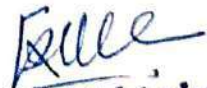
**Subject : -** Appreciation Letter for standing 1<sup>st</sup> for the Oral presentation in International e-Conference on Proteomics application to Biomedical Research-(PABR-2022).

Respected sir,

We are heartily Congratulate you for standing 1<sup>st</sup> in the oral presentation session of the International e-Conference on Proteomics application to Biomedical Research-(PABR-2022) arranged by department of chemistry in our college. We are also thankful to you for your stimulating speech on Proteomics and your current research in concerned field.

Thank you

o/c

  
**Acting Principal**  
Vidnyan Mahavidyalaya, Sangola  
Tal. Sangola Dist. Solapur



'Sangola Taluka Shetkari Shikshan Prasarak Mandal Sangola's

# VIDNYAN MAHAVIDYALAYA SANGOLA

(Arts & Science, E.C.S. & B.C.A.)

Off. (02187) 220508

Tal. Sangola Dist. Solapur Pin. 413 307 (Maharashtra)  
(Affiliated to P. A. H. Solapur University)

Mob. No. 9421045987  
Email : vidnyanms@yahoo.co.in  
Website : www.vmssangola.org

Acting Principal : Dr. R. A. Fule  
M.A., Ph.D.

Third Cycle Accredited by NAAC  
with 'B' Grade (CGPA of 2.24)

Ref. No. 43/2021-22

Date : 13/11/2022

## Appreciation Letter

To,

**Dr. Ajay N. Ambhore**  
Padmabhushan Dr. Vasantarodada Patil Mahavidyalay,  
Tasgaon Sangli,

**Subject :** - Appreciation Letter for standing 1<sup>st</sup> for the Oral presentation in International e-Conference on Proteomics application to Biomedical Research-(PABR-2022).

Respected sir,

We are heartily Congratulate you for standing 1<sup>st</sup> in the oral presentation session of the International e-Conference on Proteomics application to Biomedical Research-(PABR-2022) arranged by department of chemistry in our college. We are also thankful to you for your stimulating speech on Proteomics and your current research in concerned field.

Thank you

o/c

  
**Acting Principal**  
Vidnyan Mahavidyalaya, Sangola  
Tal. Sangola Dist. Solapur

Videos link of the conference “ Proteomics application to biomedical research 2022”

(PABR-2022)

1) Day one 10 April 2022

<https://www.youtube.com/watch?v=SMQVXipK4G0>

2) Day Two 11 April 2022

<https://www.youtube.com/watch?v=BES-m2e8cY8>



**3.2.2 - Number of workshops/seminars conducted on Research Methodology, Intellectual Property Rights (IPR) and entrepreneurship during the year-2021-22**

**Documents**

**3.2.2 RTNA-2022 Conference Proceedings**

**Online ISSN : 2395-602X**

**Print ISSN : 2395-6011**

[www.ijrst.com](http://www.ijrst.com)



**International e-Conference on  
Recent Trends in Nano-Materials  
and Its Applications  
RTNA-2022**

Organized By  
Department of Physics,  
Sangola Taluka Shetkari Shikshan Prasarak  
Mandal Sangola's, Vidnyan Mahavidyalaya, Sangola  
Tal-Sangola, Dist-Solapur, MH-413307, India  
Collaboration with  
Internal Quality Assurance Cell (IQAC)

**VOLUME 9, ISSUE 11, MARCH-APRIL-2022**

**INTERNATIONAL JOURNAL OF SCIENTIFIC  
RESEARCH IN SCIENCE AND TECHNOLOGY**

Email : [editor@ijrst.com](mailto:editor@ijrst.com) Website : <http://ijrst.com>



## **International e-Conference on Recent Trends in Nano-Materials and Its Applications (RTNA-2022)**

**22<sup>nd</sup>-23<sup>rd</sup> April, 2022**

Organised by

Department of Physics in Collaboration with Internal Quality Assurance Cell (IQAC)

Sangola Taluka Shetkari Shikshan Prasarak Mandal Sangola's Vidnyan Mahavidyalaya, Sangola

Tal-Sangola, Dist-Solapur, MH-413307, India

Affiliated to Punyashlok Ahilyadevi Holkar Solapur University, Solapur, Maharashtra, India

In Association with

International Journal of Scientific Research in Science and Technology

Print ISSN: 2395-6011 Online ISSN : 2395-602X

Volume 9, Issue 11, March-April-2022

International Peer Reviewed, Open Access Journal

Published By

Technoscience Academy



(The International Open Access Publisher)

website: [www.technoscienceacademy.com](http://www.technoscienceacademy.com)

## Resource Persons



**Prof. Jae Cheol Shin**  
Dongguk University,  
South Korea



**Dr. Sreekanth TVM**  
Yeungnam University,  
South Korea



**Dr. M. Vasudeva Reddy**  
Yeungnam University,  
South Korea



**Dr. Sonaimuthu  
Mohandoss**  
Yeungnam University,  
South Korea

## Chief Patron

**Hon'ble Mr. Chandrakant Deshmukh**  
Director, STSSPM

**Hon'ble Mr. Vitthalrao Shinde**  
Secretary, STSSPM

## Organizing Committee

**Dr. R. A. Fule**  
(Acting Principal)

**Mr. A. M. Kambale**  
(Treasurer)

**Mr. B. B. Navale**  
(Head of Dept.)

**Dr. D. K. Bandgar**  
(Member)

**Dr. S. S. Dhasade,**  
(Convener)

**Dr. S. M. Mane**  
(South Korea)

**Dr. J. V. Thombare**  
(Organizing Secretary)

**Dr. S. T. Navale**  
(Spain)

## About US

The Institution, Sangola Taluka Shetkari Shikshan Prasarak Mandal Sangola, was established in 23-Sep-1991, with the aim of giving availability and facility of education to socially backward society, to Bahujan society including Harijan, Girijan, farmers, labours and socially deprived from progress in the region of sangola taluka since its establishment, the sansthas has started highschool department, professional courses of +2 section and vidnyan mahavidyalay, etc. vidnyan mahavidyalay was established 23rd september 1991. There is the facility of B .C .S, B.C.A (degree courses), Bsc(comp) & Msc education in the college. The college has started M.A (english) course from the year 2004 & Msc (comp science) from 2009 from 2012 since its establishment the college has been progressing ahead and has now become an important academic center in the region of sangola taluka the college is accredited by NAAC with Grade "B" in the year 2004 Along with an intellectual & all round development of students, to develop their academic carrier, there are various departments under Arts & Science College facilities During the last year the no. of students in this college were 1600. The big building of the college, with its large play ground, is near by S.T stand.

## CONTENTS

Sr. No	Article/Paper	Page No
2	<b>Synthesis, Characterization of Cr<sup>+3</sup>, Mn<sup>+2</sup> Metal Ion Chelates with Newly Synthesized Benzothiazolyl Hydrazone Derivatives</b> Bhagat S. M	11-18
3	<b>An Efficient One Pot Synthesis of Polyhydroquinolines Using TS1 Catalyst Under Solvent Free Conditions</b> S.K. Ghumbre, A. S. Renge	19-21
4	<b>One Pot Three Component Eco-Friendly Synthesis of Quinoline-3-Carbonitrile Derivatives</b> Kadam S. N, Ambhore Ajay, Shringare S. N., Shinde S. R., Gaikwad R. S., Adlinge N. P., Ingawale A. R.	22-27
5	<b>Highly Proficient Extractive Studies on The Behaviour of Neodymium (III) Assisted By 2-Octylaminopyridine from Weak Succinate Media</b> Gurupad D. Kore, Sunil B. Zanje, Mansing A. Anuse, Sanjay S. Kolekar	28-37
6	<b>Ammonium Chloride in PEG As an Efficient Catalyst for Synthesis Dihydropyrano [3,2-C] Chromene-3-Carbonitrile Derivatives</b> Manojkumar R. Tapare, Rahul Kamble	38-45
7	<b>Synthesis of Spiro-fused Heterocycles under Aerobic Conditions by using Polymer Gel Entrapped Catalyst</b> Shinde S. R, Gaikwad R. S, Adlinge N. P, Ingawale A. R, Kadam S. N, Rajashri Salunkhe	46-51

## Variation of Magnetic Susceptibility of Nanoparticle Sized Copper Cobalt Ferrites

S. S. Karande<sup>1</sup>, M. S. Kavale<sup>1</sup>, B. R. Karche<sup>2</sup>

<sup>1</sup>Department of Physics, Sangameshwar College, Solapur, Maharashtra, India

<sup>2</sup>Material Science and Thin Film Laboratory, Shankarrao Mohite Mahavidyalaya, Akluj, Dist. Solapur, Maharashtra, India

### ABSTRACT

The polycrystalline aluminium substituted nano-particle sized copper cobalt ferrite samples  $Cu_xCo_{1-x}Fe_2-2yAl_2yO_4$  (where  $x= 0.0, 0.2, 0.4, 0.6, 0.8, 1.0$ ;  $y= 0.05, 0.15$  and  $0.25$ ) have been prepared by standard ceramic technique. Phase formation is investigated using X-ray diffraction, Infrared absorption technique and Scanning electron microscope technique. The lattice constants of the all samples are evaluated from x-ray diffraction data. The Magnetic susceptibility decreases with aluminium and copper content.

**Keywords:** Polycrystalline, nanoparticle size, standard ceramic technique and Inverse cubic spinel, Magnetic susceptibility

### I. INTRODUCTION

In a way, every material utilized today is a composite. Composite materials are a physical mixture of two or more compatible micro or macro constituent particles which differ in form and chemical composition and are essentially insoluble in each other. Composite materials are best suited for scientific applications which could not be achieved by any one component acting on its own. Ferrite / ferroelectric composites are termed as magneto electric (ME) composites due to the coupling between the electric and magnetic fields in the materials. The conversion of magnetic to electric fields in such ME composite originates from the elastic interaction between ferrite and ferroelectric subsystems [1]. In the presence of the magnetic field, the magnetostriction in the ferrite phase gives rise to mechanical stresses that are transferred to the ferroelectric phase, resulting in electric polarization of the ferroelectric phase owing to its magneto electric effect. ME materials find applications as smart materials in actuators, sensors, magnetic probes, phase inverters, rectifiers, modulators, and transducers in solid state microelectronics and microwave devices [2,3].

Spinel ferrite nanoparticles are being intensively investigated in recent years because of their remarkable electrical and magnetic properties and wide practical applications in information storage system, ferro-fluid technology, magnetocaloric refrigeration and medical diagnosis [4]. Among the spinels, mixed Zn ferrites and especially Ni-Zn ferrites are widely used in applications like transformer cores, chokes, coils, noise filters

recording heads etc. [5]. While Ni–Zn ferrite possesses higher resistivity and saturation magnetization, cobalt ferrite possesses high cubic magneto crystalline anisotropy and hence high coercivity. The high coercivity is driven by large anisotropy of the cobalt ions due to its important spin orbit coupling. It is ferromagnetic with a Curie temperature ( $T_c$ ) around 520°C, [6] and shows a relatively large magnetic hysteresis which distinguishes it from rest of the spinels. The synthesis of ultra fine magnetic particles has been extensively investigated in recent years because of their potential applications in high density magnetic recording and magnetic fluids [7]. Among the current methods for synthesis of mixed ferrite the combustion reaction method stands out as an alternative and highly promising method for the synthesis of these ferrites [8]. Magnetic properties measured at room temperature by vibrating sample magnetometer (VSM) reveal an increase in saturation magnetization with increase in cobalt concentration [9].

## II. EXPERIMENTAL

### Materials:

High purity starting materials are used as Cobalt Oxide (CoO):- 74.9326 gm, Copper Oxide (CuO):- 74.5454 gm, Ferric oxide( $Fe_2O_3$ ):- 159.6922 gm, Aluminum Oxide ( $Al_2O_3$ ):- 101.9612 gm

### Preparation of ferrite:

Nano crystalline powder samples of  $Cu_xCo_{1-x}Fe_{2-2y}Al_{2y}O_4$  (where  $x= 0.0, 0.2, 0.4, 0.6, 0.8, 1.0$ ;  $y = 0.05, 0.15$  and  $0.25$ ) were prepared by the standard ceramic technique. Starting materials CuO, CoO,  $Fe_2O_3$  and  $Al_2O_3$  of AR grade obtained from Sigma – Aldrich, India were used. These samples were heated at ramping rate of 80 °C hr<sup>-1</sup> at 1000°C for 48 hours. XRD and IR analysis revealed the cubic spinel structure of the synthesized samples and functional groups in the samples respectively. The absence of any extra line confirms the formation of single phase ferrite. The average particle size 'D' was determined from line broadening (311) reflection using the Debye Scherer formula discussed elsewhere [10]. Calculations of lattice constant, physical density, X-ray density, porosity, site radii and ionic bond lengths on both sites were calculated by using formulae discussed elsewhere [11] and graphically shown in fig.4. Infrared absorption spectra of powdered samples were recorded in the range 350-800 cm<sup>-1</sup> using Perkin-Elmer FTIR spectrum and spectrometer by KBr pellet technique and presented in (fig.2). The scanning electron microscopes are shown in fig.3

## III. RESULTS AND DISCUSSION

The X-ray diffraction patterns of the samples are presented in (fig.1). Powder X-ray diffractometer of the ferrite samples reveals the single phase spinel structure, as well defined reflection is observed without any ambiguity. The diffraction peaks are corresponding to (200), (311), (400), (422), (333/511), (440) and (533) planes. The lattice constants 'a' and 'c' for all prepared samples are calculated by using prominent (311) XRD peak. The calculated and observed values of inter planer distance (d) are found in good agreement with each

other for all reflections. The physical density ( $\rho$ ), x-ray density ( $\rho_x$ ), and porosity ( $p$ ), are calculated from the formulae given by Gadkari et.al [12].

From the calculations of lattice constants 'a' and 'c' for all the prepared ferrites it is observed that  $c > a$  and tetragonality ratio ( $c/a$ ) is found in the range of 1.03 to 1.07. This result is in good agreement with previous report [13-14]. In this present report tetragonality ratio for copper ferrite is 1.06. It means 70% copper resides on B site and it exhibits prolate type distortions in the crystal lattice. The previous report [15] well supports the present results reported this communication. Both  $\text{Fe}^{3+}$  and  $\text{Cu}^{2+}$  are Jahn-Teller ion which produces prolate type distortions on (B) site and hence  $c > a$  and  $(c/a) = 1.06$ . Therefore copper ferrite exhibits tetragonal spinel structure in host crystal lattice of cobalt ferrite. In addition of copper content in tetragonality ratio is found increasing but due to addition of aluminium tetragonality ratio decreases. It means that  $\text{Al}^{3+}$  and copper suppress the tetragonal prolate type.

The crystallite sizes ( $t$ ) of all the prepared samples were computed by Scherer rule utilizing the peak width at one-half intensity of the maximum intensity peak (311).

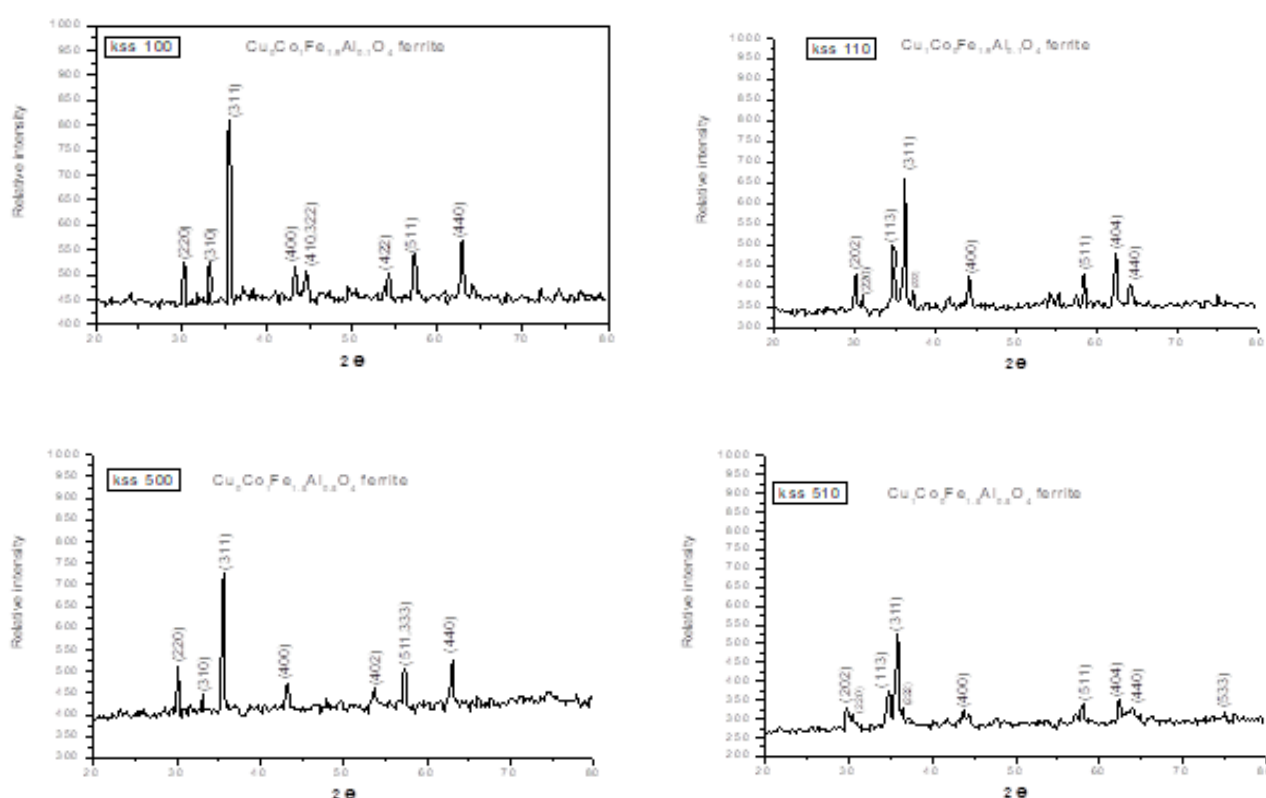


**Fig: 1 XRD patterns of system  $\text{Cu}_x\text{Co}_{1-x}\text{Fe}_{2-2y}\text{Al}_{2y}\text{O}_4$**

The Al ( $y = 0.05-0.25$ ) doped copper cobalt ferrite samples show a higher grain growth and the crystallite size ( $t$ ) lies in the extent of 52.53-94.4 nm. The mean particle size calculated from diffractograms is in the range of 50 to 100 nm. That suggest the particles in the ferrites samples are fine and there is continuous grain growth in all compositions. It gives the confirmation of suitable microstructure formation in all compositions.

The width of the reflection peak (311) for all the compositions is approximately the same due to the nearly equal particle size.

The infrared absorption spectra are showing two distinct absorption bands  $\nu_1$  due to tetrahedral (A) site interstitial voids near  $600\text{ cm}^{-1}$  and other  $\nu_2$  due to octahedral (B) site interstitial voids near  $400\text{ cm}^{-1}$ . Our results in this present communication are well supported by previous reports [16, 17].

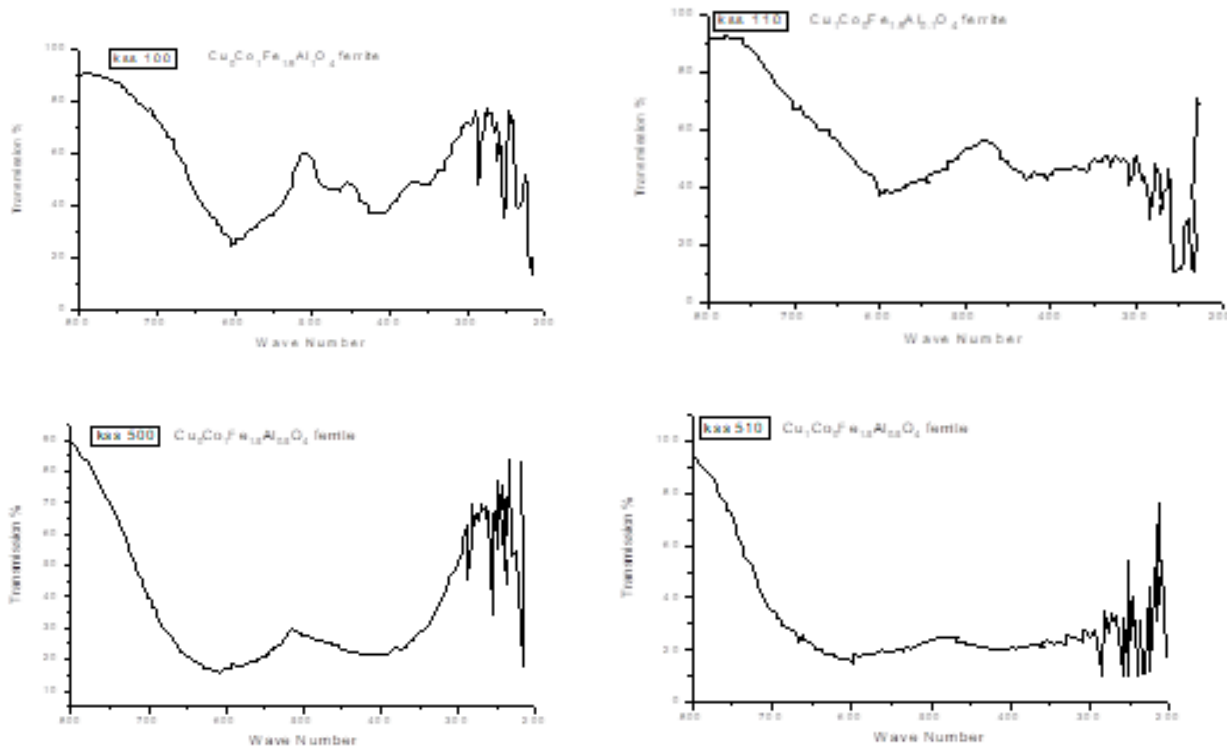


**Figure 2: Absorption spectra for system  $\text{Cu}_x\text{Co}_{1-x}\text{Fe}_{2-2y}\text{Al}_{2y}\text{O}_4$**

The close inspection of all micrographs revealed that there is continuous grain growth with well – defined grain boundaries formed. The present system shows multi domain behavior. No exaggerated grain growth is observed in any composition. The average grain size is found to decrease with increase in Al content in copper cobalt ferrite. However in the present system the grain growth shows generally a decreasing trend with aluminum content, which is rather expected because of multi-domain behavior of these compositions in copper cobalt ferrite. Grain growth is almost accompanied with grain size, which is increasing with copper and aluminum content. So it appears that copper and aluminum content favors the grain growth. The scanning electron micrographs shown below

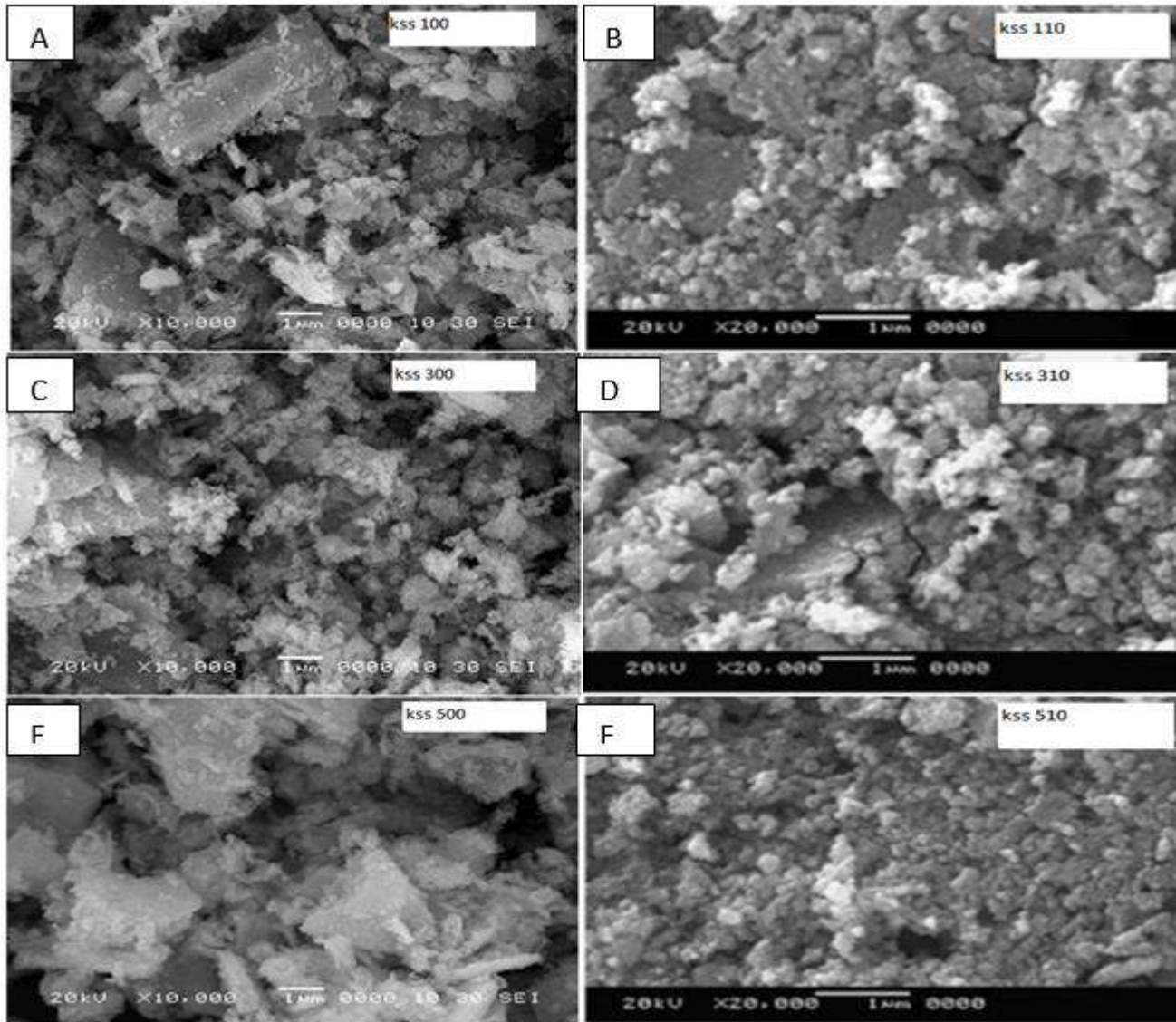


**Fig: 3 (A) to (F) scanning electron microscopes of  $\text{Cu}_x\text{Co}_{1-x}\text{Fe}_{2-2y}\text{Al}_y\text{O}_4$  :**

- (A) KSS 100- $\text{Cu}_0\text{Co}_1\text{Fe}_{1.9}\text{Al}_{0.1}\text{O}_4$ , (B) KSS 110-  $\text{Cu}_1\text{Co}_0\text{Fe}_{1.9}\text{Al}_{0.1}\text{O}_4$ ,  
 (C) KSS 300-  $\text{Cu}_0\text{Co}_1\text{Fe}_{1.7}\text{Al}_{0.3}\text{O}_4$ , (D) KSS 310-  $\text{Cu}_1\text{Co}_0\text{Fe}_{1.7}\text{Al}_{0.3}\text{O}_4$ ,  
 (E) KSS 500-  $\text{Cu}_0\text{Co}_1\text{Fe}_{1.5}\text{Al}_{0.5}\text{O}_4$  & (F) KSS 510-  $\text{Cu}_1\text{Co}_0\text{Fe}_{1.5}\text{Al}_{0.5}\text{O}_4$

The susceptibility is measured at room temperature [Fig. 2(a)] then susceptibility is found increasing up to 20 % of copper content and thereafter decreases. The susceptibility is measured at various temperatures [Fig. 2(b)], the compositions shows gradual decrease in normalized susceptibility with temperature which suggest that they exhibit super paramagnetic (SP) structure having fine particles. The susceptibility is decreases and curie temperature also shifts towards minimum value as copper as well as aluminum content increases.

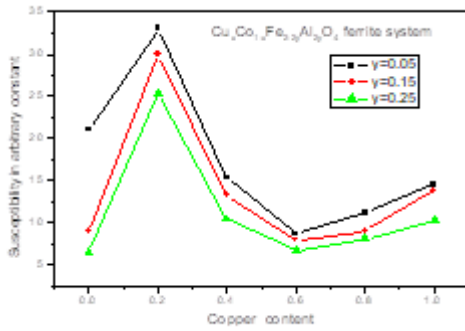


Fig. 4(a)

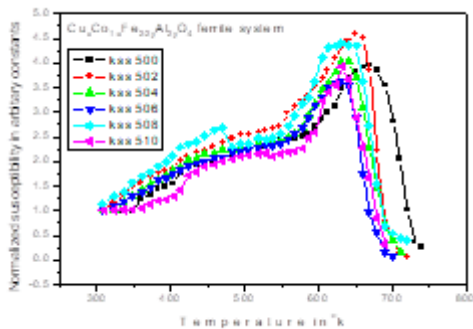
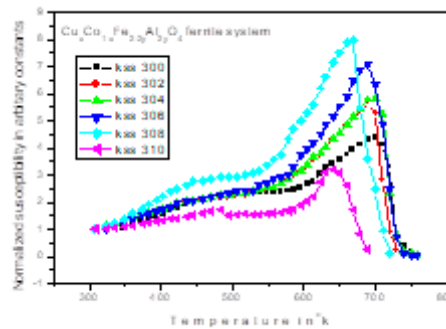
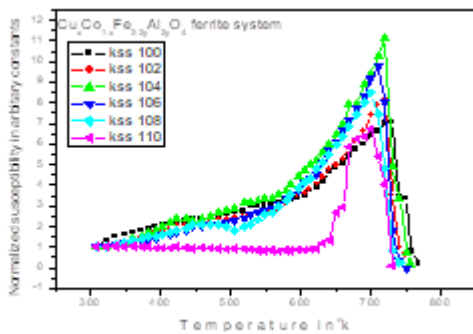


Fig. 4(b)

**Fig 4: Variation of A. C. susceptibility with copper and aluminum content at room temperature and various temperature for  $\text{Cu}_x\text{Co}_{1-x}\text{Fe}_{2-2y}\text{Al}_y\text{O}_4$  ferrite system**

#### IV. CONCLUSIONS

Copper cobalt ferrite is partially inverse spinel ferrite. Addition of  $\text{Al}^{3+}$  ions replaces  $\text{Fe}^{3+}$  on (B) site resulting in increase of lattice constant  $a$ , decrease in ionic radii ( $R_A$ ) and bond length ( $\text{O}-\text{A}$ ). The lattice constant obtained from XRD data shows increases. The A. C. susceptibility goes on decreasing with copper and aluminum content.

## V. REFERENCES

- [1]. R. S. Devan, S. A. Lokare, S. S. Chougule, D. R. Patil, Y. D. Kolekar, and B. K. Chougule, *J. Phys. Chem. Solids* 67, 1524 (2006).
- [2]. K. Zhao, K. Chen, Y. R. Dai, J. G. Wan, and J. S. Zhu, *Appl. Phys. Lett.* 87, 162901 (2005).
- [3]. S. R. Kulkarni, C. M. Kanamadi, and B. K. Chougule, *Mater. Res. Bull.* 40, 2064 (2005).
- [4]. Zhao L, Yang H, Yu L, Cui Y, Zhao X, Zou B, Feng SJ. *MagnMagn Mater* 2006;301:445–51.
- [5]. Rath C, Sahu KK, Anand S, Date SK, Mishra NC, Das RP. *J MagnMagn Mater* 1999;202:77–84.
- [6]. Rajendran M, Pullar RC, Bhattacharya AK, Das D, Chintalapudi SN, Majumdar CK. *J MagnMagn Mater* 2001;232:71–83.
- [7]. Ozaki M. *Mater Res Bull* 1989;12:35–43.
- [8]. Costa ACM, Tortella E, Morelli MR, Kaufman M, Kiminami RHGA. *J Mater Sci* 2002;37:3569–72.
- [9]. M.M. Mallapur, B.K. Chougule; *Materials Letters*; Vol. 64 (2010); P. 231–234.
- [10]. H. P. Klug, L. E. Alexander, *X-ray diffraction procedure for polycrystalline and amorphous materials*, Wiley N.Y, 1997, 637.
- [11]. A. B. Gadkari, T. J. Shinde, P. N. Vasambekar, *J. Mater Sci: Mater Electron* 21 2010, 96 , 103.
- [12]. Prince E., Treuting R.G; *Acta Crystallographica*, 1956, 9, 1025.
- [13]. Sagal K., Tabellen F. *Rontegenstrukturanalyse*, Springer, Berlin, 1958.
- [14]. Borisenko A., Toropov N. A; *Z. Prikl Chem*, 1950, 23, 1165.
- [15]. Goodenough J.B and Loeb A. L, *Phys. Rev.*, 1955, 98, 391.
- [16]. Waldron R.D, *Phy. Rev*, 1955, 99(6), 1727.
- [17]. K. V. S. Badarinath, *Phys. Stat. Solidi (a)* 1985, 91, 19-23.

## DC Resistivity of La<sup>3+</sup> Substituted Mg-Zn Ferrite Nanoparticles by Co-Precipitation Method

R.A. Bugad<sup>1\*</sup>, B.G. Pawar<sup>1</sup>, B.B. Navale<sup>2</sup>, P.G. Pawar<sup>3</sup>

<sup>1</sup>Department of Science, Sangola Mahavidyalaya, Sangola, Dist. Solapur 413307, Maharashtra, India

<sup>2</sup>Department of Science, Vidnyan Mahavidyalaya, Sangola, Dist. Solapur 413307, Maharashtra, India

<sup>3</sup>Department of Science, Shivaji Polytechnic College, Sangola, Dist. Solapur 413307, Maharashtra, India

### ABSTRACT

Lanthanum (La) substituted magnesium zinc ferrite nanoparticles with general formula  $Mg_{0.6}Zn_{0.4}La_{2y}Fe_{2-2y}O_4$  (where  $y = 0.00, 0.05, 0.10, 0.15, 0.20$  and  $0.25$ ) have been synthesized by co-precipitation method. The XRD analysis was carried out to confirm the single phase cubic structure of La<sup>3+</sup> substituted Mg-Zn ferrite. The nature of DC resistivity of ferrite was studied with substitution of La<sup>3+</sup> content. The effects of La<sup>3+</sup> substitution in Mg-Zn ferrite on structural and electric properties were studied.

**Keywords:** Lanthanum, Mg-Zn ferrites, Co-precipitation, DC Resistivity,

### I. INTRODUCTION

Ferrites are usually non-conductive ferrimagnetic ceramic material. Most of the ferrites have a spinel structure [1]. The general formula of a spinel can be written as  $AB_2O_4$ . Nano-particles of mixed spinel ferrites have been the subject of current interest because of their interesting electric, optical and magnetic properties, which are considerably different from that of their bulk ferrites [2]. The ferrites are also widely used in high frequency cores, antennas, high frequency transformers, deflecting coil, motor generator and microwave devices such as modulators, phase shifter and circulators etc.[3]. The coercive force is related with saturation magnetization, anisotropy, internal stresses and porosity. The ferrites having low coercive force (HC) is known as Soft ferrites [4]. Generally, soft ferrite shows high electrical resistivity, superior magnetic and structural properties and hence they have low eddy current losses at high frequency [5]. Demand for electronic and computer components with high density and light weight performance is greatly increasing, which step up the demand for soft ferrites with high performance and thus contributes to the development of soft magnetic ferrites on the direction of higher frequency and lower power consumption [6].

## II. EXPERIMENTAL

### 2.1. Synthesis of La<sup>3+</sup> substituted Mg-Zn ferrite

The  $\text{Mg}_{0.6}\text{Zn}_{0.4}\text{La}_{2y}\text{Fe}_{2-2y}\text{O}_4$  (where  $y = 0.00, 0.05, 0.10, 0.15, 0.20$  &  $0.25$ ) have been prepared by the oxalate co-precipitation method as per reported in earlier literature [7]. The high purity AR grade starting materials  $\text{MgSO}_4 \cdot 7\text{H}_2\text{O}$ ,  $\text{ZnSO}_4 \cdot 7\text{H}_2\text{O}$ ,  $\text{LaSO}_4 \cdot 7\text{H}_2\text{O}$  and  $\text{Fe}_2\text{SO}_4 \cdot 7\text{H}_2\text{O}$  were used for preparation of samples. These chemicals were weighted in desired stoichiometric proportion and dissolved in distilled water. The pH of the solution was maintained at 4.8 by drop wise addition of concentrated  $\text{H}_2\text{SO}_4$ . The resulting solution was heated at  $80^\circ\text{C}$  for 1 h in order to complete the ionization of metal sulfates. The precipitating reagent was prepared in distilled water by adding required proportion of AR grade ammonium oxalate. Ammonium oxalate was taken in burette and was added drop by drop until the precipitation was formed. The co-precipitate product was dried and calcined at  $450^\circ\text{C}$  for 5h in air. The calcined powders were milled in an agate mortar with AR grade acetone as a base. The powders were pre-sintered at  $700^\circ\text{C}$  for 5h. The pre-sintered powders were pressed under hydraulic pressure of 5 tones / $\text{cm}^3$  to form pellet using polyvinyl alcohol as binder. Then pellets were finally sintered at  $900^\circ\text{C}$  for 12h.

### 2.2. Characterization Techniques

XRD patterns of lanthanum substituted magnesium zinc ferrites sintered at  $900^\circ\text{C}$  for 12h were recorded by Philips X-Ray Diffractometer model PW 1710 using Cu Ka radiation ( $\lambda = 1.5405 \text{ \AA}$ ). Two probe method was used for measurement of the dc electrical resistivity of ferrite in the temperature range  $25^\circ\text{C}$  to  $575^\circ\text{C}$ . The resistivity was obtained by using formula  $\rho = \frac{\pi r^2}{t} \times \frac{V}{I} = \frac{\pi r^2 R}{t}$ , Where, t is thickness and r is radius of the pellet in cm.

## III. RESULTS AND DISCUSSIONS

### 3.1. XRD studies

The XRD patterns of  $\text{Mg}_{0.6}\text{Zn}_{0.4}\text{La}_{2y}\text{Fe}_{2-2y}\text{O}_4$  (where  $y = 0.00, 0.05, 0.10, 0.15, 0.20, 0.25$ ) ferrite system sintered at temperature  $900^\circ\text{C}$  for 12h are shown in Fig. 1. The XRD patterns reveals the well resolved, sharp and intense peaks corresponding to planes (220), (311), (222), (400), (422), (511), (440), (620) and (533). The peaks obtained in the diffractogram closely match the data in the JCPDS file card number (04-002-5442). The XRD peak pattern corresponds to all allowed planes, which hint outs single phase cubic structure with the traces of secondary phase. Moreover, the peak at  $2\theta = 32.10^\circ$  corresponds to plane (121) which is attributed to secondary phase for  $\text{LaFeO}_3$  indexed as per ICDD file No. 01-74-9045. With increase in La content, intensity of characteristics peak (311) for  $\text{Fe}_2\text{O}_4$  gradually decreases, while intensity of peak (121) of  $\text{LaFeO}_3$  increases. It implies that the substituted  $\text{La}^{3+}$  ion has a solubility limit in the spinel lattice.

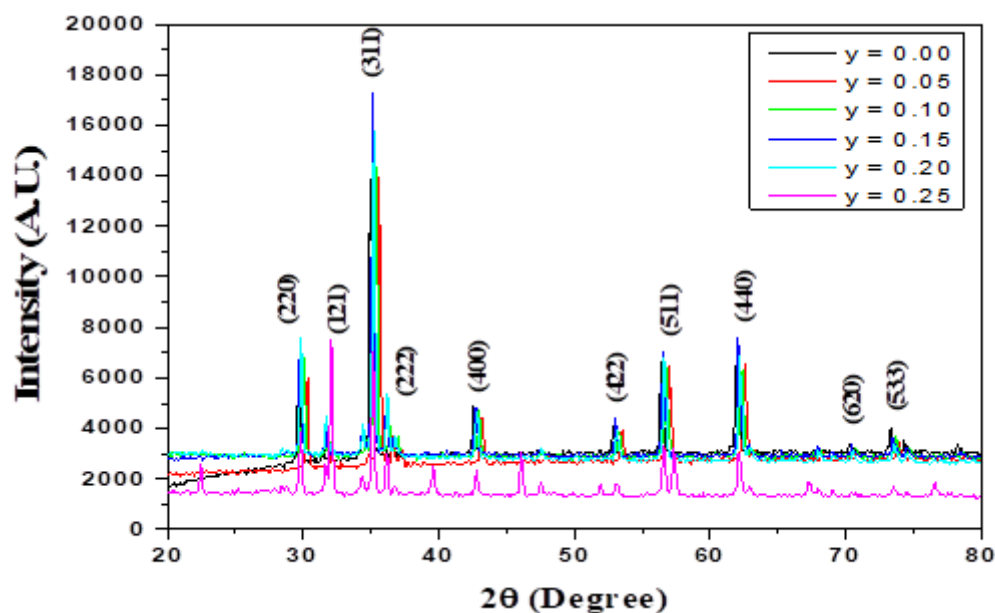


**Fig.1** : XRD patterns of  $\text{Mg}_{0.6}\text{Zn}_{0.4}\text{La}_{2y}\text{Fe}_{2-2y}\text{O}_4$  ferrite system

The degree of substitution of  $\text{Fe}^{3+}$  by  $\text{La}^{3+}$  ion is limited in the spinel lattice due to larger ionic radii of  $\text{La}^{3+}$  ions compared to  $\text{Fe}^{3+}$  ions. There is always some  $\text{La}^{3+}$  ions do not enter into spinel lattice. These  $\text{La}^{3+}$  ions react with  $\text{Fe}^{3+}$  ions and form second phase  $\text{LaFeO}_3$  usually locating at the grain boundaries. Similar observation have been reported in lanthanum substituted nickel [8], Cadmium [9] and Ni-Zi ferrites [10, 11].

### 3.2. DC Resistivity study

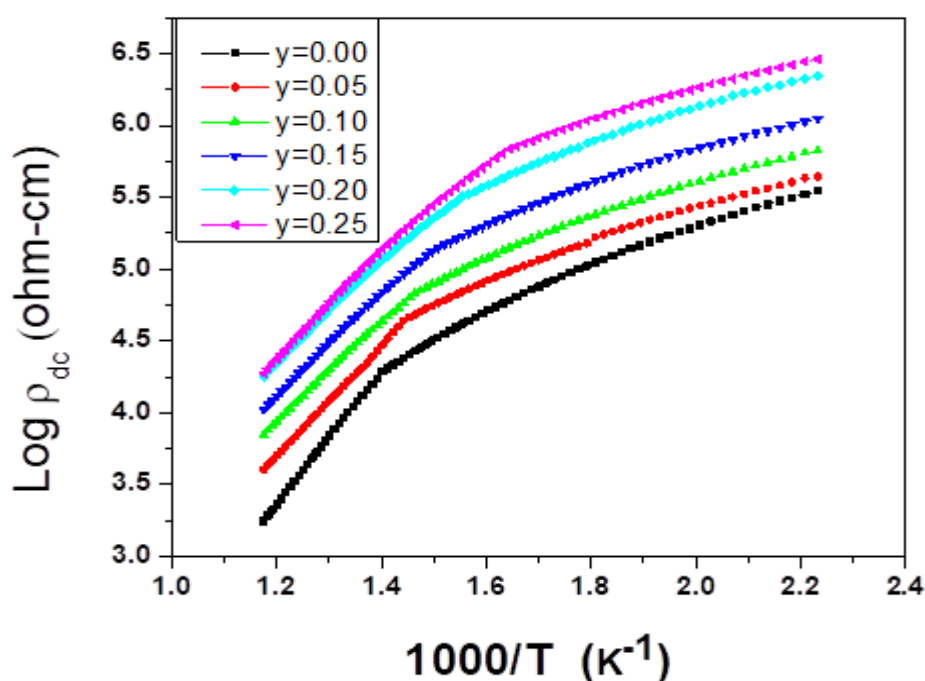


**Fig.2:** Variation of dc resistivity with inverse temperature for  $\text{Mg}_{0.6}\text{Zn}_{0.4}\text{La}_{2y}\text{Fe}_{2-2y}\text{O}_4$  ferrite system

The variation of log of dc electrical resistivity ( $\log \rho_{dc}$ ) as a function of inverse of temperature ( $1000/T$ ) for various composition of  $Mg_{0.6}Zn_{0.4}La_{2y}Fe_{2-2y}O_4$  ferrite is shown in Fig.2, The dc resistivity of the ferrites gets decreased with an increase in temperature indicates semiconducting behavior of the ferrites. All the samples show the break at Curie temperatures due to the change in conduction mechanism [12]. The slope change at Curie temperature corresponds to the samples transform from an ordered ferrimagnetic state to disordered paramagnetic state [13]. The value of Curie temperature obtained from the graph of  $\log \rho_{dc}$  verses  $1/T$  is calculated. The Curie temperature decreases with increase of  $La^{3+}$  content. It is due to the nonmagnetic nature of  $La^{3+}$  ions, which may break linkage between magnetic cations [14]. Rare earth  $La^{3+}$  ions have a strong preference to occupy on octahedral site and therefore replace  $Fe^{3+}$  ions at octahedral site (B) in spinel lattice by  $La^{3+}$ . Upon increase in the  $La^{3+}$  ions in B-site, A-B interaction weakens. Thus the decrease in Curie temperature is probably due to weakening of the A-B interaction. Similar observations have also been reported by Patil et al. [15]. The conduction phenomenon in polycrystalline ferrites was explained on the basis of Verwey and de Boer mechanism [16]. The conduction in ferrites is due to hopping of electrons between  $Fe^{2+}$  and  $Fe^{3+}$  ions on the octahedral (B) sites. In addition of lanthanum in Mg-Zn ferrite, it found that,  $Zn^{2+}$  ion have strong tendency to occupy A-site and  $Mg^{2+}$  ion have strong preference to occupy B-site, While  $La^{3+}$  preferentially occupy to octahedral B site, where it replaced  $Fe^{3+}$  ions in the B-site as per the modified cation distribution in magnetic study. The resistivity of the ferrite is controlled by  $Fe^{3+}$  concentration on B-site. The increase in resistivity with  $La^{3+}$  content is due to overall decrease in  $Fe^{3+}$  ions concentration on B-site. It causes decrease in hopping of electrons between  $Fe^{2+}$  and  $Fe^{3+}$  ions, results in decrease in conduction in ferrite with increase of resistivity [17]. Several researchers have been reported that resistivity of ferrites increases with the substitution of rare earth [18]. Gul and Ahmed also reported the effect of grain size, porosity and grain boundary area on resistivity of ferrite [19]. It is found that one of the factors for higher resistivity in ferrite is the decrease in grain size upon the addition of lanthanum. Smaller grain size produces larger number of insulating grain boundaries which produces inhomogeneous structure and greater energy is required for electron conduction which affects on AC and DC resistivity of ferrites [20].

#### IV. CONCLUSIONS

In conclusion, we report the preparation of lanthanum substituted magnesium zinc ferrites by co-precipitation method. A study on DC resistivity shows all sample have semiconducting behavior and break at Curie temperature. The conduction phenomenon in polycrystalline ferrites was explained on the basis of Verwey and de Boer mechanism. The increase in DC resistivity is due to low concentration of  $Fe^{2+}$  ions, which is responsible for decrease in electronic polarization. The increase of dc resistivity with La content was mainly attributed to decreases in drift mobility with lanthanum content. This study reveals that Lanthanum substitution alters the structural and electric properties of Mg-Zn ferrites.

## V. REFERENCES

- [1]. M. Kaur, B.S. Randhawa, J. Singh, D. Utreja , Thermolysis studies on magnesium zinc bis(citrato)ferrate pentahydrate precursor for synthesis of ferrite nanoparticles, *J. Ceramics Int.*, 39 (2013) 325-328.
- [2]. V. Provenzano, & R. L. Holtz, Nanocomposites for high temperature applications. *Mat.Sci. and Eng. A*, 204(1-2) (1995)125-134.
- [3]. S. R. Hoh, "Evaluation of High Performance Core Materials", *Tele. Tech.* 2 (1953) 86.
- [4]. E.W. Lee, Soft magnetic material, *Advances in Physics*, 8 (1959) 292.
- [5]. E.E. Richards and A.C. Lynch, "Soft Magnetic Materials for Telecommunications", Pergamon Press Ltd. (1953).
- [6]. A. Sharma, K.S. Pallavi, R. Sharma, "Optical Properties of Tin Oxide Nanoparticles", *ISST Journal of Applied Physics*, 2(2)(2011) 13-14.
- [7]. R. A. Bugad, T. R. Mane, B. B. Navale, J. V. Thombare, A. R. Babar, B. R. Karche, Structural, morphological and compositional properties of La<sup>3+</sup> substituted Mg-Zn ferrite interlocked nanoparticles by co-precipitation method, *J. Mater. Sci.: Mater. Electron.* 28 (2017) 1590-1596.
- [8]. S. E. Shirsath, B. G. Toksha, K. M. Jadhav, Structural and Magnetic properties of La<sup>(3+)</sup> substituted NiFe<sub>2</sub>O<sub>4</sub>, *Mater. Chem. Phys.* 117(2009)163-168.
- [9]. A. Gadkari, T. Shinde, P. Vasambekar, Influence of rare-earth ions on structural and Magnetic properties of CdFe<sub>2</sub>O<sub>4</sub>, *Rare Metal*, 29(2) (2010)148.
- [10]. Y. K. Dasan, B. H. Guan, M. H. Zahari, L. K. Chuan, Influence of La<sup>(3+)</sup> substitution on structure, Morphology and Magnetic properties of Nanocrystalline Ni-Zn ferrite, *PLoS ONE* 12(1) (2017)75.
- [11]. M. Soka, M. Usakova, R. Dosoudil, E. Usak, J. Lokaj, Effect of lanthanum substitution on structural and magnetic properties of nickel zinc ferrites, *AIP Advances* 8 (2018) 047802.
- [12]. D. Ravinder, B. Ravikumar, A study on elastic behaviour of rare earth substituted Mn-Zn ferrites, *Mater. Lett.* 57 (2003) 4471-4473.
- [13]. A.A. Sattar, Egypt., Temperature Dependence of the Electrical Resistivity and Thermoelectric Power of Rare Earth Substituted Cu-Cd ferrite *J. Sol.*, 26(2003)113.
- [14]. A. I. Ali, M. A. Ahmed, N. Okashad, M. Hammam, J. Y. Son, Effect of the La<sup>3+</sup> ions substitution on the magnetic properties of spinal Li-Zn-ferrites at low temperature, *J. Mater. Res. Technol.* 2 (2013) 356-361.
- [15]. S. B. Patil, R. P. Patil, J. S. Ghodake, B. K. Chougule, Temperature and frequency dependent dielectric properties of Ni-Mg-Zn-Co ferrites, *J. Magn. Magn. Mater.* 350 (2014) 179-182.
- [16]. E. J. W. Verwey, F. de Boer and J.H. Van Santen, Cation Arrangement in Spinels, *J. Chem. Phys.* 16 (1948) 1091.
- [17]. K. Torkar & O. Fredriksen, The effect of grain size on saturation magnetization of barium ferrite powders, *J. Powder Metallurgy*, (2014) 105-107.
- [18]. G. L. Sun, J. B. Li, J. J. Sun, X-Z Yang, The influences of Zn<sup>2+</sup> and some rare-earth ions on the magnetic properties of nickel-zinc ferrites, *J. Magn. Magn. Mater.* 281 (2004)173.

- [19].I. H. Gul, W. Ahmed and A. Maqsood, Electrical and magnetic characterization of nanocrystalline Ni-Zn ferrite synthesis by co-precipitation route, *J. Magn. Magn. Mater.* 320 (2008) 270-275.
- [20].T. J. Shinde, A. B. Gadkari, P. N. Vasembekar, Effect of Nd<sup>3+</sup> substitution on structural electrical properties of nanocrystalline zinc ferrite, *J. Magn. Magn. Mater.* 322(2010) 2777-2781.

## Self-Focusing of Gaussian Laser Beam in Collision less Plasma with Linear Absorption

K.Y. Khandale<sup>1</sup>, P.T. Takale<sup>1</sup>, T.U. Urunkar<sup>1</sup>, S.S. Patil<sup>2</sup>, P.P. Nikam<sup>2</sup>, M.B. Mane<sup>2</sup>, V.S. Pawar<sup>2</sup>, S.D. Patil<sup>2</sup>,  
M.V. Takale<sup>1</sup>

<sup>1</sup>Department of Physics, Shivaji University, Kolhapur 416 004, Maharashtra, India

<sup>2</sup>Department of Physics, Devchand College, Arjunnagar, Kolhapur 591 237, Maharashtra, India

### ABSTRACT

In the present work, authors have studied the effect of linear absorption on the self-focusing of Gaussian laser beam propagating in the collisionless plasma. The non-linear dependence of the dielectric constant inside collisionless plasma is mainly due to the ponderomotive force. The field distribution in the medium is expressed in terms of linear absorption coefficient as well as beam-width parameter. By following Akhmanov's parabolic equation approach under Wentzel-Kramers-Brillouin (WKB) approximation and Paraxial approximations, the differential equation is set up for the beam width parameter  $f$  which is solved numerically. It is noticed that the absorption coefficient plays an important role in propagation of Gaussian laser beam in collisionless plasma. The graphical results are presented and are discussed at the end.

**Keywords:** Gaussian laser beam, Collisionless Plasma, Linear absorption, Self-focusing.

### I. INTRODUCTION

With the invention of laser nearly six decades (1960-2020) ago, a fascinating new field of research known by the name "Nonlinear Optics" is introduced to the scientific community. Nonlinear optics has its origin when researchers P.A. Franken and his co-workers in 1961 noticed that a weak optical signal at  $3472 \text{ \AA}$  could be generated in quartz crystal when the material is illuminated with a high power Ruby laser at  $6943 \text{ \AA}$  on optical second-harmonic generation in 1961 the theoretical work of J.A. Armstrong and his co-workers on optical wave mixing in 1962-3. Self-focusing is one of the phenomena in which the intense beam of laser light incident on material medium changes the optical properties in such a way that beam comes to focus within the medium. There are three major mechanisms that lead to a change in the dielectric constant of plasma in laser-plasma interaction, as follows: (i) the relativistic effect (ii) the collisional and (iii) the ponderomotive force<sup>4-6</sup>.

With the availability of high power laser beams, a large number of interesting nonlinear phenomena have been studied, both theoretically and experimentally. The redistribution of carriers is caused by the ponderomotive force and is mainly important in collisionless plasmas. When an intense laser beam propagates

through collisionless plasma, the drift velocity of electrons is relativistic so that their mass is intensity dependant but for long pulse experiments, the relativistic effects can be ignored and ponderomotive force of the beam nonlinearity perturbs electron density resulting in the excitation of electron plasma wave<sup>7,8</sup>. Light absorption has played an important role in studies on the self-focusing of laser beams in different situations. The contribution of light absorption has been ignored in the most of investigations on self-focusing of laser beams in plasmas<sup>9–14</sup>. Furthermore, Navare et al.<sup>15</sup>, M. A. Wani et al.<sup>16</sup>, L. Ouahid et al.<sup>17</sup>, R. Kashyap et al.<sup>18</sup>, T. U. Urunkar et al.<sup>19</sup>, K. M. Gavade et al.<sup>20</sup>, B. D. Vhanmore et al.<sup>21</sup> and S. D. Patil et al.<sup>22–25</sup> have investigated the effect of linear absorption on the self-focusing of a Gaussian, Chirped Gaussian, Airy-Gaussian, q-Gaussian, Gaussian, Cosh-Gaussian, elegant Hermite-cosh-Gaussian, Cosh-Gaussian, Gaussian laser beam respectively by considering the different nonlinearities in different situations. The aim of the present investigation is to study the effect of linear absorption on the self-focusing of Gaussian laser beam propagating in the collisionless plasma. The present analysis is carried through parabolic equation approach under WKB and paraxial approximations.

## II. THEORETICAL FRAMEWORK

Consider the propagation of Gaussian laser beam in homogeneous collisionless plasma along the z-direction, initial intensity distribution of Gaussian laser beam at  $z = 0$  can be expressed as

$$\bar{E}\bar{E}^* = E_0^2 \exp\left(-\frac{r^2}{r_0^2}\right), \quad (1)$$

where  $E_0$  is the amplitude of Gaussian intensity distribution,  $r$  is the radial coordinate of cylindrical coordinate system,  $r_0$  is the initial beam width of the laser beam. The wave equation governing the electric field  $\bar{E}$  of the laser beam in homogeneous plasma along with the effective dielectric constant  $\varepsilon$ , in the cylindrical co-ordinate system is given by,

$$\frac{\partial^2 \bar{E}}{\partial z^2} + \frac{\partial^2 \bar{E}}{\partial r^2} + \frac{1}{r} \frac{\partial \bar{E}}{\partial r} + \frac{\omega^2}{c^2} \varepsilon \bar{E} = 0 \quad (2)$$

When a laser beam propagates through homogeneous gaseous plasma, the effective dielectric constant changes significantly and can be, in general represented as<sup>5</sup>

$$\varepsilon = \varepsilon_0 + \phi(EE^*) - i\varepsilon_i, \quad (3)$$

where  $\varepsilon_0 = 1 - (\omega_p / \omega)^2$  is linear part and  $\phi$  is nonlinear part of the dielectric constant,  $\omega_p$  is the plasma frequency  $\omega_p^2 = (4\pi n_e e^2 / m_0)$ , here  $e$ ,  $m_0$  and  $n_e$  are the charge of electron, rest mass of electron and density of plasma electrons in the absence of laser beam respectively and  $\varepsilon_i$  takes care of absorption. The second term in the equation (3) is the nonlinear dielectric constant for collisionless plasma can be represented as<sup>5</sup>

$$\phi(EE^*) = \frac{\omega_p^2}{\omega^2} \left[ 1 - \exp\left(-\frac{3m\alpha EE^*}{4M}\right) \right], \quad (4)$$

with

$$\alpha = \left( \frac{e^2 M}{6 k_B T_0 \omega^2 m^2} \right),$$

where  $M$ ,  $m$ ,  $k_B$  and  $T_0$  are mass of ion, mass of electron, Boltzmann constant and equilibrium plasma temperature respectively. By using WKB and paraxial approximations the coupled equations in terms of eikonal  $S$  and intensity of laser beam  $A_0^2$  can be expressed as

$$2 \frac{\partial S}{\partial z} + \left( \frac{\partial S}{\partial r} \right)^2 = \frac{\omega_p^2}{\epsilon_0 \omega^2} \left[ 1 - \exp \left( - \frac{3m \alpha E E^*}{4M} \right) \right] + \frac{1}{k^2 A_0} \nabla_{\perp}^2 A_0 \quad (5)$$

And

$$\frac{\partial A_0^2}{\partial z} + \frac{\partial S}{\partial r} \frac{\partial A_0^2}{\partial r} + \left( \frac{\partial^2 S}{\partial r^2} + \frac{1}{r} \frac{\partial S}{\partial r} - k \frac{\epsilon_i}{\epsilon_0} \right) A_0^2 = 0. \quad (6)$$

The solution for equations (5) and (6) which satisfies the initial conditions for a Gaussian beam's intensity distribution is as follows:

$$S = \frac{r^2}{2f} \frac{\partial f}{\partial z} + \phi(z), \quad (7)$$

And

$$A_0^2 = \frac{E_0^2}{f^2} \exp \left( - \frac{r^2}{r_0^2 f^2} - 2k_i z \right), \quad (8)$$

where  $\phi$  is the axial phase and  $k_i$  is the absorption coefficient. By following the approach given by Akhmanov et al.<sup>4</sup> and its simple extension by Sodha et al.<sup>5</sup> the dimensionless beamwidth parameter  $f$  is obtained as,

$$\frac{d^2 f}{d\xi^2} = \frac{1}{f^3} - \frac{3m p \rho_0 e^{-\frac{3m p e^{-2k_i' \xi}}{4M f}} - 4k_i' \xi}{4M f^3} \quad (9)$$

where  $\xi = z/R_d$  known as dimensionless distance of propagation,  $p = \alpha E_0^2$  is the initial intensity parameter,  $R_d = k r_0^2$  is known as Rayleigh diffraction length,  $\rho_0 = (\omega_p r_0)/c$  is the normalized equilibrium beam radius and  $k_i' = k_i R_d$  is the normalized absorption coefficient. The equation (9) can be solved numerically with appropriate boundary conditions such as  $f = 1$ ,  $\xi = 0$  and  $\partial f / \partial z = 0$ . By using critical condition in equation (9) one may obtain equilibrium beam radius as follows. Here  $p$  is known as critical beam power.

$$\rho_0 = \sqrt{\frac{4M}{3m p e^{-\frac{3m p e^{-2k_i' \xi}}{4M}} - 4k_i' \xi}} \quad (10)$$

### III. RESULT AND DISCUSSION

Equation (9) is a nonlinear, ordinary second order differential equation which shows the variation of dimensionless beam-width parameter  $f$  with respect to normalized propagation distance  $\xi$  into the collisionless plasma. First term on the right hand side of the equation (9) is the diffraction divergence which is responsible for defocusing and second term is the convergence arising from the collisionless nonlinearity and also depends on normalized absorption coefficient  $k_i'$  which is responsible for self-focusing of the beam. The equation (9) is a second order nonlinear ordinary differential equation and is solved numerically by choosing following laser-plasma parameters:  $\omega_p = 1.7760 \times 10^{15}$  rad/s,  $r_0 = 20 \times 10^{-4}$  cm,  $c = 3 \times 10^{10}$  cm/s,  $n_0 = 10^{18}$  cm<sup>-3</sup>,  $\rho_0 = 65$ ,  $p = \alpha E_0^2 = 10$ , to study the effect of linear absorption on the self-focusing of the beam in collisionless plasma.

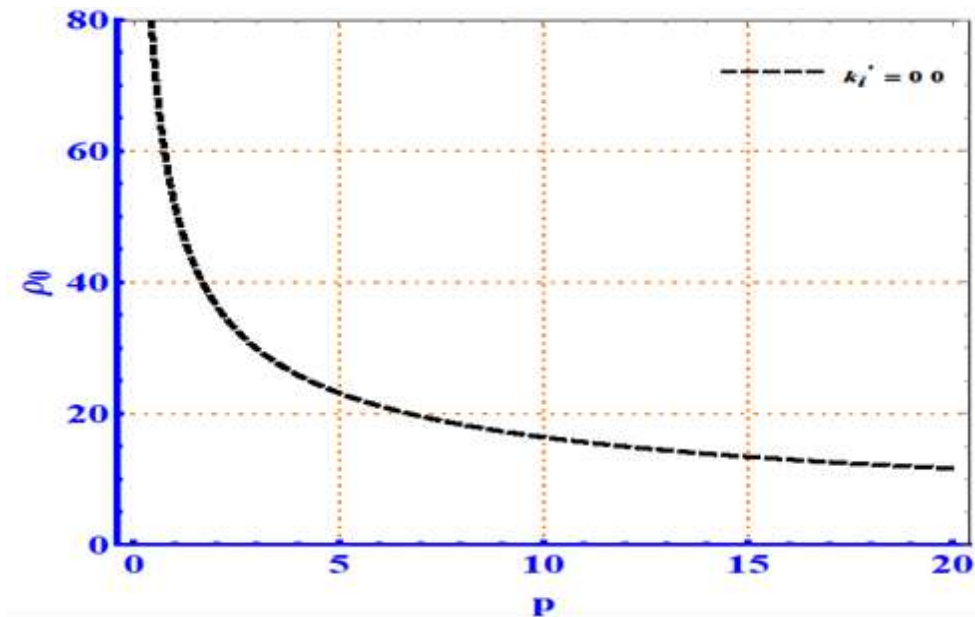


Figure 1: Dependence of normalized equilibrium beam radius  $\rho_0$  as a function of initial intensity parameter  $p$ .  $\omega_p = 1.7760 \times 10^{15}$  rad/s,  $r_0 = 20 \times 10^{-4}$  cm,  $n_0 = 10^{18}$  cm $^{-3}$ ,  $\rho_0 = 65$ ,  $p = \alpha E_0^2 = 10$ .

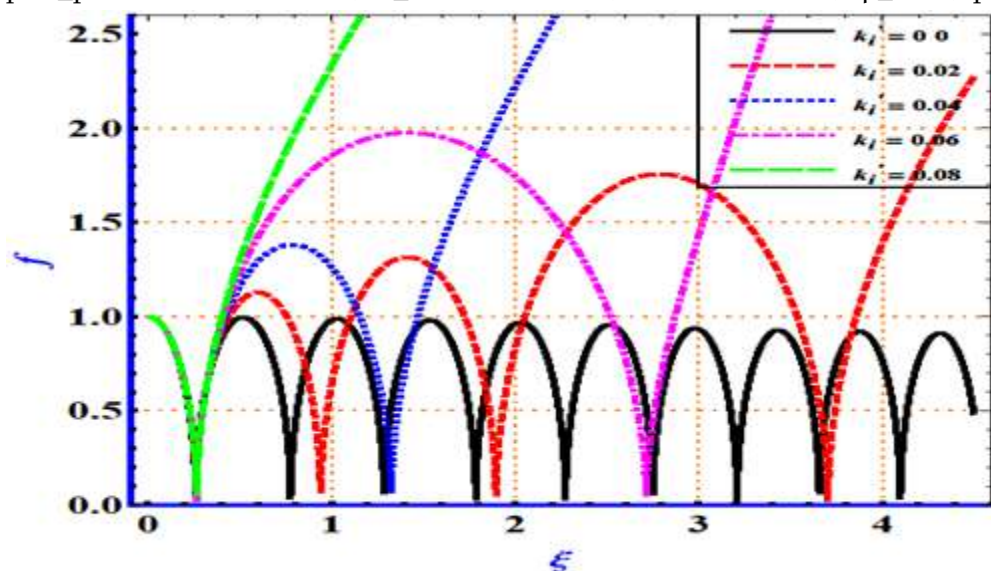


Figure 2: Variation of beam-width parameter  $f$  as a function of normalized propagation distance  $\xi$  for different linear absorption coefficients in collisionless plasma ( $k_l' = 0.00, 0.02, 0.04, 0.06, 0.08$ ).

Figure 1 shows critical curve which is plotted from Equation (10). In figure 1 three distinct regions are observed. The region above the critical curve (supercritical region) corresponds to self-focusing region while the region below the critical curve (subcritical region) corresponds to defocusing region and for any point on the critical curve the self-trapping of the laser beam is observed. Figure 2 shows the variation of beam-width parameter  $f$  as a function of normalized propagation distance  $\xi$  for different absorption coefficients in collisionless plasma ( $k_l' = 0.00, 0.02, 0.04, 0.06$  and  $0.08$ ). In figure 2 for  $k_l' = 0.00$ , i.e. in the absence of linear

absorption, the oscillatory self-focusing of the laser beam in collisionless plasma is observed. By taking into consideration the absorption, the self-focusing of the laser beam gets destroyed. As a result, the linear absorption defeats the effect of self-focusing, and the beam subsequently becomes too weak to control diffraction, resulting in quick divergence due to high energy attenuation. The longer propagation of laser beam in plasmas decreases due to absorption. In presence of absorption alone the energy of the beam decreases as  $\propto \exp[-\alpha_0(-2k_iz)]$ , which is equivalent to a weakening of the nonlinearity effect.

#### IV. CONCLUSION

We have studied the effect of linear absorption on the self-focusing of Gaussian laser beam propagating through collisionless plasma by using parabolic equation approach under WKB and paraxial approximations. The following important conclusions are drawn from the present analysis:

- In the propagation dynamics of the laser beam in collisionless plasma, the controlling factors such as linear absorption coefficient, equilibrium beam radius, and initial intensity parameter play a vital role.
- With an increase in linear absorption in collisionless plasma, the self-focusing effect weakens.

The present results are of importance in various laser-plasma applications, where propagation of laser beam with confined energy over several Rayleigh lengths is required.

Acknowledgement: Authors are thankful to DST-PURSE Phase-II (2018-2023) and UGC DSA -Phase II (2018-2023) Programme for providing research facilities at Dept. of Physics, Shivaji University, Kolhapur, M.S., India.

#### V. REFERENCES

- [1]. Prof. Franken, P. A., Hill, A. E., Peters, C. W. and Weinreich, G. Phys. Rev. Lett. 7, 118–119 (1961).
- [2]. Armstrong, J. A., Bloembergen, N., Ducuing, J. and Pershan, P. S., Phys. Rev. 127, 1918–1939 (1962).
- [3]. Sodha, M. S., Ghatak, A. K. and Tripathi, V. K., Tata McGraw-Hill, New Delhi, (1974).
- [4]. Akhmanov, S. A., Sukhorukov, A. P. and Khokhlov, R. V. , Sov. Phys. Uspekhi 10, 609–636 (1968).
- [5]. Sodha, M. S., Ghatak, A. K. and Tripathi, V. K. , Prog. Opt. 13, 169–265 (1976).
- [6]. Nayyar, V. P. and Soni, V. S., J. Phys. D. Appl. Phys. 12, 239–247 (1979).
- [7]. Takale. M.V, Navare. S.T, Patil. S.D, Fulari. V.J. & Dongare. M.B, Opt. Commun. 282, 3157–3162 (2009).
- [8]. Valkunde. A.T., Vhanmore. B.D., Urunkar. T.U., Gavade. K.M., Patil. S.D. and Takale. M.V., AIP Conf. Proc. 1953, 140088, (2018).
- [9]. Sodha. M. S. and Sharma, A., Phys. Plasmas 13, 053105 (2006).
- [10].Patil. S.D, Takale. M.V, Fulari. V. J., Gupta. D. N. and Suk. H., Appl. Phys. B Lasers Opt. 111, 1–6 (2013).
- [11].Patil, S.D., Takale, M.V., Navare, S. T., Dongare, M. B. and Fulari, V. J., Optik 124, 180–183 (2013).
- [12].Patil, S.D. and Takale, M.V. , Phys. Plasmas 20, 072703 (2013).
- [13].Patil, S.D. and Takale, M.V., Phys. Plasmas 20, 083101 (2013).
- [14].Aggarwal, M., Kumar, H. and Kant, N., Optik 127, 2212–2216 (2016).

- [15].Navare. S.T, Takale. M.V, Patil. S.D, Fulari. V.J. & Dongare. M.B, Opt. Lasers Eng.50,1316–1320 (2012).
- [16].Wani. M.A. and Kant. N., Commun. Theor. Phys. 66, 349–354 (2016).
- [17].Ouahid. L., Dalil-Essakali, L. and Belafhal, A., Opt. Quantum Electron. 50, (2018).
- [18].Kashyap. R, Aggarwal. M, Gill. T.S, Arora. N.S, Kumar. H. and Deepshikha. M., Optik 182, 1030–1038 (2019).
- [19].Urunkar. T.U., Gavade. K.M., Vhanmore, B.D., Valkunde. A.T., Patil. S.D. and Takale. M.V., AIP Conf. Proc. 2142, (2019).
- [20].Gavade. K.M., Vhanmore. B.D., Valkunde. A.T., Urunkar. T.U., Patil. S.D. and Takale. M.V., AIP Conf. Proc. 2142, 110016 (2019).
- [21].Vhanmore. B.D., Takale. M.V. and Patil. S.D., Phys. Plasmas 27, 063104, (2020).
- [22].Patil. S.D., Navare. S.T., Takale. M.V. and Dongare. M.B., Opt. Lasers Eng. 47, 604–606 (2009).
- [23].Patil. S.D., Takale. M.V. and Gill, T.S., Eur. Phys. J. D 69: 163, (2015).
- [24].Patil. S.D. and Takale. M.V., AIP Conf. Proc. 1728, 020129 (2016).
- [25].Patil. S.D., Valkunde. A.T., Vhanmore. B.D., Urunkar. T.U., Gavade. K.M., Takale. M.V., AIP Conf. Proc. 1953, 140046 (2018).

## Simulations Commercial BJT with Temperature for Space and Radiation Rich Environment Applications

C M Dinesh<sup>1\*</sup>, K S Krishna Kumar<sup>2</sup>, M Sathish<sup>3</sup>, R. Chandrashekar<sup>1</sup>, Shivaprakash Y<sup>4</sup>

<sup>1</sup>Department of Physics, Govt. First Grade College and PG centre, Chintamani-563125, Karnataka, India

<sup>2</sup>Department of Physics, Raja Rajeshwari College of Engineering, Bengaluru-560074, Karnataka, India

<sup>3</sup>Department of Physics, Govt. First Grade College, Doddaballapur – 561203, Karnataka, India

<sup>4</sup>Department of Physics, Govt. First Grade College, Devanahalli – 562110, Karnataka, India

### ABSTRACT

The temperature variations on electronic circuits employed to onboard plays a significant impact. In this investigation silicon NPN BJT response to irradiation has been studied at room temperature and temperature variation. A temperature variation dependent analytical model for total ionising dose induced excess base current in BJT's is tested. In this model base current dependent on temperature in irradiation parts have been captured. During irradiation all the three terminals of the devices are grounded. After irradiation, the base current is captured and the concentrations of oxide defects like oxide trapped charges and interface traps created during irradiations are calculated using simulated monte-carlo programming. The base current and defect density resulting from room temperature irradiations are used as inputs to simulations and analytical model experimental data obtained from measurements at room temperature and high temperature on irradiation parts are compared with the simulated results. This work shows that the simulations can support qualifications of the chosen devices for space applications and are functional at various temperatures.

**Keywords:** Bipolar Transistor, NPN, Temperature, Total ionizing dose, Base current.

### I. INTRODUCTION

Bipolar circuits used for comparators and regulators used for large percentage of a space system's are important to understand as a part invention. The operation of the components used for these circuits can be significantly degraded by Total Ionizing Dose (TID) [1]. It has been observed that Low Dose Rate (LDR) Irradiation causes more degradation than High Dose Rate (HDR) Irradiation, for the same TID [2]. Space is a Low Radiation Dose Rate (LDR) environment. Since LDR exposures required long test time, part qualification at this rate can introduce prohibitively high costs to mission assurance. Due to this, the identification of numeral models, accelerated techniques, and test method to assist in the characterization of LDR sensitivity in linear bipolar circuits [3] has been proposed. BJT's and Bipolar circuits show degradation mainly due to emitter – base interface traps ( $N_{IT}$ ) and passivation layer oxide trapped charge ( $N_{OT}$ ) defect build up in oxides.

These build up defects in BJTs can increase recombination at the bipolar base surface can lead to an increasing in the base current ( $I_B$ )[3].

In this paper we describe the temperature dependence of BJTs current voltage characteristics after the irradiation with 108 MeV  $Si^{8+}$  ions. We also calculate the defects produced in the irradiation region using Monte-Carlo code (SRIM- Stopping and range of ions in matter). These results has been correlated to electrical degradation.

## II. EXPERIMENTAL METHODS

### BJTs Device and Oxide Defects

The transistors considered for this study are of vertical NPN BJTs the experimental devices were fabricated in BEL (Bharath Electronics Limited, India). Radiation-induced degradation due to defects that build up in base bipolar oxides alter surface recombination, which results in the increase of base current in NPN BJTs. These defects are net positive oxide trapped charge ( $N_{DIT}$ ) and interface trap ( $N_{IT}$ ). The data obtained from (SRIM) and data from the transistors were used to extract Non Ionising Energy Loss (NIEL) calculations as a function of TID.

### SRIM Data

**Table 1** SRIM simulated results for 110 MeV Si ion irradiation on silicon target.

Parameter	Value			
R ( $\mu\text{m}$ )	39.62			
$S_e$ (MeV $\text{cm}^2/\text{mg}$ )	10.21			
$S_n$ (MeV $\text{cm}^2/\text{mg}$ )	$7.698 \times 10^{-03}$			
NIEL up to R (MeV $\text{cm}^2/\text{g}$ )	42.67			
Fluence (ions/ $\text{cm}^2$ )	$5 \times 10^9$	$1 \times 10^{11}$	$1 \times 10^{12}$	$1 \times 10^{13}$
TID (rad)	0.8174	16.348	163.482	1634.82
$D_a$ (rad)	3143.4	68268	$6.8268 \times 10^5$	$6.8268 \times 10^6$

Table 1 depicts that the nuclear energy loss of 110 MeV  $Si^{8+}$  ion is much smaller than the electronic energy loss (3 orders of magnitude, Table. 1) in a Si-target material due to smaller elastic scattering cross-section. Therefore the maximum energy deposited to the material is expected mainly due to the electronic energy loss during its passage through the Si-material [5]. The device suffers non-uniform irradiation effects as the projected ion range (39.46  $\mu\text{m}$ ) is lower than the device thickness ( $\sim 600 \mu\text{m}$ ) and it is expected to implant at base-collector region. The damage caused due to the linear energy transfer [ $LET = S_e + S_n \sim 10.2177 \text{ MeV}/(\text{mg}/\text{cm}^2)$ ] in the Si target is obtained using TRIM calculations. LET dependent TID and NIEL dependent  $D_a$  are tabulated in table 1.

### Pre-and post-irradiation test results

Radiation testing was performed at Inter University accelerating Centre (IUAC) New Delhi, India. Three devices were irradiated at room temperature (RT) LDR irradiation was performed 1PNA (particle nano

ampere current) to get desired irradiation fluence. The energy of irradiating ion as choosing so that it could penetrate into emitter base junction.

The fluence has been calculated by counting the charge collected at the Faraday cup placed at the target. The another advantage of selecting low irradiation current is that BJTs are not damage due to the loss of irradiated ion energy (110 MeV Si<sup>8+</sup> heavy ion) in the BJTs, (Heating effect will not be produced/the heat produced during the irradiation get transferred to the target).

Figure.1 show the base current  $I_B$  responses exposed at 110 MeV Si<sup>8+</sup> ions for NPN BJTs. The data in these plots were collected at room temperature, 50 and 100 °C. The increase in base current with radiation can be fit approximately to

$$\Delta I_B = I_{SE} \exp\left(\frac{q|V_{BE}|}{n_E kT}\right), \quad (1)$$

Where  $I_{SE}$  is the radiation-induced change in low-injection base leakage current,  $n_E$  is the change in the low injection ideality factor,  $k$  is Boltzmann's constant,  $T$  is the junction temperature, and  $q$  is the magnitude of electronic charge. Plots of  $I_B$  and  $V_{BE}$  at constant  $V_{CE}=4V$ .

### Temperature data on BJT devices

Figure 1 – 3 shows the temperature dependent base current as a function of base – emitter voltage measured for un-irradiated and irradiated NPN BJTs to characterize the impact of thermal variation prior to and after ionizing radiation dose. The temperature testing was performed approximately 300 months after the radiation tests. No significant change was observed in the electrical response at room temperature between the end of the radiation testing and temperature testing. This showed that the defects produced during irradiations are permanent. Pre- and post unirradiated and irradiated devices were placed in a thermal chamber (hot air oven) with an internal thermocouple to automatically monitor the temperature near the devices during the tests. Temperature response testing was performed from 27 °C up to a maximum temperature of 100 °C in order to avoid annealing effects. Temperatures above 100 °C may lead to the annealing of some oxide defects (both interface and oxide traps) and a reduction in the excess base current measured for BJT [4]. Electrical measurements are performed a few minutes after the temperature is fixed in order to ensure thermal equilibrium during measurement. Each devices has been tested for electrical measurements before and after irradiation in order to test the effect of irradiation, it has been observed all devices show approximately same I-V characteristics before and after irradiation. Hence one devices were tested for each condition, electrical characterization at room temperature were performed after each temperature step in order to ensure no significant temperature dependent annealing of the parts of NPN BJTs [5].

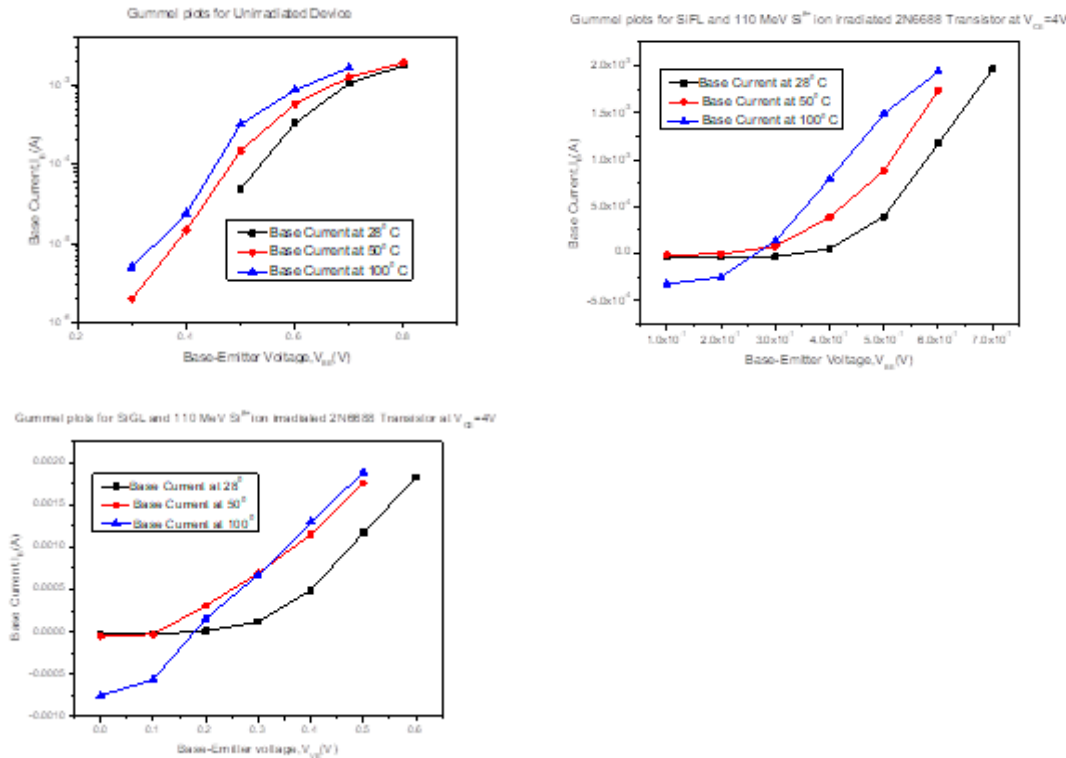


Figure. 1, 2 and 3 show the pre-irradiation,  $1 \times 10^{11}$  and  $1 \times 10^{12}$  ions/cm<sup>2</sup> LDR irradiated base currents for NPN BJTs over the specified temperature range (27°, 50°C 100°C).

It can be observed that both the pre- and post-irradiated PNP BJTs show similar trends, i.e., a monotonic increase in base current with increasing temperature. Similar trend can be observed for the pre- and post-irradiated NPN BJTs. Most of the earlier studies have indicated that the impact of displacement damage is marginal compared with the total dose effect. However, it has been shown that total – dose irradiation may indirectly affect the silicon substrate by reducing the active p-type base dopant concentration, may lead to an increase in base current as shown in figure 4.

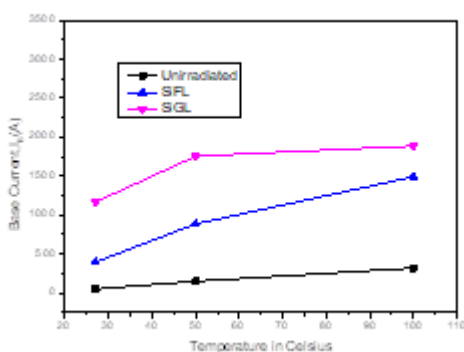


Figure. 4 show the base currents at  $|V_{BE}| = 0.5$  V as a function of temperature for un-irradiated and irradiated NPN BJTs respectively.

Table 2: Variation in base current,  $I_B$  of BJT tested for different fluence of 110 MeV  $Si^{8+}$  ions at specified temperature range (27°, 50°C 100°C)

Temperature °C	$I_B(A)$			
	Un irradiated	$5 \times 10^9$	$1 \times 10^{11}$	$1 \times 10^{12}$
27	48.66	126.666	394.66	1165.66
50	147	161	884	1755
100	317.66	3200	1488.33	1885.333

The enhanced  $I_B$  is related to an increase in the surface recombination velocity, as the density of electrons and holes is coming more comparable, due to base neutralization. From the figure we can also see that there are large increase in the base current tested at higher temperatures (50°C and 100°C) due to increased surface recombination current at the base surface. An increase in the midgap-level interface-trap density in the low-field, thick oxide over the p-type base increases the recombination current, more importantly an increase in the positive-oxide-charge density modulates the base surface potential to even more strongly increases the surfaces recombination current [6-9].

The current gain of modern bipolar transistors in an ionizing radiation environment decreases due to increased recombination in the emitter-base depletion region [7-8,10-11]. The recombination centers are related to the net charge introduced into the oxide by ionizing radiation, since it is positive the depletion region spreads on the p-side of a PN junction. For NPN transistors, this means that the depletion region separates into relatively lightly doped P-type base region. As the depletion region increases in size, recombination current increases at the oxide interface over the base and in the newly-depleted silicon bulk. In BJTs the excess base current depends on the number of interface states (recombination centers) near midgap and threshold. The excess base current due to changes in surface potential depends on the total radiation induced oxide charge at the bias condition these variations in excess base current is as shown in table 2.

### III. CONCLUSIONS

This work reports the effect of 110MeV  $Si^{8+}$  ion irradiation on silicon NPN transistors devices with fluences of  $5 \times 10^9$  ions  $cm^{-2}$  to  $1 \times 10^{13}$  ions  $cm^{-2}$ . An effort is made successfully to correlate the electrical degradation with the non-ionizing energy deposition due to MeV ion irradiation using TRIM Monte Carlo Code. Fluence dependent TID and  $D_{ais}$  calculated for 100 MeV silicon ion in silicon target. The shift in collector saturation current and collector emitter voltage is mainly due to the total displacement dose. In addition to these shifts, Si-ion irradiation causes increase in forward resistance of the collector emitter region.

The current gain of the transistors decreases with increases in silicon ion fluences. It has in addition been observed that the base current increases with increase in TID and test temperature. The excess base current due to changes in surface potential depends on the total radiation induced oxide charge at the bias condition. This is again related to the reduction of the base doping concentration after exposure. In BJTs the excess base

current depends on number of interface traps (recombination centres) near the midgap. At higher total doses, sufficient charge as the accumulated in the oxide to cause significant recombination to occur through-out the lightly doped based region. The swift heavy ion irradiation on silicon will result in increase in lattice temperature. Hence in the present device case the transistor performance is severely affected due to silicon ion irradiation. The switching time of the transistor may decrease due to an increased base currents as a function of silicon ion fluence.

#### IV. REFERENCES

- [1]. H.J. Barnaby, R.D. Schrimpf, R.L. Pease, P Cole, T.Turflinger, J.Krieg, J.T.Titus, D. Emily, M. Gehlhausen, S.C. Witczak, M.C. Maher, D.Van Nort, Identification of degradation mechanisms in a bipolar linear voltage comparator through correalation of transistor circuit response, IEEE Trans, Nucl. Sci. 46(6)(Dec.1999) 1666-1673.
- [2]. A.H. Johnston, B.G. Rax, C.I. Lee, Enhanced damage in linear bipolar integrated circuits at low dose rate, IEEE Trans. Nucl.Sci. 42(6)(Dec 1995)1650-1659.
- [3]. P.C. Adell, R.L. Pease, H.J. Barnby, B.Rax, X.J. Chen, S.McClure, Irradiation with molecular hydrogen as an accelerator total dose hardness occurrence test method for bipolar linear circuits, IEEE Trans. Nucl. Sci. 56(6)(Dec.2009) 3326-3333.
- [4]. X.Li,W.Lu, Q.Guo, D.M. Fleetwood, C.He, X.Wang, X.Yu, J.Sun, M.Liu, S.Yao, Temperature-switching during irradiation as a test for ELDRS in linear bipolar devices, IEEE trans. Nucl. Sci.66(1)(Jan. 2019)199-206.
- [5]. H.J. Barnaby, B.Vermeire, M.J. Campola, Improved model for increased surface recombination current in irradiated bipolar junction transistors, IEEE Trans Nucl. Sci.62(4)(Aug.2015) 1658-1664.
- [6]. B.S. Tolleson, P.G. Adell, B.Rax, H.J. Barnaby, A.Privat, X.Han, A.Mahmud, I.Livingston, Improved model for excess base current in irradiated lateral PNP bipolar junction transistors, IEEE Trans. Nucl.sci, Aug,2018.
- [7]. C. M. Dinesh, Ramani, M. C. Radhakrishna et al., Nucl. Instr. and Meth. in Phys. Res. B 266, (2008) 1713.
- [8]. K.S. Krishnakumar, C.M. Dinesh, KV Madhu, et al., Carbon ion irradiation damage effects on electrical characteristics of silicon PNP power BJTs, IEEE Trans. On Device and Mat. Relia. 15 (1), (2015), 101-108.
- [9]. R. Nathan Nowlin, D. M. Fleetwood, and R. D. Schrimpf, IEEE Trans. Nucl. Sci. 41, (6), (1994) 2637.
- [10].R. L. Pease, R. M. Turfler, D. Platteter, D. Emily, and R. Blice, IEEE Trans. Nucl. Sci. NS-30, (1983) 4216.
- [11].A. R. Hart, J. B. Smyth Jr. V. A. J van Lint, D. P. Snowden, and R. E. Leadon, IEEE Trans. Nucl. Sci. NS-25, (1978) 1502.
- [12].J. Boch, F. Faigne, T. Maurel, F. Giustino, L. Dusseau, R.D. Schrimpf, K.F. Galloway, J. P. David, R. Ecoffet, J. Fesquet et.al. IEEE Trans. Nucl. Sci. 49, (3), (2002) 1474.

## Green Synthesis and Characterization of CdS Quantum Dots Mediated by Aegle Marmelos Leaves

M.D. Dhiware<sup>1</sup>, T.R. Deore<sup>2</sup>, S.B. Nahire<sup>3</sup>, A.B. Gawande<sup>2\*</sup>

<sup>1</sup>Department of Physics, KVNN Arts, Commerce and Science College, Nashik, Maharashtra, India

<sup>2</sup>Department of Physics, K.S.K.W. Arts, Science and Commerce College, CIDCO, Nashik, Maharashtra, India

<sup>3</sup>Department of Physics, National Senior College, Nashik, Maharashtra, India

### ABSTRACT

Herein, we report the green synthesis of CdS quantum dots (QDs) by Aegle Marmelos leaves extract. Green synthesis method is novel, simple, eco-friendly, nontoxic compared to conventional physical and chemical methods. Aegle Marmelos used as a capping and reducing agent owing to their extraordinary medical applications. The synthesized CdS QDs characterized by various characterization techniques Such as X-Ray Diffraction (XRD) showing cubic structure with average particle size about 4 nm determined by using Debye Scherrer formula. Field emission scanning electron microscope (FE-SEM) reveals a spherical shape of CdS QDs.

### I. INTRODUCTION

In past two decades green synthesis method is drawing more attention owing to its facile, nontoxic, eco-friendly and low temperature characteristics compared other methods. Green synthesis approach uses bioactive agents such as plant materials, microorganism and various biogases etc. The various nanomaterials are synthesized by green method such as CdS, CeO<sub>2</sub>, Ag, ZnS, SnO<sub>2</sub> etc.[1-5]. There are different methods are used for synthesis of CdS QDs by like chemical deposition [6], Hydrothermal [7], Sol-Gel [8], etc. In this method uses the collides with harmful chemicals. These can be avoiding if we used green synthesis plant extract approach.

Cadmium sulfide (CdS) is a direct band gap semiconductor with energy band gap  $E_g = 2.42$  eV. The colour tunability of semiconductor QDs as a function of size is one of their most attractive characteristics. CdS is a promising material because of their applications in optoelectronics, photocatalysts, x-ray detectors, nonlinear optical material and as a window material for hetro-junction solar cells [9].

*Aegle Marmelos* leaves contains broadly alkoids, prphynols, terepnoids and other polyphenols, which are well recognized for their healing power toward variety of bacterial and fungal infections [10]. In the present research work we report green synthesis of CdS QDs mediated by *Aegle Marmelos*.

## II. MATERIALS AND METHODS

Cadmium Chloride ( $\text{CdCl}_2 \cdot \text{H}_2\text{O}$ ), Sodium sulphide ( $\text{Na}_2\text{S} \cdot \text{H}_2\text{O}$ ) and Ethanol are easily available commercial materials. *Aegle Marmelos* leaves were gathered from local trees. Distilled water used as solvent in the method.

### 2.1 Synthesis of CdS QDs:

CdS QDs synthesized greens approach, typical synthesis in 5 ml extract of *Aegle Marmelos* leaves added 90 ml of distilled water in the proceeding step 0.2 gm of  $\text{CdCl}_2$  was added and placed on hot plate with magnetic stirring at temperature  $100^\circ\text{C}$  for 2 hrs. After that 0.078 gm of  $\text{Na}_2\text{S}$  was added in the mixture and again kept for constant magnetic stirring for 2 hrs. Then final yellow colour product was filtered, centrifuged and finally dried at room temperature 12 Hrs. The final yellow powder was used for further characterisation.

## III. RESULT AND DISCUSSION

### X-ray Diffraction (XRD):

XRD pattern as shown in the figure 1. X-ray diffraction used to study crystal structure, nanoparticle size, interplanar spacing. The XRD peaks was found to be very broad which indicates formation of very small size QDs. The diffraction peaks assigns at  $2\theta = 26.9^\circ$ ,  $46.78^\circ$  and  $53.5^\circ$  which corresponds to the miller indices for the crystal plane of (111), (220) and (311) with cubic crystalline structures of synthesized CdS QDs, respectively, (JCPDS Card no.00-010-0454). XRD of prepared sample materials was found to be in good agreement with (JCPDS file no.00-010-0454). The average particle size was found to be 4 nm which was determined by using the Debye Scherrer formula i. e. nanoparticle size ( $D$ ) =  $(k \lambda) / (d \cos \theta)$  Where,  $D$  is the particle in nm,  $K$  is crystallite shape factor a good approximation is 0.9 for spherical shape nanoparticles,  $\lambda$  is the X-ray wavelength used for X-ray diffraction,  $d$  is the full width at half the maximum (FWHM) in radians of the X-ray diffraction peak and  $\theta$  is the Bragg's angle (deg.). [11]

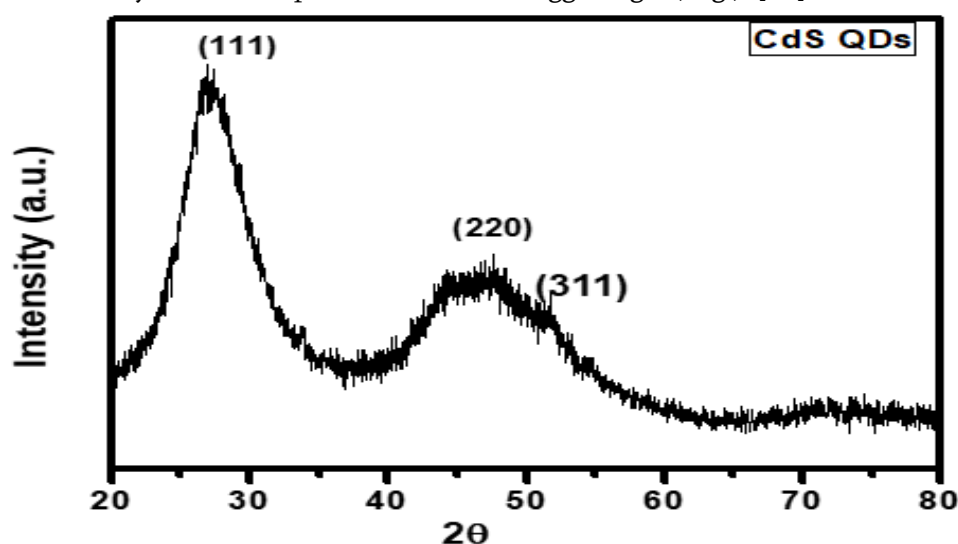


Figure 1: XRD pattern of CdS QDs

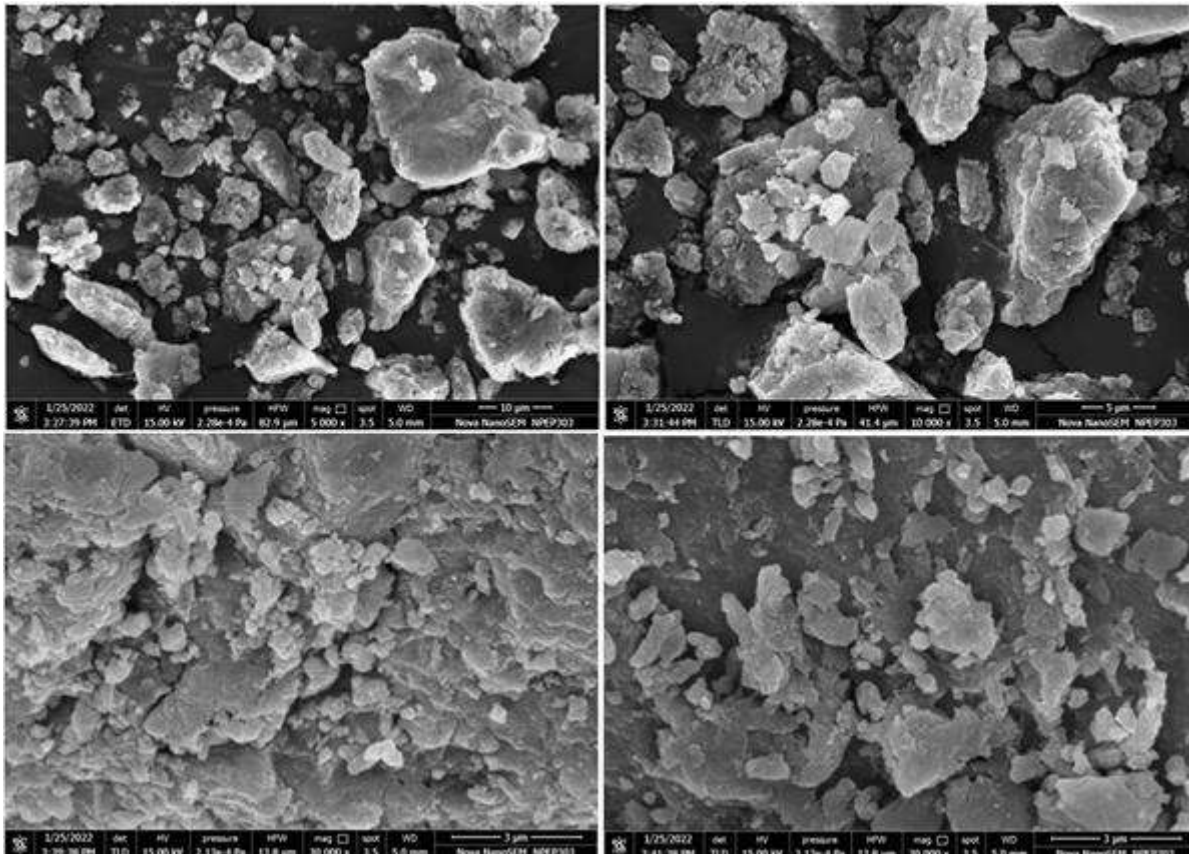
**Field Emission Scanning Electron Microscope (FESEM) study:**

Figure 2: FESEM images of CdS QDs

The synthesized product of CdS QDs characterized by using FESEM technique which is used for the study of surface morphology. CdS QDs shows particles are nearly spherical in shape morphology with slightly agglomeration as shown in the figure 2.

#### IV. CONCLUSION

In summary, plant mediated synthesis of nanoparticles have several advantages over physical and chemical methods..CdS QDs synthesized by green synthesis method with leaves extract of *Aegle Marmelos*. The leaves extract bioactive components play vital role for formation of CdS QDs Moreover, the prepared CdS QDs average nanoparticle size was found to be 4 nm determined by using XRD technique. Field emission scanning electron microscope (FE-SEM) reveals a spherical shape of CdS QDs with agglomerate morphology and. Synthesized CdS QDs can be explored for various biomedical applications such as antibacterial, antibiofilm, antifungal, antiviral, anticarcinogenic and anticandidal activities.

## V. ACKNOWLEDGEMENTS

Authors thanks to Principle, KSKW Arts, Science and Commerce College, Nashik for providing instrumental facilities to carry out this research work and Authors also wants to thanks to Vice Principle Dr. Latesh Nikam from Baburanji Gholap College, Sangvi, Pune for providing characterization facility.

## VI. REFERENCES

- [1]. Prof. Biogenic synthesis of photocatalytic activity of CdS NPs, A. Bhadwal, et al. , RSC. adv, 2014,4,9484.
- [2]. Green synthesis of CeO<sub>2</sub> NPs from the abelmoschus esculentus Extract of antioxidant, Anticancer ,Antibacterial and wound- Healing Activities. H. E. Ahemad, et al. Molecules 2021,26,4659.
- [3]. Green synthesis of silver NPs using white sugar, S. Mesharam , et al. IET Nanobiotechnology (2013), 7,1, 28-32.
- [4]. Green synthesis of ZnO Using S.Frutesences Plant extract for photocatalytic degradation of dye and antibiotics S. Munjai, et al. Mate Res Express, 9, (2022), 015001.
- [5]. Green synthesis of SnO<sub>2</sub> NPs using delonaelataleaf: Evaluation of its structural, optical, morphological and photocatalytic properties. K.C.Suresh et al, SN applied science (2020)2:1735.
- [6]. Photoaucstic study of CdS QDs for application in QDs sensitized solar cells. S. Abdallah, et al., Journal of nanomaterials,498286,1-6, 2012
- [7]. One step of hydrothermal synthesis of thioglycolic acid capped CdS QDs as fluroscsnces determination of cobalt ion, Z. wang, et al Scientific Reports, (2018) 8:8953.
- [8]. Sol Gel synthesis, characterization and effect of CdS nanoparticles on activity of liver Enzymes, Asmaa. J Al-lamei, Journal of Advanced Sciences and Engineering Technologies, 2019, 35-42.
- [9]. W.V. Huynh, J.J. Dittmer, A.P. Alivisatos, "Hybrid nanorod-polymer solar cells", Science 295 (2002), 2425–2427.
- [10].One-step biofabrication of copper nanoparticles from Aegle marmelos correa aqueous leaf extract and evaluation of its anti-inflammatory and mosquito larvicidal efficacy, Gangadhara Angajala, Pasupala Pavan and R. Subashini, RSC Adv., 2014, 4, 51459.
- [11].Room Temperature Synthesis And Characterization Of Cadmium Sulphide (CdS) Semiconductor Quantum Dots, S.I. Khan, G.K.Kande, L.D.Sonawane, A. S. Mandawade, L.J. Jondhale, P.G.Loche, Journal of Scientific Research in Science and Technology,9,2, 2021.

## Electrodeposited Nanoleaves (NLs) like $Mn_3O_4$ thin film for electrochemical supercapacitor

P. M. Kharade<sup>1\*</sup>, J. V. Thombare<sup>2</sup>, S. S. Dhasade<sup>2</sup>, S. D. Patil<sup>3</sup>, P.B.Abhange<sup>4</sup>, D. J. Salunkhe<sup>5</sup>

<sup>1</sup>Department of Physics, Shankarrao Mohite Patil Mahavidyalaya, Akluj, Dist-Solapur (MH), India 413101

<sup>2</sup>Department of Physics, Vidnyan Mahavidyalaya, Sangola, Dist-Solapur (MH), India 413307

<sup>3</sup>Department of Physics, Pratapsinh Mohite Patil Mahavidyalaya, Karmala, Dist-Solapur (MH), India 413203

<sup>4</sup>Department of Physics, G.M. Vedak College of Science, Tala, Raigad (MH), India 402111

<sup>5</sup>Nanocomposite Research Laboratory, K.B.P. Mahavidyalaya, Pandharpur, Dist-Solapur (MH), India 413303

\*Corresponding Author E-mail:pravink150@gmail.com

### ABSTRACT

In the present study, we report here synthesis and characterization of manganese oxide ( $Mn_3O_4$ ) thin films by potentiostatic electrodeposition for supercapacitor application. The structural and surface morphological behaviour of  $Mn_3O_4$  thin film were carried out by using X-ray diffraction (XRD) and Scanning Electron Microscopy (SEM) study. The structural study of  $Mn_3O_4$  thin film shows hausmannite tetragonal crystal structure. The surface morphological study showed that the formation of nanoleaves (NLs) of  $Mn_3O_4$  thin film. The electrochemical supercapacitive performance of  $Mn_3O_4$ NLs was characterized by using cyclic voltammetry (CV), charging-discharging (CD) and electrochemical impedance spectroscopy (EIS) techniques. The  $Mn_3O_4$ NLs shows maximum specific capacitance of 460  $F.g^{-1}$  at scan rate 5  $mV.s^{-1}$  and 92% cycling stability in 0.5 M  $Na_2SO_4$  electrolyte solution. Hence, potentiostatically deposited  $Mn_3O_4$ NLs is best for energy storage application.

**Keywords:** supercapacitor, electrodeposition,  $Mn_3O_4$ , XRD, FESEM, CV.

### I. INTRODUCTION

In the 21<sup>st</sup> century more and more research focused on highly renewable and sustainable energy storage devices. Electrochemical capacitor or supercapacitor have gained more attention due to their excellent electrochemical properties such as, environmental friendly, fast charging and discharging rate, good reversibility, high power density, long cycle life and safety in operation. Due to this features electrochemical

capacitor can be used in variety of potential applications such as, memory back up devices, portable electronic devices, hybrid electric vehicles, elevator, forklifts, cranes, lasers and industry [1-4]. The Electrochemical capacitor or supercapacitor mainly categorized into two types viz, electrochemical double layer capacitor (EDLC) and Pseudocapacitor (PC). In EDLC, charge is stored electrostatically, i.e charge accumulation takes place at the electrode/electrolyte interface. Example, carbon materials. In pseudocapacitor (PCs) faradic process takes place. Example, conducting polymers and Transition metal oxides (TMOs) etc. Electrode materials used in TMOs are  $\text{RuO}_2$  [5],  $\text{MnO}_2$  [6],  $\text{Co}_3\text{O}_4$  [7],  $\text{NiO}$  [8],  $\text{IrO}_2$  [9],  $\text{Cr}_2\text{O}_3$  [10] and  $\text{CuO}$  [11] etc. Among these TMOs, Manganese oxide electrode is widely studied in supercapacitor because of better electrochemical performance, natural abundant, low cost, easy synthesis and non-toxic [12-13]. Manganese oxide also have several oxidation states such as,  $\text{MnO}$ ,  $\text{MnO}_2$ ,  $\text{Mn}_2\text{O}_3$  and  $\text{Mn}_3\text{O}_4$  etc. Among these oxides,  $\text{Mn}_3\text{O}_4$  is one of the most stable state of manganese oxide and have attracted considerable attention due to its low cost, environmental friendly, natural abundant and good electrochemical properties [14-15].

Manganese oxide have been synthesized by different physical and chemical methods such as, hydrothermal method [16], co-precipitation method [17], sol-gel method [18], chemical bath deposition method [19], self-reacting microemulsion method [20], sonochemical method [21], electrodeposition method [22], room-temperature solid reaction [23] and SILAR method [24] etc. Among all the various methods, electrodeposition method is one of the best method for synthesis of metal oxides because of low cost, binder free, single step and large scale production. It also leads direct deposition of oxide/hydroxide electrodes on low cost substrates. Nguyen et al. [22] have reported nanoflakes like morphology of  $\text{Mn}_3\text{O}_4$  thin film by cathodic electrodeposition method for supercapacitor application. Yousefi et al. [25] have reported porous nanospheres of  $\text{Mn}_3\text{O}_4$  by cathodic electrodeposition method and studied their electrochemical properties. Porous and nanostructured material is key requirement for electrochemical capacitor because it provides large surface area, shorten the diffusion path of electrons and ions, which promotes the fast insertion and extraction of electrons and ions. Which improves the specific capacitance of the electrode [26].

In the present report, efforts have been taken to study structural, morphological and electrochemical supercapacitive behaviour of potentiostatically deposited  $\text{Mn}_3\text{O}_4$  NLs for supercapacitor application.

## 2. Experimental:

### 2.2 (a) Characterization techniques

The crystal structural study of  $\text{Mn}_3\text{O}_4$  NLs was carried out with the help of XRD using Bruker axes D8 Advance Model with copper radiation ( $K_\alpha$  of  $\lambda = 1.54 \text{ \AA}$ ) within  $2\theta$  range between  $20^\circ$  to  $80^\circ$ . The surface morphology of  $\text{Mn}_3\text{O}_4$  NLs was carried out by using field emission scanning electron microscopy (FESEM) technique (Model: JSM-6160). The electrochemical supercapacitive study of  $\text{Mn}_3\text{O}_4$  NLs was studied by using CV, GCD and EIS techniques by using electrochemical workstation (CHI 660 A). The electrochemical cell includes three electrode systems.  $\text{Mn}_3\text{O}_4$  NLs was used as a working electrode, graphite was used as a counter electrode and saturated calomel electrode (SCE) was used as a reference electrode. The 0.5 M  $\text{Na}_2\text{SO}_4$  was used an electrolyte solution for overall measurements.

### 3. Result and Discussion

#### 3.1 XRD Study:

X-ray diffraction (XRD) techniques have been carried out to examine the crystal structure of the  $Mn_3O_4$  NLs. Fig.1 shows the XRD pattern of  $Mn_3O_4$  NLs in the  $2\theta$  range from  $20^\circ$  to  $80^\circ$ . The observed diffraction peaks indexed in the XRD pattern of  $Mn_3O_4$  NLs was well matched with JCPDs card no.89-4837. The XRD study shows hausmannite tetragonal crystal structure of electrodeposited  $Mn_3O_4$  NLs. The peak marked with (SS) in the XRD spectrum is due to stainless steel substrate only.

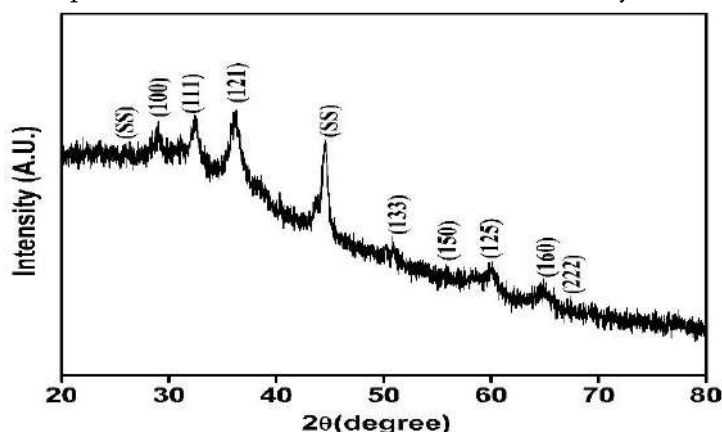


**Figure 1.** X-ray Diffraction (XRD) spectra of  $Mn_3O_4$  NLs.

The average crystallite size of  $Mn_3O_4$  NLs was calculated by using the Debye's Scherer's equation,

$$D = \frac{0.9\lambda}{\beta \cos\theta} \text{ ----- (3)}$$

Where, D is the crystallite size,  $\lambda$  is the wavelength of X-ray ( $1.54.4 \text{ \AA}$ ) and  $\beta$  is full width at half maximum (FWHM). For determination of crystallite size, the most intense peak (121) is centered at FWHM in term of radian is 0.807. The crystallite size of  $Mn_3O_4$  NLs is found to be 34 nm.

#### 3.2. Surface Morphological Studies

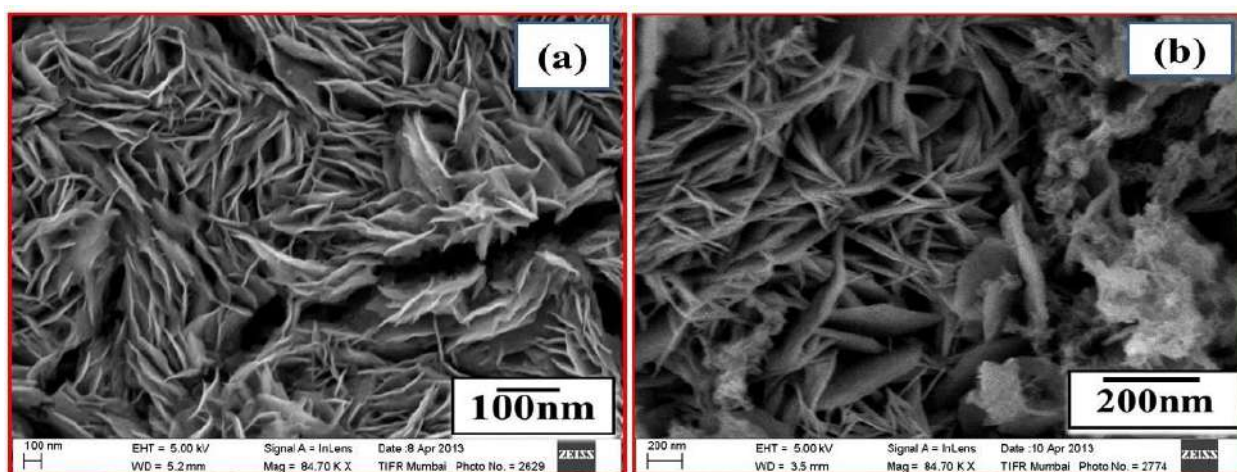


**Figure 2 :** Scanning Electron Microscope (SEM) images of  $Mn_3O_4$  thin film at (a) 100kX and (b) 200kX magnifications respectively.

Surface morphology of the  $Mn_3O_4$  NLs was studied by using FESEM technique. Fig. 2(a-b) demonstrate the FESEM micrographs of  $Mn_3O_4$  thin film with two different magnifications (100 kX and 200 kX) respectively. In Fig. 2(a) SEM micrograph of  $Mn_3O_4$  thin film at low magnifications shows the compact and nanoflakes like morphology [28]. At high magnification in Fig. 2(b), the  $Mn_3O_4$  thin film gives highly resolved, porous and interconnected Nano leaves (NLs) like structure. Such structures have a larger specific surface area, providing the active material to sufficiently react with ions in the solution, and hence reducing the electron transport distance [29]. Therefore, it enhances the electrochemical supercapacitive properties.

### 3.3 Supercapacitive studies:

#### 3.3.1 Cyclic voltammetry (CV) studies:

The specific capacity of  $Mn_3O_4$  NLs was carried out by using CV study. Fig. 3(a) display typical CV curves of  $Mn_3O_4$  NLs at different scan rates such as; 5, 10, 50 and 100 mV/s within potential limit of +1.2 V to -1.2 V vs SCE, respectively. From CV curves, it is observed that as scan rate increases current under curve increases and the cathodic and anodic peaks shifts more towards positive and negative sideward. This result shows that current is directly proportional to scan rate, i.e. scan rate dependent current-voltage indicate that ideal capacitive behaviour of  $Mn_3O_4$  NLs. Similar results reported by Dubal and More et al. prepared by  $Mn_3O_4$  thin film by chemical bath deposition and spray pyrolysis method for supercapacitor application respectively [19, 30].

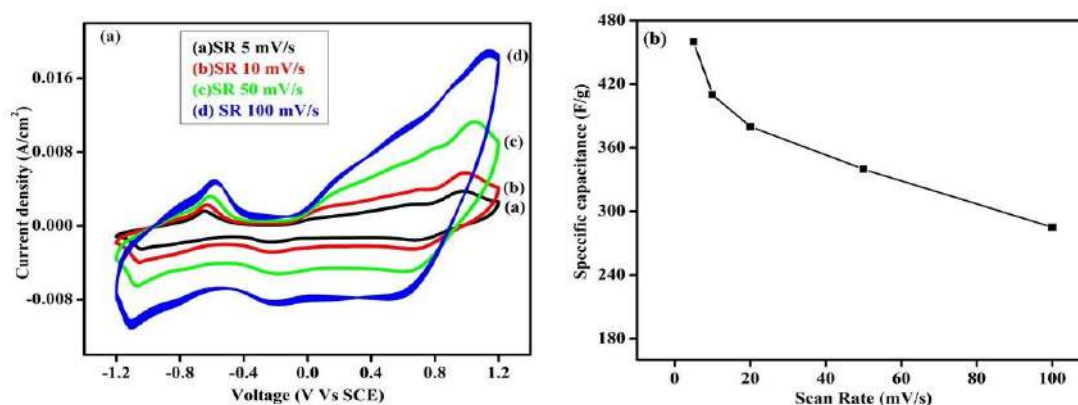


**Figure 3** (a) Cyclic Voltammetry (CV) study of  $Mn_3O_4$  NLs at scan rate of 5, 10, 50 and 100 mV/s and 4 (b) Variation of specific capacitance vs scan rate of  $Mn_3O_4$  NLs.

The capacitance of  $Mn_3O_4$  thin film was calculated by using the following relation,

$$C = \frac{\int Idt}{dv/dt} \text{ ----- (4)}$$

Where,  $\int Idt$  is area under curve of CV and  $dv/dt$  is voltage scanning rate in mV/s.

The specific capacitance of  $Mn_3O_4$  NLs was calculated by following relation,

$$\text{Specific capacitance } (C_s) = \frac{C}{W} \text{ ----- (5)}$$

Where, C – capacitance in farad and W – the mass of active electrode materials in gm. The active mass of  $Mn_3O_4$  NLs was 0.0024 gm, calculated from weight difference method. The  $Mn_3O_4$  NLs show specific

capacitance of  $460 \text{ F.g}^{-1}$  at scan rate of  $5 \text{ mV.s}^{-1}$ . It was observed that as scan rate increases specific capacitance decreases shown in Fig. 3 (b). Decrease in specific capacitance suggests that at higher scan rate most of the inner active sites of nanoflakes network are not involved in the reaction. So, specific capacitance obtained at low scan rate are due to full utilization of the active electrode materials.

Material	Specific Capacitance ( $\text{F.g}^{-1}$ )	Electrolyte	Method of synthesis	Reference
$\text{Mn}_3\text{O}_4$ Nano leaves	460	0.5 M $\text{Na}_2\text{SO}_4$	Potentiostatic Electrodeposition	Our work
$\text{Mn}_3\text{O}_4$ nanoparticles	375	1.0 M $\text{Na}_2\text{SO}_4$	SILAR	[31]
$\text{Mn}_3\text{O}_4$ nanocubes	223	1.0 M $\text{Na}_2\text{SO}_4$	CBD	[32]
$\text{Mn}_3\text{O}_4$ nanograins	314	1.0 M $\text{Na}_2\text{SO}_4$	SILAR	[24]
$\text{Mn}_3\text{O}_4$ nanograins	289	1.0 M $\text{Na}_2\text{SO}_4$	SILAR	[33]

**Table: 1** Comparison of specific capacitance between our work and previously reported work to synthesis the  $\text{Mn}_3\text{O}_4$  electrodes by considering scan rate of  $5 \text{ mV/s}$ .

Table 1 represents a comparison of specific capacitance between our work and previously reported work by keeping scan rate of  $5 \text{ mV/s}$  vs SCE. The specific capacitance obtained in the present study is higher due nanostructured and porous morphology of  $\text{Mn}_3\text{O}_4$  NLs. It depends upon optimum electrodeposition time.

### 3.3.3 Galvanostatic charging-discharging (GCD) studies:

The specific energy and specific power associated with  $\text{Mn}_3\text{O}_4$  NLs was carried with the help of GCD techniques. Fig 4 (a) shows typical charge-discharge curves of  $\text{Mn}_3\text{O}_4$  NLs at constant current density of  $5 \text{ mA.cm}^{-2}$  in  $0.5 \text{ M Na}_2\text{SO}_4$  electrolyte solution. The charging-discharging curves of  $\text{Mn}_3\text{O}_4$  NLs show symmetrical characteristics, which reveals that  $\text{Mn}_3\text{O}_4$  NLs thin film have good capacitive behaviour and the reversible redox process. The GCD curve of  $\text{Mn}_3\text{O}_4$  NLs shows very small voltage drop at the initial of the discharge curve which is due to very low internal resistance between the current collector and  $\text{Mn}_3\text{O}_4$  NLs.

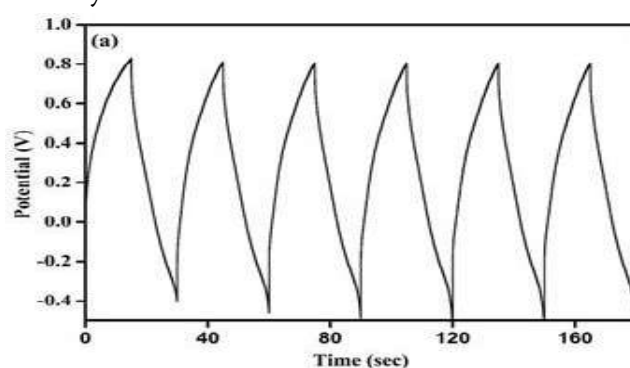


**Figure 4** Galvanostatic charge-discharge (GCD) study of  $\text{Mn}_3\text{O}_4$  NLs

The coulombic efficiency, specific energy and power of  $\text{Mn}_3\text{O}_4$  NLs was calculated using following formulae:

$$\text{Coulombic Efficiency } (\eta) = \frac{T_d}{T_c} \times 100 \text{ ----- (6)}$$

$$\text{Specific power } (P) = \frac{V \times I_d}{W} \text{ ----- (7)}$$

$$\text{Specific energy (E)} = \frac{V \times I_d \times T_d}{W} \text{----- (8)}$$

Where,  $T_d$  and  $T_c$  is discharge and charge time in sec,  $V$  is voltage window in volt,  $I_d$  is discharge current mA and  $W$  is the mass of the active material in gm. The coulombic efficiency of  $Mn_3O_4$  NLs was found to be 98.42% whereas the specific power and specific energy were observed to be 6.40 kW.kg<sup>-1</sup> and 3.85 Wh.kg<sup>-1</sup>, respectively.

#### 4. Conclusions:

In summary, we have successfully synthesized  $Mn_3O_4$  NLs by electrodeposition method on low cost conducting stainless steel substrate for supercapacitor application. The XRD study reveals that hausmannite tetragonal crystal structure with average crystallite size of 34 nm. The surface morphology study  $Mn_3O_4$  thin film shows NLs type morphology at higher magnification. The electrodeposited  $Mn_3O_4$  NLs shows higher specific capacitance of 460 F.g<sup>-1</sup> with 92% cyclic stability, which is better achievement than earlier reported values because of nano structured materials. The GCD study shows better values specific energy and specific power and coulombic efficiency of  $Mn_3O_4$  NLs. EIS study reveals that small values of  $R_s$  and  $R_{ct}$  of  $Mn_3O_4$  NLs based thin film electrode, providing better ability of electronic and ionic conductivity of  $Mn_3O_4$  materials. Thus, electrodeposited  $Mn_3O_4$  NLs based thin film electrode is suitable material for electrochemical supercapacitor device.

#### References:

- [1] G. Wee, W.F. Mak, iN. Phonthammacha, A. Kiebele, M.V. Reddy, B.V.R. Chowdari, G. Gruner, M. Srinivasan, S.G. Mhaisalkar, J. Electrochem. Soc. 157, A179 (2010)
- [2] J.K. Chang, Y.L. Chen, W.T.T. Sai, J. Power Sources. 135, 344 (2004)
- [3] P. Simon, Y. Gogotsi, Nat. Mater. 7, 845 (2008)
- [4] D. Wei, Scherer MR, Bower C, Andrew P, Ryhanen T, U. Steiner, Nano Lett. 12, 1857 (2012)
- [5] K.H. Chang, C.C. Hu, C.Y. Chou, Chem. Mater. 19, 2112 (2007)
- [6] Z. Yu, B. Duong, D. Abbott, J. Thomas, Adv. Mater. 25, 3302 (2013)
- [7] P.M. Kharade, J.V. Thombare, A.R. Babar, R.N. Bulakhe, S.B. Kulkarni, D.J. Salunkhe, J Phys Chem Solids. 120, 207 (2018)
- [8] L. Gu, Y. Wang, R. Lu, L. Guan, X. Peng, J. Sha J. Mater. Chem. A. 2, 1761 (2014)
- [9] D.Q. Liu, S.H. Yu, S.W. Son, and S.K. Joo, ECS Trans. 16, 103 (2008)
- [10] P.M. Kharade, A.R. Babar, S.S. Dhasade, B.R. Karche, D.J. Salunkhe, Mater. 7, 342 (2018)
- [11] A.S. Patil, M.D. Patil, G.M. Lohar, S.T. Jadhav, V.J. Fulari, Ionics. 23, 1259 (2017)
- [12] S.F. Chin, S.C. Pang, and M.A. Anderson, J. Electrochemical Society. 149, A379 (2002)
- [13] S.F. Chin, and S.C. Pang, Mater. Chem. Phys. 124, 29 (2010)
- [14] X. Zhang, X. Sun, Y. Chen, D. Zhang, Y. Ma, Mater. Lett. 68, 336 (2012)
- [15] X. Zhang, P. Yu, D. Zhang, H. Zhang, X. Sun, Y. Ma, Mater. Lett. 92, 401 (2013)
- [16] J.L. Liu, L.Z. Fan, X. Qu, Electrochim. Acta. 66, 302 (2012)
- [17] R. Jiang, T. Huang, J. Liu, J. Zhuang, A. Yu, Electrochim. Acta. 54, 3047 (2009)
- [18] C.K. Lin, K.H. Chuang, C.Y. Lin, C.Y. Tsay, C.Y. Chen, Surf. Coat. Technol. 202, 1272 (2007)

- [19] D.P. Dubal, D.S. Dhawale, R.R. Salunkhe, V.J. Fulari, C.D. Lokhande, *J. Alloy. Compd.* 497,166(2010)
- [20] C. Xu, B. Li, H. Du, F. Kang, and Y. Zeng, *J of Power Sources.*180,664 (2008)
- [21] A. Zolfaghari, F. Ataherian, M. Ghaemi, and A. Gholami, *Electrochimica Acta.* 52,2806(2007)
- [22] T. Nguyen, M.J. Carmezim, M. Boudard, M. Montemor, *J. Hydrog. Energy.* 40,16355(2015)
- [23] A. Yuan, X. Wang, Y. Wang, J. Hu, *Electrochim. Acta.* 54,1021(2009)
- [24] D.P. Dubal, D.S. Dhawale, R.R. Salunkhe, S.M. Pawar, C.D. Lokhande, *Appl Surf Sci.*256,4411(2010)
- [25] T. Yousefi, A.N. Golikand, M.H. Mashhadizadeh, M. Aghazadeh, *Curr. Appl. Phys.* 12, 544(2012)
- [26] M. Kim, Y. Hwang, J. Kim, *J. Power Sources.* 239, 225(2013)
- [27] X. Dai, M. Zhang, J. Li, D. Yang, *RSC Adv.*10, 15860(2020)
- [28] P.M. Kharade, S.G. Chavan, D.J. Salunkhe, P.B. Joshi, S.M. Mane, S.B. Kulkarni, *J. Mater. Sci. Mater. Electron.* 52, 37(2014)
- [29] M. Zhang, X. Dai, C. Zhang, Y. Fuan, D. Yang, *J. Li, Mater.*13, 181(2020)
- [30] P.D. More, P.R. Jadhav, S.M. Ingole, Y.H. Navale, V.B. Patil, *J Mater Sci: Mater Electron.* 28,707(2017)
- [31] A.A. Shaikh, M.R. Waikar, R.G. Sonkawade, *Synth. Met.* 247, 1(2019)
- [32] D.P. Dubal, D.S. Dhawale, R.R. Salunkhe, C.D. Lokhande, *J. Electrochem. Soc.* 157,A812 (2010)
- [33] G.S. Gund, D.P. Dubal, B.H. Patil, S.S. Shinde, C.D. Lokhande, *Electrochim. Acta.* 92,205 (2013)

## Investigation The Temperature and Volume Fraction Effects on The Thermal and Rheological Properties of The TiO<sub>2</sub> Nanofluid

N B Girhe<sup>1</sup>, S N Botewad<sup>2\*</sup>, P P Pawar<sup>2</sup>, A B Kadam<sup>2</sup>

<sup>1</sup>Department of Physics, Jawahar Science, Commerce and Arts College, Andoor, Tuljapur 413603, Maharashtra, India

<sup>2</sup>Department of Physics, Dr. Babasaheb Ambedkar Marathwada University, Aurangabad 431004, Maharashtra, India

### ABSTRACT

The present investigation has been reported the preparation of water-based TiO<sub>2</sub> nanofluid using a two-step method. The temperature and volume fraction dependent thermal conductivity and viscosity TiO<sub>2</sub> was studied. The different volume fraction of TiO<sub>2</sub> (0.1,0.2,0.3,0.4 and 0.5) were used dispersed in water using harsh ultrasonic treatment and tested the thermal conductivities for temperature range of 20–50 °C. The experimental results reveal that increase in temperature and volume fraction increases the thermal conductivity of nanofluid. The viscosity of the nanofluid with same concentration of TiO<sub>2</sub> was measured and shows the decrease viscosity by increasing temperature whereas increases when increase the volume concentration. Thus, the experimental results are much more useful for the practical application of nanofluids in thermal management.

**Keywords:** Nanofluid; Nanoparticles; Thermal Conductivity; Viscosity;

### I. INTRODUCTION

Thermal management becomes the very critical task in various industries for getting the efficient productivity. Worldwide various conventional fluids were used for the thermal management such as water, oil, ethylene glycol etc. But unfortunately, these fluids do not achieve the desired thermal properties for practical application. To improve the thermal conductivities of these conventional fluids firstly in 1873 Maxwell proposed the single-phase fluids with the addition of solid particles [1]. The idea of Maxwell worked and it improves the thermal properties of the conventional fluids but it has the drawbacks such as sedimentation, clogging and erosion during the flow. After this inventive research idea and experimental results in 1995, Choi introduced the idea of nanofluids with his own experimental results. The nanofluid which solely overcomes the sedimentation, clogging and erosion problems [2].

An emerging nanotechnology provides the superior physical, thermal, optoelectronics properties of the material in nanosized dimension. The very new trending application of nanotechnology is the nanofluid

research. Nanofluid is an engineering fluid in which nanometre sized solid particles homogeneously dispersed in base fluid such as water, engine oil, propylene glycol, ethylene glycol, etc [3]. Recently various types of nanomaterials were found to be used for the preparation of nanofluid such as metal, metal oxides, carbon materials etc. Nowadays metal oxide nanoparticles ( $\text{TiO}_2$ ,  $\text{SiO}_2$ ,  $\text{Fe}_2\text{O}_3$ ,  $\text{Fe}_3\text{O}_4$ ,  $\text{Al}_2\text{O}_3$ ,  $\text{BaTiO}_3$ ,  $\text{CuO}$ , etc.) extensively employed for the preparation of nanofluid [4]. The preference for metal oxide nanoparticles is due to the superior physicochemical, optoelectronics, thermal properties, and ease of preparation with tuned properties. The potential of nanofluids to enhances the thermal conductivity and rheological behaviour of base fluid it applicable in heat transfer, including fuel cells, cooling of microelectronic equipment, pharmaceutical processes and hybrid engines etc [5,6].

Worldwide different research groups have been reported the thermal conductivity and viscosity of the nanofluids using the different types of nanoparticles with different volume fraction in the base fluid. M.Kh. Abdolbaqi et. al studied the thermal conductivity and viscosity of BioGlycol/water based  $\text{TiO}_2$  nanofluids and experimental results shows that enhancement of thermal conductivity depends on volume concentration, temperature and thermal conductivity of base fluid [7]. M.H. Ahmadi et.al investigate the thermal performance of  $\text{TiO}_2$  nanofluid using four different neural networks [8]. D. Cabaleiro et.al reported the ethylene and propylene glycol-based  $\text{TiO}_2$  (anatase and rutile) nanofluids. The experimental results shows that thermal conductivity increases 15.4%. and enhancements are higher for propylene than ethylene glycol-based nanofluids [9]. W.H. Azmi et.al investigate the heat transfer performance of  $\text{TiO}_2$  nanofluids in water-EG mixture at different operating temperatures. On the basis of experimental results concluded that maximum enhancement of thermal conductivity was 15.4% at 1.5% volume concentration and temperature of  $60^\circ\text{C}$ . and relative viscosities fluctuate at a range of 4.6 to 33.3% with variation of temperature [10].

## II. EXPERIMENTAL

### 2.1 Materials and Characterization

In present investigation  $\text{TiO}_2$  (Rutile) nano particles with particles size 20 nm procured from the Sisco Research Laboratory Mumbai, India. KD2 Pro thermal analyser (Decagan Devices Inc., USA) was use to study the thermal conductivity and before measurements the device prob was calibrated with standard fluid. The viscosity of all nanofluid were measured by means of an AR-G2 rheometer (TA Instruments, USA) at different temperatures.

### 2.2 Nanofluid Preparation

Nanofluids reported in the present investigation were prepared via two-step method.  $\text{TiO}_2$  nanoparticles of volume fraction (0.1, 0.2, 0.3, 0.4, and 0.5 Wt.%) were used for the preparation of nanofluid. The above-mentioned proportion of  $\text{TiO}_2$  nanoparticles was dispersed in the base fluid double distilled water (DDW) separately and stirred for 2 hours forcefully using magnetic stirrer. Then the stable dispersion was attained by ultrasonic probe via ultrasonication for 6 h.

### III. RESULTS AND DISCUSSION

#### 3.1 Thermal conductivity

The thermal conductivity of prepared water based  $\text{TiO}_2$ -nanofluids concentrations of (0.1, 0.2, 0.3 and 0.4) wt. % were measured at temperatures of 300 K-350 K in 15 k interval. Fig. 1 shows the thermal conductivity of prepared nanofluid for different volume concentrations and fig. 2 shows for different temperatures. It is observed that by increasing both parameters volume concentrations and temperatures, thermal conductivity is enhanced of all the studied samples. Increment of the nanoparticles loading in the base fluid reduces the interparticle distances that improves heat conduction and the outcome is enriched thermal conductivity. The basic phenomenon of the increment in the thermal conductivity is propagation of lattice vibration between electrons and phonons. The thermal conductivity significantly increases by increasing temperatures due to the Brownian motion which provide the direct solid-solid transport between the incorporated particles.

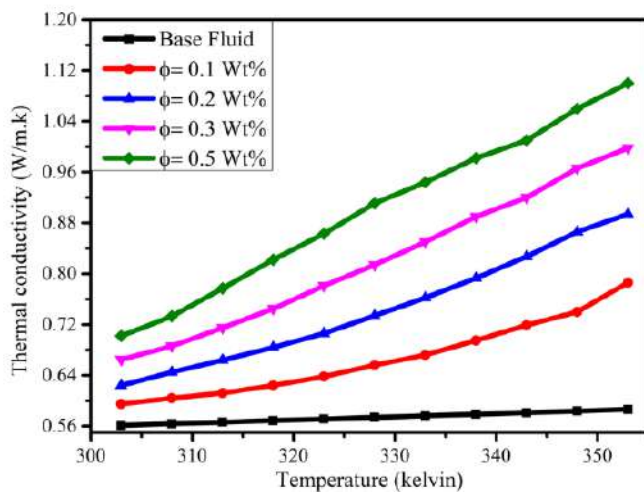


Figure 1. Thermal conductivity for various volume fraction at different temperature

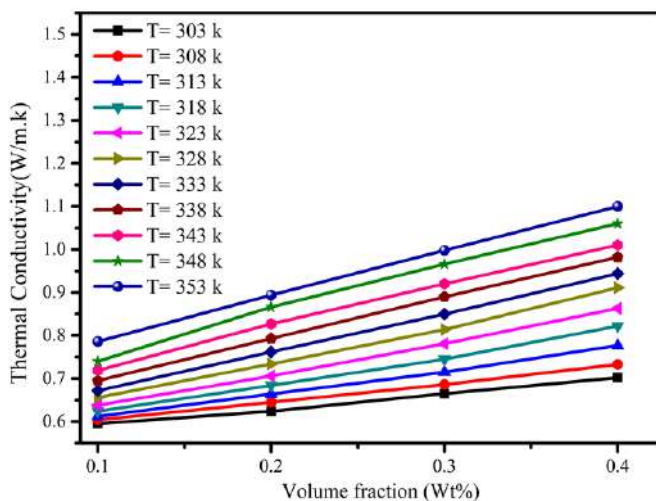


Figure 2. Thermal conductivity for different temperatures of various concentration

### 3.2 Viscosity

Rheological behaviors of all prepared nanofluid samples viscosity were examined at different temperature points of 300 K-360 K at equal interval for each volume concentrations. Fig. 3 shows the dependency of viscosity on the volume concentration and temperature of TiO<sub>2</sub> nanofluid. The considerable effects were observed for both parameters, temperature as well as volume concentrations. As concerned to the volume concentration viscosity of all the nanofluid samples observed to be increased. The reason behind the increasing viscosity may be due to the formation of agglomeration of nanoparticles in suspension. The temperature effect slightly reduces the viscosity due to the feeble intermolecular interaction and adhesion forces between molecules which is further attributed to Brownian motion, thermal movement of molecules and their average speed.

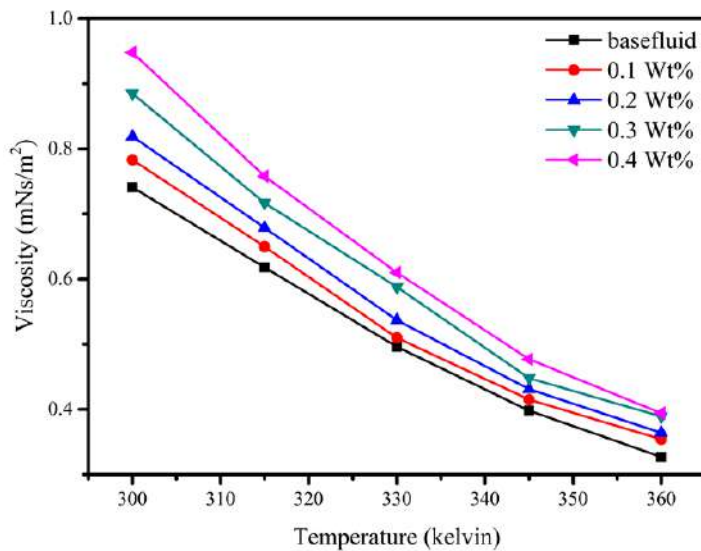


Figure 3. Viscosity of TiO<sub>2</sub> nanofluid at different temperature

## IV. CONCLUSION

In short, present investigation successfully encloses the preparation and analysis of the thermal as well as rheological properties of TiO<sub>2</sub> nanofluids. The investigational findings reveal the considerable enhanced thermal conductivity of nanofluids with increased temperature and volume concentration. The viscosity of the nanofluid increased with volume concentration whereas decreased with increased temperature. Thus, the present investigation exhibits the applicability of the ternary TiO<sub>2</sub> nanofluid for the various application wherever the necessity of cooling.

## V. REFERENCES

- [1]. Vanaki, S. M., Ganesan, P., & Mohammed, H. A. (2016). Numerical study of convective heat transfer of nanofluids: a review. *Renewable and Sustainable Energy Reviews*, 54, 1212-1239.

- [2]. Das, S. K., & Stephen, U. S. (2009). A review of heat transfer in nanofluids. *Advances in Heat transfer*, 41, 81-197.
- [3]. Ali, H. M., Babar, H., Shah, T. R., Sajid, M. U., Qasim, M. A., & Javed, S. (2018). Preparation techniques of TiO<sub>2</sub> nanofluids and challenges: a review. *Applied Sciences*, 8(4), 587.
- [4]. Sidik, N. A. C., Mohammed, H. A., Alawi, O. A., & Samion, S. (2014). A review on preparation methods and challenges of nanofluids. *International Communications in Heat and Mass Transfer*, 54, 115-125.
- [5]. Puliti, G., Paolucci, S., & Sen, M. (2011). Nanofluids and their properties. *Applied Mechanics Reviews*, 64(3).
- [6]. Suganthi, K. S., & Rajan, K. S. (2017). Metal oxide nanofluids: Review of formulation, thermo-physical properties, mechanisms, and heat transfer performance. *Renewable and Sustainable Energy Reviews*, 76, 226-255.
- [7]. Abdolbaqi, M. K., Sidik, N. A. C., Aziz, A., Mamat, R., Azmi, W. H., Yazid, M. N. A. W. M., & Najafi, G. (2016). An experimental determination of thermal conductivity and viscosity of BioGlycol/water based TiO<sub>2</sub> nanofluids. *International Communications in Heat and Mass Transfer*, 77, 22-32.
- [8]. Ahmadi, M. H., Baghban, A., Sadeghzadeh, M., Hadipoor, M., & Ghazvini, M. (2020). Evolving connectionist approaches to compute thermal conductivity of TiO<sub>2</sub>/water nanofluid. *Physica A: Statistical Mechanics and its Applications*, 540, 122489.
- [9]. Cabaleiro, D., Nimo, J., Pastoriza-Gallego, M. J., Piñeiro, M. M., Legido, J. L., & Lugo, L. (2015). Thermal conductivity of dry anatase and rutile nano-powders and ethylene and propylene glycol-based TiO<sub>2</sub> nanofluids. *The Journal of Chemical Thermodynamics*, 83, 67-76.
- [10]. Azmi, W. H., Hamid, K. A., Mamat, R., Sharma, K. V., & Mohamad, M. S. (2016). Effects of working temperature on thermo-physical properties and forced convection heat transfer of TiO<sub>2</sub> nanofluids in water–Ethylene glycol mixture. *Applied Thermal Engineering*, 106, 1190-1199.

## Variation of Magnetic Susceptibility of Nanoparticle Sized Copper Cobalt Ferrites

S. S. Karande<sup>1</sup>, M. S. Kavale<sup>1</sup>, B. R. Karche<sup>2</sup>

<sup>1</sup>Department of Physics, Sangameshwar College, Solapur, Maharashtra, India

<sup>2</sup>Material Science and Thin Film Laboratory, Shankarrao Mohite Mahavidyalaya, Akluj, Dist. Solapur, Maharashtra, India

### ABSTRACT

The polycrystalline aluminium substituted nano-particle sized copper cobalt ferrite samples  $Cu_xCo_{1-x}Fe_2-2yAl_2yO_4$  (where  $x= 0.0, 0.2, 0.4, 0.6, 0.8, 1.0$ ;  $y= 0.05, 0.15$  and  $0.25$ ) have been prepared by standard ceramic technique. Phase formation is investigated using X-ray diffraction, Infrared absorption technique and Scanning electron microscope technique. The lattice constants of the all samples are evaluated from x-ray diffraction data. The Magnetic susceptibility decreases with aluminium and copper content.

**Keywords:** Polycrystalline, nanoparticle size, standard ceramic technique and Inverse cubic spinel, Magnetic susceptibility

### I. INTRODUCTION

In a way, every material utilized today is a composite. Composite materials are a physical mixture of two or more compatible micro or macro constituent particles which differ in form and chemical composition and are essentially insoluble in each other. Composite materials are best suited for scientific applications which could not be achieved by any one component acting on its own. Ferrite / ferroelectric composites are termed as magneto electric (ME) composites due to the coupling between the electric and magnetic fields in the materials. The conversion of magnetic to electric fields in such ME composite originates from the elastic interaction between ferrite and ferroelectric subsystems [1]. In the presence of the magnetic field, the magnetostriction in the ferrite phase gives rise to mechanical stresses that are transferred to the ferroelectric phase, resulting in electric polarization of the ferroelectric phase owing to its magneto electric effect. ME materials find applications as smart materials in actuators, sensors, magnetic probes, phase inverters, rectifiers, modulators, and transducers in solid state microelectronics and microwave devices [2,3].

Spinel ferrite nanoparticles are being intensively investigated in recent years because of their remarkable electrical and magnetic properties and wide practical applications in information storage system, ferro-fluid technology, magnetocaloric refrigeration and medical diagnosis [4]. Among the spinels, mixed Zn ferrites and especially Ni-Zn ferrites are widely used in applications like transformer cores, chokes, coils, noise filters

recording heads etc. [5]. While Ni–Zn ferrite possesses higher resistivity and saturation magnetization, cobalt ferrite possesses high cubic magneto crystalline anisotropy and hence high coercivity. The high coercivity is driven by large anisotropy of the cobalt ions due to its important spin orbit coupling. It is ferromagnetic with a Curie temperature ( $T_c$ ) around 520°C, [6] and shows a relatively large magnetic hysteresis which distinguishes it from rest of the spinels. The synthesis of ultra fine magnetic particles has been extensively investigated in recent years because of their potential applications in high density magnetic recording and magnetic fluids [7]. Among the current methods for synthesis of mixed ferrite the combustion reaction method stands out as an alternative and highly promising method for the synthesis of these ferrites [8]. Magnetic properties measured at room temperature by vibrating sample magnetometer (VSM) reveal an increase in saturation magnetization with increase in cobalt concentration [9].

## II. EXPERIMENTAL

### Materials:

High purity starting materials are used as Cobalt Oxide (CoO):- 74.9326 gm, Copper Oxide (CuO):- 74.5454 gm, Ferric oxide( $Fe_2O_3$ ):- 159.6922 gm, Aluminum Oxide ( $Al_2O_3$ ):- 101.9612 gm

### Preparation of ferrite:

Nano crystalline powder samples of  $Cu_xCo_{1-x}Fe_{2-2y}Al_{2y}O_4$  (where  $x= 0.0, 0.2, 0.4, 0.6, 0.8, 1.0$ ;  $y = 0.05, 0.15$  and  $0.25$ ) were prepared by the standard ceramic technique. Starting materials CuO, CoO,  $Fe_2O_3$  and  $Al_2O_3$  of AR grade obtained from Sigma – Aldrich, India were used. These samples were heated at ramping rate of 80 °C hr<sup>-1</sup> at 1000°C for 48 hours. XRD and IR analysis revealed the cubic spinel structure of the synthesized samples and functional groups in the samples respectively. The absence of any extra line confirms the formation of single phase ferrite. The average particle size 'D' was determined from line broadening (311) reflection using the Debye Scherer formula discussed elsewhere [10]. Calculations of lattice constant, physical density, X-ray density, porosity, site radii and ionic bond lengths on both sites were calculated by using formulae discussed elsewhere [11] and graphically shown in fig.4. Infrared absorption spectra of powdered samples were recorded in the range 350-800 cm<sup>-1</sup> using Perkin-Elmer FTIR spectrum and spectrometer by KBr pellet technique and presented in (fig.2). The scanning electron microscopes are shown in fig.3

## III. RESULTS AND DISCUSSION

The X-ray diffraction patterns of the samples are presented in (fig.1). Powder X-ray diffractometer of the ferrite samples reveals the single phase spinel structure, as well defined reflection is observed without any ambiguity. The diffraction peaks are corresponding to (200), (311), (400), (422), (333/511), (440) and (533) planes. The lattice constants 'a' and 'c' for all prepared samples are calculated by using prominent (311) XRD peak. The calculated and observed values of inter planer distance (d) are found in good agreement with each

other for all reflections. The physical density ( $\rho$ ), x-ray density ( $\rho_x$ ), and porosity ( $p$ ), are calculated from the formulae given by Gadkari et.al [12].

From the calculations of lattice constants 'a' and 'c' for all the prepared ferrites it is observed that  $c > a$  and tetragonality ratio ( $c/a$ ) is found in the range of 1.03 to 1.07. This result is in good agreement with previous report [13-14]. In this present report tetragonality ratio for copper ferrite is 1.06. It means 70% copper resides on B site and it exhibits prolate type distortions in the crystal lattice. The previous report [15] well supports the present results reported this communication. Both  $\text{Fe}^{3+}$  and  $\text{Cu}^{2+}$  are Jahn-Teller ion which produces prolate type distortions on (B) site and hence  $c > a$  and  $(c/a) = 1.06$ . Therefore copper ferrite exhibits tetragonal spinel structure in host crystal lattice of cobalt ferrite. In addition of copper content in tetragonality ratio is found increasing but due to addition of aluminium tetragonality ratio decreases. It means that  $\text{Al}^{3+}$  and copper suppress the tetragonal prolate type.

The crystallite sizes ( $t$ ) of all the prepared samples were computed by Scherer rule utilizing the peak width at one-half intensity of the maximum intensity peak (311).

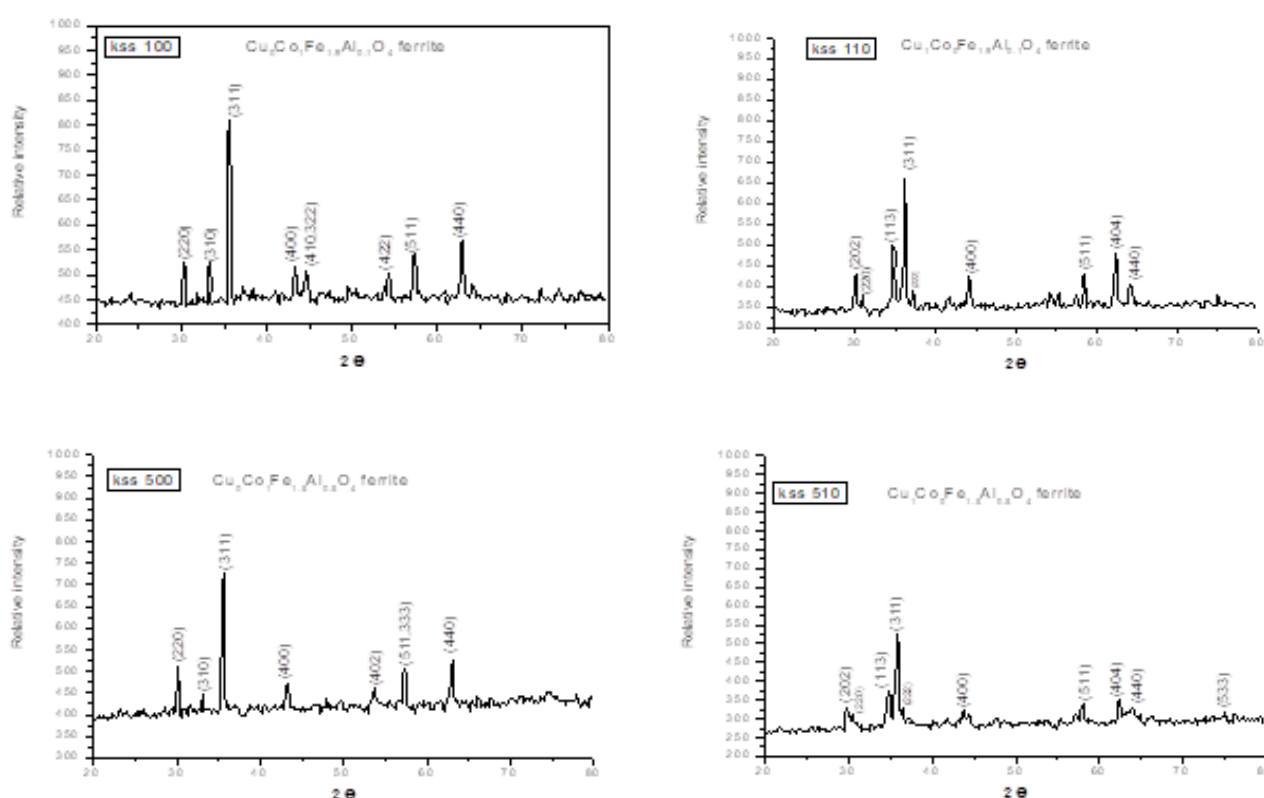


**Fig: 1 XRD patterns of system  $\text{Cu}_x\text{Co}_{1-x}\text{Fe}_{2-2y}\text{Al}_{2y}\text{O}_4$**

The Al ( $y = 0.05-0.25$ ) doped copper cobalt ferrite samples show a higher grain growth and the crystallite size ( $t$ ) lies in the extent of 52.53-94.4 nm. The mean particle size calculated from diffractograms is in the range of 50 to 100 nm. That suggest the particles in the ferrites samples are fine and there is continuous grain growth in all compositions. It gives the confirmation of suitable microstructure formation in all compositions.

The width of the reflection peak (311) for all the compositions is approximately the same due to the nearly equal particle size.

The infrared absorption spectra are showing two distinct absorption bands  $\nu_1$  due to tetrahedral (A) site interstitial voids near  $600\text{ cm}^{-1}$  and other  $\nu_2$  due to octahedral (B) site interstitial voids near  $400\text{ cm}^{-1}$ . Our results in this present communication are well supported by previous reports [16, 17].

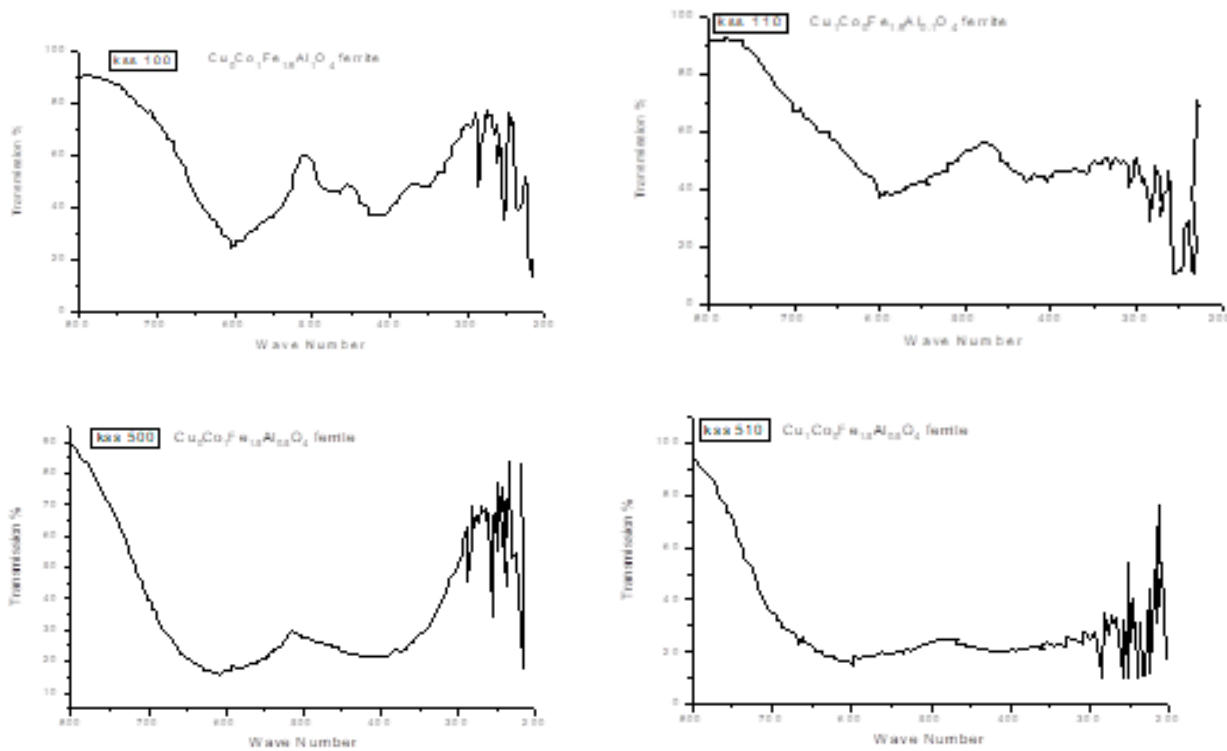


**Figure 2: Absorption spectra for system  $\text{Cu}_x\text{Co}_{1-x}\text{Fe}_{2-2y}\text{Al}_{2y}\text{O}_4$**

The close inspection of all micrographs revealed that there is continuous grain growth with well – defined grain boundaries formed. The present system shows multi domain behavior. No exaggerated grain growth is observed in any composition. The average grain size is found to decrease with increase in Al content in copper cobalt ferrite. However in the present system the grain growth shows generally a decreasing trend with aluminum content, which is rather expected because of multi-domain behavior of these compositions in copper cobalt ferrite. Grain growth is almost accompanied with grain size, which is increasing with copper and aluminum content. So it appears that copper and aluminum content favors the grain growth. The scanning electron micrographs shown below

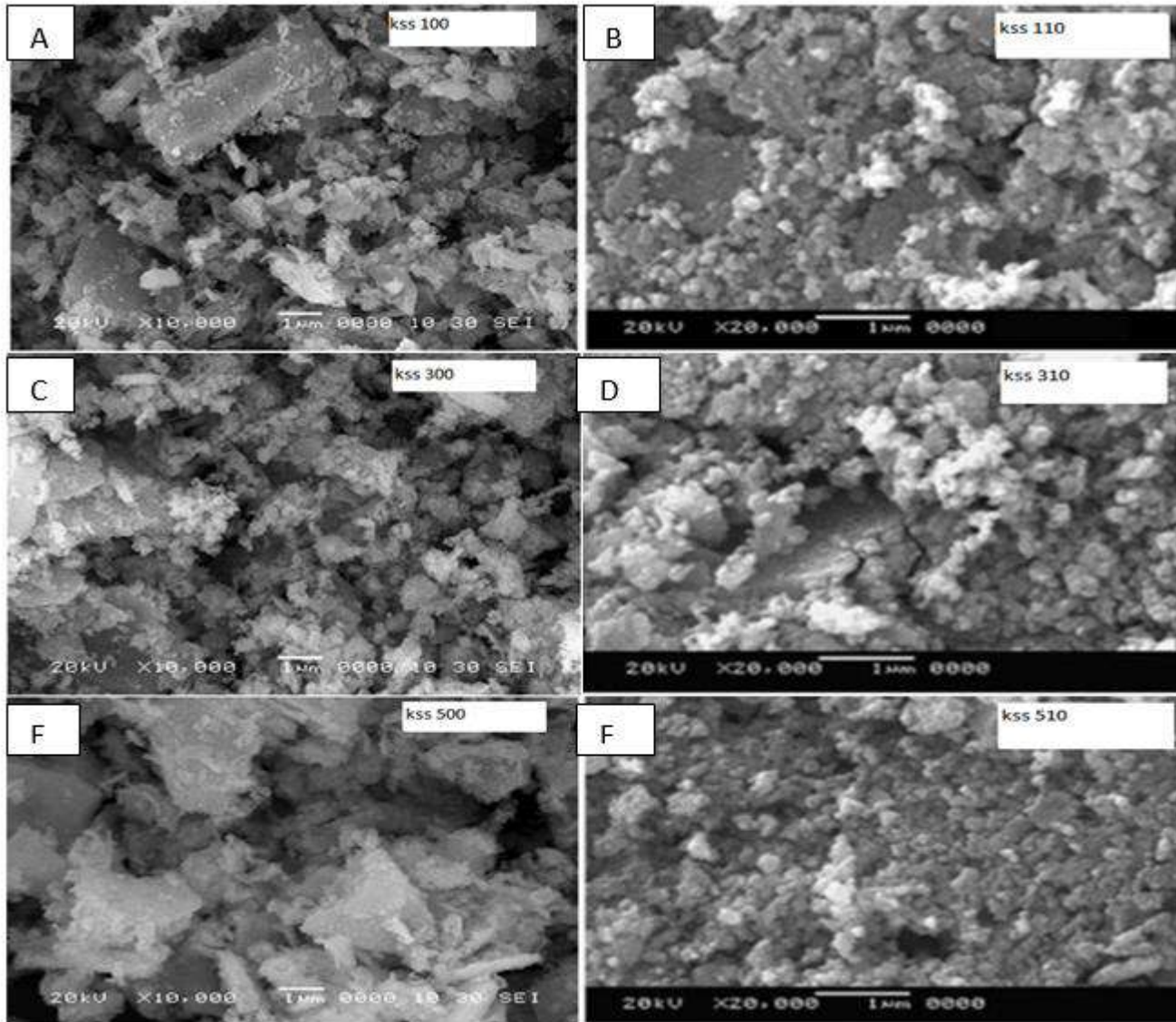


**Fig: 3 (A) to (F) scanning electron microscopes of  $Cu_xCo_{1-x}Fe_{2-2y}Al_yO_4$  :**

- (A) KSS 100-  $Cu_0Co_1Fe_{1.9}Al_{0.1}O_4$ , (B) KSS 110-  $Cu_1Co_0Fe_{1.9}Al_{0.1}O_4$ ,  
 (C) KSS 300-  $Cu_0Co_1Fe_{1.7}Al_{0.3}O_4$ , (D) KSS 310-  $Cu_1Co_0Fe_{1.7}Al_{0.3}O_4$ ,  
 (E) KSS 500-  $Cu_0Co_1Fe_{1.5}Al_{0.5}O_4$  & (F) KSS 510-  $Cu_1Co_0Fe_{1.5}Al_{0.5}O_4$

The susceptibility is measured at room temperature [Fig. 2(a)] then susceptibility is found increasing up to 20 % of copper content and thereafter decreases. The susceptibility is measured at various temperatures [Fig. 2(b)], the compositions shows gradual decrease in normalized susceptibility with temperature which suggest that they exhibit super paramagnetic (SP) structure having fine particles. The susceptibility is decreases and curie temperature also shifts towards minimum value as copper as well as aluminum content increases.

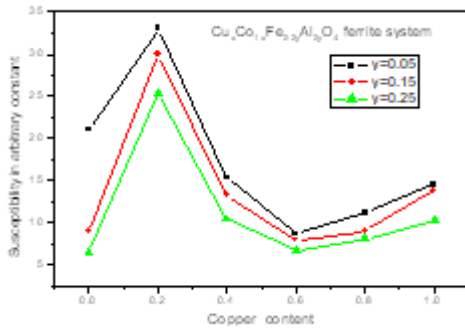


Fig. 4(a)

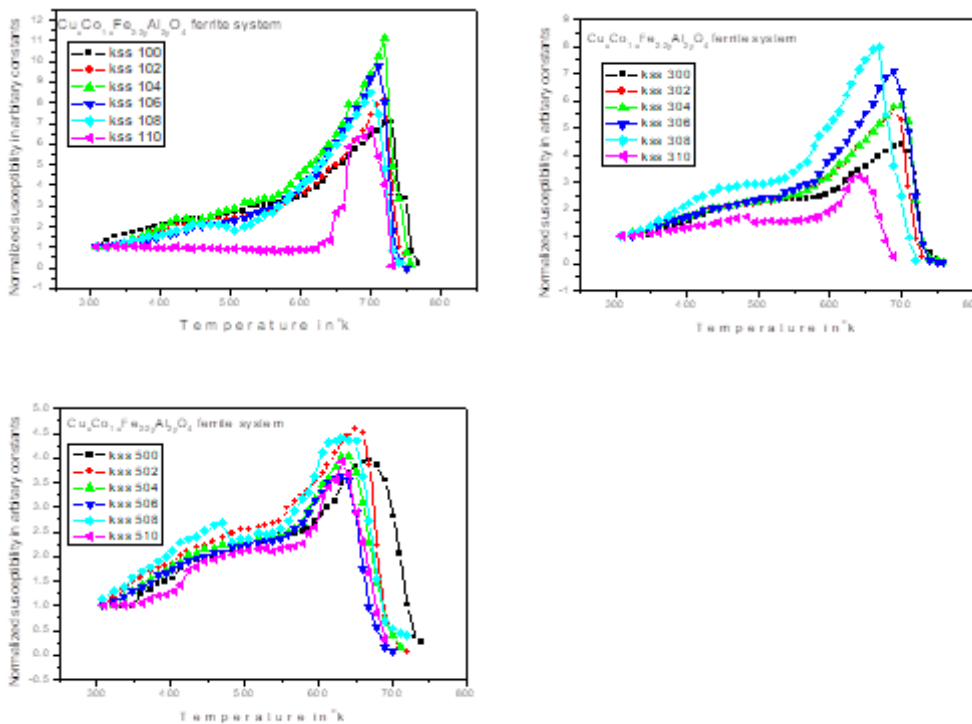


Fig. 4(b)

**Fig 4: Variation of A. C. susceptibility with copper and aluminum content at room temperature and various temperature for  $\text{Cu}_x\text{Co}_{1-x}\text{Fe}_{2-2y}\text{Al}_y\text{O}_4$  ferrite system**

#### IV. CONCLUSIONS

Copper cobalt ferrite is partially inverse spinel ferrite. Addition of  $\text{Al}^{3+}$  ions replaces  $\text{Fe}^{3+}$  on (B) site resulting in increase of lattice constant  $a$ , decrease in ionic radii ( $R_A$ ) and bond length ( $\text{O}-\text{A}$ ). The lattice constant obtained from XRD data shows increases. The A. C. susceptibility goes on decreasing with copper and aluminum content.

## V. REFERENCES

- [1]. R. S. Devan, S. A. Lokare, S. S. Chougule, D. R. Patil, Y. D. Kolekar, and B. K. Chougule, *J. Phys. Chem. Solids* 67, 1524 (2006).
- [2]. K. Zhao, K. Chen, Y. R. Dai, J. G. Wan, and J. S. Zhu, *Appl. Phys. Lett.* 87, 162901 (2005).
- [3]. S. R. Kulkarni, C. M. Kanamadi, and B. K. Chougule, *Mater. Res. Bull.* 40, 2064 (2005).
- [4]. Zhao L, Yang H, Yu L, Cui Y, Zhao X, Zou B, Feng SJ. *MagnMagn Mater* 2006;301:445–51.
- [5]. Rath C, Sahu KK, Anand S, Date SK, Mishra NC, Das RP. *J MagnMagn Mater* 1999;202:77–84.
- [6]. Rajendran M, Pullar RC, Bhattacharya AK, Das D, Chintalapudi SN, Majumdar CK. *J MagnMagn Mater* 2001;232:71–83.
- [7]. Ozaki M. *Mater Res Bull* 1989;12:35–43.
- [8]. Costa ACM, Tortella E, Morelli MR, Kaufman M, Kiminami RHGA. *J Mater Sci* 2002;37:3569–72.
- [9]. M.M. Mallapur, B.K. Chougule; *Materials Letters*; Vol. 64 (2010); P. 231–234.
- [10]. H. P. Klug, L. E. Alexander, *X-ray diffraction procedure for polycrystalline and amorphous materials*, Wiley N.Y, 1997, 637.
- [11]. A. B. Gadkari, T. J. Shinde, P. N. Vasambekar, *J. Mater Sci: Mater Electron* 21 2010, 96 , 103.
- [12]. Prince E., Treuting R.G; *Acta Crystallographica*, 1956, 9, 1025.
- [13]. Sagal K., Tabellen F. *Rontegenstrukturanalyse*, Springer, Berlin, 1958.
- [14]. Borisenko A., Toropov N. A; *Z. Prikl Chem*, 1950, 23, 1165.
- [15]. Goodenough J.B and Loeb A. L ,*Phys. Rev.*, 1955, 98, 391.
- [16]. Waldron R.D, *Phy. Rev*, 1955, 99(6), 1727.
- [17]. K. V. S. Badarinath, *Phys. Stat. Solidi (a)* 1985, 91, 19-23.

## DC Resistivity of La<sup>3+</sup> Substituted Mg-Zn Ferrite Nanoparticles by Co-Precipitation Method

R.A. Bugad<sup>1\*</sup>, B.G. Pawar<sup>1</sup>, B.B. Navale<sup>2</sup>, P.G. Pawar<sup>3</sup>

<sup>1</sup>Department of Science, Sangola Mahavidyalaya, Sangola, Dist. Solapur 413307, Maharashtra, India

<sup>2</sup>Department of Science, Vidnyan Mahavidyalaya, Sangola, Dist. Solapur 413307, Maharashtra, India

<sup>3</sup>Department of Science, Shivaji Polytechnic College, Sangola, Dist. Solapur 413307, Maharashtra, India

### ABSTRACT

Lanthanum (La) substituted magnesium zinc ferrite nanoparticles with general formula  $Mg_{0.6}Zn_{0.4}La_{2y}Fe_{2-2y}O_4$  (where  $y = 0.00, 0.05, 0.10, 0.15, 0.20$  and  $0.25$ ) have been synthesized by co-precipitation method. The XRD analysis was carried out to confirm the single phase cubic structure of La<sup>3+</sup> substituted Mg-Zn ferrite. The nature of DC resistivity of ferrite was studied with substitution of La<sup>3+</sup> content. The effects of La<sup>3+</sup> substitution in Mg-Zn ferrite on structural and electric properties were studied.

**Keywords:** Lanthanum, Mg-Zn ferrites, Co-precipitation, DC Resistivity,

### I. INTRODUCTION

Ferrites are usually non-conductive ferrimagnetic ceramic material. Most of the ferrites have a spinel structure [1]. The general formula of a spinel can be written as  $AB_2O_4$ . Nano-particles of mixed spinel ferrites have been the subject of current interest because of their interesting electric, optical and magnetic properties, which are considerably different from that of their bulk ferrites [2]. The ferrites are also widely used in high frequency cores, antennas, high frequency transformers, deflecting coil, motor generator and microwave devices such as modulators, phase shifter and circulators etc.[3]. The coercive force is related with saturation magnetization, anisotropy, internal stresses and porosity. The ferrites having low coercive force (HC) is known as Soft ferrites [4]. Generally, soft ferrite shows high electrical resistivity, superior magnetic and structural properties and hence they have low eddy current losses at high frequency [5]. Demand for electronic and computer components with high density and light weight performance is greatly increasing, which step up the demand for soft ferrites with high performance and thus contributes to the development of soft magnetic ferrites on the direction of higher frequency and lower power consumption [6].

## II. EXPERIMENTAL

### 2.1. Synthesis of La<sup>3+</sup> substituted Mg-Zn ferrite

The  $\text{Mg}_{0.6}\text{Zn}_{0.4}\text{La}_{2y}\text{Fe}_{2-2y}\text{O}_4$  (where  $y = 0.00, 0.05, 0.10, 0.15, 0.20$  &  $0.25$ ) have been prepared by the oxalate co-precipitation method as per reported in earlier literature [7]. The high purity AR grade starting materials  $\text{MgSO}_4 \cdot 7\text{H}_2\text{O}$ ,  $\text{ZnSO}_4 \cdot 7\text{H}_2\text{O}$ ,  $\text{LaSO}_4 \cdot 7\text{H}_2\text{O}$  and  $\text{Fe}_2\text{SO}_4 \cdot 7\text{H}_2\text{O}$  were used for preparation of samples. These chemicals were weighted in desired stoichiometric proportion and dissolved in distilled water. The pH of the solution was maintained at 4.8 by drop wise addition of concentrated  $\text{H}_2\text{SO}_4$ . The resulting solution was heated at  $80^\circ\text{C}$  for 1 h in order to complete the ionization of metal sulfates. The precipitating reagent was prepared in distilled water by adding required proportion of AR grade ammonium oxalate. Ammonium oxalate was taken in burette and was added drop by drop until the precipitation was formed. The co-precipitate product was dried and calcined at  $450^\circ\text{C}$  for 5h in air. The calcined powders were milled in an agate mortar with AR grade acetone as a base. The powders were pre-sintered at  $700^\circ\text{C}$  for 5h. The pre-sintered powders were pressed under hydraulic pressure of 5 tones / $\text{cm}^3$  to form pellet using polyvinyl alcohol as binder. Then pellets were finally sintered at  $900^\circ\text{C}$  for 12h.

### 2.2. Characterization Techniques

XRD patterns of lanthanum substituted magnesium zinc ferrites sintered at  $900^\circ\text{C}$  for 12h were recorded by Philips X-Ray Diffractometer model PW 1710 using Cu Ka radiation ( $\lambda = 1.5405 \text{ \AA}$ ). Two probe method was used for measurement of the dc electrical resistivity of ferrite in the temperature range  $25^\circ\text{C}$  to  $575^\circ\text{C}$ . The resistivity was obtained by using formula  $\rho = \frac{\pi r^2}{t} \times \frac{V}{I} = \frac{\pi r^2 R}{t}$ , Where, t is thickness and r is radius of the pellet in cm.

## III. RESULTS AND DISCUSSIONS

### 3.1. XRD studies

The XRD patterns of  $\text{Mg}_{0.6}\text{Zn}_{0.4}\text{La}_{2y}\text{Fe}_{2-2y}\text{O}_4$  (where  $y = 0.00, 0.05, 0.10, 0.15, 0.20, 0.25$ ) ferrite system sintered at temperature  $900^\circ\text{C}$  for 12h are shown in Fig. 1. The XRD patterns reveals the well resolved, sharp and intense peaks corresponding to planes (220), (311), (222), (400), (422), (511), (440), (620) and (533). The peaks obtained in the diffractogram closely match the data in the JCPDS file card number (04-002-5442). The XRD peak pattern corresponds to all allowed planes, which hint outs single phase cubic structure with the traces of secondary phase. Moreover, the peak at  $2\theta = 32.10^\circ$  corresponds to plane (121) which is attributed to secondary phase for  $\text{LaFeO}_3$  indexed as per ICDD file No. 01-74-9045. With increase in La content, intensity of characteristics peak (311) for  $\text{Fe}_2\text{O}_4$  gradually decreases, while intensity of peak (121) of  $\text{LaFeO}_3$  increases. It implies that the substituted  $\text{La}^{3+}$  ion has a solubility limit in the spinel lattice.

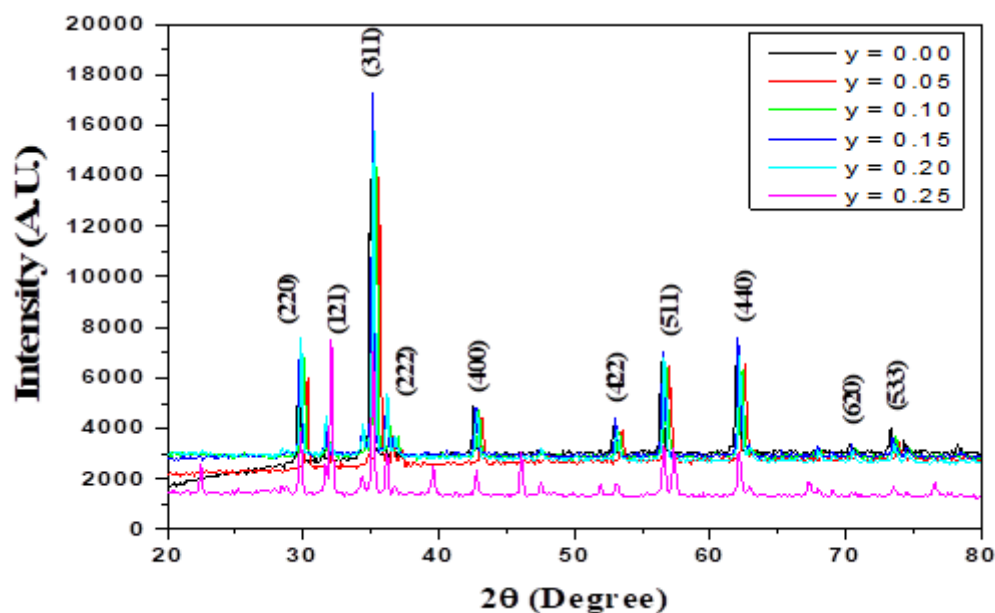


**Fig.1** : XRD patterns of  $\text{Mg}_{0.6}\text{Zn}_{0.4}\text{La}_{2y}\text{Fe}_{2-2y}\text{O}_4$  ferrite system

The degree of substitution of  $\text{Fe}^{3+}$  by  $\text{La}^{3+}$  ion is limited in the spinel lattice due to larger ionic radii of  $\text{La}^{3+}$  ions compared to  $\text{Fe}^{3+}$  ions. There is always some  $\text{La}^{3+}$  ions do not enter into spinel lattice. These  $\text{La}^{3+}$  ions react with  $\text{Fe}^{3+}$  ions and form second phase  $\text{LaFeO}_3$  usually locating at the grain boundaries. Similar observation have been reported in lanthanum substituted nickel [8], Cadmium [9] and Ni-Zi ferrites [10, 11].

### 3.2. DC Resistivity study

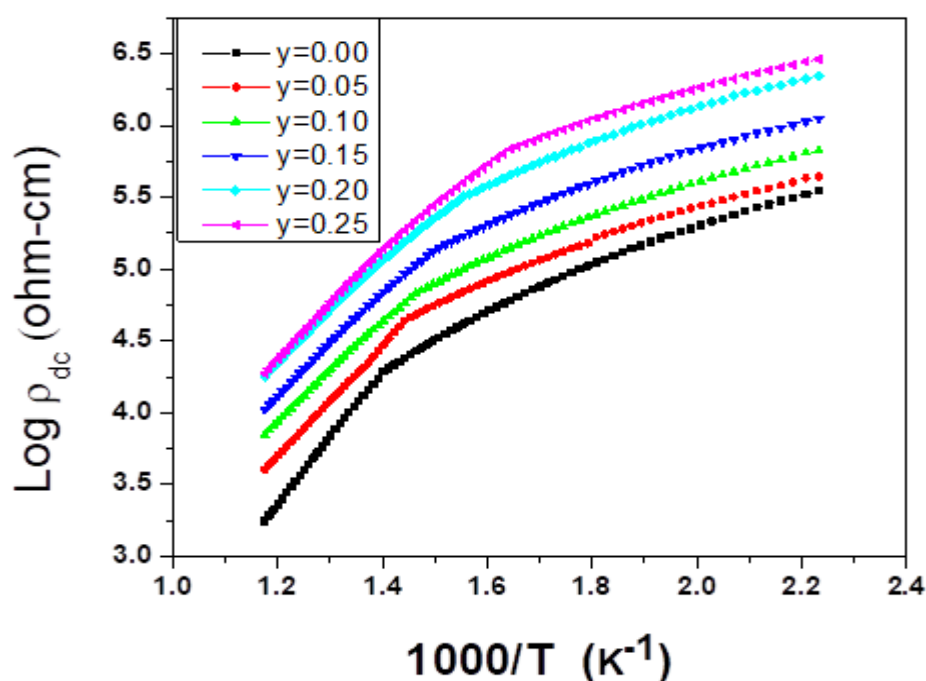


**Fig.2:** Variation of dc resistivity with inverse temperature for  $\text{Mg}_{0.6}\text{Zn}_{0.4}\text{La}_{2y}\text{Fe}_{2-2y}\text{O}_4$  ferrite system

The variation of log of dc electrical resistivity ( $\log \rho_{dc}$ ) as a function of inverse of temperature ( $1000/T$ ) for various composition of  $Mg_{0.6}Zn_{0.4}La_{2y}Fe_{2-2y}O_4$  ferrite is shown in Fig.2, The dc resistivity of the ferrites gets decreased with an increase in temperature indicates semiconducting behavior of the ferrites. All the samples show the break at Curie temperatures due to the change in conduction mechanism [12]. The slope change at Curie temperature corresponds to the samples transform from an ordered ferrimagnetic state to disordered paramagnetic state [13]. The value of Curie temperature obtained from the graph of  $\log \rho_{dc}$  verses  $1/T$  is calculated. The Curie temperature decreases with increase of  $La^{3+}$  content. It is due to the nonmagnetic nature of  $La^{3+}$  ions, which may break linkage between magnetic cations [14]. Rare earth  $La^{3+}$  ions have a strong preference to occupy on octahedral site and therefore replace  $Fe^{3+}$  ions at octahedral site (B) in spinel lattice by  $La^{3+}$ . Upon increase in the  $La^{3+}$  ions in B-site, A-B interaction weakens. Thus the decrease in Curie temperature is probably due to weakening of the A-B interaction. Similar observations have also been reported by Patil et al. [15]. The conduction phenomenon in polycrystalline ferrites was explained on the basis of Verwey and de Boer mechanism [16]. The conduction in ferrites is due to hopping of electrons between  $Fe^{2+}$  and  $Fe^{3+}$  ions on the octahedral (B) sites. In addition of lanthanum in Mg-Zn ferrite, it found that,  $Zn^{2+}$  ion have strong tendency to occupy A-site and  $Mg^{2+}$  ion have strong preference to occupy B-site, While  $La^{3+}$  preferentially occupy to octahedral B site, where it replaced  $Fe^{3+}$  ions in the B-site as per the modified cation distribution in magnetic study. The resistivity of the ferrite is controlled by  $Fe^{3+}$  concentration on B-site. The increase in resistivity with  $La^{3+}$  content is due to overall decrease in  $Fe^{3+}$  ions concentration on B-site. It causes decrease in hopping of electrons between  $Fe^{2+}$  and  $Fe^{3+}$  ions, results in decrease in conduction in ferrite with increase of resistivity [17]. Several researchers have been reported that resistivity of ferrites increases with the substitution of rare earth [18]. Gul and Ahmed also reported the effect of grain size, porosity and grain boundary area on resistivity of ferrite [19]. It is found that one of the factors for higher resistivity in ferrite is the decrease in grain size upon the addition of lanthanum. Smaller grain size produces larger number of insulating grain boundaries which produces inhomogeneous structure and greater energy is required for electron conduction which affects on AC and DC resistivity of ferrites [20].

#### IV. CONCLUSIONS

In conclusion, we report the preparation of lanthanum substituted magnesium zinc ferrites by co-precipitation method. A study on DC resistivity shows all sample have semiconducting behavior and break at Curie temperature. The conduction phenomenon in polycrystalline ferrites was explained on the basis of Verwey and de Boer mechanism. The increase in DC resistivity is due to low concentration of  $Fe^{2+}$  ions, which is responsible for decrease in electronic polarization. The increase of dc resistivity with La content was mainly attributed to decreases in drift mobility with lanthanum content. This study reveals that Lanthanum substitution alters the structural and electric properties of Mg-Zn ferrites.

## V. REFERENCES

- [1]. M. Kaur, B.S. Randhawa, J. Singh, D. Utreja , Thermolysis studies on magnesium zinc bis(citrato)ferrate pentahydrate precursor for synthesis of ferrite nanoparticles, *J. Ceramics Int.*, 39 (2013) 325-328.
- [2]. V. Provenzano, & R. L. Holtz, Nanocomposites for high temperature applications. *Mat.Sci. and Eng. A*, 204(1-2) (1995)125-134.
- [3]. S. R. Hoh, "Evaluation of High Performance Core Materials", *Tele. Tech.* 2 (1953) 86.
- [4]. E.W. Lee, Soft magnetic material, *Advances in Physics*, 8 (1959) 292.
- [5]. E.E. Richards and A.C. Lynch, "Soft Magnetic Materials for Telecommunications", Pergamon Press Ltd. (1953).
- [6]. A. Sharma, K.S. Pallavi, R. Sharma, "Optical Properties of Tin Oxide Nanoparticles", *ISST Journal of Applied Physics*, 2(2)(2011) 13-14.
- [7]. R. A. Bugad, T. R. Mane, B. B. Navale, J. V. Thombare, A. R. Babar, B. R. Karche, Structural, morphological and compositional properties of La<sup>3+</sup> substituted Mg-Zn ferrite interlocked nanoparticles by co-precipitation method, *J. Mater. Sci.: Mater. Electron.* 28 (2017) 1590-1596.
- [8]. S. E. Shirsath, B. G. Toksha, K. M. Jadhav, Structural and Magnetic properties of La<sup>(3+)</sup> substituted NiFe<sub>2</sub>O<sub>4</sub>, *Mater. Chem. Phys.* 117(2009)163-168.
- [9]. A. Gadkari, T. Shinde, P. Vasambekar, Influence of rare-earth ions on structural and Magnetic properties of CdFe<sub>2</sub>O<sub>4</sub>, *Rare Metal*, 29(2) (2010)148.
- [10]. Y. K. Dasan, B. H. Guan, M. H. Zahari, L. K. Chuan, Influence of La<sup>(3+)</sup> substitution on structure, Morphology and Magnetic properties of Nanocrystalline Ni-Zn ferrite, *PLoS ONE* 12(1) (2017)75.
- [11]. M. Soka, M. Usakova, R. Dosoudil, E. Usak, J. Lokaj, Effect of lanthanum substitution on structural and magnetic properties of nickel zinc ferrites, *AIP Advances* 8 (2018) 047802.
- [12]. D. Ravinder, B. Ravikumar, A study on elastic behaviour of rare earth substituted Mn-Zn ferrites, *Mater. Lett.* 57 (2003) 4471-4473.
- [13]. A.A. Sattar, Egypt., Temperature Dependence of the Electrical Resistivity and Thermoelectric Power of Rare Earth Substituted Cu-Cd ferrite *J. Sol.*, 26(2003)113.
- [14]. A. I. Ali, M. A. Ahmed, N. Okashad, M. Hammam, J. Y. Son, Effect of the La<sup>3+</sup> ions substitution on the magnetic properties of spinal Li-Zn-ferrites at low temperature, *J. Mater. Res. Technol.* 2 (2013) 356-361.
- [15]. S. B. Patil, R. P. Patil, J. S. Ghodake, B. K. Chougule, Temperature and frequency dependent dielectric properties of Ni-Mg-Zn-Co ferrites, *J. Magn. Magn. Mater.* 350 (2014) 179-182.
- [16]. E. J. W. Verwey, F. de Boer and J.H. Van Santen, Cation Arrangement in Spinels, *J. Chem. Phys.* 16 (1948) 1091.
- [17]. K. Torkar & O. Fredriksen, The effect of grain size on saturation magnetization of barium ferrite powders, *J. Powder Metallurgy*, (2014) 105-107.
- [18]. G. L. Sun, J. B. Li, J. J. Sun, X-Z Yang, The influences of Zn<sup>2+</sup> and some rare-earth ions on the magnetic properties of nickel-zinc ferrites, *J. Magn. Magn. Mater.* 281 (2004)173.

- [19].I. H. Gul, W. Ahmed and A. Maqsood, Electrical and magnetic characterization of nanocrystalline Ni-Zn ferrite synthesis by co-precipitation route, *J. Magn. Magn. Mater.* 320 (2008) 270-275.
- [20].T. J. Shinde, A. B. Gadkari, P. N. Vasembekar, Effect of Nd<sup>3+</sup> substitution on structural electrical properties of nanocrystalline zinc ferrite, *J. Magn. Magn. Mater.* 322(2010) 2777-2781.

## Self-Focusing of Gaussian Laser Beam in Collision less Plasma with Linear Absorption

K.Y. Khandale<sup>1</sup>, P.T. Takale<sup>1</sup>, T.U. Urunkar<sup>1</sup>, S.S. Patil<sup>2</sup>, P.P. Nikam<sup>2</sup>, M.B. Mane<sup>2</sup>, V.S. Pawar<sup>2</sup>, S.D. Patil<sup>2</sup>,  
M.V. Takale<sup>1</sup>

<sup>1</sup>Department of Physics, Shivaji University, Kolhapur 416 004, Maharashtra, India

<sup>2</sup>Department of Physics, Devchand College, Arjunnagar, Kolhapur 591 237, Maharashtra, India

### ABSTRACT

In the present work, authors have studied the effect of linear absorption on the self-focusing of Gaussian laser beam propagating in the collisionless plasma. The non-linear dependence of the dielectric constant inside collisionless plasma is mainly due to the ponderomotive force. The field distribution in the medium is expressed in terms of linear absorption coefficient as well as beam-width parameter. By following Akhmanov's parabolic equation approach under Wentzel-Kramers-Brillouin (WKB) approximation and Paraxial approximations, the differential equation is set up for the beam width parameter  $f$  which is solved numerically. It is noticed that the absorption coefficient plays an important role in propagation of Gaussian laser beam in collisionless plasma. The graphical results are presented and are discussed at the end.

**Keywords:** Gaussian laser beam, Collisionless Plasma, Linear absorption, Self-focusing.

### I. INTRODUCTION

With the invention of laser nearly six decades (1960-2020) ago, a fascinating new field of research known by the name "Nonlinear Optics" is introduced to the scientific community. Nonlinear optics has its origin when researchers P.A. Franken and his co-workers in 1961 noticed that a weak optical signal at  $3472 \text{ \AA}$  could be generated in quartz crystal when the material is illuminated with a high power Ruby laser at  $6943 \text{ \AA}$  on optical second-harmonic generation in 1961 the theoretical work of J.A. Armstrong and his co-workers on optical wave mixing in 1962-3. Self-focusing is one of the phenomena in which the intense beam of laser light incident on material medium changes the optical properties in such a way that beam comes to focus within the medium. There are three major mechanisms that lead to a change in the dielectric constant of plasma in laser-plasma interaction, as follows: (i) the relativistic effect (ii) the collisional and (iii) the ponderomotive force<sup>4-6</sup>.

With the availability of high power laser beams, a large number of interesting nonlinear phenomena have been studied, both theoretically and experimentally. The redistribution of carriers is caused by the ponderomotive force and is mainly important in collisionless plasmas. When an intense laser beam propagates

through collisionless plasma, the drift velocity of electrons is relativistic so that their mass is intensity dependant but for long pulse experiments, the relativistic effects can be ignored and ponderomotive force of the beam nonlinearity perturbs electron density resulting in the excitation of electron plasma wave<sup>7,8</sup>. Light absorption has played an important role in studies on the self-focusing of laser beams in different situations. The contribution of light absorption has been ignored in the most of investigations on self-focusing of laser beams in plasmas<sup>9–14</sup>. Furthermore, Navare et al.<sup>15</sup>, M. A. Wani et al.<sup>16</sup>, L. Ouahid et al.<sup>17</sup>, R. Kashyap et al.<sup>18</sup>, T. U. Urunkar et al.<sup>19</sup>, K. M. Gavade et al.<sup>20</sup>, B. D. Vhanmore et al.<sup>21</sup> and S. D. Patil et al.<sup>22–25</sup> have investigated the effect of linear absorption on the self-focusing of a Gaussian, Chirped Gaussian, Airy-Gaussian, q-Gaussian, Gaussian, Cosh-Gaussian, elegant Hermite-cosh-Gaussian, Cosh-Gaussian, Gaussian laser beam respectively by considering the different nonlinearities in different situations. The aim of the present investigation is to study the effect of linear absorption on the self-focusing of Gaussian laser beam propagating in the collisionless plasma. The present analysis is carried through parabolic equation approach under WKB and paraxial approximations.

## II. THEORETICAL FRAMEWORK

Consider the propagation of Gaussian laser beam in homogeneous collisionless plasma along the z-direction, initial intensity distribution of Gaussian laser beam at  $z = 0$  can be expressed as

$$\bar{E}\bar{E}^* = E_0^2 \exp\left(-\frac{r^2}{r_0^2}\right), \quad (1)$$

where  $E_0$  is the amplitude of Gaussian intensity distribution,  $r$  is the radial coordinate of cylindrical coordinate system,  $r_0$  is the initial beam width of the laser beam. The wave equation governing the electric field  $\bar{E}$  of the laser beam in homogeneous plasma along with the effective dielectric constant  $\varepsilon$ , in the cylindrical co-ordinate system is given by,

$$\frac{\partial^2 \bar{E}}{\partial z^2} + \frac{\partial^2 \bar{E}}{\partial r^2} + \frac{1}{r} \frac{\partial \bar{E}}{\partial r} + \frac{\omega^2}{c^2} \varepsilon \bar{E} = 0 \quad (2)$$

When a laser beam propagates through homogeneous gaseous plasma, the effective dielectric constant changes significantly and can be, in general represented as<sup>5</sup>

$$\varepsilon = \varepsilon_0 + \phi(EE^*) - i\varepsilon_i, \quad (3)$$

where  $\varepsilon_0 = 1 - (\omega_p / \omega)^2$  is linear part and  $\phi$  is nonlinear part of the dielectric constant,  $\omega_p$  is the plasma frequency  $\omega_p^2 = (4\pi n_e e^2 / m_0)$ , here  $e$ ,  $m_0$  and  $n_e$  are the charge of electron, rest mass of electron and density of plasma electrons in the absence of laser beam respectively and  $\varepsilon_i$  takes care of absorption. The second term in the equation (3) is the nonlinear dielectric constant for collisionless plasma can be represented as<sup>5</sup>

$$\phi(EE^*) = \frac{\omega_p^2}{\omega^2} \left[ 1 - \exp\left(-\frac{3m\alpha EE^*}{4M}\right) \right], \quad (4)$$

with

$$\alpha = \left( \frac{e^2 M}{6 k_B T_0 \omega^2 m^2} \right),$$

where  $M$ ,  $m$ ,  $k_B$  and  $T_0$  are mass of ion, mass of electron, Boltzmann constant and equilibrium plasma temperature respectively. By using WKB and paraxial approximations the coupled equations in terms of eikonal  $S$  and intensity of laser beam  $A_0^2$  can be expressed as

$$2 \frac{\partial S}{\partial z} + \left( \frac{\partial S}{\partial r} \right)^2 = \frac{\omega_p^2}{\epsilon_0 \omega^2} \left[ 1 - \exp \left( - \frac{3m \alpha E E^*}{4M} \right) \right] + \frac{1}{k^2 A_0} \nabla_{\perp}^2 A_0 \quad (5)$$

And

$$\frac{\partial A_0^2}{\partial z} + \frac{\partial S}{\partial r} \frac{\partial A_0^2}{\partial r} + \left( \frac{\partial^2 S}{\partial r^2} + \frac{1}{r} \frac{\partial S}{\partial r} - k \frac{\epsilon_i}{\epsilon_0} \right) A_0^2 = 0. \quad (6)$$

The solution for equations (5) and (6) which satisfies the initial conditions for a Gaussian beam's intensity distribution is as follows:

$$S = \frac{r^2}{2f} \frac{\partial f}{\partial z} + \phi(z), \quad (7)$$

And

$$A_0^2 = \frac{E_0^2}{f^2} \exp \left( - \frac{r^2}{r_0^2 f^2} - 2k_i z \right), \quad (8)$$

where  $\phi$  is the axial phase and  $k_i$  is the absorption coefficient. By following the approach given by Akhmanov et al.<sup>4</sup> and its simple extension by Sodha et al.<sup>5</sup> the dimensionless beamwidth parameter  $f$  is obtained as,

$$\frac{d^2 f}{d\xi^2} = \frac{1}{f^3} - \frac{3m p \rho_0 e^{-\frac{3m p e^{-2k_i' \xi}}{4M f}} - 4k_i' \xi}{4M f^3} \quad (9)$$

where  $\xi = z/R_d$  known as dimensionless distance of propagation,  $p = \alpha E_0^2$  is the initial intensity parameter,  $R_d = k r_0^2$  is known as Rayleigh diffraction length,  $\rho_0 = (\omega_p r_0)/c$  is the normalized equilibrium beam radius and  $k_i' = k_i R_d$  is the normalized absorption coefficient. The equation (9) can be solved numerically with appropriate boundary conditions such as  $f = 1$ ,  $\xi = 0$  and  $\partial f / \partial z = 0$ . By using critical condition in equation (9) one may obtain equilibrium beam radius as follows. Here  $p$  is known as critical beam power.

$$\rho_0 = \sqrt{\frac{4M}{3m p e^{-\frac{3m p e^{-2k_i' \xi}}{4M}} - 4k_i' \xi}} \quad (10)$$

### III. RESULT AND DISCUSSION

Equation (9) is a nonlinear, ordinary second order differential equation which shows the variation of dimensionless beam-width parameter  $f$  with respect to normalized propagation distance  $\xi$  into the collisionless plasma. First term on the right hand side of the equation (9) is the diffraction divergence which is responsible for defocusing and second term is the convergence arising from the collisionless nonlinearity and also depends on normalized absorption coefficient  $k_i'$  which is responsible for self-focusing of the beam. The equation (9) is a second order nonlinear ordinary differential equation and is solved numerically by choosing following laser-plasma parameters:  $\omega_p = 1.7760 \times 10^{15}$  rad/s,  $r_0 = 20 \times 10^{-4}$  cm,  $c = 3 \times 10^{10}$  cm/s,  $n_0 = 10^{18}$  cm<sup>-3</sup>,  $\rho_0 = 65$ ,  $p = \alpha E_0^2 = 10$ , to study the effect of linear absorption on the self-focusing of the beam in collisionless plasma.

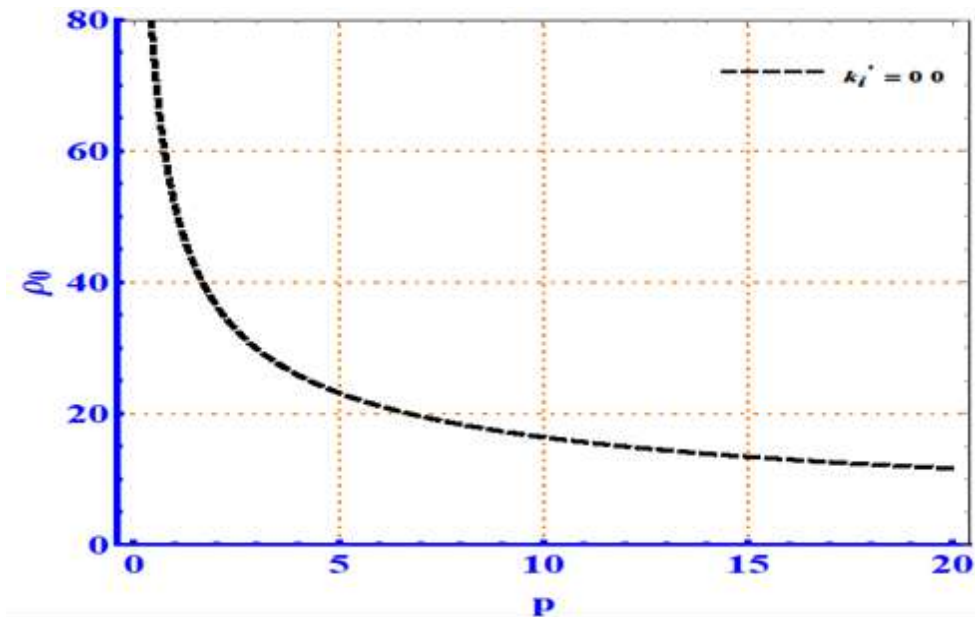


Figure 1: Dependence of normalized equilibrium beam radius  $\rho_0$  as a function of initial intensity parameter  $p$ .  $\omega_p = 1.7760 \times 10^{15}$  rad/s,  $r_0 = 20 \times 10^{-4}$  cm,  $n_0 = 10^{18}$  cm $^{-3}$ ,  $\rho_0 = 65$ ,  $p = \alpha E_0^2 = 10$ .

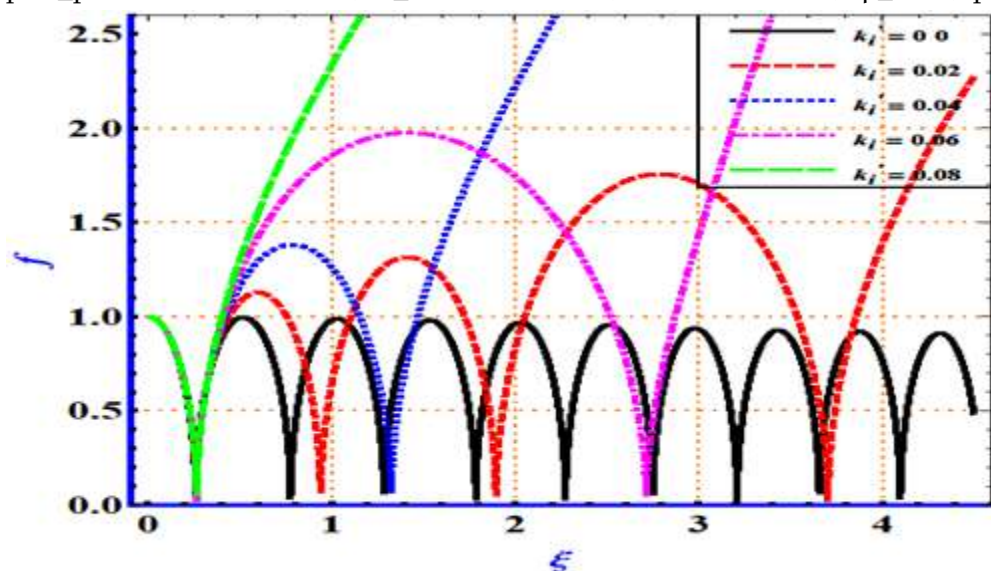


Figure 2: Variation of beam-width parameter  $f$  as a function of normalized propagation distance  $\xi$  for different linear absorption coefficients in collisionless plasma ( $k_l' = 0.00, 0.02, 0.04, 0.06, 0.08$ ).

Figure 1 shows critical curve which is plotted from Equation (10). In figure 1 three distinct regions are observed. The region above the critical curve (supercritical region) corresponds to self-focusing region while the region below the critical curve (subcritical region) corresponds to defocusing region and for any point on the critical curve the self-trapping of the laser beam is observed. Figure 2 shows the variation of beam-width parameter  $f$  as a function of normalized propagation distance  $\xi$  for different absorption coefficients in collisionless plasma ( $k_l' = 0.00, 0.02, 0.04, 0.06$  and  $0.08$ ). In figure 2 for  $k_l' = 0.00$ , i.e. in the absence of linear

absorption, the oscillatory self-focusing of the laser beam in collisionless plasma is observed. By taking into consideration the absorption, the self-focusing of the laser beam gets destroyed. As a result, the linear absorption defeats the effect of self-focusing, and the beam subsequently becomes too weak to control diffraction, resulting in quick divergence due to high energy attenuation. The longer propagation of laser beam in plasmas decreases due to absorption. In presence of absorption alone the energy of the beam decreases as  $\propto \exp[-\alpha_0(-2k_iz)]$ , which is equivalent to a weakening of the nonlinearity effect.

#### IV. CONCLUSION

We have studied the effect of linear absorption on the self-focusing of Gaussian laser beam propagating through collisionless plasma by using parabolic equation approach under WKB and paraxial approximations. The following important conclusions are drawn from the present analysis:

- In the propagation dynamics of the laser beam in collisionless plasma, the controlling factors such as linear absorption coefficient, equilibrium beam radius, and initial intensity parameter play a vital role.
- With an increase in linear absorption in collisionless plasma, the self-focusing effect weakens.

The present results are of importance in various laser-plasma applications, where propagation of laser beam with confined energy over several Rayleigh lengths is required.

Acknowledgement: Authors are thankful to DST-PURSE Phase-II (2018-2023) and UGC DSA -Phase II (2018-2023) Programme for providing research facilities at Dept. of Physics, Shivaji University, Kolhapur, M.S., India.

#### V. REFERENCES

- [1]. Prof. Franken, P. A., Hill, A. E., Peters, C. W. and Weinreich, G. Phys. Rev. Lett. 7, 118–119 (1961).
- [2]. Armstrong, J. A., Bloembergen, N., Ducuing, J. and Pershan, P. S., Phys. Rev. 127, 1918–1939 (1962).
- [3]. Sodha, M. S., Ghatak, A. K. and Tripathi, V. K., Tata McGraw-Hill, New Delhi, (1974).
- [4]. Akhmanov, S. A., Sukhorukov, A. P. and Khokhlov, R. V. , Sov. Phys. Uspekhi 10, 609–636 (1968).
- [5]. Sodha, M. S., Ghatak, A. K. and Tripathi, V. K. , Prog. Opt. 13, 169–265 (1976).
- [6]. Nayyar, V. P. and Soni, V. S., J. Phys. D. Appl. Phys. 12, 239–247 (1979).
- [7]. Takale. M.V, Navare. S.T, Patil. S.D, Fulari. V.J. & Dongare. M.B, Opt. Commun. 282, 3157–3162 (2009).
- [8]. Valkunde. A.T., Vhanmore. B.D., Urunkar. T.U., Gavade. K.M., Patil. S.D. and Takale. M.V., AIP Conf. Proc. 1953, 140088, (2018).
- [9]. Sodha. M. S. and Sharma, A., Phys. Plasmas 13, 053105 (2006).
- [10].Patil. S.D, Takale. M.V, Fulari. V. J., Gupta. D. N. and Suk. H., Appl. Phys. B Lasers Opt. 111, 1–6 (2013).
- [11].Patil, S.D., Takale, M.V., Navare, S. T., Dongare, M. B. and Fulari, V. J., Optik 124, 180–183 (2013).
- [12].Patil, S.D. and Takale, M.V. , Phys. Plasmas 20, 072703 (2013).
- [13].Patil, S.D. and Takale, M.V., Phys. Plasmas 20, 083101 (2013).
- [14].Aggarwal, M., Kumar, H. and Kant, N., Optik 127, 2212–2216 (2016).

- [15].Navare. S.T, Takale. M.V, Patil. S.D, Fulari. V.J. & Dongare. M.B, Opt. Lasers Eng.50,1316–1320 (2012).
- [16].Wani. M.A. and Kant. N., Commun. Theor. Phys. 66, 349–354 (2016).
- [17].Ouahid. L., Dalil-Essakali, L. and Belafhal, A., Opt. Quantum Electron. 50, (2018).
- [18].Kashyap. R, Aggarwal. M, Gill. T.S, Arora. N.S, Kumar. H. and Deepshikha. M., Optik 182, 1030–1038 (2019).
- [19].Urunkar. T.U., Gavade. K.M., Vhanmore, B.D., Valkunde. A.T., Patil. S.D. and Takale. M.V., AIP Conf. Proc. 2142, (2019).
- [20].Gavade. K.M., Vhanmore. B.D., Valkunde. A.T., Urunkar. T.U., Patil. S.D. and Takale. M.V., AIP Conf. Proc. 2142, 110016 (2019).
- [21].Vhanmore. B.D., Takale. M.V. and Patil. S.D., Phys. Plasmas 27, 063104, (2020).
- [22].Patil. S.D., Navare. S.T., Takale. M.V. and Dongare. M.B., Opt. Lasers Eng. 47, 604–606 (2009).
- [23].Patil. S.D., Takale. M.V. and Gill, T.S., Eur. Phys. J. D 69: 163, (2015).
- [24].Patil. S.D. and Takale. M.V., AIP Conf. Proc. 1728, 020129 (2016).
- [25].Patil. S.D., Valkunde. A.T., Vhanmore. B.D., Urunkar. T.U., Gavade. K.M., Takale. M.V., AIP Conf. Proc. 1953, 140046 (2018).

## Simulations Commercial BJT with Temperature for Space and Radiation Rich Environment Applications

C M Dinesh<sup>1\*</sup>, K S Krishna Kumar<sup>2</sup>, M Sathish<sup>3</sup>, R. Chandrashekar<sup>1</sup>, Shivaprakash Y<sup>4</sup>

<sup>1</sup>Department of Physics, Govt. First Grade College and PG centre, Chintamani-563125, Karnataka, India

<sup>2</sup>Department of Physics, Raja Rajeshwari College of Engineering, Bengaluru-560074, Karnataka, India

<sup>3</sup>Department of Physics, Govt. First Grade College, Doddaballapur – 561203, Karnataka, India

<sup>4</sup>Department of Physics, Govt. First Grade College, Devanahalli – 562110, Karnataka, India

### ABSTRACT

The temperature variations on electronic circuits employed to onboard plays a significant impact. In this investigation silicon NPN BJT response to irradiation has been studied at room temperature and temperature variation. A temperature variation dependent analytical model for total ionising dose induced excess base current in BJT's is tested. In this model base current dependent on temperature in irradiation parts have been captured. During irradiation all the three terminals of the devices are grounded. After irradiation, the base current is captured and the concentrations of oxide defects like oxide trapped charges and interface traps created during irradiations are calculated using simulated monte-carlo programming. The base current and defect density resulting from room temperature irradiations are used as inputs to simulations and analytical model experimental data obtained from measurements at room temperature and high temperature on irradiation parts are compared with the simulated results. This work shows that the simulations can support qualifications of the chosen devices for space applications and are functional at various temperatures.

**Keywords:** Bipolar Transistor, NPN, Temperature, Total ionizing dose, Base current.

### I. INTRODUCTION

Bipolar circuits used for comparators and regulators used for large percentage of a space system's are important to understand as a part invention. The operation of the components used for these circuits can be significantly degraded by Total Ionizing Dose (TID) [1]. It has been observed that Low Dose Rate (LDR) Irradiation causes more degradation than High Dose Rate (HDR) Irradiation, for the same TID [2]. Space is a Low Radiation Dose Rate (LDR) environment. Since LDR exposures required long test time, part qualification at this rate can introduce prohibitively high costs to mission assurance. Due to this, the identification of numeral models, accelerated techniques, and test method to assist in the characterization of LDR sensitivity in linear bipolar circuits [3] has been proposed. BJT's and Bipolar circuits show degradation mainly due to emitter – base interface traps ( $N_{IT}$ ) and passivation layer oxide trapped charge ( $N_{OT}$ ) defect build up in oxides.

These build up defects in BJTs can increase recombination at the bipolar base surface can lead to an increasing in the base current ( $I_B$ )[3].

In this paper we describe the temperature dependence of BJTs current voltage characteristics after the irradiation with 108 MeV  $Si^{8+}$  ions. We also calculate the defects produced in the irradiation region using Monte-Carlo code (SRIM- Stopping and range of ions in matter). These results has been correlated to electrical degradation.

## II. EXPERIMENTAL METHODS

### BJTs Device and Oxide Defects

The transistors considered for this study are of vertical NPN BJTs the experimental devices were fabricated in BEL (Bharath Electronics Limited, India). Radiation-induced degradation due to defects that build up in base bipolar oxides alter surface recombination, which results in the increase of base current in NPN BJTs. These defects are net positive oxide trapped charge ( $N_{DIT}$ ) and interface trap ( $N_{IT}$ ). The data obtained from (SRIM) and data from the transistors were used to extract Non Ionising Energy Loss (NIEL) calculations as a function of TID.

### SRIM Data

**Table 1** SRIM simulated results for 110 MeV Si ion irradiation on silicon target.

Parameter	Value			
R ( $\mu\text{m}$ )	39.62			
$S_e$ (MeV $\text{cm}^2/\text{mg}$ )	10.21			
$S_n$ (MeV $\text{cm}^2/\text{mg}$ )	$7.698 \times 10^{-03}$			
NIEL up to R (MeV $\text{cm}^2/\text{g}$ )	42.67			
Fluence (ions/ $\text{cm}^2$ )	$5 \times 10^9$	$1 \times 10^{11}$	$1 \times 10^{12}$	$1 \times 10^{13}$
TID (rad)	0.8174	16.348	163.482	1634.82
$D_a$ (rad)	3143.4	68268	$6.8268 \times 10^5$	$6.8268 \times 10^6$

Table 1 depicts that the nuclear energy loss of 110 MeV  $Si^{8+}$  ion is much smaller than the electronic energy loss (3 orders of magnitude, Table. 1) in a Si-target material due to smaller elastic scattering cross-section. Therefore the maximum energy deposited to the material is expected mainly due to the electronic energy loss during its passage through the Si-material [5]. The device suffers non-uniform irradiation effects as the projected ion range (39.46  $\mu\text{m}$ ) is lower than the device thickness ( $\sim 600 \mu\text{m}$ ) and it is expected to implant at base-collector region. The damage caused due to the linear energy transfer [ $LET = S_e + S_n \sim 10.2177 \text{ MeV}/(\text{mg}/\text{cm}^2)$ ] in the Si target is obtained using TRIM calculations. LET dependent TID and NIEL dependent  $D_a$  are tabulated in table 1.

### Pre-and post-irradiation test results

Radiation testing was performed at Inter University accelerating Centre (IUAC) New Delhi, India. Three devices were irradiated at room temperature (RT) LDR irradiation was performed 1PNA (particle nano

ampere current) to get desired irradiation fluence. The energy of irradiating ion as choosing so that it could penetrate into emitter base junction.

The fluence has been calculated by counting the charge collected at the Faraday cup placed at the target. The another advantage of selecting low irradiation current is that BJTs are not damage due to the loss of irradiated ion energy (110 MeV Si<sup>8+</sup> heavy ion) in the BJTs, (Heating effect will not be produced/the heat produced during the irradiation get transferred to the target).

Figure.1 show the base current  $I_B$  responses exposed at 110 MeV Si<sup>8+</sup> ions for NPN BJTs. The data in these plots were collected at room temperature, 50 and 100 °C. The increase in base current with radiation can be fit approximately to

$$\Delta I_B = I_{SE} \exp\left(\frac{q|V_{BE}|}{n_E kT}\right), \quad (1)$$

Where  $I_{SE}$  is the radiation-induced change in low-injection base leakage current,  $n_E$  is the change in the low injection ideality factor,  $k$  is Boltzmann's constant,  $T$  is the junction temperature, and  $q$  is the magnitude of electronic charge. Plots of  $I_B$  and  $V_{BE}$  at constant  $V_{CE}=4V$ .

### Temperature data on BJT devices

Figure 1 – 3 shows the temperature dependent base current as a function of base – emitter voltage measured for un-irradiated and irradiated NPN BJTs to characterize the impact of thermal variation prior to and after ionizing radiation dose. The temperature testing was performed approximately 300 months after the radiation tests. No significant change was observed in the electrical response at room temperature between the end of the radiation testing and temperature testing. This showed that the defects produced during irradiations are permanent. Pre- and post unirradiated and irradiated devices were placed in a thermal chamber (hot air oven) with an internal thermocouple to automatically monitor the temperature near the devices during the tests. Temperature response testing was performed from 27 °C up to a maximum temperature of 100 °C in order to avoid annealing effects. Temperatures above 100 °C may lead to the annealing of some oxide defects (both interface and oxide traps) and a reduction in the excess base current measured for BJT [4]. Electrical measurements are performed a few minutes after the temperature is fixed in order to ensure thermal equilibrium during measurement. Each devices has been tested for electrical measurements before and after irradiation in order to test the effect of irradiation, it has been observed all devices show approximately same I-V characteristics before and after irradiation. Hence one devices were tested for each condition, electrical characterization at room temperature were performed after each temperature step in order to ensure no significant temperature dependent annealing of the parts of NPN BJTs [5].

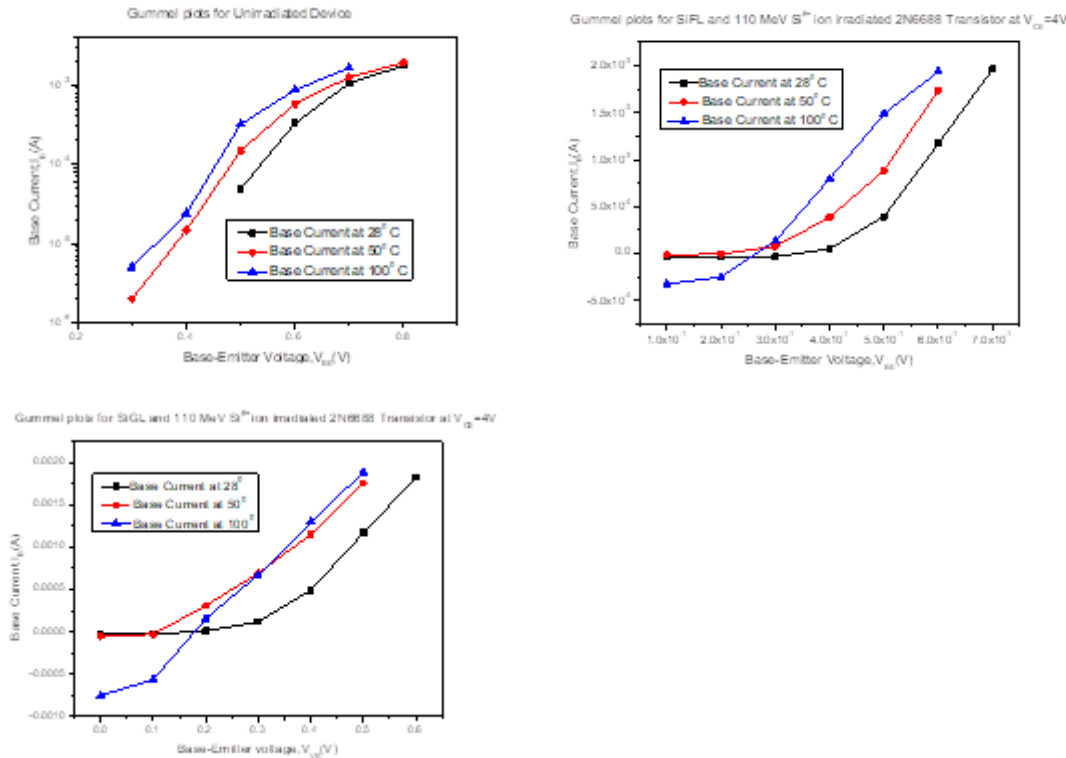


Figure. 1, 2 and 3 show the pre-irradiation,  $1 \times 10^{11}$  and  $1 \times 10^{12}$  ions/cm<sup>2</sup> LDR irradiated base currents for NPN BJTs over the specified temperature range (27°, 50°C 100°C).

It can be observed that both the pre- and post-irradiated PNP BJTs show similar trends, i.e., a monotonic increase in base current with increasing temperature. Similar trend can be observed for the pre- and post-irradiated NPN BJTs. Most of the earlier studies have indicated that the impact of displacement damage is marginal compared with the total dose effect. However, it has been shown that total – dose irradiation may indirectly affect the silicon substrate by reducing the active p-type base dopant concentration, may lead to an increase in base current as shown in figure 4.

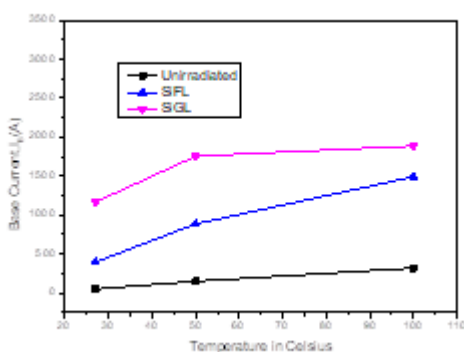


Figure. 4 show the base currents at  $|V_{BE}| = 0.5$  V as a function of temperature for un-irradiated and irradiated NPN BJTs respectively.

Table 2: Variation in base current,  $I_B$  of BJT tested for different fluence of 110 MeV  $Si^{8+}$  ions at specified temperature range (27°, 50°C 100°C)

Temperature °C	$I_B(A)$			
	Un irradiated	$5 \times 10^9$	$1 \times 10^{11}$	$1 \times 10^{12}$
27	48.66	126.666	394.66	1165.66
50	147	161	884	1755
100	317.66	3200	1488.33	1885.333

The enhanced  $I_B$  is related to an increase in the surface recombination velocity, as the density of electrons and holes is coming more comparable, due to base neutralization. From the figure we can also see that there are large increase in the base current tested at higher temperatures (50°C and 100°C) due to increased surface recombination current at the base surface. An increase in the midgap-level interface-trap density in the low-field, thick oxide over the p-type base increases the recombination current, more importantly an increase in the positive-oxide-charge density modulates the base surface potential to even more strongly increases the surfaces recombination current [6-9].

The current gain of modern bipolar transistors in an ionizing radiation environment decreases due to increased recombination in the emitter-base depletion region [7-8,10-11]. The recombination centers are related to the net charge introduced into the oxide by ionizing radiation, since it is positive the depletion region spreads on the p-side of a PN junction. For NPN transistors, this means that the depletion region separates into relatively lightly doped P-type base region. As the depletion region increases in size, recombination current increases at the oxide interface over the base and in the newly-depleted silicon bulk. In BJTs the excess base current depends on the number of interface states (recombination centers) near midgap and threshold. The excess base current due to changes in surface potential depends on the total radiation induced oxide charge at the bias condition these variations in excess base current is as shown in table 2.

### III. CONCLUSIONS

This work reports the effect of 110MeV  $Si^{8+}$  ion irradiation on silicon NPN transistors devices with fluences of  $5 \times 10^9$  ions  $cm^{-2}$  to  $1 \times 10^{13}$  ions  $cm^{-2}$ . An effort is made successfully to correlate the electrical degradation with the non-ionizing energy deposition due to MeV ion irradiation using TRIM Monte Carlo Code. Fluence dependent TID and  $D_{ais}$  calculated for 100 MeV silicon ion in silicon target. The shift in collector saturation current and collector emitter voltage is mainly due to the total displacement dose. In addition to these shifts, Si-ion irradiation causes increase in forward resistance of the collector emitter region.

The current gain of the transistors decreases with increases in silicon ion fluences. It has in addition been observed that the base current increases with increase in TID and test temperature. The excess base current due to changes in surface potential depends on the total radiation induced oxide charge at the bias condition. This is again related to the reduction of the base doping concentration after exposure. In BJTs the excess base

current depends on number of interface traps (recombination centres) near the midgap. At higher total doses, sufficient charge as the accumulated in the oxide to cause significant recombination to occur through-out the lightly doped based region. The swift heavy ion irradiation on silicon will result in increase in lattice temperature. Hence in the present device case the transistor performance is severely affected due to silicon ion irradiation. The switching time of the transistor may decrease due to an increased base currents as a function of silicon ion fluence.

#### IV. REFERENCES

- [1]. H.J. Barnaby, R.D. Schrimpf, R.L. Pease, P Cole, T.Turflinger, J.Krieg, J.T.Titus, D. Emily, M. Gehlhausen, S.C. Witczak, M.C. Maher, D.Van Nort, Identification of degradation mechanisms in a bipolar linear voltage comparator through correalation of transistor circuit response, IEEE Trans, Nucl. Sci. 46(6)(Dec.1999) 1666-1673.
- [2]. A.H. Johnston, B.G. Rax, C.I. Lee, Enhanced damage in linear bipolar integrated circuits at low dose rate, IEEE Trans. Nucl.Sci. 42(6)(Dec 1995)1650-1659.
- [3]. P.C. Adell, R.L. Pease, H.J. Barnby, B.Rax, X.J. Chen, S.McClure, Irradiation with molecular hydrogen as an accelerator total dose hardness occurrence test method for bipolar linear circuits, IEEE Trans. Nucl. Sci. 56(6)(Dec.2009) 3326-3333.
- [4]. X.Li,W.Lu, Q.Guo, D.M. Fleetwood, C.He, X.Wang, X.Yu, J.Sun, M.Liu, S.Yao, Temperature-switching during irradiation as a test for ELDRS in linear bipolar devices, IEEE trans. Nucl. Sci.66(1)(Jan. 2019)199-206.
- [5]. H.J. Barnaby, B.Vermeire, M.J. Campola, Improved model for increased surface recombination current in irradiated bipolar junction transistors, IEEE Trans Nucl. Sci.62(4)(Aug.2015) 1658-1664.
- [6]. B.S. Tolleson, P.G. Adell, B.Rax, H.J. Barnaby, A.Privat, X.Han, A.Mahmud, I.Livingston, Improved model for excess base current in irradiated lateral PNP bipolar junction transistors, IEEE Trans. Nucl.sci, Aug,2018.
- [7]. C. M. Dinesh, Ramani, M. C. Radhakrishna et al., Nucl. Instr. and Meth. in Phys. Res. B 266, (2008) 1713.
- [8]. K.S. Krishnakumar, C.M. Dinesh, KV Madhu, et al., Carbon ion irradiation damage effects on electrical characteristics of silicon PNP power BJTs, IEEE Trans. On Device and Mat. Relia. 15 (1), (2015), 101-108.
- [9]. R. Nathan Nowlin, D. M. Fleetwood, and R. D. Schrimpf, IEEE Trans. Nucl. Sci. 41, (6), (1994) 2637.
- [10].R. L. Pease, R. M. Turfler, D. Platteter, D. Emily, and R. Blice, IEEE Trans. Nucl. Sci. NS-30, (1983) 4216.
- [11].A. R. Hart, J. B. Smyth Jr. V. A. J van Lint, D. P. Snowden, and R. E. Leadon, IEEE Trans. Nucl. Sci. NS-25, (1978) 1502.
- [12].J. Boch, F. Faigne, T. Maurel, F. Giustino, L. Dusseau, R.D. Schrimpf, K.F. Galloway, J. P. David, R. Ecoffet, J. Fesquet et.al. IEEE Trans. Nucl. Sci. 49, (3), (2002) 1474.

## Green Synthesis and Characterization of CdS Quantum Dots Mediated by Aegle Marmelos Leaves

M.D. Dhiware<sup>1</sup>, T.R. Deore<sup>2</sup>, S.B. Nahire<sup>3</sup>, A.B. Gawande<sup>2\*</sup>

<sup>1</sup>Department of Physics, KVNN Arts, Commerce and Science College, Nashik, Maharashtra, India

<sup>2</sup>Department of Physics, K.S.K.W. Arts, Science and Commerce College, CIDCO, Nashik, Maharashtra, India

<sup>3</sup>Department of Physics, National Senior College, Nashik, Maharashtra, India

### ABSTRACT

Herein, we report the green synthesis of CdS quantum dots (QDs) by Aegle Marmelos leaves extract. Green synthesis method is novel, simple, eco-friendly, nontoxic compared to conventional physical and chemical methods. Aegle Marmelos used as a capping and reducing agent owing to their extraordinary medical applications. The synthesized CdS QDs characterized by various characterization techniques Such as X-Ray Diffraction (XRD) showing cubic structure with average particle size about 4 nm determined by using Debye Scherrer formula. Field emission scanning electron microscope (FE-SEM) reveals a spherical shape of CdS QDs.

### I. INTRODUCTION

In past two decades green synthesis method is drawing more attention owing to its facile, nontoxic, eco-friendly and low temperature characteristics compared other methods. Green synthesis approach uses bioactive agents such as plant materials, microorganism and various biogases etc. The various nanomaterials are synthesized by green method such as CdS, CeO<sub>2</sub>, Ag, ZnS, SnO<sub>2</sub> etc.[1-5]. There are different methods are used for synthesis of CdS QDs by like chemical deposition [6], Hydrothermal [7], Sol-Gel [8], etc. In this method uses the collides with harmful chemicals. These can be avoiding if we used green synthesis plant extract approach.

Cadmium sulfide (CdS) is a direct band gap semiconductor with energy band gap  $E_g = 2.42$  eV. The colour tunability of semiconductor QDs as a function of size is one of their most attractive characteristics. CdS is a promising material because of their applications in optoelectronics, photocatalysts, x-ray detectors, nonlinear optical material and as a window material for hetro-junction solar cells [9].

*Aegle Marmelos* leaves contains broadly alkoids, prphynols, terepnoids and other polyphenols, which are well recognized for their healing power toward variety of bacterial and fungal infections [10]. In the present research work we report green synthesis of CdS QDs mediated by *Aegle Marmelos*.

## II. MATERIALS AND METHODS

Cadmium Chloride ( $\text{CdCl}_2 \cdot \text{H}_2\text{O}$ ), Sodium sulphide ( $\text{Na}_2\text{S} \cdot \text{H}_2\text{O}$ ) and Ethanol are easily available commercial materials. *Aegle Marmelos* leaves were gathered from local trees. Distilled water used as solvent in the method.

### 2.1 Synthesis of CdS QDs:

CdS QDs synthesized greens approach, typical synthesis in 5 ml extract of *Aegle Marmelos* leaves added 90 ml of distilled water in the proceeding step 0.2 gm of  $\text{CdCl}_2$  was added and placed on hot plate with magnetic stirring at temperature  $100^\circ\text{C}$  for 2 hrs. After that 0.078 gm of  $\text{Na}_2\text{S}$  was added in the mixture and again kept for constant magnetic stirring for 2 hrs. Then final yellow colour product was filtered, centrifuged and finally dried at room temperature 12 Hrs. The final yellow powder was used for further characterisation.

## III. RESULT AND DISCUSSION

### X-ray Diffraction (XRD):

XRD pattern as shown in the figure 1. X-ray diffraction used to study crystal structure, nanoparticle size, interplanar spacing. The XRD peaks was found to be very broad which indicates formation of very small size QDs. The diffraction peaks assigns at  $2\theta = 26.9^\circ$ ,  $46.78^\circ$  and  $53.5^\circ$  which corresponds to the miller indices for the crystal plane of (111), (220) and (311) with cubic crystalline structures of synthesized CdS QDs, respectively, (JCPDS Card no.00-010-0454). XRD of prepared sample materials was found to be in good agreement with (JCPDS file no.00-010-0454). The average particle size was found to be 4 nm which was determined by using the Debye Scherrer formula i. e. nanoparticle size ( $D$ ) =  $(k \lambda) / (d \cos \theta)$  Where,  $D$  is the particle in nm,  $K$  is crystallite shape factor a good approximation is 0.9 for spherical shape nanoparticles,  $\lambda$  is the X-ray wavelength used for X-ray diffraction,  $d$  is the full width at half the maximum (FWHM) in radians of the X-ray diffraction peak and  $\theta$  is the Bragg's angle (deg.). [11]

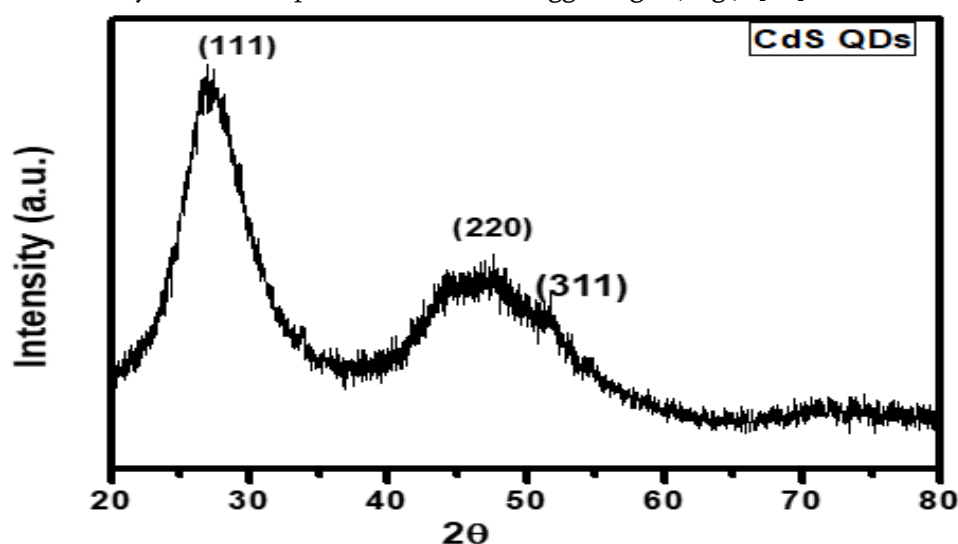


Figure 1: XRD pattern of CdS QDs

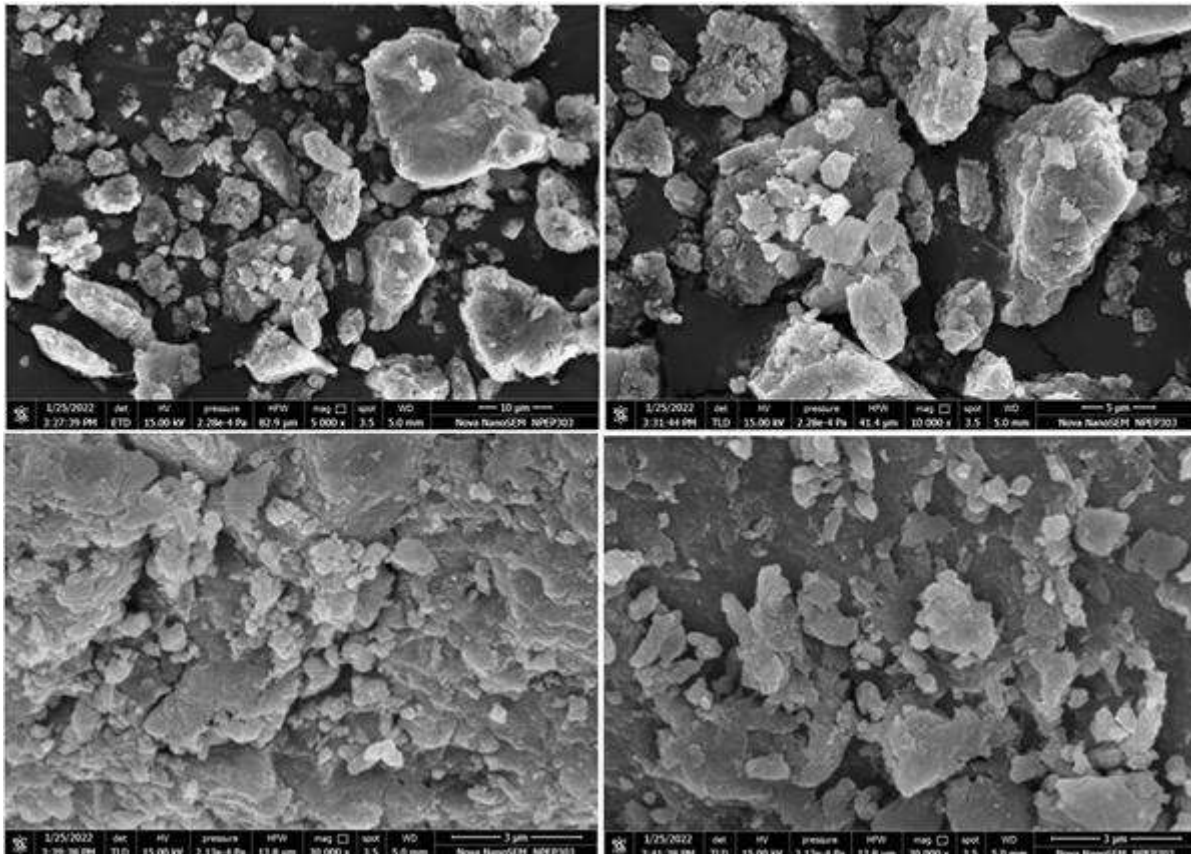
**Field Emission Scanning Electron Microscope (FESEM) study:**

Figure 2: FESEM images of CdS QDs

The synthesized product of CdS QDs characterized by using FESEM technique which is used for the study of surface morphology. CdS QDs shows particles are nearly spherical in shape morphology with slightly agglomeration as shown in the figure 2.

#### IV. CONCLUSION

In summary, plant mediated synthesis of nanoparticles have several advantages over physical and chemical methods..CdS QDs synthesized by green synthesis method with leaves extract of *Aegle Marmelos*. The leaves extract bioactive components play vital role for formation of CdS QDs Moreover, the prepared CdS QDs average nanoparticle size was found to be 4 nm determined by using XRD technique. Field emission scanning electron microscope (FE-SEM) reveals a spherical shape of CdS QDs with agglomerate morphology and. Synthesized CdS QDs can be explored for various biomedical applications such as antibacterial, antibiofilm, antifungal, antiviral, anticarcinogenic and anticandidal activities.

## V. ACKNOWLEDGEMENTS

Authors thanks to Principle, KSKW Arts, Science and Commerce College, Nashik for providing instrumental facilities to carry out this research work and Authors also wants to thanks to Vice Principle Dr. Latesh Nikam from Baburanji Gholap College, Sangvi, Pune for providing characterization facility.

## VI. REFERENCES

- [1]. Prof. Biogenic synthesis of photocatalytic activity of CdS NPs, A. Bhadwal, et al. , RSC. adv, 2014,4,9484.
- [2]. Green synthesis of CeO<sub>2</sub> NPs from the abelmoschus esculentus Extract of antioxidant, Anticancer ,Antibacterial and wound- Healing Activities. H. E. Ahemad, et al. Molecules 2021,26,4659.
- [3]. Green synthesis of silver NPs using white sugar, S. Mesharam , et al. IET Nanobiotechnology (2013), 7,1, 28-32.
- [4]. Green synthesis of ZnO Using S.Frutesences Plant extract for photocatalytic degradation of dye and antibiotics S. Munjai, et al. Mate Res Express, 9, (2022), 015001.
- [5]. Green synthesis of SnO<sub>2</sub> NPs using delonaelataleaf: Evaluation of its structural, optical, morphological and photocatalytic properties. K.C.Suresh et al, SN applied science (2020)2:1735.
- [6]. Photoaucstic study of CdS QDs for application in QDs sensitized solar cells. S. Abdallah, et al., Journal of nanomaterials,498286,1-6, 2012
- [7]. One step of hydrothermal synthesis of thioglycolic acid capped CdS QDs as fluroscsnces determination of cobalt ion, Z. wang, et al Scientific Reports, (2018) 8:8953.
- [8]. Sol Gel synthesis, characterization and effect of CdS nanoparticles on activity of liver Enzymes, Asmaa. J Al-lamei, Journal of Advanced Sciences and Engineering Technologies, 2019, 35-42.
- [9]. W.V. Huynh, J.J. Dittmer, A.P. Alivisatos, "Hybrid nanorod-polymer solar cells", Science 295 (2002), 2425–2427.
- [10].One-step biofabrication of copper nanoparticles from Aegle marmelos correa aqueous leaf extract and evaluation of its anti-inflammatory and mosquito larvicidal efficacy, Gangadhara Angajala, Pasupala Pavan and R. Subashini, RSC Adv., 2014, 4, 51459.
- [11].Room Temperature Synthesis And Characterization Of Cadmium Sulphide (CdS) Semiconductor Quantum Dots, S.I. Khan, G.K.Kande, L.D.Sonawane, A. S. Mandawade, L.J. Jondhale, P.G.Loche, Journal of Scientific Research in Science and Technology,9,2, 2021.

## Electrodeposited Nanoleaves (NLs) like $Mn_3O_4$ thin film for electrochemical supercapacitor

P. M. Kharade<sup>1\*</sup>, J. V. Thombare<sup>2</sup>, S. S. Dhasade<sup>2</sup>, S. D. Patil<sup>3</sup>, P.B.Abhange<sup>4</sup>, D. J. Salunkhe<sup>5</sup>

<sup>1</sup>Department of Physics, Shankarrao Mohite Patil Mahavidyalaya, Akluj, Dist-Solapur (MH), India 413101

<sup>2</sup>Department of Physics, Vidnyan Mahavidyalaya, Sangola, Dist-Solapur (MH), India 413307

<sup>3</sup>Department of Physics, Pratapsinh Mohite Patil Mahavidyalaya, Karmala, Dist-Solapur (MH), India 413203

<sup>4</sup>Department of Physics, G.M. Vedak College of Science, Tala, Raigad (MH), India 402111

<sup>5</sup>Nanocomposite Research Laboratory, K.B.P. Mahavidyalaya, Pandharpur, Dist-Solapur (MH), India 413303

\*Corresponding Author E-mail:pravink150@gmail.com

### ABSTRACT

In the present study, we report here synthesis and characterization of manganese oxide ( $Mn_3O_4$ ) thin films by potentiostatic electrodeposition for supercapacitor application. The structural and surface morphological behaviour of  $Mn_3O_4$  thin film were carried out by using X-ray diffraction (XRD) and Scanning Electron Microscopy (SEM) study. The structural study of  $Mn_3O_4$  thin film shows hausmannite tetragonal crystal structure. The surface morphological study showed that the formation of nanoleaves (NLs) of  $Mn_3O_4$  thin film. The electrochemical supercapacitive performance of  $Mn_3O_4$ NLs was characterized by using cyclic voltammetry (CV), charging-discharging (CD) and electrochemical impedance spectroscopy (EIS) techniques. The  $Mn_3O_4$ NLs shows maximum specific capacitance of 460  $F.g^{-1}$  at scan rate 5  $mV.s^{-1}$  and 92% cycling stability in 0.5 M  $Na_2SO_4$  electrolyte solution. Hence, potentiostatically deposited  $Mn_3O_4$ NLs is best for energy storage application.

**Keywords:** supercapacitor, electrodeposition,  $Mn_3O_4$ , XRD, FESEM, CV.

### I. INTRODUCTION

In the 21<sup>st</sup> century more and more research focused on highly renewable and sustainable energy storage devices. Electrochemical capacitor or supercapacitor have gained more attention due to their excellent electrochemical properties such as, environmental friendly, fast charging and discharging rate, good reversibility, high power density, long cycle life and safety in operation. Due to this features electrochemical

capacitor can be used in variety of potential applications such as, memory back up devices, portable electronic devices, hybrid electric vehicles, elevator, forklifts, cranes, lasers and industry [1-4]. The Electrochemical capacitor or supercapacitor mainly categorized into two types viz, electrochemical double layer capacitor (EDLC) and Pseudocapacitor (PC). In EDLC, charge is stored electrostatically, i.e charge accumulation takes place at the electrode/electrolyte interface. Example, carbon materials. In pseudocapacitor (PCs) faradic process takes place. Example, conducting polymers and Transition metal oxides (TMOs) etc. Electrode materials used in TMOs are  $\text{RuO}_2$  [5],  $\text{MnO}_2$  [6],  $\text{Co}_3\text{O}_4$  [7],  $\text{NiO}$  [8],  $\text{IrO}_2$  [9],  $\text{Cr}_2\text{O}_3$  [10] and  $\text{CuO}$  [11] etc. Among these TMOs, Manganese oxide electrode is widely studied in supercapacitor because of better electrochemical performance, natural abundant, low cost, easy synthesis and non-toxic [12-13]. Manganese oxide also have several oxidation states such as,  $\text{MnO}$ ,  $\text{MnO}_2$ ,  $\text{Mn}_2\text{O}_3$  and  $\text{Mn}_3\text{O}_4$  etc. Among these oxides,  $\text{Mn}_3\text{O}_4$  is one of the most stable state of manganese oxide and have attracted considerable attention due to its low cost, environmental friendly, natural abundant and good electrochemical properties [14-15].

Manganese oxide have been synthesized by different physical and chemical methods such as, hydrothermal method [16], co-precipitation method [17], sol-gel method [18], chemical bath deposition method [19], self-reacting microemulsion method [20], sonochemical method [21], electrodeposition method [22], room-temperature solid reaction [23] and SILAR method [24] etc. Among all the various methods, electrodeposition method is one of the best method for synthesis of metal oxides because of low cost, binder free, single step and large scale production. It also leads direct deposition of oxide/hydroxide electrodes on low cost substrates. Nguyen et al. [22] have reported nanoflakes like morphology of  $\text{Mn}_3\text{O}_4$  thin film by cathodic electrodeposition method for supercapacitor application. Yousefi et al. [25] have reported porous nanospheres of  $\text{Mn}_3\text{O}_4$  by cathodic electrodeposition method and studied their electrochemical properties. Porous and nanostructured material is key requirement for electrochemical capacitor because it provides large surface area, shorten the diffusion path of electrons and ions, which promotes the fast insertion and extraction of electrons and ions. Which improves the specific capacitance of the electrode [26].

In the present report, efforts have been taken to study structural, morphological and electrochemical supercapacitive behaviour of potentiostatically deposited  $\text{Mn}_3\text{O}_4$  NLs for supercapacitor application.

## 2. Experimental:

### 2.2 (a) Characterization techniques

The crystal structural study of  $\text{Mn}_3\text{O}_4$  NLs was carried out with the help of XRD using Bruker axes D8 Advance Model with copper radiation ( $K_\alpha$  of  $\lambda = 1.54 \text{ \AA}$ ) within  $2\theta$  range between  $20^\circ$  to  $80^\circ$ . The surface morphology of  $\text{Mn}_3\text{O}_4$  NLs was carried out by using field emission scanning electron microscopy (FESEM) technique (Model: JSM-6160). The electrochemical supercapacitive study of  $\text{Mn}_3\text{O}_4$  NLs was studied by using CV, GCD and EIS techniques by using electrochemical workstation (CHI 660 A). The electrochemical cell includes three electrode systems.  $\text{Mn}_3\text{O}_4$  NLs was used as a working electrode, graphite was used as a counter electrode and saturated calomel electrode (SCE) was used as a reference electrode. The 0.5 M  $\text{Na}_2\text{SO}_4$  was used an electrolyte solution for overall measurements.

### 3. Result and Discussion

#### 3.1 XRD Study:

X-ray diffraction (XRD) techniques have been carried out to examine the crystal structure of the  $Mn_3O_4$  NLs. Fig.1 shows the XRD pattern of  $Mn_3O_4$  NLs in the  $2\theta$  range from  $20^\circ$  to  $80^\circ$ . The observed diffraction peaks indexed in the XRD pattern of  $Mn_3O_4$  NLs was well matched with JCPDs card no.89-4837. The XRD study shows hausmannite tetragonal crystal structure of electrodeposited  $Mn_3O_4$  NLs. The peak marked with (SS) in the XRD spectrum is due to stainless steel substrate only.

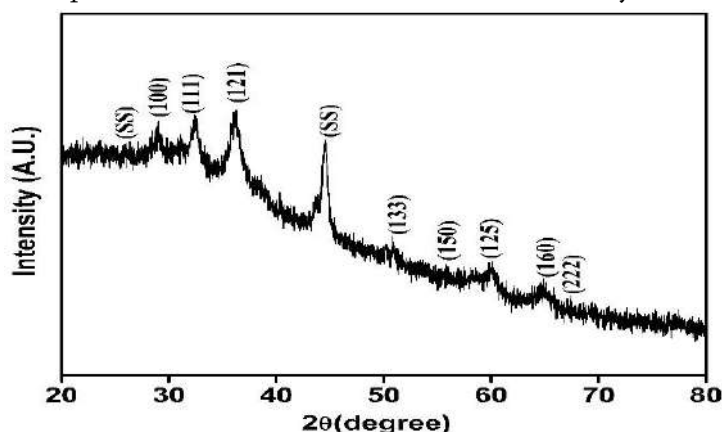


**Figure 1.** X-ray Diffraction (XRD) spectra of  $Mn_3O_4$  NLs.

The average crystallite size of  $Mn_3O_4$  NLs was calculated by using the Debye's Scherer's equation,

$$D = \frac{0.9\lambda}{\beta \cos\theta} \text{ ----- (3)}$$

Where, D is the crystallite size,  $\lambda$  is the wavelength of X-ray ( $1.54.4 \text{ \AA}$ ) and  $\beta$  is full width at half maximum (FWHM). For determination of crystallite size, the most intense peak (121) is centered at FWHM in term of radian is 0.807. The crystallite size of  $Mn_3O_4$  NLs is found to be 34 nm.

#### 3.2. Surface Morphological Studies

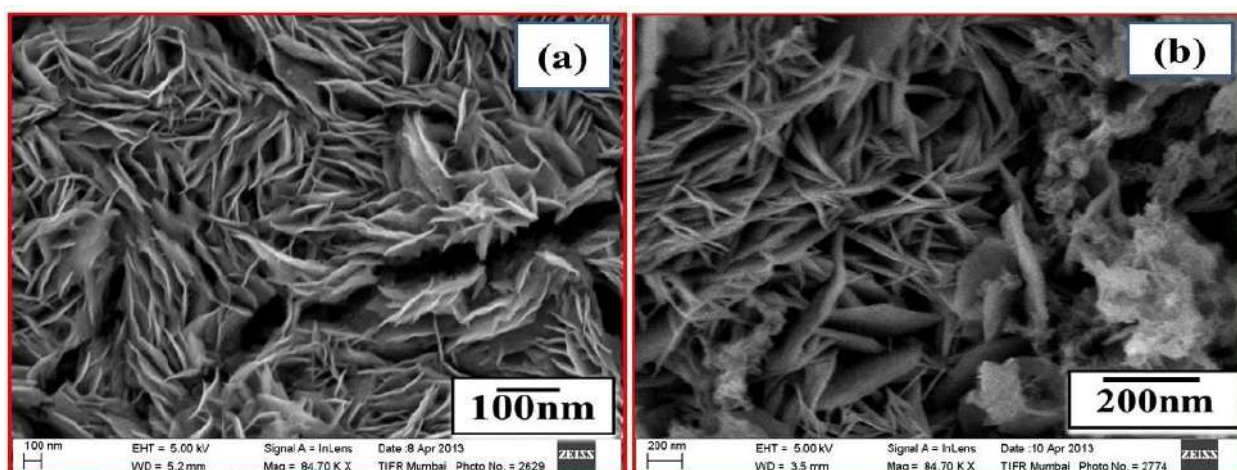


**Figure 2 :** Scanning Electron Microscope (SEM) images of  $Mn_3O_4$  thin film at (a) 100kX and (b) 200kX magnifications respectively.

Surface morphology of the  $Mn_3O_4$  NLs was studied by using FESEM technique. Fig. 2(a-b) demonstrate the FESEM micrographs of  $Mn_3O_4$  thin film with two different magnifications (100 kX and 200 kX) respectively. In Fig. 2(a) SEM micrograph of  $Mn_3O_4$  thin film at low magnifications shows the compact and nanoflakes like morphology [28]. At high magnification in Fig. 2(b), the  $Mn_3O_4$  thin film gives highly resolved, porous and interconnected Nano leaves (NLs) like structure. Such structures have a larger specific surface area, providing the active material to sufficiently react with ions in the solution, and hence reducing the electron transport distance [29]. Therefore, it enhances the electrochemical supercapacitive properties.

### 3.3 Supercapacitive studies:

#### 3.3.1 Cyclic voltammetry (CV) studies:

The specific capacity of  $Mn_3O_4$  NLs was carried out by using CV study. Fig. 3(a) display typical CV curves of  $Mn_3O_4$  NLs at different scan rates such as; 5, 10, 50 and 100 mV/s within potential limit of +1.2 V to -1.2 V vs SCE, respectively. From CV curves, it is observed that as scan rate increases current under curve increases and the cathodic and anodic peaks shifts more towards positive and negative sideward. This result shows that current is directly proportional to scan rate, i.e. scan rate dependent current-voltage indicate that ideal capacitive behaviour of  $Mn_3O_4$  NLs. Similar results reported by Dubal and More et al. prepared by  $Mn_3O_4$  thin film by chemical bath deposition and spray pyrolysis method for supercapacitor application respectively [19, 30].

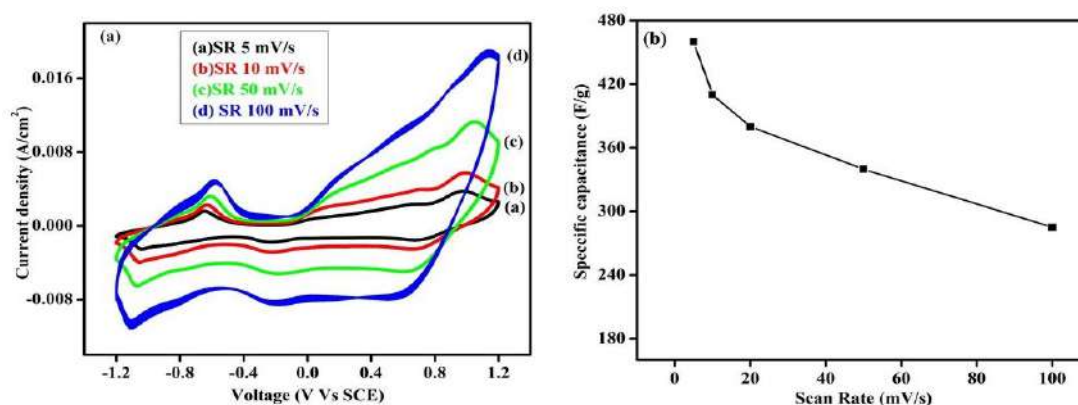


**Figure 3** (a) Cyclic Voltammetry (CV) study of  $Mn_3O_4$  NLs at scan rate of 5, 10, 50 and 100 mV/s and 4 (b) Variation of specific capacitance vs scan rate of  $Mn_3O_4$  NLs.

The capacitance of  $Mn_3O_4$  thin film was calculated by using the following relation,

$$C = \frac{\int Idt}{dv/dt} \text{ ----- (4)}$$

Where,  $\int Idt$  is area under curve of CV and  $dv/dt$  is voltage scanning rate in mV/s.

The specific capacitance of  $Mn_3O_4$  NLs was calculated by following relation,

$$\text{Specific capacitance } (C_s) = \frac{C}{W} \text{ ----- (5)}$$

Where, C – capacitance in farad and W – the mass of active electrode materials in gm. The active mass of  $Mn_3O_4$  NLs was 0.0024 gm, calculated from weight difference method. The  $Mn_3O_4$  NLs show specific

capacitance of  $460 \text{ F.g}^{-1}$  at scan rate of  $5 \text{ mV.s}^{-1}$ . It was observed that as scan rate increases specific capacitance decreases shown in Fig. 3 (b). Decrease in specific capacitance suggests that at higher scan rate most of the inner active sites of nanoflakes network are not involved in the reaction. So, specific capacitance obtained at low scan rate are due to full utilization of the active electrode materials.

Material	Specific Capacitance ( $\text{F.g}^{-1}$ )	Electrolyte	Method of synthesis	Reference
$\text{Mn}_3\text{O}_4$ Nano leaves	460	0.5 M $\text{Na}_2\text{SO}_4$	Potentiostatic Electrodeposition	Our work
$\text{Mn}_3\text{O}_4$ nanoparticles	375	1.0 M $\text{Na}_2\text{SO}_4$	SILAR	[31]
$\text{Mn}_3\text{O}_4$ nanocubes	223	1.0 M $\text{Na}_2\text{SO}_4$	CBD	[32]
$\text{Mn}_3\text{O}_4$ nanograins	314	1.0 M $\text{Na}_2\text{SO}_4$	SILAR	[24]
$\text{Mn}_3\text{O}_4$ nanograins	289	1.0 M $\text{Na}_2\text{SO}_4$	SILAR	[33]

**Table: 1** Comparison of specific capacitance between our work and previously reported work to synthesis the  $\text{Mn}_3\text{O}_4$  electrodes by considering scan rate of  $5 \text{ mV/s}$ .

Table 1 represents a comparison of specific capacitance between our work and previously reported work by keeping scan rate of  $5 \text{ mV/s}$  vs SCE. The specific capacitance obtained in the present study is higher due nanostructured and porous morphology of  $\text{Mn}_3\text{O}_4$  NLs. It depends upon optimum electrodeposition time.

### 3.3.3 Galvanostatic charging-discharging (GCD) studies:

The specific energy and specific power associated with  $\text{Mn}_3\text{O}_4$  NLs was carried with the help of GCD techniques. Fig 4 (a) shows typical charge-discharge curves of  $\text{Mn}_3\text{O}_4$  NLs at constant current density of  $5 \text{ mA.cm}^{-2}$  in  $0.5 \text{ M Na}_2\text{SO}_4$  electrolyte solution. The charging-discharging curves of  $\text{Mn}_3\text{O}_4$  NLs show symmetrical characteristics, which reveals that  $\text{Mn}_3\text{O}_4$  NLs thin film have good capacitive behaviour and the reversible redox process. The GCD curve of  $\text{Mn}_3\text{O}_4$  NLs shows very small voltage drop at the initial of the discharge curve which is due to very low internal resistance between the current collector and  $\text{Mn}_3\text{O}_4$  NLs.

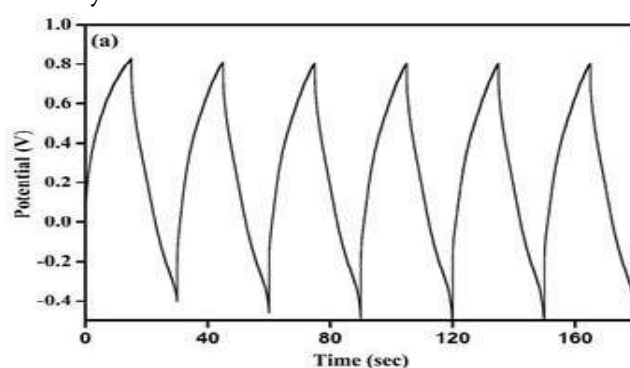


**Figure 4** Galvanostatic charge-discharge (GCD) study of  $\text{Mn}_3\text{O}_4$  NLs

The coulombic efficiency, specific energy and power of  $\text{Mn}_3\text{O}_4$  NLs was calculated using following formulae:

$$\text{Coulombic Efficiency } (\eta) = \frac{T_d}{T_c} \times 100 \text{ ----- (6)}$$

$$\text{Specific power } (P) = \frac{V \times I_d}{W} \text{ ----- (7)}$$

$$\text{Specific energy (E)} = \frac{V \times I_d \times T_d}{W} \text{----- (8)}$$

Where,  $T_d$  and  $T_c$  is discharge and charge time in sec,  $V$  is voltage window in volt,  $I_d$  is discharge current mA and  $W$  is the mass of the active material in gm. The coulombic efficiency of  $Mn_3O_4$  NLs was found to be 98.42% whereas the specific power and specific energy were observed to be 6.40 kW.kg<sup>-1</sup> and 3.85 Wh.kg<sup>-1</sup>, respectively.

#### 4. Conclusions:

In summary, we have successfully synthesized  $Mn_3O_4$  NLs by electrodeposition method on low cost conducting stainless steel substrate for supercapacitor application. The XRD study reveals that hausmannite tetragonal crystal structure with average crystallite size of 34 nm. The surface morphology study  $Mn_3O_4$  thin film shows NLs type morphology at higher magnification. The electrodeposited  $Mn_3O_4$  NLs shows higher specific capacitance of 460 F.g<sup>-1</sup> with 92% cyclic stability, which is better achievement than earlier reported values because of nano structured materials. The GCD study shows better values specific energy and specific power and coulombic efficiency of  $Mn_3O_4$  NLs. EIS study reveals that small values of  $R_s$  and  $R_{ct}$  of  $Mn_3O_4$  NLs based thin film electrode, providing better ability of electronic and ionic conductivity of  $Mn_3O_4$  materials. Thus, electrodeposited  $Mn_3O_4$  NLs based thin film electrode is suitable material for electrochemical supercapacitor device.

#### References:

- [1] G. Wee, W.F. Mak, iN. Phonthammacha, A. Kiebele, M.V. Reddy, B.V.R. Chowdari, G. Gruner, M. Srinivasan, S.G. Mhaisalkar, J. Electrochem. Soc. 157, A179 (2010)
- [2] J.K. Chang, Y.L. Chen, W.T.T. Sai, J. Power Sources. 135, 344 (2004)
- [3] P. Simon, Y. Gogotsi, Nat. Mater. 7, 845 (2008)
- [4] D. Wei, Scherer MR, Bower C, Andrew P, Ryhanen T, U. Steiner, Nano Lett. 12, 1857 (2012)
- [5] K.H. Chang, C.C. Hu, C.Y. Chou, Chem. Mater. 19, 2112 (2007)
- [6] Z. Yu, B. Duong, D. Abbott, J. Thomas, Adv. Mater. 25, 3302 (2013)
- [7] P.M. Kharade, J.V. Thombare, A.R. Babar, R.N. Bulakhe, S.B. Kulkarni, D.J. Salunkhe, J Phys Chem Solids. 120, 207 (2018)
- [8] L. Gu, Y. Wang, R. Lu, L. Guan, X. Peng, J. Sha J. Mater. Chem. A. 2, 1761 (2014)
- [9] D.Q. Liu, S.H. Yu, S.W. Son, and S.K. Joo, ECS Trans. 16, 103 (2008)
- [10] P.M. Kharade, A.R. Babar, S.S. Dhasade, B.R. Karche, D.J. Salunkhe, Mater. 7, 342 (2018)
- [11] A.S. Patil, M.D. Patil, G.M. Lohar, S.T. Jadhav, V.J. Fulari, Ionics. 23, 1259 (2017)
- [12] S.F. Chin, S.C. Pang, and M.A. Anderson, J. Electrochemical Society. 149, A379 (2002)
- [13] S.F. Chin, and S.C. Pang, Mater. Chem. Phys. 124, 29 (2010)
- [14] X. Zhang, X. Sun, Y. Chen, D. Zhang, Y. Ma, Mater. Lett. 68, 336 (2012)
- [15] X. Zhang, P. Yu, D. Zhang, H. Zhang, X. Sun, Y. Ma, Mater. Lett. 92, 401 (2013)
- [16] J.L. Liu, L.Z. Fan, X. Qu, Electrochim. Acta. 66, 302 (2012)
- [17] R. Jiang, T. Huang, J. Liu, J. Zhuang, A. Yu, Electrochim. Acta. 54, 3047 (2009)
- [18] C.K. Lin, K.H. Chuang, C.Y. Lin, C.Y. Tsay, C.Y. Chen, Surf. Coat. Technol. 202, 1272 (2007)

- [19] D.P. Dubal, D.S. Dhawale, R.R. Salunkhe, V.J. Fulari, C.D. Lokhande, *J. Alloy. Compd.* 497,166(2010)
- [20] C. Xu, B. Li, H. Du, F. Kang, and Y. Zeng, *J of Power Sources.*180,664 (2008)
- [21] A. Zolfaghari, F. Ataherian, M. Ghaemi, and A. Gholami, *Electrochimica Acta.* 52,2806(2007)
- [22] T. Nguyen, M.J. Carmezim, M. Boudard, M. Montemor, *J. Hydrog. Energy.* 40,16355(2015)
- [23] A. Yuan, X. Wang, Y. Wang, J. Hu, *Electrochim. Acta.* 54,1021(2009)
- [24] D.P. Dubal, D.S. Dhawale, R.R. Salunkhe, S.M. Pawar, C.D. Lokhande, *Appl Surf Sci.*256,4411(2010)
- [25] T. Yousefi, A.N. Golikand, M.H. Mashhadizadeh, M. Aghazadeh, *Curr. Appl. Phys.* 12, 544(2012)
- [26] M. Kim, Y. Hwang, J. Kim, *J. Power Sources.* 239, 225(2013)
- [27] X. Dai, M. Zhang, J. Li, D. Yang, *RSC Adv.*10, 15860(2020)
- [28] P.M. Kharade, S.G. Chavan, D.J. Salunkhe, P.B. Joshi, S.M. Mane, S.B. Kulkarni, *J. Mater. Sci. Mater. Electron.* 52, 37(2014)
- [29] M. Zhang, X. Dai, C. Zhang, Y. Fuan, D. Yang, *J. Li, Mater.*13, 181(2020)
- [30] P.D. More, P.R. Jadhav, S.M. Ingole, Y.H. Navale, V.B. Patil, *J Mater Sci: Mater Electron.* 28,707(2017)
- [31] A.A. Shaikh, M.R. Waikar, R.G. Sonkawade, *Synth. Met.* 247, 1(2019)
- [32] D.P. Dubal, D.S. Dhawale, R.R. Salunkhe, C.D. Lokhande, *J. Electrochem. Soc.* 157,A812 (2010)
- [33] G.S. Gund, D.P. Dubal, B.H. Patil, S.S. Shinde, C.D. Lokhande, *Electrochim. Acta.* 92,205 (2013)

## Investigation The Temperature and Volume Fraction Effects on The Thermal and Rheological Properties of The TiO<sub>2</sub> Nanofluid

N B Girhe<sup>1</sup>, S N Botewad<sup>2\*</sup>, P P Pawar<sup>2</sup>, A B Kadam<sup>2</sup>

<sup>1</sup>Department of Physics, Jawahar Science, Commerce and Arts College, Andoor, Tuljapur 413603, Maharashtra, India

<sup>2</sup>Department of Physics, Dr. Babasaheb Ambedkar Marathwada University, Aurangabad 431004, Maharashtra, India

### ABSTRACT

The present investigation has been reported the preparation of water-based TiO<sub>2</sub> nanofluid using a two-step method. The temperature and volume fraction dependent thermal conductivity and viscosity TiO<sub>2</sub> was studied. The different volume fraction of TiO<sub>2</sub> (0.1,0.2,0.3,0.4 and 0.5) were used dispersed in water using harsh ultrasonic treatment and tested the thermal conductivities for temperature range of 20–50 °C. The experimental results reveal that increase in temperature and volume fraction increases the thermal conductivity of nanofluid. The viscosity of the nanofluid with same concentration of TiO<sub>2</sub> was measured and shows the decrease viscosity by increasing temperature whereas increases when increase the volume concentration. Thus, the experimental results are much more useful for the practical application of nanofluids in thermal management.

**Keywords:** Nanofluid; Nanoparticles; Thermal Conductivity; Viscosity;

### I. INTRODUCTION

Thermal management becomes the very critical task in various industries for getting the efficient productivity. Worldwide various conventional fluids were used for the thermal management such as water, oil, ethylene glycol etc. But unfortunately, these fluids do not achieve the desired thermal properties for practical application. To improve the thermal conductivities of these conventional fluids firstly in 1873 Maxwell proposed the single-phase fluids with the addition of solid particles [1]. The idea of Maxwell worked and it improves the thermal properties of the conventional fluids but it has the drawbacks such as sedimentation, clogging and erosion during the flow. After this inventive research idea and experimental results in 1995, Choi introduced the idea of nanofluids with his own experimental results. The nanofluid which solely overcomes the sedimentation, clogging and erosion problems [2].

An emerging nanotechnology provides the superior physical, thermal, optoelectronics properties of the material in nanosized dimension. The very new trending application of nanotechnology is the nanofluid

research. Nanofluid is an engineering fluid in which nanometre sized solid particles homogeneously dispersed in base fluid such as water, engine oil, propylene glycol, ethylene glycol, etc [3]. Recently various types of nanomaterials were found to be used for the preparation of nanofluid such as metal, metal oxides, carbon materials etc. Nowadays metal oxide nanoparticles ( $\text{TiO}_2$ ,  $\text{SiO}_2$ ,  $\text{Fe}_2\text{O}_3$ ,  $\text{Fe}_3\text{O}_4$ ,  $\text{Al}_2\text{O}_3$ ,  $\text{BaTiO}_3$ ,  $\text{CuO}$ , etc.) extensively employed for the preparation of nanofluid [4]. The preference for metal oxide nanoparticles is due to the superior physicochemical, optoelectronics, thermal properties, and ease of preparation with tuned properties. The potential of nanofluids to enhances the thermal conductivity and rheological behaviour of base fluid it applicable in heat transfer, including fuel cells, cooling of microelectronic equipment, pharmaceutical processes and hybrid engines etc [5,6].

Worldwide different research groups have been reported the thermal conductivity and viscosity of the nanofluids using the different types of nanoparticles with different volume fraction in the base fluid. M.Kh. Abdolbaqi et. al studied the thermal conductivity and viscosity of BioGlycol/water based  $\text{TiO}_2$  nanofluids and experimental results shows that enhancement of thermal conductivity depends on volume concentration, temperature and thermal conductivity of base fluid [7]. M.H. Ahmadi et.al investigate the thermal performance of  $\text{TiO}_2$  nanofluid using four different neural networks [8]. D. Cabaleiro et.al reported the ethylene and propylene glycol-based  $\text{TiO}_2$  (anatase and rutile) nanofluids. The experimental results shows that thermal conductivity increases 15.4%. and enhancements are higher for propylene than ethylene glycol-based nanofluids [9]. W.H. Azmi et.al investigate the heat transfer performance of  $\text{TiO}_2$  nanofluids in water-EG mixture at different operating temperatures. On the basis of experimental results concluded that maximum enhancement of thermal conductivity was 15.4% at 1.5% volume concentration and temperature of  $60^\circ\text{C}$ . and relative viscosities fluctuate at a range of 4.6 to 33.3% with variation of temperature [10].

## II. EXPERIMENTAL

### 2.1 Materials and Characterization

In present investigation  $\text{TiO}_2$  (Rutile) nano particles with particles size 20 nm procured from the Sisco Research Laboratory Mumbai, India. KD2 Pro thermal analyser (Decagan Devices Inc., USA) was use to study the thermal conductivity and before measurements the device prob was calibrated with standard fluid. The viscosity of all nanofluid were measured by means of an AR-G2 rheometer (TA Instruments, USA) at different temperatures.

### 2.2 Nanofluid Preparation

Nanofluids reported in the present investigation were prepared via two-step method.  $\text{TiO}_2$  nanoparticles of volume fraction (0.1, 0.2, 0.3, 0.4, and 0.5 Wt.%) were used for the preparation of nanofluid. The above-mentioned proportion of  $\text{TiO}_2$  nanoparticles was dispersed in the base fluid double distilled water (DDW) separately and stirred for 2 hours forcefully using magnetic stirrer. Then the stable dispersion was attained by ultrasonic probe via ultrasonication for 6 h.

### III. RESULTS AND DISCUSSION

#### 3.1 Thermal conductivity

The thermal conductivity of prepared water based  $\text{TiO}_2$ -nanofluids concentrations of (0.1, 0.2, 0.3 and 0.4) wt. % were measured at temperatures of 300 K-350 K in 15 k interval. Fig. 1 shows the thermal conductivity of prepared nanofluid for different volume concentrations and fig. 2 shows for different temperatures. It is observed that by increasing both parameters volume concentrations and temperatures, thermal conductivity is enhanced of all the studied samples. Increment of the nanoparticles loading in the base fluid reduces the interparticle distances that improves heat conduction and the outcome is enriched thermal conductivity. The basic phenomenon of the increment in the thermal conductivity is propagation of lattice vibration between electrons and phonons. The thermal conductivity significantly increases by increasing temperatures due to the Brownian motion which provide the direct solid-solid transport between the incorporated particles.

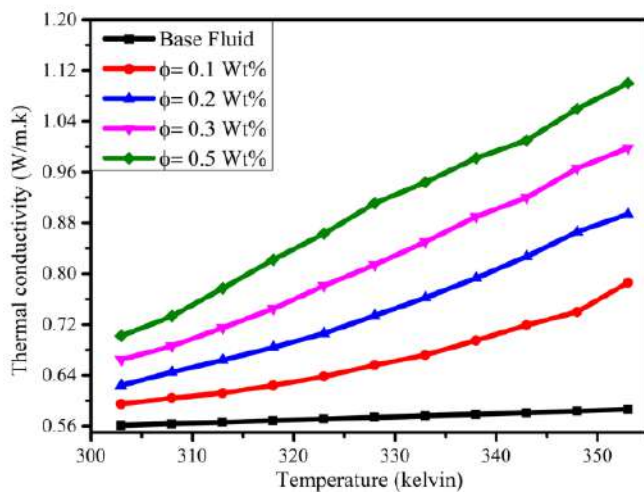


Figure 1. Thermal conductivity for various volume fraction at different temperature

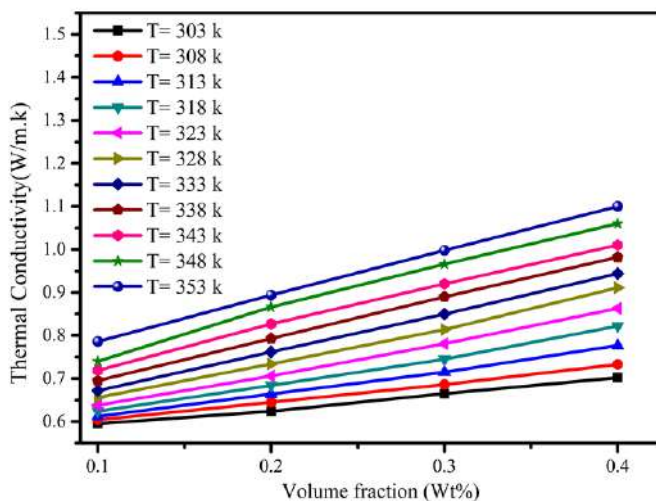


Figure 2. Thermal conductivity for different temperatures of various concentration

### 3.2 Viscosity

Rheological behaviors of all prepared nanofluid samples viscosity were examined at different temperature points of 300 K-360 K at equal interval for each volume concentrations. Fig. 3 shows the dependency of viscosity on the volume concentration and temperature of TiO<sub>2</sub> nanofluid. The considerable effects were observed for both parameters, temperature as well as volume concentrations. As concerned to the volume concentration viscosity of all the nanofluid samples observed to be increased. The reason behind the increasing viscosity may be due to the formation of agglomeration of nanoparticles in suspension. The temperature effect slightly reduces the viscosity due to the feeble intermolecular interaction and adhesion forces between molecules which is further attributed to Brownian motion, thermal movement of molecules and their average speed.

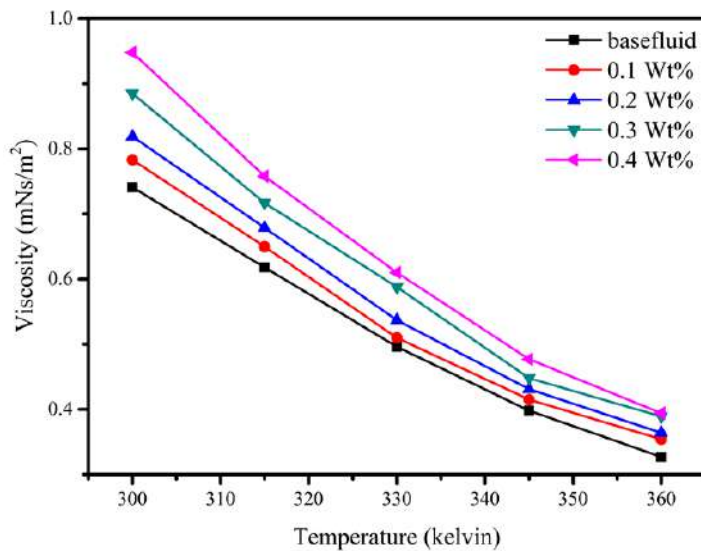


Figure 3. Viscosity of TiO<sub>2</sub> nanofluid at different temperature

## IV. CONCLUSION

In short, present investigation successfully encloses the preparation and analysis of the thermal as well as rheological properties of TiO<sub>2</sub> nanofluids. The investigational findings reveal the considerable enhanced thermal conductivity of nanofluids with increased temperature and volume concentration. The viscosity of the nanofluid increased with volume concentration whereas decreased with increased temperature. Thus, the present investigation exhibits the applicability of the ternary TiO<sub>2</sub> nanofluid for the various application wherever the necessity of cooling.

## V. REFERENCES

- [1]. Vanaki, S. M., Ganesan, P., & Mohammed, H. A. (2016). Numerical study of convective heat transfer of nanofluids: a review. *Renewable and Sustainable Energy Reviews*, 54, 1212-1239.

- [2]. Das, S. K., & Stephen, U. S. (2009). A review of heat transfer in nanofluids. *Advances in Heat transfer*, 41, 81-197.
- [3]. Ali, H. M., Babar, H., Shah, T. R., Sajid, M. U., Qasim, M. A., & Javed, S. (2018). Preparation techniques of TiO<sub>2</sub> nanofluids and challenges: a review. *Applied Sciences*, 8(4), 587.
- [4]. Sidik, N. A. C., Mohammed, H. A., Alawi, O. A., & Samion, S. (2014). A review on preparation methods and challenges of nanofluids. *International Communications in Heat and Mass Transfer*, 54, 115-125.
- [5]. Puliti, G., Paolucci, S., & Sen, M. (2011). Nanofluids and their properties. *Applied Mechanics Reviews*, 64(3).
- [6]. Suganthi, K. S., & Rajan, K. S. (2017). Metal oxide nanofluids: Review of formulation, thermo-physical properties, mechanisms, and heat transfer performance. *Renewable and Sustainable Energy Reviews*, 76, 226-255.
- [7]. Abdolbaqi, M. K., Sidik, N. A. C., Aziz, A., Mamat, R., Azmi, W. H., Yazid, M. N. A. W. M., & Najafi, G. (2016). An experimental determination of thermal conductivity and viscosity of BioGlycol/water based TiO<sub>2</sub> nanofluids. *International Communications in Heat and Mass Transfer*, 77, 22-32.
- [8]. Ahmadi, M. H., Baghban, A., Sadeghzadeh, M., Hadipoor, M., & Ghazvini, M. (2020). Evolving connectionist approaches to compute thermal conductivity of TiO<sub>2</sub>/water nanofluid. *Physica A: Statistical Mechanics and its Applications*, 540, 122489.
- [9]. Cabaleiro, D., Nimo, J., Pastoriza-Gallego, M. J., Piñeiro, M. M., Legido, J. L., & Lugo, L. (2015). Thermal conductivity of dry anatase and rutile nano-powders and ethylene and propylene glycol-based TiO<sub>2</sub> nanofluids. *The Journal of Chemical Thermodynamics*, 83, 67-76.
- [10]. Azmi, W. H., Hamid, K. A., Mamat, R., Sharma, K. V., & Mohamad, M. S. (2016). Effects of working temperature on thermo-physical properties and forced convection heat transfer of TiO<sub>2</sub> nanofluids in water–Ethylene glycol mixture. *Applied Thermal Engineering*, 106, 1190-1199.



# International e-Conference on Recent Trends in Nano-Materials and Its Applications RTNA-2022

Organized By  
Department of Physics,  
Sangola Taluka Shetkari Shikshan Prasarak  
Mandal Sangola's, Vidnyan Mahavidyalaya, Sangola  
Tal-Sangola, Dist-Solapur, MH-413307, India  
Collaboration with  
Internal Quality Assurance Cell (IQAC)

## Publisher

Technoscience Academy



Website : [www.technoscienceacademy.com](http://www.technoscienceacademy.com)



Email : [editor@ijsrst.com](mailto:editor@ijsrst.com) Website : <http://ijsrst.com>



**3.2.2 - Number of workshops/seminars conducted  
on Research Methodology, Intellectual  
Property Rights (IPR) and entrepreneurship  
during the year-2021-22**

**Documents**

**3.2.2 Oral and poster presentations and  
Broacher of the conference**



Sangola Taluka Shetkari Shikshan Prasarak Mandal Sangola's

# Vidnyan Mahavidyalaya, Sangola.

Tal-Sangola, Dist-Solapur, MH-413307, India.

(Affiliated to Punyashlok Ahilyadevi Holkar Solapur University, Solapur.)

**Department of Physics in Collaboration with Internal Quality Assurance Cell (IQAC)**

organizes

## International e-Conference on Recent Trends in Nano-Materials and Its Applications-2022(RTNA-2022)

(dated April 22-23, 2022)

### Resource Persons



**Prof. Jae Cheol Shin**  
Dongguk University,  
South Korea



**Dr. Sreekanth TVM**  
Yeungnam University,  
South Korea



**Dr. M. Vasudeva Reddy**  
Yeungnam University,  
South Korea



**Dr. Sonaimuthu Mohandoss**  
Yeungnam University,  
South Korea

### Chief Patron

**Hon'ble Mr. Chandrakant Deshmukh**  
Director, STSSPM

**Hon'ble Mr. Vitthalrao Shinde**  
Secretary, STSSPM

### Organizing Committee

**Dr. R. A. Fule**  
(Acting Principal)

**Mr. B. B. Navale**  
(Head of Dept.)

**Dr. S. S. Dhasade,**  
(Convener)

**Dr. J. V. Thombare**  
(Organizing Secretary)

**Mr. A. M. Kambale**  
(Treasurer)

**Dr. D. K. Bandgar**  
(Member)

**Dr. S. M. Mane**  
(South Korea)

**Dr. S. T. Navale**  
(Spain)

### About Registration & Conference Proceeding

E-Certificate to be provided to those who will register, attend and fill the feedback form.

**Last date of registration:** 20 April, 2022.

**Registration Link:**

<https://forms.gle/sThctfpXEuhjbHVYA>

Email: 2022rtna@gmail.com

Conference Date: April 22-23, 2022

Paper Publication

Research papers will be published in

•UGC Approved Journal Number 64011

•International Peer reviewed Thomson

Reuters, Open access Scientific Journal

•Online ISSN: 2395-602X

•Print ISSN: 2395-6011

•DOI: 10.32628, Index Copernicus :49.58

•Individual certificate to soft copy to all authors

Soft copy of CD cover and proceeding of the conference if needed.

Contact No.: 9422652388, 9284555463, 9890776585, 9860477067, 9673922572, 7798033087

Registration Fees submission details: The registration fees along with paper publication charges may be paid online/ Paytm/ Phone pay / Internet Banking to

Account Name: VidnyanMahavidyalaya, Sangola

Bank Name: Bank of Maharashtra

Branch: Sangola, Account Number: 60101820852

IFSC: MAHB0001467; MICR Code: 413014079

Fees details:

Category	Registration fee	Paper Publication charges
Students	Rs. 100/-	Rs. 800/-
Academics	Rs. 200/-	Rs. 800/-
Industry	Rs. 1000/-	Rs. 800/-
Foreign Delegates	USD 20	USD 50

Submission of Papers: Interested authors are requested to submit full-length manuscript of research paper in MS-Word 2007 or MS-Word 2010 including Paper Title, Names of all the authors and e-mail address of corresponding authors. The font should be Times New Roman, Size-12. The maximum length of manuscripts is limited to four pages. Paper sent by e-mail to conference E-mail address: 2022rtna@gmail.com.



Sangola Taluka Shetkari Shikshan Prasarak Mandal Sangola's

## **Vidnyan Mahavidyalaya, Sangola**

Tal-Sangola, Dist-Solapur, MH- 413307, India.

(Affiliated to Punyashlok Ahilyadevi Holkar Solapur University, Solapur)

Department of Physics in collaboration with Internal Quality Assurance Cell (IQAC) organizes an **International e-Conference on Recent Trends in Nano-Materials and Its Applications-2022 (RTNA-2022)** Dated on April 22-23, 2022, Conference E-mail:2022rtna@gmail.com

**-:Oral and Poster Presentations:-**

### **Oral Presentations**

**(Date: April 22, 2022)**

**OP1)** Self-focusing of Gaussian Laser Beam in Collisionless Plasma with Linear Absorption

Author: **Mr. Kalyani Y. Khandale**, Shivaji University, Kolhapur

**OP2)** Simulations Commercial BJT with Temperature for Space and Radiation Rich Environment Applications.

Author: **C M Dinesh**, Department of Physics, Govt. First Grade College and PG centre, Chintamani-563125, India.

**OP3)** Study of Dielectric and Field Modulation studies in Polymer Nanocomposites,

Author: **C. V. Chanmal**, DBF Dayanand College of Arts and Science, Solapur

### **Poster Presentations**

**(Date: April 23, 2022)**

**PP1)** Antimicrobial activity of CdS quantum dots mediated by *Aegle marmelos* leaves

Authors: **T.R. Deore**, M D Dhiware, S.B. Nahire, A.B. Gawande

**PP2)** CuO nanoparticles mediated by Coffee powder extract: An Impeder of *Candida albicans* biofilm

Authors: **P. G. Jadhav**, A.B. Gawande

**PP3)** High stability  $Mn_2O_3/MnCO_3$  microcubes synthesized by hydrothermal method for supercapacitor application

Authors: **O. C. Pore**, D. S. Sawant, A. S. Shelake, D. B. Mane, V. J. Fulari, G. M. Lohar

**PP4)** Growth study on entire replacement of Zn by Mn into  $\text{Cu}_2\text{ZnSnS}_4$  thin films by SILAR method

Authors: **H. C. Yadav**, B. V. Patil, S. S. Dhere, R. M. Shaikh , S. B. Duchal , A. M. More

**PP5)** Thin Films of  $\text{Cu}_2\text{ZnSnS}_4$  (CZTS) grown via replacement of Zn by Mg using SILAR method

Authors: **A. K. Bagal**, M. S. Shinde, K. S. Gund, G .V. Patil, A. M. Rajage, A. M. More



Sangola Taluka Shetkari Shikshan Prasarak Mandal Sangola's

## **Vidnyan Mahavidyalaya, Sangola**

Tal-Sangola, Dist-Solapur, MH- 413307, India.

(Affiliated to Punyashlok Ahilyadevi Holkar Solapur University, Solapur)

Department of Physics in collaboration with Internal Quality Assurance Cell (IQAC) organizes an **International e-Conference on Recent Trends in Nano-Materials and Its Applications-2022 (RTNA-2022)** Dated on April 22-23, 2022, Conference E-mail:2022rtna@gmail.com

**-:Oral and Poster Presentations:-**

### **Oral Presentations**

**(Date: April 22, 2022)**

**OP1)** Self-focusing of Gaussian Laser Beam in Collisionless Plasma with Linear Absorption

Author: **Mr. Kalyani Y. Khandale**, Shivaji University, Kolhapur

**OP2)** Simulations Commercial BJT with Temperature for Space and Radiation Rich Environment Applications.

Author: **C M Dinesh**, Department of Physics, Govt. First Grade College and PG centre, Chintamani-563125, India.

**OP3)** Study of Dielectric and Field Modulation studies in Polymer Nanocomposites,

Author: **C. V. Chanmal**, DBF Dayanand College of Arts and Science, Solapur

### **Poster Presentations**

**(Date: April 23, 2022)**

**PP1)** Antimicrobial activity of CdS quantum dots mediated by *Aegle marmelos* leaves

Authors: **T.R. Deore**, M D Dhiware, S.B. Nahire, A.B. Gawande

**PP2)** CuO nanoparticles mediated by Coffee powder extract: An Impeder of *Candida albicans* biofilm

Authors: **P. G. Jadhav**, A.B. Gawande

**PP3)** High stability  $Mn_2O_3/MnCO_3$  microcubes synthesized by hydrothermal method for supercapacitor application

Authors: **O. C. Pore**, D. S. Sawant, A. S. Shelake, D. B. Mane, V. J. Fulari, G. M. Lohar

**PP4)** Growth study on entire replacement of Zn by Mn into  $\text{Cu}_2\text{ZnSnS}_4$  thin films by SILAR method

Authors: **H. C. Yadav**, B. V. Patil, S. S. Dhere, R. M. Shaikh , S. B. Duchal , A. M. More

**PP5)** Thin Films of  $\text{Cu}_2\text{ZnSnS}_4$  (CZTS) grown via replacement of Zn by Mg using SILAR method

Authors: **A. K. Bagal**, M. S. Shinde, K. S. Gund, G .V. Patil, A. M. Rajage, A. M. More



**3.2.2 - Number of workshops/seminars conducted  
on Research Methodology, Intellectual  
Property Rights (IPR) and entrepreneurship  
during the year-2021-22**

**Documents**

**3.2.2 RTNA-2022 letters\_Broucher-plan**



Sangola Taluka Shetkari Shikshan Prasarak Mandal Sangola's

# Vidnyan Mahavidyalaya, Sangola.

Tal-Sangola, Dist-Solapur, MH-413307, India.

(Affiliated to Punyashlok Ahilyadevi Holkar Solapur University, Solapur.)

Department of Physics in Collaboration with Internal Quality Assurance Cell (IQAC)

organizes

## International e-Conference on Recent Trends in Nano-Materials and Its Applications-2022(RTNA-2022)

(dated April 22-23, 2022)

### Resource Persons



**Prof. Jae Cheol Shin**  
Dongguk University,  
South Korea



**Dr. Sreekanth TVM**  
Yeungnam University,  
South Korea



**Dr. M. Vasudeva Reddy**  
Yeungnam University,  
South Korea



**Dr. Sonaimuthu Mohandoss**  
Yeungnam University,  
South Korea

### Chief Patron

**Hon'ble Mr. Chandrakant Deshmukh**  
Director, STSSPM

**Hon'ble Mr. Vitthalrao Shinde**  
Secretary, STSSPM

### Organizing Committee

**Dr. R. A. Fule**  
(Acting Principal)

**Mr. B. B. Navale**  
(Head of Dept.)

**Dr. S. S. Dhasade,**  
(Convener)

**Dr. J. V. Thombare**  
(Organizing Secretary)

**Mr. A. M. Kambale**  
(Treasurer)

**Dr. D. K. Bandgar**  
(Member)

**Dr. S. M. Mane**  
(South Korea)

**Dr. S. T. Navale**  
(Spain)

### About Registration & Conference Proceeding

E-Certificate to be provided to those who will register, attend and fill the feedback form.

**Last date of registration:** 20 April, 2022.

**Registration Link:**

<https://forms.gle/sThtcfpXEuhjbHVYA>

Email: 2022rtna@gmail.com

Conference Date: April 22-23, 2022

Paper Publication

Research papers will be published in

• UGC Approved Journal Number 64011

• International Peer reviewed Thomson

Reuters, Open access Scientific Journal

• Online ISSN: 2395-602X

• Print ISSN: 2395-6011

• DOI: 10.32628, Index Copernicus : 49.58

• Individual certificate to soft copy to all authors

Soft copy of CD cover and proceeding of the conference if needed.

Contact No.: 9422652388, 9284555463, 9890776585, 9860477067, 9673922572, 7798033087

Registration Fees submission details: The registration fees along with paper publication charges may be paid online/ Paytm/ Phone pay / Internet Banking to

Account Name: VidnyanMahavidyalaya, Sangola

Bank Name: Bank of Maharashtra

Branch: Sangola, Account Number: 60101820852

IFSC: MAHB0001467; MICR Code: 413014079

Fees details:

Category	Registration fee	Paper Publication charges
Students	Rs. 100/-	Rs. 800/-
Academics	Rs. 200/-	Rs. 800/-
Industry	Rs. 1000/-	Rs. 800/-
Foreign Delegates	USD 20	USD 50

Submission of Papers: Interested authors are requested to submit full-length manuscript of research paper in MS-Word 2007 or MS-Word 2010 including Paper Title, Names of all the authors and e-mail address of corresponding authors. The font should be Times New Roman, Size-12. The maximum length of manuscripts is limited to four pages. Paper sent by e-mail to conference E-mail address: 2022rtna@gmail.com.



*Sangola Taluka Shetkari Shikshan Prasarak Mandal Sangola's*

## **Vidnyan Mahavidyalaya, Sangola**

Tal-Sangola, Dist-Solapur, MH- 413307, India.

(Affiliated to Punyashlok Ahilyadevi Holkar Solapur University, Solapur)

Department of Physics in collaboration with Internal Quality Assurance Cell (IQAC) organizes an **International e-Conference on Recent Trends in Nano-Materials and Its Applications-2022 (RTNA-2022)** Dated on April 22-23, 2022, Conference E-mail:2022rtna@gmail.com

**-:Program Schedule:-**

**Day 1<sup>st</sup>: Friday**

**Date: April 22, 2022**

**Session-I: Inauguration of Conference; Session Coordinator: Dr. J. V. Thombare**

Sr. No.	Time in IST*	Description/Name of Program	Name
01	10:00 am to 10:05 am	Introduction and Welcome	Dr. S. S. Dhasade Convener & Coordinator IQAC
02	10:05 am to 10:50 am	Keynote Address	<b>Resource Person:</b> Prof. (Dr.) Jae Cheol Shin Dongguk University, South Korea
03	10:50 am to 10:55 am	Presidential Address	Hon'ble Dr. Aniket Chandrakant Deshmukh Director, STSSPM, Sangola
04	10:55 am to 11:00 am	Vote of thanks	Dr. R. A. Fule, Acting Principal, V. M. Sangola

**Session-II: Invited Talk; Session Coordinator: Dr. J. V. Thombare**

05	11:00 am to 11:45 am	<b>Resource Person:</b> Dr. Rajshekhar, Yeungnam University, South Korea	<b>Chairperson:</b> Prof.(Dr.) S. B. Kulkarni Director, Innovation, Incubation and Linkages, Dr. Homi Bhabha State University, Mumbai
06	11:45 am to 11:50 am	Discussion	
07	11:50 am to 12:05 pm : Short break		

**Session-III: Oral Presentations; Session Coordinator: Mr. B. B. Navale**

08	12:05 pm to 12:35 pm	OP-01 to OP-03	<b>Chairperson:</b> Dr. S. M. Mane, Dongguk University, South Korea
----	----------------------	----------------	---

**Zoom meeting link for joining:**

**<https://us02web.zoom.us/j/5328645418?pwd=OXRXaHNHdjRtNERZalcxHE1QTjZz09>**

\*IST-Indian Standard Time (Time is mentioned in IST)

Day 2<sup>nd</sup>: Saturday

Date: April 23, 2022

**Session-IV: Invited Talk; Session Coordinator: Dr. S. S. Dhasade**

09	10:00 am to 10:45 am	<b>Resource Person:</b> Dr. Sonaimuthu Mohandoss Yeungnam University, South Korea	<b>Chairperson:</b> Dr. A. R. Babar, Shankararao Mohite Patil Mahavidyalaya, Akluj
10	10:45 am to 10:50 am	Discussion	

**Session-V: Invited Talk; Session Coordinator: Dr. J. V. Thombare**

11	10:50 am to 11:35 am	<b>Resource Person:</b> Dr. M. Vasudeva Reddy Yeungnam University, South Korea	<b>Chairperson:</b> Dr. R. A. Bugad, Sangola College, Sangola
12	11:35 am to 11:40 am	Discussion	

**Session-VI: Poster Presentation; Session Coordinator: Prof. R. S. Gaikwad**

13	11:40 am to 12:10 pm	PP-01 to PP-05	<b>Chairperson:</b> Dr. S. D. Patil Pratapsinh Mohite Patil Mahavidyalaya, Karmala
14	12:10 pm to 12:15 pm	Short break	

**Session-VII: Valedictory Function; Session Coordinator: Dr. J. V. Thombare**

15	12:15 pm to 12:20 pm	Conference Overview	<b>Dr. S. S. Dhasade</b> Convener
16	12:20 pm to 12:30 pm	Feedback from Participants	--
17	12:30 pm to 12:40 pm	Valedictory address	<b>Chief Guest:</b> Dr. Anamika Kadam Professor, Institute of Science, Mumbai Young Scientist, DST, New Delhi
18	12:40 pm to 12:45 pm	Presidential remark	<b>Dr. R. A. Fule,</b> Acting Principal, V. M. Sangola
19	12:45 pm to 12:50 pm	Vote of Thanks	<b>Mr. B. B. Navale</b> Head, Dept. of Physics

\*IST-Indian Standard Time (Time is mentioned in IST)



Sangola Taluka Shetkari Shikshan Prasarak Mandal Sangola's

## **Vidnyan Mahavidyalaya, Sangola**

Tal-Sangola, Dist-Solapur, MH- 413307, India.

(Affiliated to Punyashlok Ahilyadevi Holkar Solapur University, Solapur)

Department of Physics in collaboration with Internal Quality Assurance Cell (IQAC) organizes an **International e-Conference on Recent Trends in Nano-Materials and Its Applications-2022 (RTNA-2022)** Dated on April 22-23, 2022, Conference E-mail:2022rtna@gmail.com

-:Oral and Poster Presentations:-

### Oral Presentations

(Date: April 22, 2022)

**OP1)** Self-focusing of Gaussian Laser Beam in Collisionless Plasma with Linear Absorption

Author: **Mr. Kalyani Y. Khandale**, Shivaji University, Kolhapur

**OP2)** Simulations Commercial BJT with Temperature for Space and Radiation Rich Environment Applications.

Author: **C M Dinesh**, Department of Physics, Govt. First Grade College and PG centre, Chintamani-563125, India.

**OP3)** Study of Dielectric and Field Modulation studies in Polymer Nanocomposites,

Author: **C. V. Chanmal**, DBF Dayanand College of Arts and Science, Solapur

### Poster Presentations

(Date: April 23, 2022)

**PP1)** Antimicrobial activity of CdS quantum dots mediated by *Aegle marmelos* leaves

Authors: **T.R. Deore**, M D Dhiware, S.B. Nahire, A.B. Gawande

**PP2)** CuO nanoparticles mediated by Coffee powder extract: An Impeder of *Candida albicans* biofilm

Authors: **P. G. Jadhav**, A.B. Gawande

**PP3)** High stability  $Mn_2O_3/MnCO_3$  microcubes synthesized by hydrothermal method for supercapacitor application

Authors: **O. C. Pore**, D. S. Sawant, A. S. Shelake, D. B. Mane, V. J. Fulari, G. M. Lohar

**PP4)** Growth study on entire replacement of Zn by Mn into  $\text{Cu}_2\text{ZnSnS}_4$  thin films by SILAR method

Authors: **H. C. Yadav**, B. V. Patil, S. S. Dhere, R. M. Shaikh , S. B. Duchal , A. M. More

**PP5)** Thin Films of  $\text{Cu}_2\text{ZnSnS}_4$  (CZTS) grown via replacement of Zn by Mg using SILAR method

Authors: **A. K. Bagal**, M. S. Shinde, K. S. Gund, G .V. Patil, A. M. Rajage, A. M. More

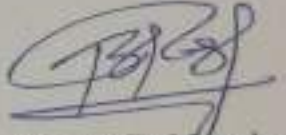
## NOTICE

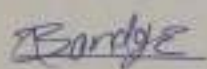
Date: 10-03-2022

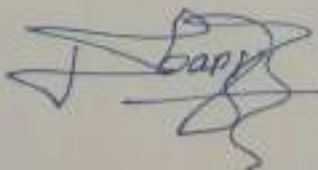
All faculty members are hereby informed that Department of Physics in collaboration with IQAC is planning to organize an **International e-Conference on Recent Trends in Nano-Materials and Its Applications-2022(RTNA-2022)**. So, for planning of RTNA-2022, you are notified that a meeting is held on 11-03-2022 at 10:00 am at Department of Physics.

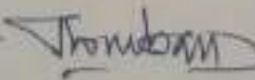
Agenda:

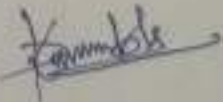
- 1) To final the dates of conference.
- 2) To allot the division of work.
- 3) To prepare conference brochure.
- 3) Any related issues.

  
Mr. B. B. Navale

1) Dr. D. K. Bandgar 

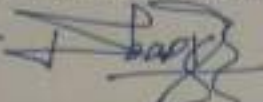
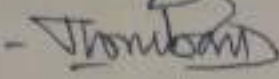
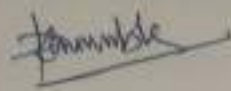
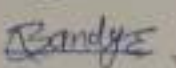
2) Dr. S. S. Dhasade 

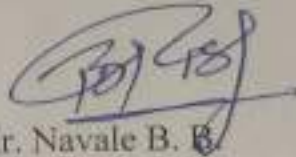
3) Dr. J. V. Thombare - 

4) Mr. A. M. Kambale - 

**Date: 11-03-2022**

A meeting of Physics faculty was held at staff room of Department of Physics on March 11, 2022 on 10:00 am. Following members were presents.

- 1) Dr. Dhasade S. S. - 
- 2) Dr. Thombare J. V. - 
- 3) Mr. Kambale A. M. - 
- 4) Dr. Bandgar D. K. - 



Mr. Navale B. B.

Head

Department of Physics

## Minutes of the meeting

Date: 11-03-2022

A meeting of Physics faculty was held at staff room of Department of Physics on March 11, 2022 on 10:00 am. Mr. Navale B. B. has worked as president of meeting and following decisions were taken;

1) As per discussion held in the meetings, the dates of RTNA-2022 are finalized as April 22-23, 2022.

2) As per interest of faculty members and requirements the division of work has been allotted as;

Mr. B. B. Navale (Head of Dept.)

Dr. S. S. Dhasade, (Convener)

Dr. J. V. Thombare (Organizing Secretary)

Mr. A. M. Kambale (Treasurer)

Dr. D. K. Bandgar (Member)

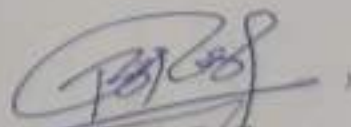
Dr. S. M. Mane (South Korea)

Dr. S. T. Navale (Spain)

3) It is decided that the RTNA-2022 brochure will be prepared by Dr. Thombare J. V. and Dr. Dhasade S. S. within time.

4) It is decided that all other related issues were discussed when they were raised.

5) At the end of meeting the vote of thanks were shared by Dr. Bandgar D. K.



Mr. Navale B.B.

Head

Department of Physics

Date: 12-03-2022

To,  
Acting Principal,  
Vidnyan Mahavidyalaya Sangola

Subject: Regarding International e-Conference.

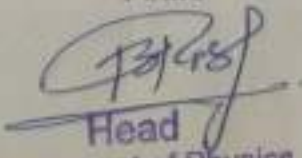
Dear Sir,

Subject mentioned above we may please inform you that, Department of Physics in collaboration with IQAC has planned to organize an **International e-Conference on Recent Trends in Nano-Materials and Its Applications-2022(RTNA-2022) dated April 22-23, 2022**. The division of work is as follows:

- Mr. B. B. Navale (Head of Dept.)
- Dr. S. S. Dhasade, (Convener)
- Dr. J. V. Thombare (Organizing Secretary)
- Mr. A. M. Kambale (Treasurer)
- Dr. D. K. Bandgar (Member)
- Dr. S. M. Mane (South Korea)
- Dr. S. T. Navale (Spain)

So, herewith I am requesting to you to allow us to organize RTNA-2022 and do the necessary communication with Punyashlok Ahilyadevi Holkar Solapur University, Solapur within time.

%c. Received  
12/3/22

Yours  
  
Head  
Department of Physics  
Vidnyan Mahavidyalaya, Sangola  
Tal - Sangola Dist - Solapur



'Sangola Taluka Shetkari Shikshan Prasarak Mandal Sangola's

# VIDNYAN MAHAVIDYALAYA SANGOLA

(Arts & Science, E.C.S. & B.C.A.)

Off. (02187) 220508

Tal. Sangola Dist. Solapur Pin. 413 307 (Maharashtra)

Mob. No. 9421045987

(Affiliated to P. A. H. Solapur University)

Email : vidnyanma@yahoo.co.in

Website : www.vmsangola.org

Acting Principal : Dr. R. A. Fule

M.A., Ph.D.

Third Cycle Accredited by NAAC

with 'B' Grade (CGPA of 2.24)

Ref. No. Email

Date : 15/03/2022

## Invitation letter

To

Prof. Jae Cheol Shin  
Dongguk University,  
South Korea

**Subject:** Invitation letter

Respected Prof. J. C. Shin sir...

Greetings from Vidnyan Mahavidyalaya, Sangola !!!!

The subject mentioned above I may please inform you that Department of Physics in Collaboration with Internal Quality Assurance Cell (IQAC), Vidnyan Mahavidyalaya, Sangola has organized International e-Conference on Recent Trends in Nano-Materials and Its Applications-2022 (RTNA-2022) dated April 22-23, 2022.

As per discussion with you, we are requesting to you to work as a resource person for the RTNA-2022. Hope you will accept the same. Shortly we will send the detailed technical program.

Thanking you

Yours

  
Acting Principal  
Vidnyan Mahavidyalaya, Sangola  
Tal. Sangola Dist. Solapur



\*Sangola Taluka Shetkari Shikshan Prasarak Mandal Sangola's

# VIDNYAN MAHAVIDYALAYA SANGOLA

(Arts & Science, E.C.S. & B.C.A.)

Tal. Sangola Dist. Solapur Pin. 413 307 (Maharashtra)  
(Affiliated to P. A. H. Solapur University)

Off. (02187) 220508

Mob. No. 9421045987

Email : vidnyanms@yahoo.co.in  
Website : www.vmsangola.org

Acting Principal : Dr. R. A. Fule  
M.A., Ph.D.

Third Cycle Accredited by NAAC  
with 'B' Grade (CGPA of 2.24)

Ref. No. - E-mail.

Date : 15/03/2022

## Invitation letter

To  
Dr. Sonaimuthu Mohandoss  
Yeungnam University,  
South Korea

Subject: Invitation letter

Dear Dr. Sonaimuthu Mohandoss sir...

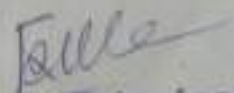
Greetings from Vidnyan Mahavidyalaya, Sangola !!!!

The subject mentioned above I may please inform you that Department of Physics in Collaboration with Internal Quality Assurance Cell (IQAC), Vidnyan Mahavidyalaya, Sangola has organized International e-Conference on Recent Trends in Nano-Materials and Its Applications-2022 (RTNA-2022) dated April 22-23, 2022.

As per discussion with you, we are requesting to you to work as a resource person for the RTNA-2022. Hope you will accept the same. Shortly we will send the detailed technical program.

Thanking you

Yours

  
Acting Principal  
Vidnyan Mahavidyalaya, Sangola  
Tal. Sangola Dist. Solapur



'Sangola Taluka Shetkari Shikshan Prasarak Mandal Sangola's

# VIDNYAN MAHAVIDYALAYA SANGOLA

(Arts & Science, E.C.S. & B.C.A.)

Off. (02187) 220508

Tal. Sangola Dist. Solapur Pin. 413 307 (Maharashtra)

Mob. No. 9421045987

(Affiliated to P. A. H. Solapur University)

Email vidnyanma@yahoo.co.in

Website www.vmasangola.org

Acting Principal : Dr. R. A. Fule  
M.A., Ph.D.

Third Cycle Accredited by NAAC  
with 'B' Grade (CGPA of 2.24)

Ref. No. - E-mail-

Date : 15/03/2022

## Invitation letter

To  
Dr. M. Vasudeva Reddy  
Yeungnam University,  
South Korea

Subject: Invitation letter

Dear Dr. M. Vasudeva Reddy sir...

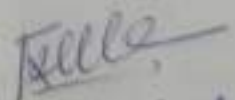
Greetings from Vidnyan Mahavidyalaya, Sangola !!!!

The subject mentioned above I may please inform you that Department of Physics in Collaboration with Internal Quality Assurance Cell (IQAC), Vidnyan Mahavidyalaya, Sangola has organized International e-Conference on Recent Trends in Nano-Materials and Its Applications-2022 (RTNA-2022) dated April 22-23, 2022.

As per discussion with you, we are requesting to you to work as a resource person for the RTNA-2022. Hope you will accept the same. Shortly we will send the detailed technical program.

Thanking you

Yours

  
Acting Principal  
Vidnyan Mahavidyalaya, Sangola  
Tal. Sangola Dist. Solapur



'Sangola Taluka Shetkari Shikshan Prasarak Mandal Sangola's

# VIDNYAN MAHAVIDYALAYA SANGOLA

(Arts & Science, E.C.S. & B.C.A.)

Off. (02187) 220508

Tal. Sangola Dist. Solapur Pin. 413 307 (Maharashtra)

Mob. No. 9421045987

(Affiliated to P. A. H. Solapur University)

Email : vidnyanms@yahoo.co.in  
Website : www.vmsangola.org

Acting Principal : Dr. R. A. Fule

M.A., Ph.D.

Third Cycle Accredited by NAAC  
with 'B' Grade (CGPA of 2.24)

Ref. No. E-mail.

Date : 15/03/2022

## Invitation letter

To

Dr. Sreekanth TVM  
Yeungnam University,  
South Korea

**Subject:** Invitation letter

Dear Dr. Sreekanth TVM sir...

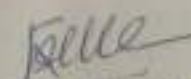
Greetings from Vidnyan Mahavidyalaya, Sangola !!!!

The subject mentioned above I may please inform you that Department of Physics in Collaboration with Internal Quality Assurance Cell (IQAC), Vidnyan Mahavidyalaya, Sangola has organized International e-Conference on Recent Trends in Nano-Materials and Its Applications-2022 (RTNA-2022) dated April 22-23, 2022.

As per discussion with you, we are requesting to you to work as a resource person for the RTNA-2022. Hope you will accept the same. Shortly we will send the detailed technical program.

Thanking you

Yours

  
**Acting Principal**  
Vidnyan Mahavidyalaya, Sangola  
Tal. Sangola Dist. Solapur



'Sangola Taluka Shetkari Shikshan Prasarak Mandal Sangola's

# VIDNYAN MAHAVIDYALAYA SANGOLA

(Arts & Science, E.C.S. & B.C.A.)

Off. (02187) 220508

Tal. Sangola Dist. Solapur Pin. 413 307 (Maharashtra)

Mob. No. 9421045987

(Affiliated to P. A. H. Solapur University)

Email : vidnyanms@yahoo.co.in  
Website : www.vmsangola.org

Acting Principal : Dr. R. A. Fule  
M.A., Ph.D.

Third Cycle Accredited by NAAC  
with 'B' Grade (CGPA of 2.24)

Ref. No. 622/2021-22

Date : 15/03/2022

To  
Registrar  
Punyashlok Ahilyadevi Holkar Solapur University,  
Solapur.

Subject: Regarding International e-Conference RTNA-2022.

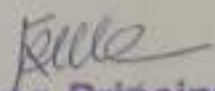
Dear sir/madam,

The subject mentioned above I may please inform you that Department of Physics in collaboration with IQAC has organized **International e-Conference on Recent Trends in Nano-Materials and Its Applications-2022 (RTNA-2022)** dated April 22-23, 2022.

So, herewith I am requesting to you to allow us to organize RTNA-2022. Also, allow us to use University Logo for RTNA-2022 purpose only.

Thanking you,

Yours

  
Acting Principal  
Vidnyan Mahavidyalaya, Sangola  
Tal. Sangola Dist. Solapur

O/c



'Sangola Taluka Shetkari Shikshan Prasarak Mandal Sangola's

# VIDNYAN MAHAVIDYALAYA SANGOLA

(Arts & Science, E.C.S. & B.C.A.)

Off. (02187) 220508

Tal. Sangola Dist. Solapur Pin. 413 307 (Maharashtra)

Mob. No. 9421045987

(Affiliated to P. A. H. Solapur University)

Email - vidnyanma@yahoo.co.in

Website : www.vmsangola.org

Acting Principal : Dr. R. A. Fule

M.A., Ph.D.

Third Cycle Accredited by NAAC  
with 'B' Grade (CGPA of 2.24)

Ref. No. - 2022-RTNA

Date : 19/04/2022

## Invitation letter

To  
Dr. Rajshekhar  
Yeungnam University,  
South Korea

**Subject:** Invitation letter

Respected Dr. Rajshekhar sir...

Greetings from Vidnyan Mahavidyalaya, Sangola !!!!

The subject mentioned above I may please inform you that Department of Physics in Collaboration with Internal Quality Assurance Cell (IQAC), Vidnyan Mahavidyalaya, Sangola has organized International e-Conference on Recent Trends in Nano-Materials and Its Applications-2022 (RTNA-2022) dated April 22-23, 2022.

As per discussion with you, we are requesting to you to work as a resource person for the RTNA-2022. Hope you will accept the same. Shortly we will send the detailed technical program.

Thanking you

Yours

**Acting Principal**  
Vidnyan Mahavidyalaya, Sangola  
Tal. Sangola Dist. Solapur



'Sangola Taluka Shetkari Shikshan Prasarak Mandal Sangola's

# VIDNYAN MAHAVIDYALAYA SANGOLA

(Arts & Science, E.C.S. & B.C.A.)

Tal. Sangola Dist. Solapur Pin. 413 307 (Maharashtra)

(Affiliated to P. A. H. Solapur University)

Off. (02187) 220508

Mob. No. 9421045987

Email - vidnyanms@yahoo.co.in

Website - www.vmsangola.org

Acting Principal : Dr. R. A. Fule

M.A., Ph.D.

Third Cycle Accredited by NAAC  
with 'B' Grade (CGPA of 2.24)

Ref. No. - RTNA-2022

Date : 19/04/2022

## Invitation letter

To  
Dr. Anamika Kadam  
Professor,  
Institute of Science, Mumbai  
Young Scientist, DST, New Delhi

**Subject:** Invitation letter

Respected Dr. Anamika Kadam madam...

Greetings from Vidnyan Mahavidyalaya, Sangola !!!!

The subject mentioned above I may please inform you that Department of Physics in Collaboration with Internal Quality Assurance Cell (IQAC), Vidnyan Mahavidyalaya, Sangola has organized International e-Conference on Recent Trends in Nano-Materials and Its Applications-2022 (RTNA-2022) dated April 22-23, 2022.

As per discussion with you, we are requesting to you to work as a **Chief Guest** for valedictory session of RTNA-2022. Hope you will accept the same.

Thanking you

Yours

**Acting Principal**

Vidnyan Mahavidyalaya, Sangola

Tal. Sangola Dist. Solapur



'Sangola Taluka Shetkari Shikshan Prasarak Mandal Sangola's

# VIDNYAN MAHAVIDYALAYA SANGOLA

(Arts & Science, E.C.S. & B.C.A.)

Off. (02187) 220508

Tal. Sangola Dist. Solapur Pin. 413 307 (Maharashtra)  
(Affiliated to P. A. H. Solapur University)

Mob. No. 9421045987  
Email : vidnyanms@yahoo.co.in  
Website : www.vmsangola.org

Acting Principal : Dr. R. A. Fule  
M.A., Ph.D.

Third Cycle Accredited by NAAC  
with 'B' Grade (CGPA of 2.24)

Ref. No. 2021-22/Email

Date : 23/04/2022

To,  
Dr. Rajshekhar,  
Yeungnam University,  
South Korea

Subject: Regarding RTNA-2022.

Dear Esteemed Professor Dr. Rajshekhar sir,

I am grateful for your invited talk at International e-Conference on Recent Trends in Nano-Materials and Its Applications (RTNA)-2022 dated April 22-23, 2022 organized by Department of Physics in collaboration with Internal Quality Assurance Cell (IQAC).

Your Invited talk on Morphology dependent electrochemical performance of electrodes has explained many things related to Supercapacitors. Particularly, you have explained morphology controlled electrodes for supercapacitors. The participants may get benefited from your Invited Talk.

I appreciate your generosity.

Thanking you,

Yours

Acting Principal  
Vidnyan Mahavidyalaya, Sangola  
Tal. Sangola Dist. Solapur



'Sangola Taluka Shetkari Shikshan Prasarak Mandal Sangola's

# VIDNYAN MAHAVIDYALAYA SANGOLA

(Arts & Science, E.C.S. & B.C.A.)

Off. (02187) 220508

Tal. Sangola Dist. Solapur Pin. 413 307 (Maharashtra)

Mob. No. 9421045987

(Affiliated to P. A. H. Solapur University)

Email: vidnyanms@yahoo.co.in

Website: www.vmsangola.org

Acting Principal : Dr. R. A. Fule

M.A., Ph.D.

Third Cycle Accredited by NAAC  
with 'B' Grade (CGPA of 2.24)

Ref. No. 2021-22/Email

Date : 23/04/2022

To,  
Dr. Sonaimuthu Mohandoss  
Yeungnam University,  
South Korea.

Subject: Regarding RTNA-2022.

Dear Esteemed Professor Dr. Sonaimuthu Mohandoss sir,

I am grateful for your invited talk at International e-Conference on Recent Trends in Nano-Materials and Its Applications (RTNA)-2022 dated April 22-23, 2022 organized by Department of Physics in collaboration with Internal Quality Assurance Cell (IQAC).

Your Invited talk on Carbon dots and its application has explained many things related to Nanotechnology. Particularly, you have explained the uses of Carbon dots in sensing and Bio-imaging. The participants may get benefited from your Invited Talk.

I appreciate your generosity.

Thanking you,

Yours

Acting Principal  
Vidnyan Mahavidyalaya, Sangola  
Tal. Sangola Dist. Solapur



'Sangola Taluka Shetkari Shikshan Prasarak Mandal Sangola's

# VIDNYAN MAHAVIDYALAYA SANGOLA

(Arts & Science, E.C.S. & B.C.A.)

Tal. Sangola Dist. Solapur Pin. 413 307 (Maharashtra)  
(Affiliated to P. A. H. Solapur University)

Off. (02187) 220508

Mob. No. 9421045987

Email : vidnyanma@yahoo.co.in  
Website : www.vmsangola.org

Acting Principal : **Dr. R. A. Fule**  
M.A., Ph.D.

Third Cycle Accredited by NAAC  
with 'B' Grade (CGPA of 2.24)

Ref. No. 2021-22 / Email

Date : 23/04/2022

To,  
**Dr. M. Vasudeva Reddy**  
Yeungnam University,  
South Korea.

**Subject: Regarding RTNA-2022.**

Dear Esteemed Professor Dr. M. Vasudeva Reddy sir,

I am grateful for your invited talk at International e-Conference on Recent Trends in Nano-Materials and Its Applications (RTNA)-2022 dated April 22-23, 2022 organized by Department of Physics in collaboration with Internal Quality Assurance Cell (IQAC).

Your Invited talk on earth abundant and ultra low cost solar cell has explained many things related to Nanotechnology. Particularly, you have explained the basics of solar cell and current status of research in solar cell. The participants may get benefited from your Invited Talk.

I appreciate your generosity.

Thanking you,

Yours

**Acting Principal**  
Vidnyan Mahavidyalaya, Sangola  
Tal. Sangola Dist. Solapur



'Sangola Taluka Shetkari Shikshan Prasarak Mandal Sangola's

# VIDNYAN MAHAVIDYALAYA SANGOLA

(Arts & Science, E.C.S. & B.C.A.)

Tal. Sangola Dist. Solapur Pin. 413 307 (Maharashtra)  
(Affiliated to P. A. H. Solapur University)

Off. (02187) 220508

Mob. No. 9421045987

Email: vidnyanme@yahoo.co.in  
Website: www.vmsangola.org

Acting Principal : Dr. R. A. Fule  
M.A., Ph.D.

Third Cycle Accredited by NAAC  
with 'B' Grade (CGPA of 2.24)

Ref. No. 2021 -22 /Email

Date : 23/04/2022

To,  
Prof.(Dr.) S. B. Kulkarni  
Associate Professor in Physics,  
Institute of Science, Mumbai

**Subject: Regarding RTNA-2022.**

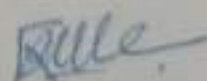
Dear Esteemed Professor Dr. Kulkarni sir,

I am grateful for your participation in International e-Conference on Recent Trends in Nano-Materials and Its Applications (RTNA)-2022 dated April 22-23, 2022 organized by Department of Physics in collaboration with Internal Quality Assurance Cell (IQAC). You have been worked as Chairperson for one the sessions.

So, on behalf of my College, I extend a really hearty vote of thanks to you for sparing time with us from your busiest schedule to grace the occasion RTNA-2022.

Thanking you,

Yours

  
Acting Principal  
Vidnyan Mahavidyalaya, Sangola  
Tal. Sangola Dist. Solapur



'Sangola Taluka Shetkari Shikshan Prasarak Mandal Sangola's

# VIDNYAN MAHAVIDYALAYA SANGOLA

(Arts & Science, E.C.S. & B.C.A.)

Tal. Sangola Dist. Solapur Pin. 413307 (Maharashtra)  
(Affiliated to P. A. H. Solapur University)

Off. (02187) 220508

Mob. No. 9421045987

Email: vidnyanms@yahoo.co.in

Website: www.vmsangola.org

Acting Principal : Dr. R. A. Fule  
M.A., Ph.D.

Third Cycle Accredited by NAAC  
with 'B' Grade (CGPA of 2.24)

Ref. No. 2021-22 / Email

Date : 23/04/2022

To,  
Dr. A. R. Babar,  
Shankarrao Mohite Mahavidyalaya,  
Akluj

Subject: Regarding RTNA-2022.

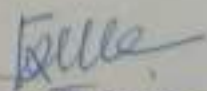
Dear Dr. Babar sir,

I am grateful for your participation in International e-Conference on Recent Trends in Nano-Materials and Its Applications (RTNA)-2022 dated April 22-23, 2022 organized by Department of Physics in collaboration with Internal Quality Assurance Cell (IQAC). You have been worked as Chairperson for one the sessions.

So, on behalf of my College, I extend a really hearty vote of thanks to you for sparing time with us from your busiest schedule to grace the occasion RTNA-2022.

Thanking you,

Yours

  
Acting Principal  
Vidnyan Mahavidyalaya, Sangola  
Tal. Sangola Dist. Solapur



'Sangola Taluka Shetkari Shikshan Prasarak Mandal Sangola's

# VIDNYAN MAHAVIDYALAYA SANGOLA

(Arts & Science, E.C.S. & B.C.A.)

Off. (02187) 220508

Tal. Sangola Dist. Solapur Pin. 413 307 (Maharashtra)  
(Affiliated to P. A. H. Solapur University)

Mob. No. 9421045987

Email : vidnyanms@yahoo.co.in  
Website : www.vmsasangola.org

Acting Principal : Dr. R. A. Fule  
M.A., Ph.D.

Third Cycle Accredited by NAAC  
with 'B' Grade (CGPA of 2.24)

Ref. No. 2021 - 22 / Email

Date : 23/04/2022

To,  
Dr. S. D. Patil  
Pratapsinh Mohite Patil Mahavidyalaya,  
Karmala

Subject: Regarding RTNA-2022.

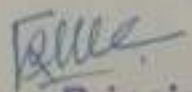
Dear Dr. Patil madam,

I am grateful for your participation in International e-Conference on Recent Trends in Nano-Materials and Its Applications (RTNA)-2022 dated April 22-23, 2022 organized by Department of Physics in collaboration with Internal Quality Assurance Cell (IQAC). You have been worked as Chairperson for one the sessions.

So, on behalf of my College, I extend a really hearty vote of thanks to you for sparing time with us from your busiest schedule to grace the occasion RTNA-2022.

Thanking you,

Yours

  
Acting Principal  
Vidnyan Mahavidyalaya, Sangola  
Tal. Sangola Dist. Solapur



\*Sangola Taluka Shetkari Shikshan Prasarak Mandal Sangola's

# VIDNYAN MAHAVIDYALAYA SANGOLA

(Arts & Science, E.C.S. & B.C.A.)

Off. (02187) 220508

Tal. Sangola Dist. Solapur Pin. 413 307 (Maharashtra)

Mob. No. 9421045987

(Affiliated to P. A. H. Solapur University)

Email : vidnyanms@yahoo.co.in

Website : www.vmssangola.org

**Acting Principal : Dr. R. A. Fule**

M.A., Ph.D.

Third Cycle Accredited by NAAC  
with 'B' Grade (CGPA of 2.24)

Ref. No. 2021 - 22 /Email

Date : 23/04/2022

To,  
Dr. R. A. Bugad,  
Sangola College,  
Sangola.

**Subject: Regarding RTNA-2022.**

Dear Dr. Bugad sir,

I am grateful for your participation in International e-Conference on Recent Trends in Nano-Materials and Its Applications (RTNA)-2022 dated April 22-23, 2022 organized by Department of Physics in collaboration with Internal Quality Assurance Cell (IQAC). You have been worked as Chairperson for one the sessions.

So, on behalf of my College, I extend a really hearty vote of thanks to you for sparing time with us from your busiest schedule to grace the occasion RTNA-2022.

Thanking you,

Yours

**Acting Principal**  
Vidnyan Mahavidyalaya, Sangola  
Tal. Sangola Dist. Solapur



\*Sangola Taluka Shetkari Shikshan Prasarak Mandal Sangola's

# VIDNYAN MAHAVIDYALAYA SANGOLA

(Arts & Science, E.C.S. & B.C.A.)

Tal. Sangola Dist. Solapur Pin. 413 307 (Maharashtra)  
(Affiliated to P. A. H. Solapur University)

Off. (02187) 220508

Mob. No. 9421045987

Email: vidnyanms@yahoo.co.in

Website: www.vmsangola.org

Acting Principal : Dr. R. A. Fule

M.A., Ph.D.

Third Cycle Accredited by NAAC  
with 'B' Grade (CGPA of 2.24)

Ref. No. 2021-22/ Email

Date : 23/04/2022

To,  
Dr. S. M. Mane,  
Dongguk University,  
South Korea.

Subject: Regarding RTNA-2022.

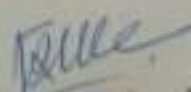
Dear Dr. Sagar Mane,

I am grateful for your participation in International e-Conference on Recent Trends in Nano-Materials and Its Applications (RTNA)-2022 dated April 22-23, 2022 organized by Department of Physics in collaboration with Internal Quality Assurance Cell (IQAC). You have been worked as Chairperson for one the sessions.

So, on behalf of my College, I extend a really hearty vote of thanks to you for sparing time with us from your busiest schedule to grace the occasion RTNA-2022.

Thanking you,

Yours

  
Acting Principal  
Vidnyan Mahavidyalaya, Sangola  
Tal. Sangola Dist. Solapur



'Sangola Taluka Shetkari Shikshan Prasarak Mandal Sangola's

# VIDNYAN MAHAVIDYALAYA SANGOLA

(Arts & Science, E.C.S. & B.C.A.)

Off. (02187) 220508

Tal. Sangola Dist. Solapur Pin. 413 307 (Maharashtra)

Mob. No. 9421045987

(Affiliated to P. A. H. Solapur University)

Email : vidnyanms@yahoo.co.in

Website : www.vmsasangola.org

Acting Principal : Dr. R. A. Fule

M.A., Ph.D.

Third Cycle Accredited by NAAC  
with 'B' Grade (CGPA of 2.24)

Ref. No. 2021-22 / Email

Date : 23/04/2022

To,  
Mr. R. S. Gaikwad,  
Vidnyan Mahavidyalaya,  
Sangola.

Subject: Regarding RTNA-2022.

Dear Mr. R. S. Gaikwad,

I am grateful for your participation in International e-Conference on Recent Trends in Nano-Materials and Its Applications (RTNA)-2022 dated April 22-23, 2022 organized by Department of Physics in collaboration with Internal Quality Assurance Cell (IQAC). You have been worked as Chairperson for one the sessions.

So, on behalf of my College, I extend a really hearty vote of thanks to you for sparing time with us from your busiest schedule to grace the occasion RTNA-2022.

Thanking you,

Yours

Acting Principal  
Vidnyan Mahavidyalaya, Sangola  
Tal. Sangola Dist. Solapur



'Sangola Taluka Shetkari Shikshan Prasarak Mandal Sangola's

# VIDNYAN MAHAVIDYALAYA SANGOLA

(Arts & Science, E.C.S. & B.C.A.)

Off. (02187) 220508

Tal. Sangola Dist. Solapur Pin. 413 307 (Maharashtra)

Mob. No. 9421045987

(Affiliated to P. A. H. Solapur University)

Email : vidnyanms@yahoo.co.in

Website : www.vmsangola.org

Acting Principal : Dr. R. A. Fule

M.A., Ph.D.

Third Cycle Accredited by NAAC  
with 'B' Grade (CGPA of 2.24)

Ref. No. 2021-22/ Email

Date : 23/04/2022

To,  
Dr. Anamika Kadam  
Professor, Institute of Science, Mumbai  
Young Scientist, DST, New Delhi

**Subject: Regarding RTNA-2022.**

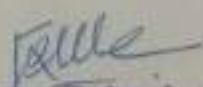
Dear Esteemed Professor Dr. Anamika Madam,

With due respect, I would like to thank you for your kind presence on Zoom meeting platform as a Chief Guest at the Valedictory Session of International e-Conference on Recent Trends in Nano-Materials and Its Applications (RTNA)-2022 dated April 22-23, 2022 organized by Department of Physics in collaboration with Internal Quality Assurance Cell (IQAC). We felt great pleasure to have you among us. You took the festivity of RTNA-2022 to a greater level by your zealous speech to the participants. Everyone appreciated your kind thoughts and motivation which you inculcated into the young researcher. Your presence was inspirational for us.

In this regard, we would like to thank you for your presence on Zoom meeting platform. We will be looking forward to having more of your presence in future events. Thanking you on the behalf of Vidnyan Mahavidyalaya, Sangola.

Thanking you,

Yours

  
Acting Principal  
Vidnyan Mahavidyalaya, Sangola  
Tal. Sangola Dist. Solapur



'Sangola Taluka Shetkari Shikshan Prasarak Mandal Sangola's

# VIDNYAN MAHAVIDYALAYA SANGOLA

(Arts & Science, E.C.S. & B.C.A.)

Off. (02187) 220508

Tal. Sangola Dist. Solapur Pin. 413 307 (Maharashtra)

Mob. No. 9421045987

(Affiliated to P. A. H. Solapur University)

Email : vidnyanms@yahoo.co.in

Website : www.umssangola.org

Acting Principal : Dr. R. A. Fule

M.A., Ph.D.

Third Cycle Accredited by NAAC  
with 'B' Grade (CGPA of 2.24)

Ref. No. 2021-22/Email

Date : 23/04/2022

"To whomsoever it may concern"

Department of Physics in collaboration with Internal Quality Assurance Cell (IQAC) has successfully organized and completed an International e-Conference on Recent Trends in Nano-Materials and Its Applications (RTNA)-2022 dated April 22-23, 2022. Dr. J. V. Thombare worked as Organizing Secretary for RTNA-2022.

Acting Principal

Vidnyan Mahavidyalaya, Sangola  
Tal. Sangola Dist. Solapur



'Sangola Taluka Shetkari Shikshan Prasarak Mandal Sangola's

# VIDNYAN MAHAVIDYALAYA SANGOLA

(Arts & Science, E.C.S. & B.C.A.)

Tal. Sangola Dist. Solapur Pin. 413 307 (Maharashtra)  
(Affiliated to P. A. H. Solapur University)

Off. (02187) 220508

Mob. No. 9421045987

Email : vidnyanms@yahoo.co.in

Website : www.vmsangola.org

**Acting Principal : Dr. R. A. Fule**  
M.A., Ph.D.

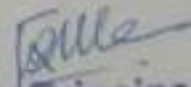
Third Cycle Accredited by NAAC  
with 'B' Grade (CGPA of 2.24)

Ref. No. 2021-22/Email

Date : 23/04/2022

**"To whomsoever it may concern"**

Department of Physics in collaboration with Internal Quality Assurance Cell (IQAC) has successfully organized and completed an International e-Conference on Recent Trends in Nano-Materials and Its Applications (RTNA)-2022 dated April 22-23, 2022. Dr. D. K. Bandgar worked as Member of Organizing Committee for RTNA-2022.

  
**Acting Principal**  
Vidnyan Mahavidyalaya, Sangola  
Tal. Sangola Dist. Solapur



'Sangola Taluka Shetkari Shikshan Prasarak Mandal Sangola's

# VIDNYAN MAHAVIDYALAYA SANGOLA

(Arts & Science, E.C.S. & B.C.A.)

Off. (02187) 220508

Tal. Sangola Dist. Solapur Pin. 413 307 (Maharashtra)

Mob. No. 9421045987

(Affiliated to P. A. H. Solapur University)

Email : vidnyanma@yahoo.co.in

Website : www.vmsangola.org

Acting Principal : Dr. R. A. Fule

M.A., Ph.D.

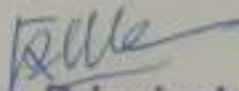
Third Cycle Accredited by NAAC  
with 'B' Grade (CGPA of 2.24)

Ref. No. 2021-22/Email

Date : 23/04/2022

"To whomsoever it may concern"

Department of Physics in collaboration with Internal Quality Assurance Cell (IQAC) has successfully organized and completed an International e-Conference on Recent Trends in Nano-Materials and Its Applications (RTNA)-2022 dated April 22-23, 2022. Mr. B. B. Navale worked as Member of Organizing Committee for RTNA-2022.

  
Acting Principal

Vidnyan Mahavidyalaya, Sangola  
Tal. Sangola Dist. Solapur



'Sangola Taluka Shetkari Shikshan Prasarak Mandal Sangola's

# VIDNYAN MAHAVIDYALAYA SANGOLA

(Arts & Science, E.C.S. & B.C.A.)

Tal. Sangola Dist. Solapur Pin. 413 307 (Maharashtra)  
(Affiliated to P. A. H. Solapur University)

Off. (02187) 220508

Mob. No. 9421045987

Email - vidnyanma@yahoo.co.in  
Website - www.vmsangola.org

Acting Principal : Dr. R. A. Fule  
M.A., Ph.D.

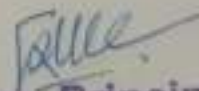
Third Cycle Accredited by NAAC  
with 'B' Grade (CGPA of 2.24)

Ref. No. 2021-22/Email

Date : 23/04/2022

"To whomsoever it may concern"

Department of Physics in collaboration with Internal Quality Assurance Cell (IQAC) has successfully organized and completed an International e-Conference on Recent Trends in Nano-Materials and Its Applications (RTNA)-2022 dated April 22-23, 2022. Dr. S. S. Dhasade worked as Convener for RTNA-2022.

  
Acting Principal  
Vidnyan Mahavidyalaya, Sangola  
Tal. Sangola Dist. Solapur



Sangola Taluka Shetkari Shikshan Prasarak Mandal Sangola's

# VIDNYAN MAHAVIDYALAYA SANGOLA

(Arts & Science, E.C.S. & B.C.A.)

Tal. Sangola Dist. Solapur Pin. 413 307 (Maharashtra)  
(Affiliated to P. A. H. Solapur University)

Off. (02187) 220508

Mob. No. 9421045987

Email: vidnyanms@yahoo.co.in

Website: www.vmsangola.org

Acting Principal : Dr. R. A. Fule  
M.A., Ph.D.

Third Cycle Accredited by NAAC  
with 'B' Grade (CGPA of 2.24)

Ref. No. 2021-22/Email

Date : 23/04/2022

To,  
Prof. (Dr.) Jae Cheol Shin  
Dongguk University, South Korea.

Subject: Regarding RTNA-2022.

Dear Esteemed Professor Dr. Shin sir,

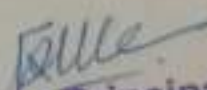
I am grateful for your keynote address at International e-Conference on Recent Trends in Nano-Materials and Its Applications (RTNA)-2022 dated April 22-23, 2022 organized by Department of Physics in collaboration with Internal Quality Assurance Cell (IQAC).

Your keynote address has explained many things related to Nanomaterials. Particularly, you have explained the use of Nanotechnology and Nano-Materials in Solar cell and related devices. The participants may get benefited from your keynote address.

I appreciate your generosity.

Thanking you,

Yours

  
Acting Principal  
Vidnyan Mahavidyalaya, Sangola  
Tal. Sangola Dist. Solapur



'Sangola Taluka Shetkari Shikshan Prasarak Mandal Sangola's

# VIDNYAN MAHAVIDYALAYA SANGOLA

(Arts & Science, E.C.S. & B.C.A.)

Tal. Sangola Dist. Solapur Pin. 413 307 (Maharashtra)  
(Affiliated to P. A. H. Solapur University)

Off. (02187) 220508

Mob. No. 9421045987

Email : vidnyanma@yahoo.co.in  
Website : www.vmasangola.org

Acting Principal : Dr. R. A. Fule  
M.A., Ph.D.

Third Cycle Accredited by NAAC  
with 'B' Grade (CGPA of 2.24)

Ref. No. 2021-22/ Email

Date : 23/04/2022

To,  
Prof. (Dr.) Jae Cheol Shin  
Dongguk University, South Korea.

Subject: Regarding RTNA-2022.

Dear Esteemed Professor Dr. Shin sir,

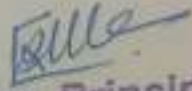
I am grateful for your keynote address at International e-Conference on Recent Trends in Nano-Materials and Its Applications (RTNA)-2022 dated April 22-23, 2022 organized by Department of Physics in collaboration with Internal Quality Assurance Cell (IQAC).

Your keynote address has explained many things related to Nanomaterials. Particularly, you have explained the use of Nanotechnology and Nano-Materials in Solar cell and related devices. The participants may get benefited from your keynote address.

I appreciate your generosity.

Thanking you,

Yours

  
Acting Principal  
Vidnyan Mahavidyalaya, Sangola  
Tal. Sangola Dist. Solapur



**3.2.2 - Number of workshops/seminars conducted  
on Research Methodology, Intellectual  
Property Rights (IPR) and entrepreneurship  
during the year-2021-22**

**Documents**

**3.2.2 conference by Botany**

## वनस्पतीशास्त्र विभाग विज्ञान महाविद्यालय सांगोला आयोजित आंतरराष्ट्रीय परिषद संपन्न

सांगोला(प्रतिनिधी):-विज्ञान महाविद्यालय सांगोला (वनस्पतीशास्त्र विभाग),इंडियन वुमन सार्वटिस्ट असोसिएशन कोल्हापूर शाखा व इतर काही महाविद्यालये यांच्या संयुक्त विद्यमाने एक दिवशीय आंतरविद्याशाखीय आंतरराष्ट्रीय परिषद (ऑन लाइन) अतिशय उत्तम प्रकारे संपन्न झाली.

'नर्चर द नेचर टू स्ट्रेनदन द फ्युचर'(उज्वल भविष्यासाठी निसर्ग संगोपन) या विषयावरती ही कार्यशाळा घेण्यात आली. या कार्यशाळेची मुख्य संकल्पना 'महिला आणि पर्यावरण' अशी होती. या कार्यशाळेचे उद्घाटन कुंडीतील वडाच्या झाडाला पाणी घालून करण्यात आले. उद्घाटन कार्यक्रमाच्या अध्यक्षता डॉ. रिटा, अध्यक्षता इंडियन वुमन सार्वटिस्ट असोसिएशन, (मुंबई) यांनी कार्यशाळेचे उद्घाटन झाल्याचे जाहीर केले. परिषदेच्या सुरुवातीला विज्ञान महाविद्यालयातर्फे वनस्पतीशास्त्र विभागाच्या प्राध्यापिका डॉ. सी. सीमा गायकवाड (सह-संयोजक- इंडियन वुमन सार्वटिस्ट असोसिएशन, कोल्हापूर शाखा) यांनी महाविद्यालयाची भूमिका स्पष्ट केली. या परिषदेत 'महिला व पर्यावरणाच्या सामाजिक फायद्यासाठी अंतराळ तंत्रज्ञानाचा उपयोग' यावर सावित्रीबाई फुले पुणे विद्यापीठातील इन्डोच्या अंतराळ तंत्रज्ञान कक्ष येथे चेअर प्रोफेसर डॉ. दीप्ती देवबागकर, तर 'महिला आणि पर्यावरणाच्या शाश्वत विकासाचे सामाजिक व आर्थिक पैलू' यावर पुण्यश्लोक अहिल्यादेवी होळकर सोलापूर विद्यापीठ सोलापूर च्या कुलगुरू डॉ.मृणालिनी फडणवीस यांनी मांडणी केली. तर 'ग्रामीण महिलांसाठी नैसर्गिक संसाधने आणि

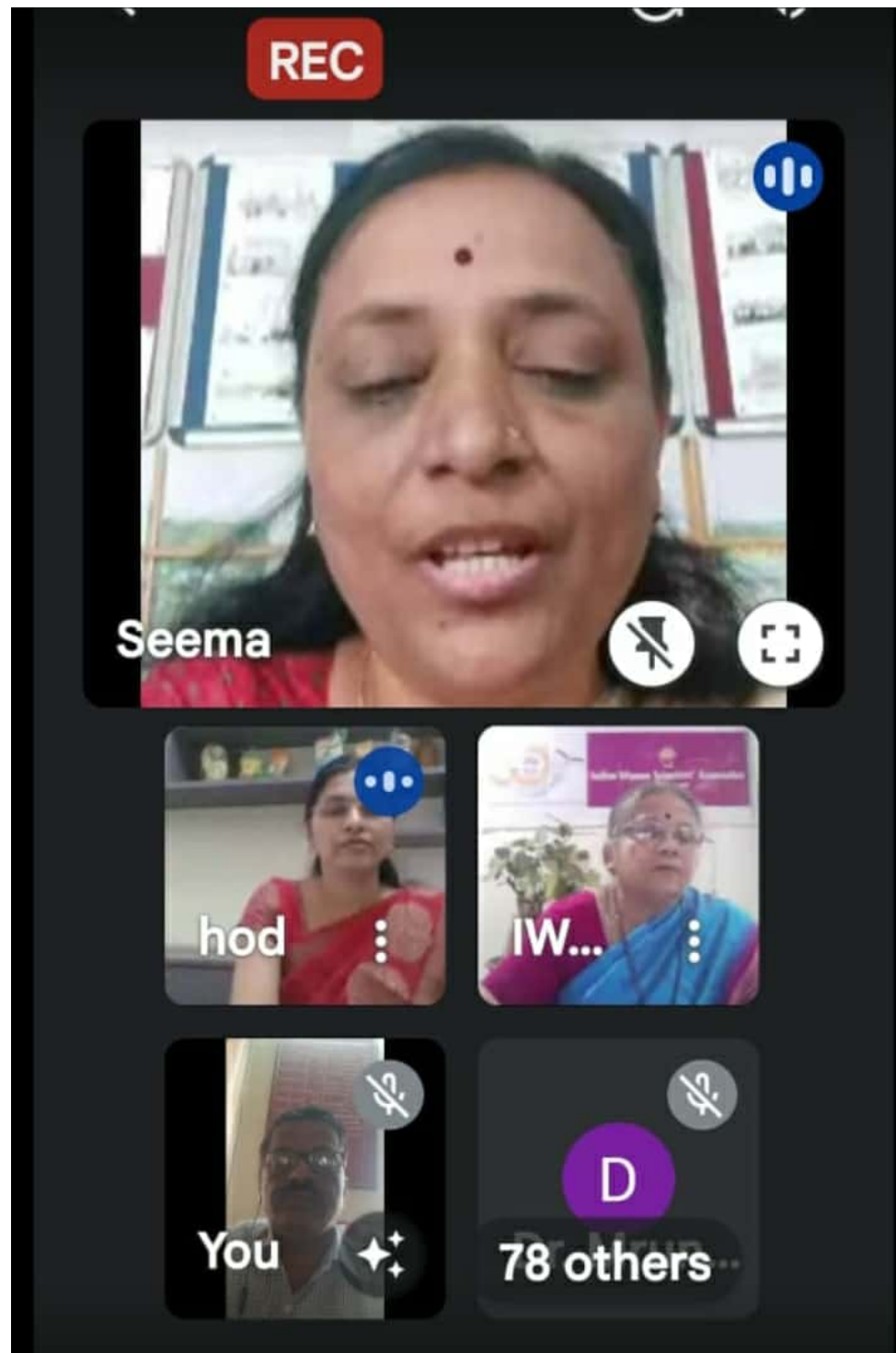
गुंतवणूक' यावर रिझर्व बँकेच्या डेप्युटी गव्हर्नर उषा थोरात, तर 'कृषी व औद्योगिक कचरा मुल्यमापन चक्रीय अर्थव्यवस्थेच्या दिशेने वाटचाल' यावर कोडोन बायोसायान्स च्या डॉ. अर्चना ठाकूर यांनी मांडणी केली. तर 'जागतिक वाजारपेठेतील बहुचर्चित पिकावर अंतर विद्याशाखीय दृष्टिकोनातून नवीन संधी ची ओळख' यावर डॉ. मनीषा राजे भोसले यांनी यूके (लंडन) येथून व डॉ.कविता माथूर (नोर्थ कॅरोलीना स्टेट युनिव्हर्सिटी, अमेरिका) यांनी इन्व्हेंस्युएशन ऑफ अँटीमायक्रोबियल अँड अँटीव्हायरल प्रॉपर्टीज ऑफ टेक्सटाइल सरफेस या विषयावरती आपली उत्कृष्ट मांडणी केली.

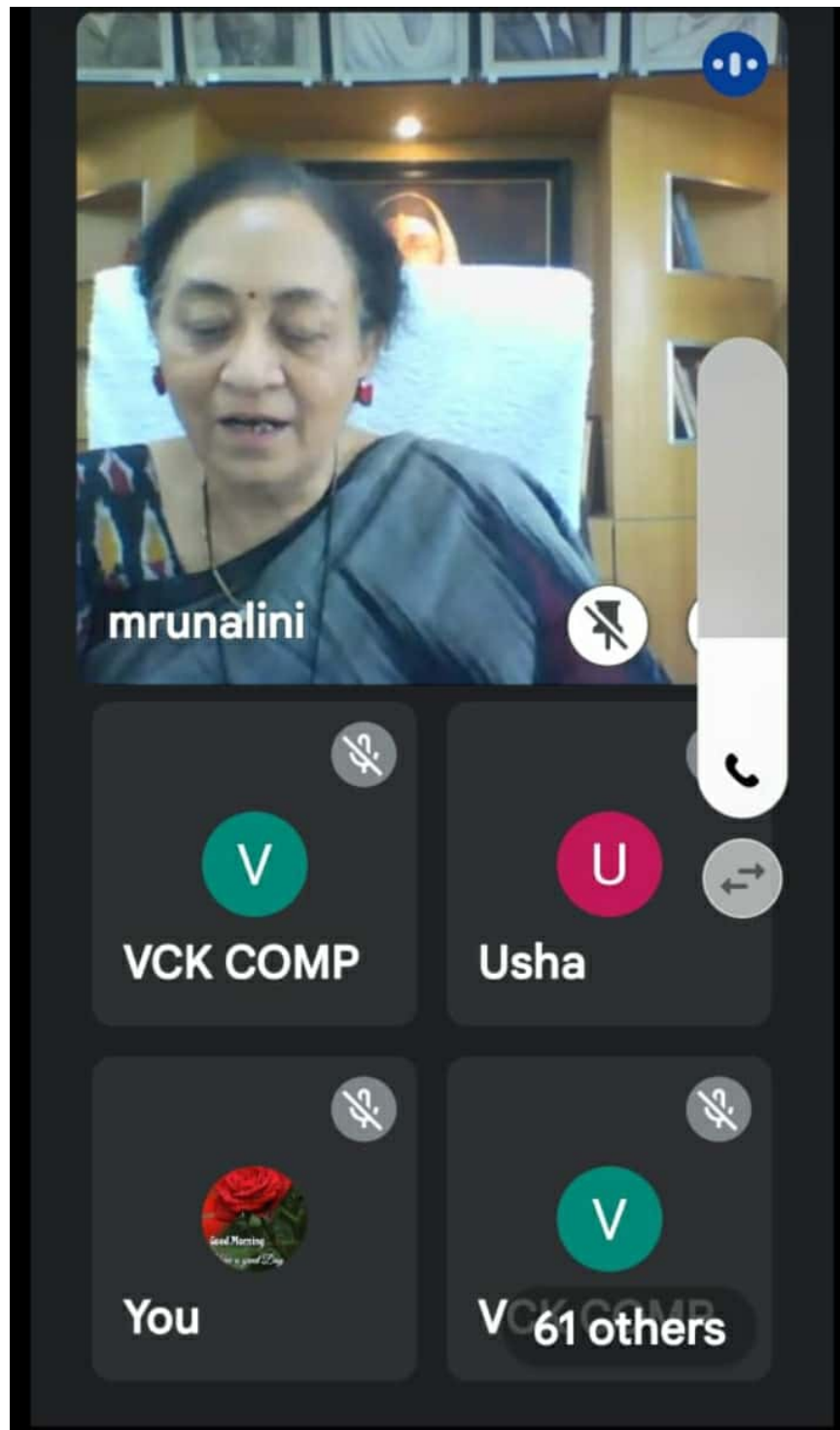
महिला व पर्यावरण व्यवस्थापन भूमिका, संबंधित पर्यावरणासह सामाजिक फायद्यासाठी अवकाश तंत्रज्ञान, तटीय जैवविविधता संवर्धन, पाणी जिर्णोध्दार, निसर्गाचे पालन-पोषण करण्यासाठी महिलांची सामाजिक पर्यावरणीय भूमिका, नैसर्गिक संशोधन संसाधन व्यवस्थापनाच्या संदर्भात अर्थशास्त्र, नैसर्गिक साधन संपत्तीवर अवलंबून उपजीविका पद्धती, सेंट्रिय शेती करणाऱ्या महिला, महिला शाश्वत निसर्ग उभारणीत भूमिका आदी विषयांवर सुमारे २० संशोधक सहभागींनी आपले पेंपर सादर केले. या सत्रासाठी अध्यक्ष म्हणून डॉ. निरंजना चव्हाण, डॉ.धनश्री पाटील, डॉ. ललीता धारेखर यांनी काम पाहिले तर रेपोटीयर म्हणून डॉ. अंजली साळवी यांनी तर पेंपर सादरीकरण सत्रात डॉ. पद्मश्री आवटे, डॉ. मृणालिनी देसाई यांनी काम पाहिले. इंडियन वुमन सार्वटिस्ट असोसिएशन च्या संयोजक दिपाली

तायवडे-पाटील यांनी सर्वांचे आभार मानले संपूर्ण कार्यक्रमाचे सुत्रसंचलन डॉ. अनुराधा सामंत यांनी केले.

टेकिनकल को-ऑर्डिनेटर म्हणून वनस्पतिशास्त्र विभागप्रमुख डॉ. राजेंद्र सूर्यवंशी व नितीन कचठणकर यांनी काम पाहिले. या परिषदेसाठी जवळजवळ १८० सहभागींनी आपला सहभाग नोंदवला होता. या परिषदेनिमित्त आलेल्या संशोधक विद्यार्थ्यांचे निबंध आय. एस. एस. एन. नंबर व उत्तम इम्पॅक्ट पॅन्टर असलेल्या आंतरराष्ट्रीय जर्नल मध्ये प्रसिद्ध केले जाणार आहेत.

या आंतरराष्ट्रीय परिषदेचा एक भाग म्हणून दि. ८ मार्च २०२२ रोजी जागतिक महिला दिनानिमित्त सेंट्रिय शेती, पर्यावरण व निसर्ग संवर्धन या क्षेत्रामध्ये काम करणाऱ्या विविध महिलांचा सत्कार समारंभ महाविद्यालयामध्ये आयोजित करण्यात आला होता. सेंट्रिय शेती बरोबरच मोरिंगा (शेवगा) पावडर निर्यात करणाऱ्या सारिका ताई घाडगे, कृषिरत्न पुरस्कार मिळालेल्या निताताई ढोबळे व वनविभागामध्ये काम करून निसर्ग संवर्धन करीत असलेल्या वनिताताई इंगोले यांना सन्मानित करण्यात आले होते. या आंतरराष्ट्रीय परिषदेच्या उत्कृष्ट आयोजनाबद्दल संस्था सचिव मा. बिठ्ठलराव शिंदे व महाविद्यालयाचे प्राचार्य डॉ. रघुनाथ फुले यांनी वनस्पती शास्त्र विभागाचे कौतुक केले केले. या परिषदेच्या यशस्वीतेसाठी वनस्पती शास्त्र विभागाचे विभाग प्रमुख डॉ. राजेंद्र सूर्यवंशी, डॉ. सीमा गायकवाड, प्रा. मारुती हाके व श्री. वसंत घुसाळे यांनी परिश्रम घेतले.







**3.2.2 - Number of workshops/seminars conducted on Research Methodology, Intellectual Property Rights (IPR) and entrepreneurship during the year-2021-22**

**Documents**

**3.2.2 workshop Organized**

- 1) Food processing and fruit preservation**
- 2) workshop on STSSP teaching and learning application**
- 3) workshop on stress management and stress removal**
- 4) Workshop on IPR**



↪ Inauguration Function ↪



# DEPARTMENT OF BOTANY

Vidnyan Mahavidyalaya, Sangola

↪ Inauguration of ↪

**"FOOD PROCESSING & FRUIT PRESERVATION"**

☆ Chairman ↪ **Dr. R. A. Fule** (Act. Principal, V. M. Sangola)

☆ Chief Guests ↪ **Dr. Ashokrao Shinde** (Member STSSPM)

**Prof. V. K. Ghadage** (Vice-Principal, V. M. Sangola)

**Mrs. Lata Kambale** (Course Trainer)

**Dr. R. S. Suryavanshi** (HoD, Dept. of Botany)



Date: 17/02/2022



Vidnyan Mahavidyalaya, Sangola  
Inauguration of,

**"FOOD PROCESSING & FRUIT PRESERVATION"**

**Organized by BOTANY DEPARTMENT**

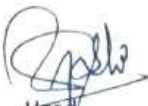
17th Feb 2022 (10 a.m.)

**•Program Schedule•**

◉Inauguration◉

1. Introduction: Prof. Dr. R. S. Suryavanshi – Head Dept. of Botany
2. Felicitation:
  - a. Dr. A. V. Shinde -Chief Guest (Member STSSPM)
  - b. Dr. R. A. Fule -President (Act. Principal V. M. Sangola)
  - c. Prof. V. K. Ghadage – Vice-Principal V. M. Sangola
  - d. Mrs. Lata Kambale – Course Trainer
  - e. Dr. Seema Gaikwad- Course Coordinator
  - f. Dr. R. S. Suryavanshi - HOD Botany VMS
3. Speech:
  - a. Chief Guest - Dr. A. V. Shinde
  - b. President - Dr. R. A. Fule
4. Vote of Thanks: Asso. Prof. Mr. Hake M. A. (2 min.)
5. Anchoring: Dr. Seema Gaikwad

  
Coordinator

  
Head  
Prof. R. S. Suryavanshi  
Head  
Dept. of Botany  
Vidnyan Mahavidyalaya,  
Sangola Dist. Solapur

  
Acting Principal  
Vidnyan Mahavidyalaya, Sangola  
Tal. Sangola Dist. Solapur



'Sangola Taluka Shetkari Shikshan Prasarak Mandal Sangola's

# VIDNYAN MAHAVIDYALAYA SANGOLA

(Arts & Science, E.C.S. & B.C.A.)

Tal.Sangola Dist.Solapur Pin. 413 307 (Maharashtra)

(Affiliated to Solapur University)

Acting Principal : **Dr. R. A. PHULE**

M.A, Ph.D.

Off. (02187) 220508

Resi. (02187) 221151

Fax : (02187) 222306

Email : vidnyanms@yahoo.co.in

Website : www.vmssangola.org

Re-Accredited by NAAC with 'B' Grade (CGPA of 2.76)

**Ref. No.**

**Date :** / /201

Date: 16.02.2022

**To**

**Dr. Ashokrao Shinde**

**Director - Sangola Taluka Shetkari Shikshan Prasarak Mandal**

**Subject: Invitation as a Chief Guest**

Respected Sir,

We cordially invite you as a Chief Guest and Speaker for Inauguration of "Food Processing and Fruit Preservation" organized by Botany Department in our college on 17.02.2022, 10.00 a.m.

Your guidance will enrich our student for their skill development.

Thanking You,

Yours Sincerely

  
Prof. R. S. Suryavanshi  
Head  
Dept. of Botany  
Vidnyan Mahavidyalaya,  
Sangola Taluka Solapur-413307

  
Acting Principal  
Vidnyan Mahavidyalaya, Sangola  
Tal. Sangola Dist. Solapur



'Sangola Taluka Shetkari Shikshan Prasarak Mandal Sangola's

# VIDNYAN MAHAVIDYALAYA SANGOLA

(Arts & Science, E.C.S. & B.C.A.)

Tal.Sangola Dist.Solapur Pin. 413 307 (Maharashtra)

Off. (02187) 220508

Resi. (02187) 221151

Fax : (02187) 222306

Acting Principal : Dr. R. A. PHULE (Affiliated to Solapur University)

M.A. Ph.D.

Email : vidnyanms@yahoo.co.in

Website : www.umssangola.org

Re-Accredited by NAAC with 'B' Grade (CGPA of 2.76)

Ref. No.

Date : / /201

Date: 17.02.2022

To

Dr. Ashokrao Shinde

Director - Sangola Taluka Shetkari Shikshan Prasarak Mandal

Subject: Vote of Thanks

Respected Sir,

We are very much pleased to have your valuable guidance as Chief Guest for "Food Processing and Fruit Preservation" organized by Botany Department in our college on 17.02.2022, 10.00 a.m.

Your speech was really important for the students. Once again we extend our heartfelt gratitude towards you. Thank you very much for your co-operation. We expect the same in future.

Thanking You,

Yours Sincerely

  
Prof. R. S. Suryavanshi  
Head  
Dept. of Botany  
Vidnyan Mahavidyalaya,  
Sangola Tal. Solapur, 413 307

  
Acting Principal  
Vidnyan Mahavidyalaya, Sangola  
Tal. Sangola Dist. Solapur

# INAUGURATION



Figure 1: Anchor- Miss. Shembade



Figure 2: Welcome speech Dr. Seema Gaiwad



**Figure 3: Introduction of Course by Dr. Rajendra Suryavanshi**



**Figure 4: Present Audience**



Figure 5: Chief Guest - Dr. Ashokrao Shinde



Figure 6: Chief Guest - Dr. Ashokrao Shinde



Figure 7: Presidential Address by Dr. R. A. Fule



Figure 8: Vote of Thanks by Prof. Hake M. A.

# COURSE WORK

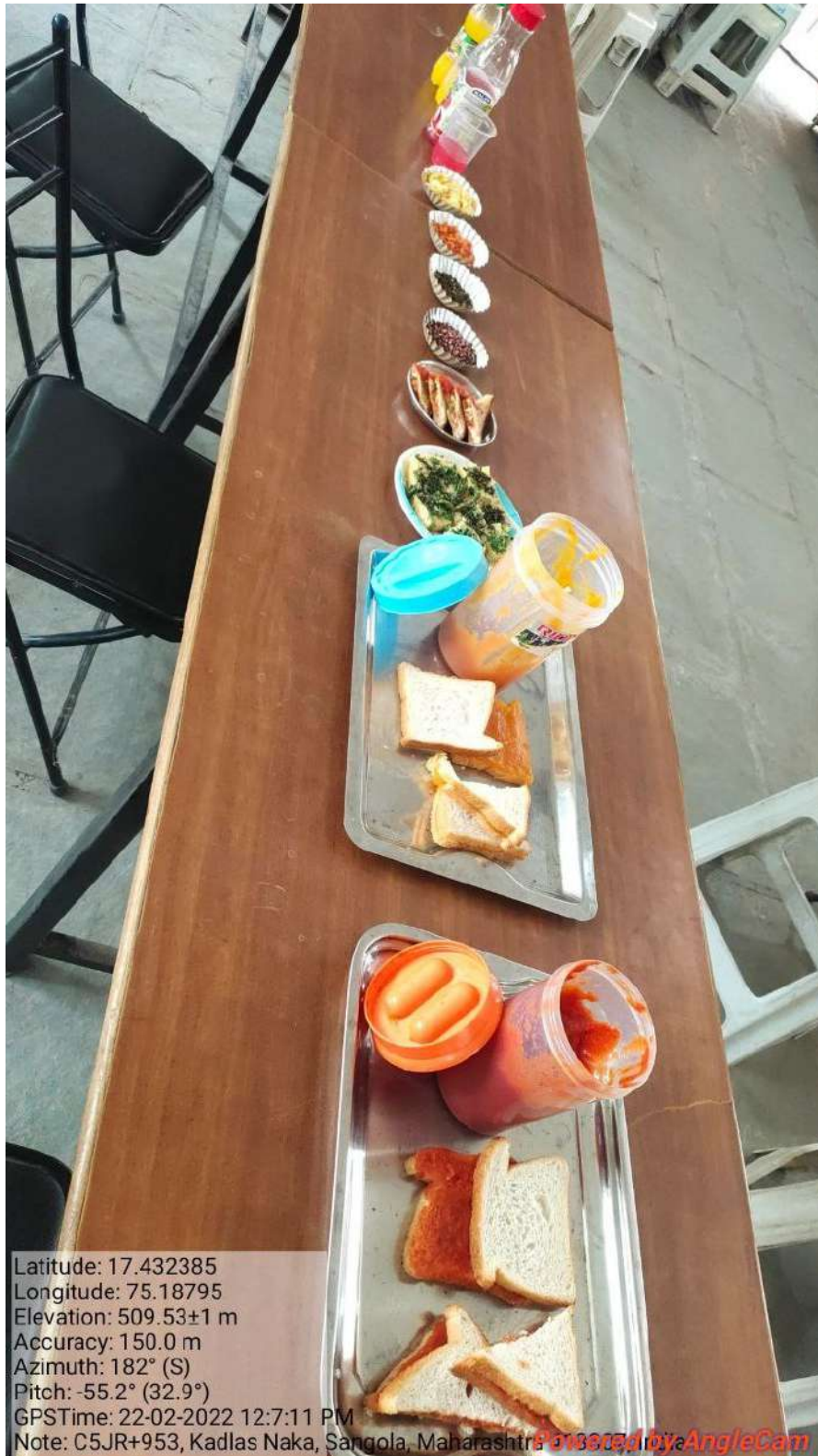
---



Figure 1: Cherry



Figure 2: Preparation of Dhokala



**Figure 3: Different Food Products prepared during Course**



Figure 4: Students during Preparations

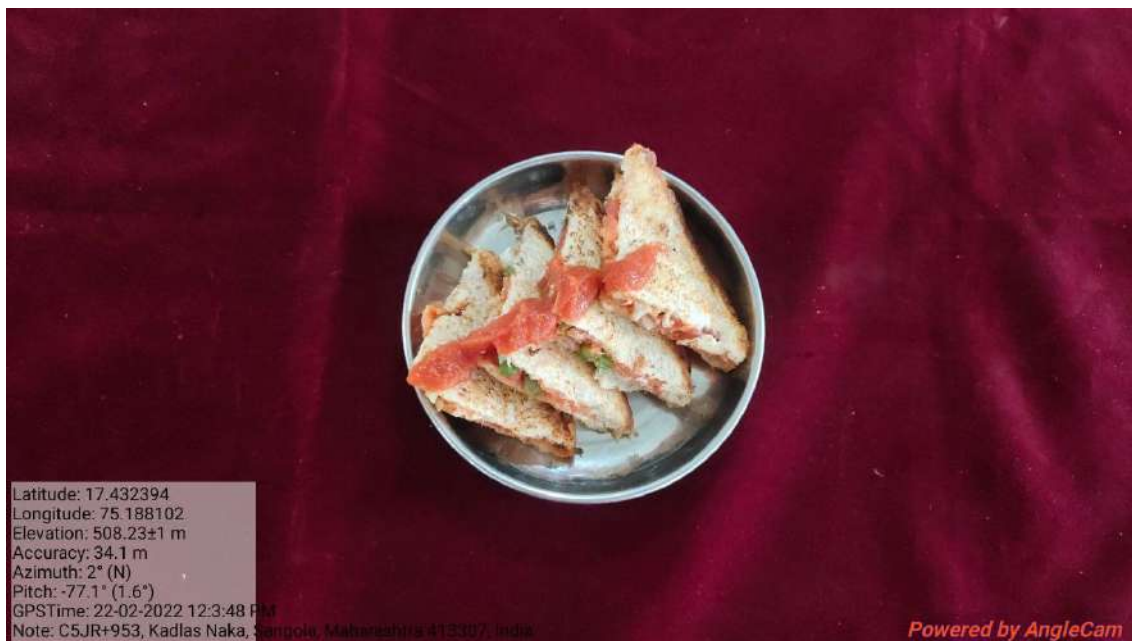


Figure 6: Jam Bread



**Figure 5: Pineapple Juice**



**Figure 7 :Pomegranate Juice**



Figure 8: Banana Wafers chips



Figure 9: Cherry



Figure 9: Preparation of Dhokala



Figure 10: Anardana



Figure 11: Masala Dry Pan



Figure 12: Pineapple Jam



Figure 13 :Tomato Sauce

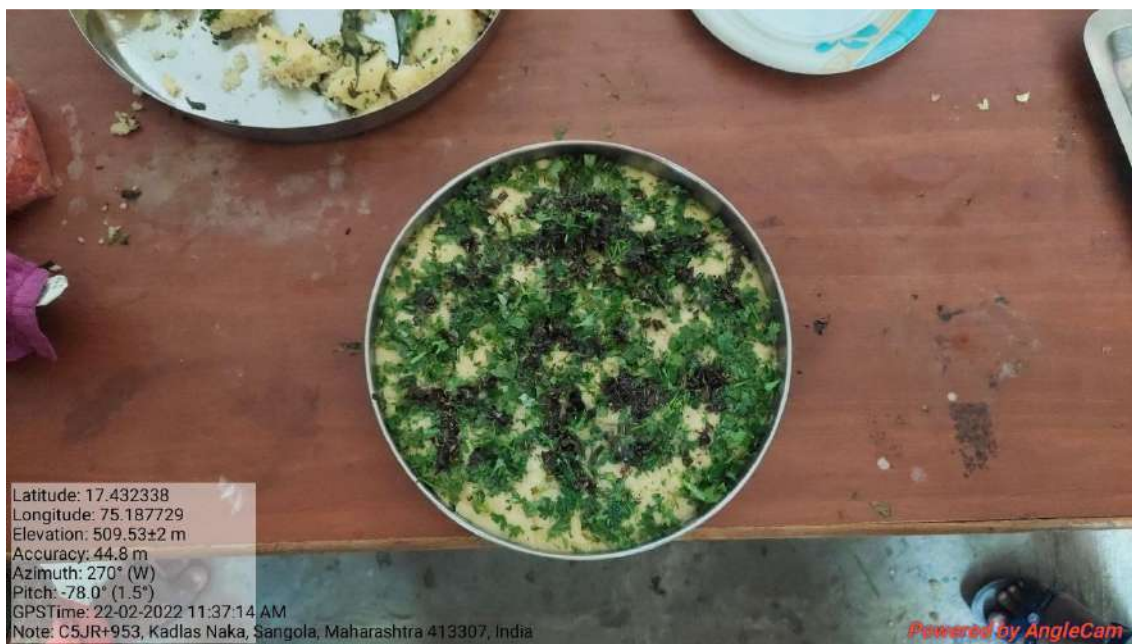


Figure 14: Preparation of Dhokala



Figure 15: Preparation of Dhokala



Figure 18: Students during Preparations



Figure 17: Students during Preparations



Figure 19: Students during Preparations



**Figure 16: Students during Preparations**



Figure 17: Students during Preparations



Figure 18: Students during Preparations



Figure 19: Students during Preparations



Figure 20: Students during Preparations



Figure 21: Students during Preparations



Figure 22: Students during Preparations



**Figure 26: Students during Preparations**



Vasud Road, Kadlas Naka, Sangola, Maharashtra  
413307, India

Latitude  
17.4323732°

Longitude  
75.188043°

Local 12:38:09 PM  
GMT 07:08:09 AM

Altitude 433.8 meters  
Friday, 18-02-2022

**Figure 27 :Principal and Chief Guest testing the Food Products**



Vasud Road, Kadlas Naka, Sangola, Maharashtra  
413307, India

Latitude  
17.4323937°

Longitude  
75.1877145°

Local 12:39:51 PM  
GMT 07:09:51 AM

Altitude 433.8 meters  
Friday, 18-02-2022

**Figure 238 :Principal and Chief Guest testing the Food Products**



Vasud Road, Kadlas Naka, Sangola, Maharashtra  
413307, India

Latitude  
17.4323624°

Longitude  
75.1880702°

Local 12:52:53 PM  
GMT 07:22:53 AM

Altitude 432.5 meters  
Friday, 18-02-2022

**Figure 29 :Principal and Chief Guest testing the Food Products**

बुधवार

दि. २३ फेब्रुवारी २०२२

दैनिक  
**सांगोला**

## विज्ञान महाविद्यालय सांगोला येथे ताणतणाव व्यवस्थापन या विषयावर कार्यशाळा संपन्न



**सांगोला/ प्रतिनिधी :**

आयक्यूएसी व स्टुडेंट वेलफेअर कमिटी यांच्या संयुक्त विद्यमाने स्ट्रेस मॅनेजमेंट ताणतणाव व्यवस्थापन या विषयावर एक दिवसीय कार्यशाळा संपन्न झाली. सदर कार्यक्रमासाठी सांगोला येथील सुप्रसिद्ध होमिओपॅथिक तज्ञ गणेश गुरव हे प्रमुख पाहुणे म्हणून उपस्थित होते.

सदर कार्यशाळेत मार्गदर्शन करताना डॉ.गणेश गुरव म्हणाले की, विद्यार्थीदशेत असताना व जीवन जगत असताना विद्यार्थ्यांना अनेक प्रकारचे ताण तणावांना सामोरे जावे लागते. ताण जीवनाचा भाग आहे. समस्या व दुःख हे सर्वांनाच असतात, पण या तणावातून व समस्येतून मार्ग काढून पुढे गेले पाहिजे. टेन्शन वर मात करणे

शिकले पाहिजे. परिस्थिती ही नेहमी बदलत असते. समस्येला संयमाची गरज असते. आपली क्षमता ओळखली पाहिजे अपेक्षा ठेवू नका व तुलना करू नका आत्मविश्वास असेल तर कोणतीही समस्या मोठी नसते नैराश्य व भीती पासून दूर राहा आभासी जगातून व खोट्या प्रतिमेतून बाहेर येऊन वास्तव याचा स्वीकार केला पाहिजे आजचे विद्यार्थी हे उद्याचे नागरिक आहेत स्वप्ने पूर्ण करण्याचा प्रयत्न करा जीवनात पुढे जात असताना विद्यार्थ्यांनी थोर महापुरुषांचा आदर डोळ्यासमोर ठेवला पाहिजे छत्रपती शिवाजी महाराज, सावित्रीबाई फुले इत्यादी थोर महापुरुषांचा जीवन चरित्रांचा अभ्यास करून त्यांच्यापासून प्रेरणा घेऊन पुढे गेले पाहिजे प्रास्ताविक करताना स्टुडेंट्स वेलफेअर कमिटीचे

चेअरमन प्रा. कैलास सगरे म्हणाले की, ताणतणावापासून मुक्त होण्यासाठी परिस्थितीचा अभ्यास केला पाहिजे व आत्मविश्वासाने पुढे गेले पाहिजे नेहमी आशावादी राहून हसत मुखाने जीवन जगले पाहिजे कार्यक्रमाचे अध्यक्ष रघुनाथ फुले म्हणाले की धोरणाचा काळ अतिशय कठीण होता पण खूप वाढला होता पण आपण बाहेर पडलो तुम्ही तुमच्या जीवनाचे शिल्पकार आहात नका रांची भवनात दूर करून नेहमी आनंदी राहा हसायला आण हसवायला आले पाहिजे. सदर कार्यक्रमाचे सूत्रसंचालन प्रा. दीपक शिंदे यांनी केले तर आभार प्रदर्शन डॉ.कदम यांनी केले. कार्यक्रमासाठी महाविद्यालयातील बहुतांश प्राध्यापक, शिक्षकेतर कर्मचारी, विद्यार्थी वर्ग मोठ्या संख्येने उपस्थित होता.

# विज्ञान महाविद्यालय सांगोला येथे ताणतणाव व्यवस्थापन या विषयावर कार्यशाळा संपन्न

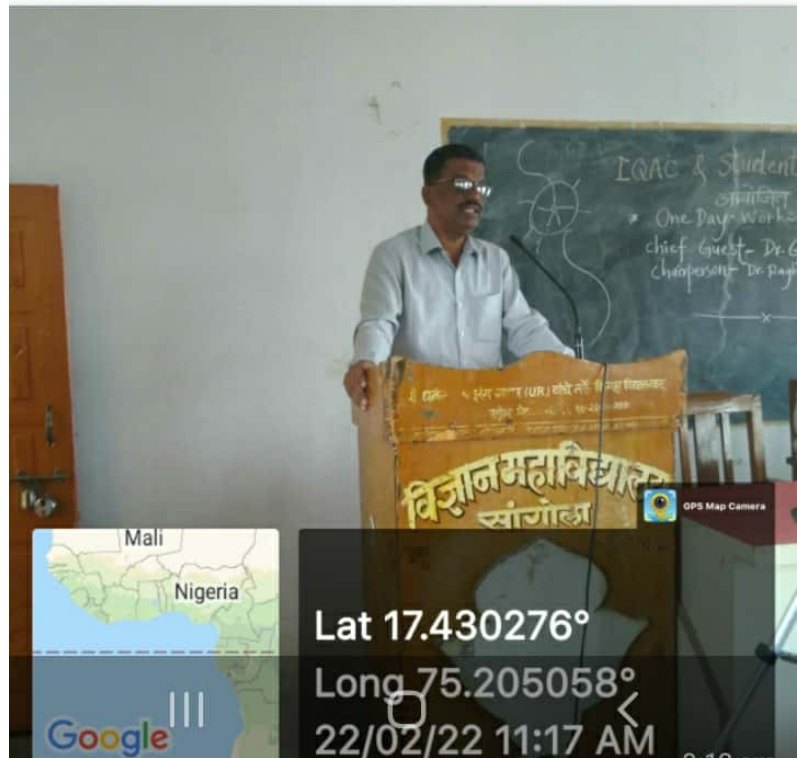
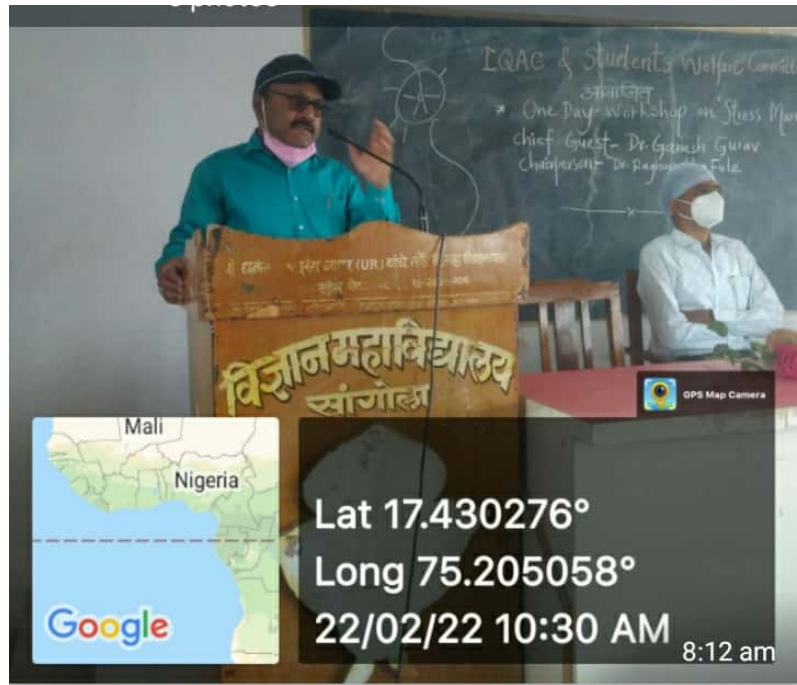
सांगोला(प्रतिनिधी):-आयक्युएसी स्टुडंट वेलफेअर कमिटी यांच्या संयुक्त विद्यमाने ताण तणाव व्यवस्थापन या विषयावर एक दिवसीय कार्यशाळा संपन्न झाली. सदर कार्यक्रमासाठी सांगोल्यातील सुप्रसिद्ध होमिओपॅथिक तज्ञ डॉ.गणेश गुरव हे प्रमुख पाहुणे म्हणून उपस्थित होते.

डॉ.गणेश गुरव म्हणाले की, विद्यार्थी दशेत असताना व जीवन जगत असताना विद्यार्थ्यांना अनेक प्रकारचे ताणतणावांना सामोरे जावे लागते. ताण हा जीवनाचा भाग आहे. समस्या व दुःख हे सर्वांनाच असतात पण या ताणातून व समस्येतून मार्ग काढून पुढे गेले पाहिजे. टेन्शन वर मात करणे शिकले पाहिजे. परिस्थितीही नेहमी बदलत असते. समस्येला संयमाची गरज असते. आजचे विद्यार्थी हे उद्याचे नागरिक आहेत. स्वप्ने पूर्ण करण्याचा प्रयत्न करा. जीवनात

पुढे जात असताना विद्यार्थ्यांनी थोर महापुरुषांचा आदर्श डोळ्यासमोर ठेवला पाहिजे. महापुरुषांच्या जीवन चरित्रांचा अभ्यास करून त्यांच्यापासून प्रेरणा घेऊन पुढे गेले पाहिजे, असे त्यांनी सांगितले.

कार्यक्रमाचे अध्यक्ष डॉ.रघुनाथ फुले म्हणाले की, कोरोनाचा काळ अतिशय कठीण होता . ताण खूप वाढला होता पण आपण बाहेर पडलो तुम्ही तुमच्या जीवनाचे शिल्पकार आहात. नकारांची भावना दूर करून नेहमी आनंदी राहा. हसायला आणि हसवायला आले पाहिजे असे त्यांनी सांगितले. यावेळी प्रा.कैलास सगरे यांनीही मनोगत व्यक्त केले.

कार्यक्रमाचे प्रास्ताविक दीपक शिंदे यांनी तर आभार प्रदर्शन डॉ.कदम यांनी केले. कार्यक्रमासाठी जिल्ह्यातील बहुतांशी प्राध्यापक व विद्यार्थी वर्ग उपस्थित होता.













\* Digital Repository Cell समितीचा अहवाल \*

Digital Repository Cell समिती माहिती

वैश्विक वर्ष 2021-22 व्याप्तीकडे काम करत असतो.

दि 20/01/2022 रोजी मा. प्राचार्य यांच्या  
समवेत जालेल्या बैठकीमध्ये एक दिवसीय

कार्यालयात HR Management System  
(GTSSPM Application) चा विषयावर संस्थेतील  
सर्व शिक्षक व शिक्षकेतर कर्मचारी यांच्यासाठी

दि 26/01/2022 रोजी. दोनवेळेने करणे. या  
कार्यालयासाठी प्रमुख पाहुणे म्हणून

Technology, पुणे मा. श्री. इमाम नदाफ  
यांना आमंत्रित केले. तसेच या कार्यालयासाठी

संस्था सदस्य मा. डॉ. अनिकेत देशमुख, सचिव.  
विठ्ठलरावजी बेशिंदे सर, व संस्थेतील सर्व  
शिक्षक व शिक्षकेतर कर्मचारी उपस्थित होते.

या कार्यालयामध्ये मा. श्री. इमाम नदाफ

या GTSSPM APP चा सवल माहिती सांगितली.

आमचे  
चेतुरमन

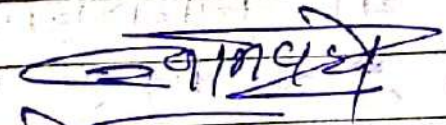
Digital Repository  
cell

Pillai  
प्रभारी प्राचार्य  
पु. वि. महाविद्यालय, सांगोल,  
ता. सांगोला जि. सोलापूर

मिडिया

मा. प्राचार्य यांच्या सहकार्याने ही सांगोला  
 रोजी Digital Repository चेा या  
 समितीची बैठक आयोजित करण्यात आली  
 या बैठकीमध्ये सांगोला तालुका सोलापूर  
 शिखर प्रयाग मंडळ सांगोला या  
 संस्थेचे Technology and Learning  
 Application (STSA) चेा या  
 व्यक्तीने उपदिवासी कार्याळा येथे  
 ठरले. या कार्याळासाठी संस्थेचे सहकार्य  
 मा. डॉ. अनिकेत (सोला) देसाय या  
 आमंत्रण देण्याचे ठरले तसेच या  
 कार्याळासाठी मा. इतम नकाफ.

Director & founder DSPUR Technology  
 Pune यांना आमंत्रण देण्याचे ठरले व ही  
 कार्याळा 26/01/2022 रोजी येथे  
 ठरले.

  
 डॉ. अनिकेत देसाय  
 Digital Repository  
 चेा

  
 डॉ. प्रभाशंपाटील  
 विज्ञान महाविद्यालय, सांगोला  
 ता. सांगोला जि. सोलापूर

'Sangola Taluka Shetkari Shikshan Prasarak Mandal Sangola's



# VIDNYAN MAHAVIDYALAYA SANGOLA

(Arts & Science, E.C.S. & B.C.A.)

Tal. Sangola Dist. Solapur Pin. 413 307 (Maharashtra)

(Affiliated to P. A. H. Solapur University)

Off. (02187) 220508

Mob. No. 9421045987

Email : vidnyanms@yahoo.co.in

Website : www.vmsangola.org

Acting Principal : Dr. R. A. Fule  
M.A., Ph.D.

Third Cycle Accredited by NAAC  
with 'B' Grade (CGPA of 2.24)

Ref. No. B7 Hemel / 2022-23

Date : 21/01/2022

## Invitation Letter

To

Mr. Imam Nadaf  
ISSTUR Technology, Pune

Subject:- An Invitation For One Day Workshop on "Institute Management System" (STSSPM Application).

Respected Sir,

We, Digital Repository Cell VidnyanMahavidyalayaSangola is please to invite you as a resource person for "Institute Management System" (STSSPM Application) For Teaching staff in the college on 26/01/2022 at 11:00 am. Please convey your acceptance.

Thank you.

Yours Faithfully

  
Coordinator  
Digital Repository Cell

  
Acting Principal  
Vidnyan Mahavidyalaya, Sangola  
Tal. Sangola Dist. Solapur



'Sangola Taluka Shetkari Shikshan Prasarak Mandal Sangola's

# VIDNYAN MAHAVIDYALAYA SANGOLA

(Arts & Science, E.C.S. & B.C.A.)

Tal. Sangola Dist. Solapur Pin. 413 307 (Maharashtra)

(Affiliated to P. A. H. Solapur University)

Off. (02187) 220508

Mob. No. 9421045987

Email : vidnyanms@yahoo.co.in

Website : www.vmssangola.org

**Acting Principal : Dr. R. A. Fule**  
M.A., Ph.D.

**Third Cycle Accredited by NAAC**  
with 'B' Grade (CGPA of 2.24)

Ref. No. *B7 Huna/2022-23*

Date : *26/01/2022*

## Thanking Letter

To

Mr. Imam Nadaf  
ISSTUR Technology, Pune

**Subject: - Thanking letter For One Day Workshop on "Institute Management System" (STSSPM Application).**

Respected Sir,

We, Digital Repository Cell Vidnyan Mahavidyalaya Sangola is please to thank you for your valuable guidance as a resource person on "Institute Management System" (STSSPM Application) Teaching staff in the college on 26/01/2022 at 11:00 am.

Thank you.

Yours Faithfully

  
Coordinator

Digital Repository Cell

  
**Acting Principal**  
Vidnyan Mahavidyalaya, Sangola  
Tal. Sangola Dist. Solapur

# STSSPM App

## **Institute Management:**

Covering each and every aspect of managing your institution like lead generation, enquiries, students, attendance, timetables etc.

**Video Sharing and Management:** Completely secure advanced video player to manage and share video content which cannot be downloaded or screen recorded and screen shared and many other such highlighting features.

**Live Online Interactive Classes:** Provides two way video live lectures with recording, screen sharing, Live Chat and many other features to give your students a classroom experience.

## **Batch Management:**

Create unlimited batches and share your content with whom you want to. Assign homework, tests and disseminate results.

**Content Sharing:** Share your study material, upload docs, pdf or images, conduct tests and assign homework.



Chairman

Digital Repository Cell  
Vidnyan Mahavidyalaya, Sangola



**Acting Principal**  
Vidnyan Mahavidyalaya, Sangola  
Tal. Sangola Dist. Solapur

**Sangola Taluka Shetkari Shikshan  
Prasarak Mandal, Sangola**  
**Teaching and Learning Application**

**One Day**

**Workshop**

**Chief Guest:**

**Hon. Chandrakantdada Deshmukh**

**Hon. Dr. Aniket Deshmukh**

**Resource Person: Imam Nadaf**

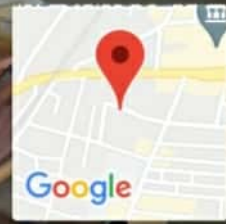
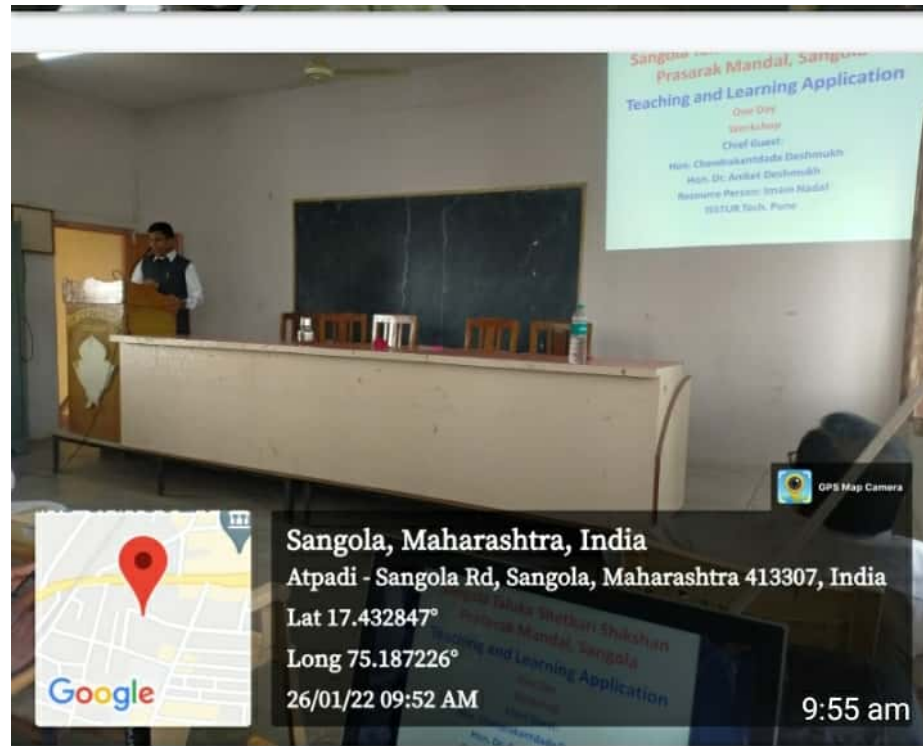
**ISSTUR Tech. Pune**



GPS Map Camera

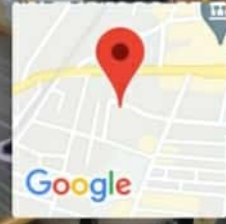
**Sangola, Maharashtra, India**

**Atnadi - Sangola Rd. Sangola, Maharashtra 413307, India**



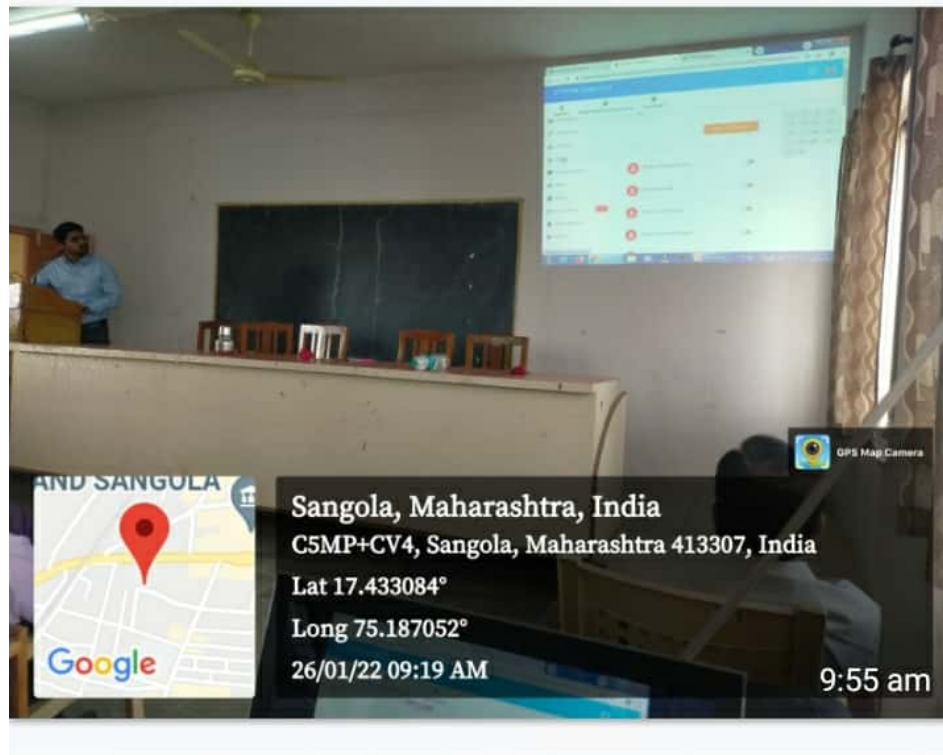
**Sangola, Maharashtra, India**  
Atpadi - Sangola Rd, Sangola, Maharashtra 413307, India  
Lat 17.432847°  
Long 75.187226°  
26/01/22 09:52 AM

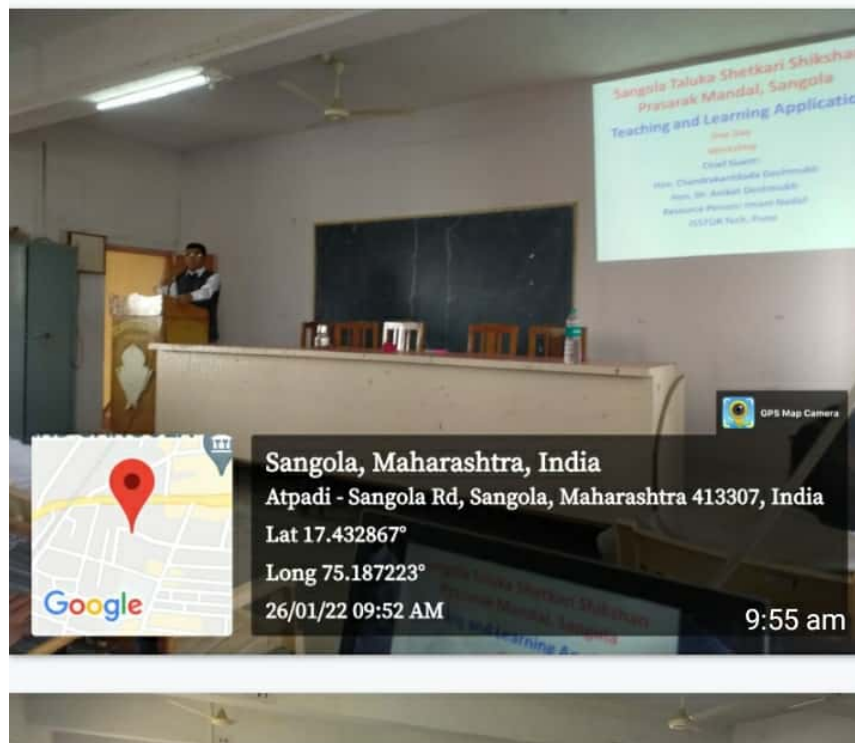
9:55 am



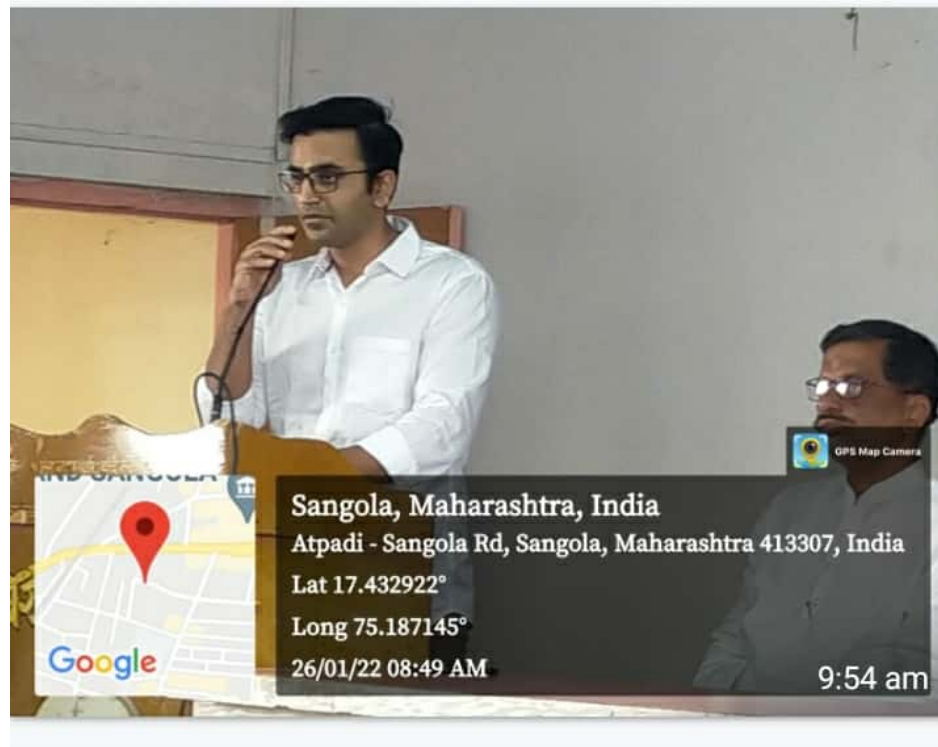
**Sangola, Maharashtra, India**  
Atpadi - Sangola Rd, Sangola, Maharashtra 413307, India  
Lat 17.432843°  
Long 75.187148°  
26/01/22 09:19 AM

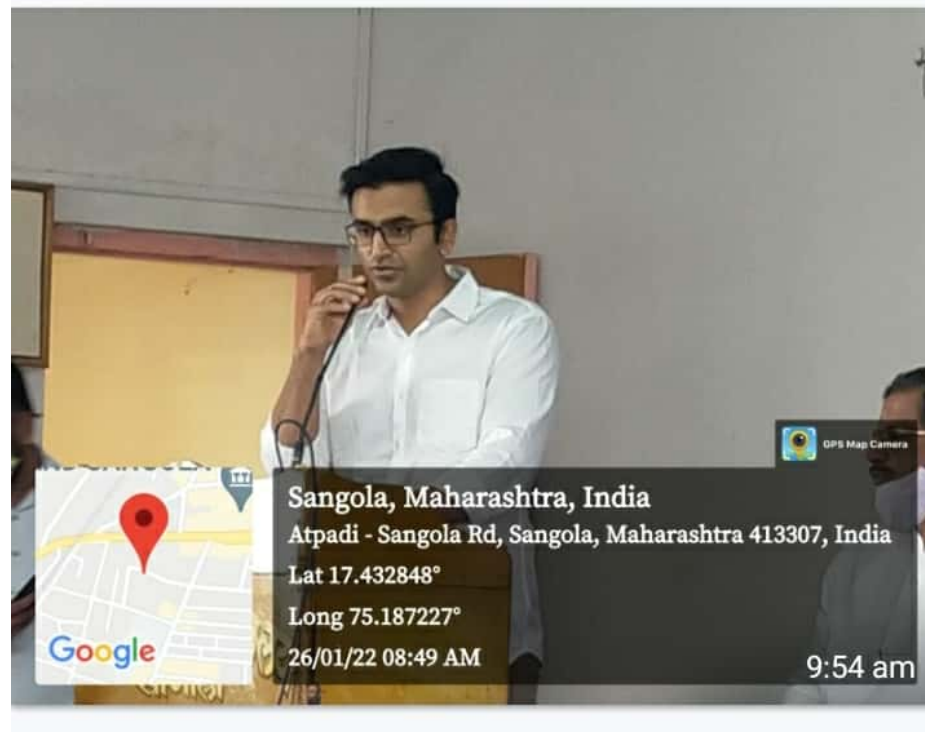
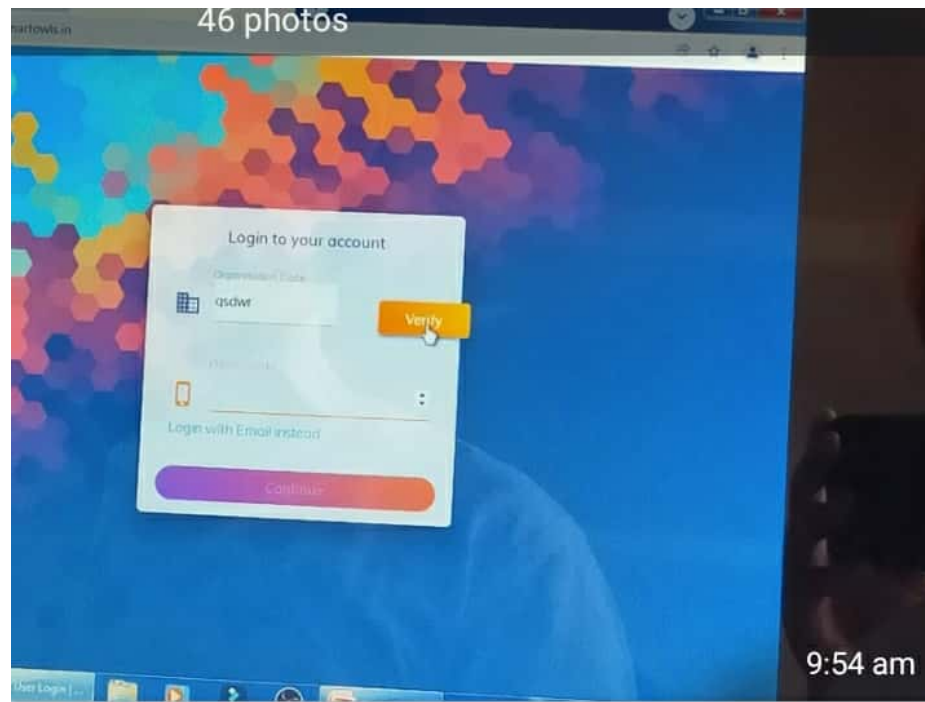
9:55 am

















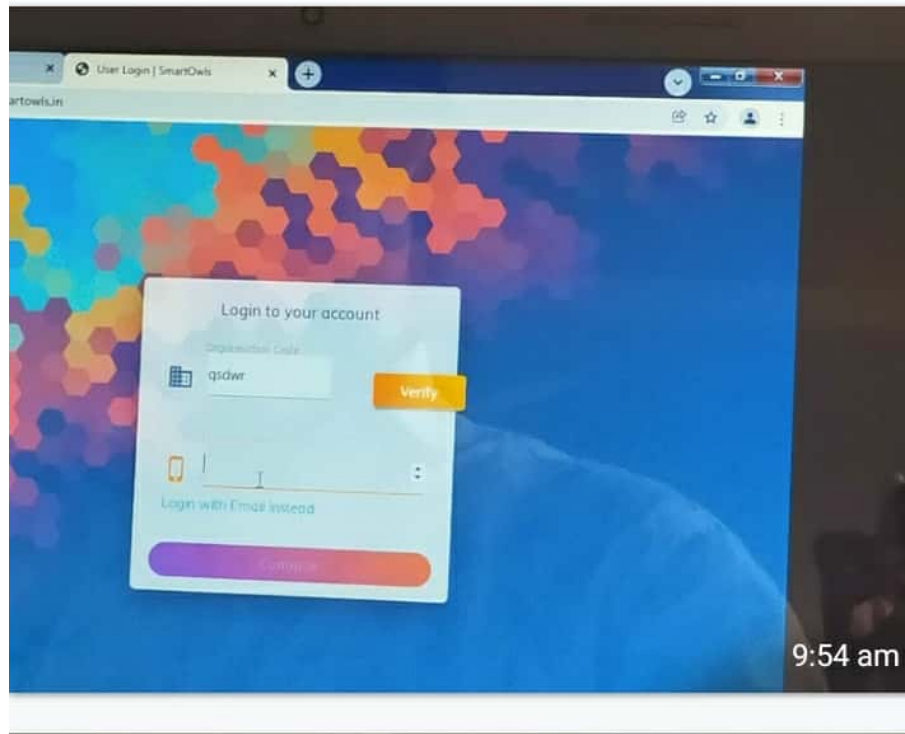


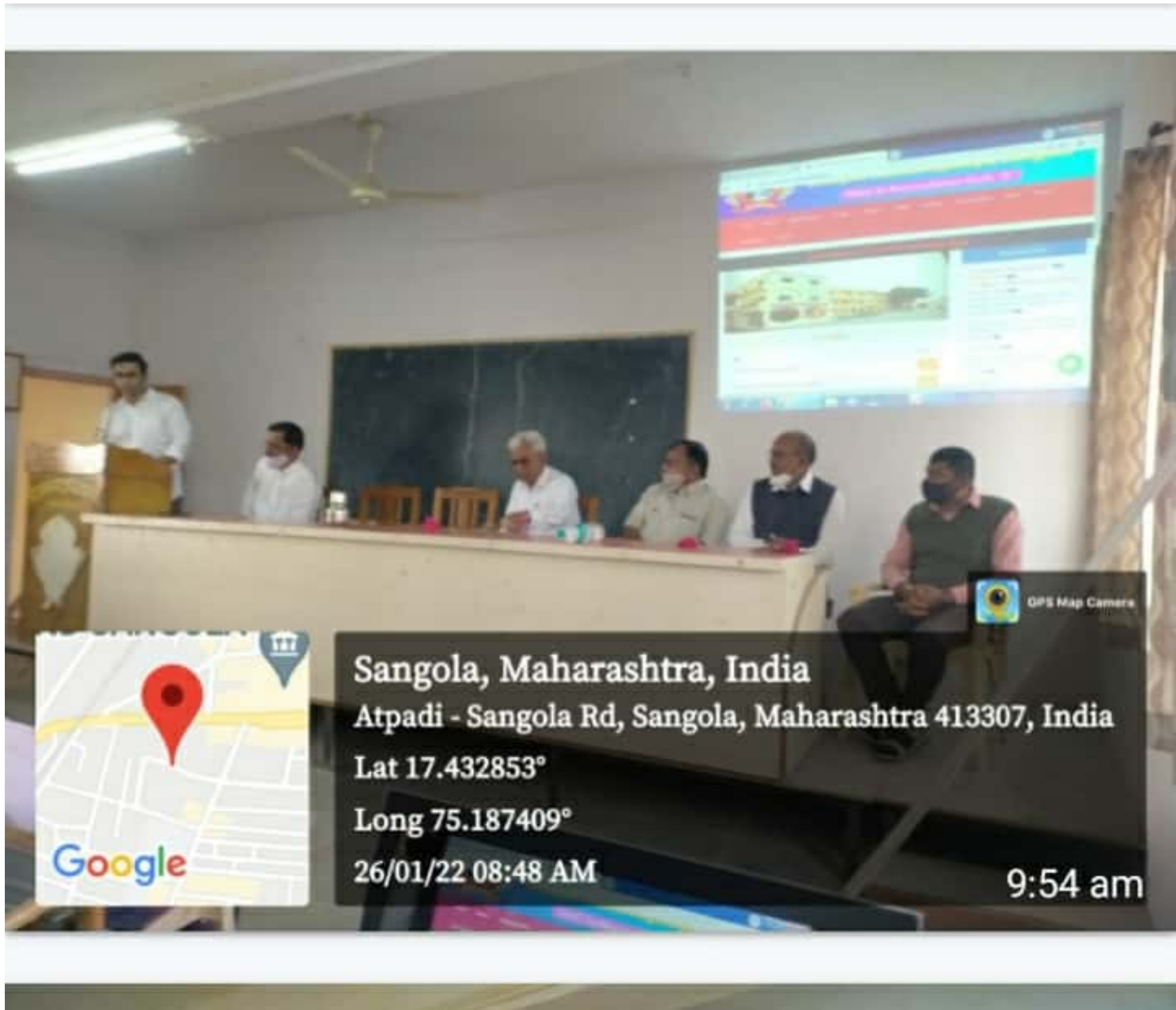












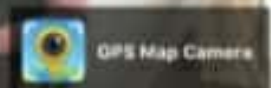
Sangola, Maharashtra, India

Atpadi - Sangola Rd, Sangola, Maharashtra 413307, India

Lat 17.432853°

Long 75.187409°

26/01/22 08:48 AM



9:54 am





